

MECHANISTIC STUDY AND APPLICATION OF DECARBONYLATION OF  
CYCLOPROPENONE DERIVATIVES

by

ZICHUN REN

(Under the Direction of Vladimir Popik)

ABSTRACT

Cyclopropenone is an organic compound consisting of a cyclopropene framework with a ketone functional group. It has been found in various natural compounds. Cyclopropenone can also undergo different reactions, and photo-decarbonylation is one of the most unique. It is clean and one of the fast photo reactions. In this dissertation, we focused on mechanistic study and application of the photo-decarbonylation of cyclopropenone derivatives. Although photodecarbonylation is the one of the most common reaction of cyclopropenones, there is very little agreement in the literature on the photoactivation mechanism. We discussed some finding we had recently on the mechanism of photo-decarbonylation reaction both in nanosuspension and in solution. In ultrafast transient absorption spectroscopy, with the help of collaborator, we proposed different mechanism for photo-decarbonylation of photo-ODIBO under 321 nm and 350 nm. In addition, we reported our latest findings on the different photo reaction quantum yield of decarbonylation in basic condition and in acidic conditions. We used fluorescent spectroscopy to study fluorescent quantum yield of solution in both conditions to explain those differences. Those findings pave ways for determination of the mechanism of the photo-decarbonylation We also discussed some synthetic work based on using carbonyl groups in

cyclopropanone as photo-labile protecting groups. With different functional groups, we achieved different linkages between SPPAC moieties, such as ODIBO or ADIBO and biomacromolecules. We hope those methods would provide with new insight of SPAAC reagents in biolabeling.

INDEX WORDS: ODIBO, ADIBO, Photo Decarbonylation, Cyclopropanone, Photo-ODIBO,  
Photo-ADIBO, Mechanism

MECHANISTIC STUDY AND APPLICATIONS OF DECARBONYLATION OF  
CYCLOPROPENONE DERIVATIVES

by

ZICHUN REN

BS, WUHAN UNIVERSITY, CHINA, 2017

A Dissertation Submitted to the Graduate Faculty of The University of Georgia in Partial  
Fulfillment of the Requirements for the Degree

DOCTOR OF PHILOSOPHY

ATHENS, GEORGIA

2022

© 2022

Zichun Ren

All Rights Reserved

MECHANISTIC STUDY AND APPLICATIONS OF DECARBONYLATION OF  
CYCLOPROPENONE DERIVATIVES

by

ZICHUN REN

Major Professor: Vladimir Popik  
Committee: George Y. Zheng  
Jin Xie

Electronic Version Approved:

Ron Walcott  
Vice Provost for Graduate Education and Dean of the Graduate School  
The University of Georgia  
August 2022

## ACKNOWLEDGEMENTS

I would like to express my appreciation to my adviser Dr. Vladimir Popik. His patience and rigorous research attitude toward science influenced me in the past five years. I also want to thank my committee members, Dr. Jin Xie, and Dr. George Y. Zheng. They have valuable vision into chemistry and provide creative suggestions for my projects. I want to make a special thank Dr. Chris McNitt who led me to the field of click chemistry and helped me finish the synthetic project during the first year of my study. I would also want to thank all my former or present group members, Dr. Nannan Lin, Dr. Kun Wang, Dr. Chen Zhao, Chris Molnar, Rohan Bhavsar, Shrey Patel, Shubham, Sharma, Ayesha Nisathar, Patrick Forster. It was a great pleasure to work with you. I must also thank my family members, especially my parents. They never hesitated to support me and give their best to me. I love you so much. At last, I want to thank my collaborator Dr. Learnmore Shenje. Without you, I cannot finish the hardest part of the project.

## TABLE OF CONTENT

ACKNOWLEDGEMENTS .....	iv
LIST OF TABLES .....	ix
LIST OF FIGURES .....	xi
LIST OF SCHEMES.....	xv
CHAPTER 1 .....	1
INTRODUCTION .....	1
1.1 Cyclopropenone and Synthesis of Cyclopropenone Derivatives.....	1
1.2 Reactions of Cyclopropenone .....	7
1.3 Application of Photo-Decarbonylation of Cyclopropenone.....	23
1.4 Conclusion.....	26
1.5 Reference.....	29
CHAPTER 2 .....	37
CYCLOPROPENONES IN THE SYNTHESIS OF MULTIPLE FUNCTIONALIZED TERMINAL SPAAC REAGENTS .....	37
2.1 Introduction .....	37
2.2 Synthesis of NHS-ester terminal SPAAC reagents.....	37
2.3 Synthesis of SPAAC Regents with Biotin .....	40

2.4 Synthesis of SPAAC Reagents with Propargyl Terminal .....	42
2.5 Water Solubility of Photo-ODIBO-OH and Photo-ADIBO-Bis-OH.....	42
2.6 Visible Light Irradiation for Transforming Photo-XDIBO Derivatives into XDIBO SPAAC Reagents .....	43
2.7 Conclusion.....	45
2.8 Experimental Section .....	46
2.9 References .....	60
CHAPTER 3 .....	63
ULTRAFAST TRANSIENT ABSORPTION SPECTROSCOPY OF PHOTODECARBONYLATION OF PHOTOOXADIBENZOCYCLOOCTYNE.....	63
3.1 Introduction .....	63
3.2 Synthesis of Photo-ODIBO-OMe .....	64
3.3 Measurement of Quantum Yield of Photo-ODIBO under 321 nm and 350 nm .....	65
3.4 Study of Triplet-State Photo-ODIBO-OMe using Nanosecond Transient Spectroscopy ...	66
3.5 Conclusion.....	67
3.6 Experimental Section .....	67
3.7 References .....	75
CHAPTER 4 .....	76
PHOTONIC AMPLIFICATION EFFECT OF PHOTOOXADIBENZYL CYCLOOCTYNE ....	76
4.1 Introduction .....	76

4.2 Preparation of Nanocrystalline Suspension and Size Measurement .....	76
4.3 Measurement of Quantum Yield of Photo-ODIBO Nanosuspension in Neutral Buffer.....	78
4.4 Measurement of pKa Value of Photo-ODIBO-OH.....	81
4.5 Measurement of Quantum Yield of Photo-ODIBO Nanosuspension in Acidic Buffer.....	81
4.6 Conclusion and Future Work .....	83
4.7 Experimental Section .....	84
4.8 References: .....	90
CHAPTER 5 .....	92
MEASUREMENT OF QUANTUM YIELD OF PHOTO-ODIBO-OH IN DIFFERENT PH ENVIRONMENT .....	92
5.1 Introduction .....	92
5.2 Measurement of Quantum Yield of Photo-ODIBO-OH in Basic Condition .....	92
5.3 Measurement of Irradiation of Actinometer.....	93
5.4 Irradiation of Photo-ODIBO-OH in Acidic Conditions.....	94
5.5 Measurement of Quantum Yield of Photo-ODIBO-Acid in Basic Conditions.....	95
5.6 Fluorescence Spectra Measurement .....	97
5.7 Conclusion.....	101
5.8 Experimental Section .....	101
5.9 References .....	104
APPENDICES .....	106

1. $^1\text{H}$ NMR and $^{13}\text{C}$ NMR .....	106
2. Measurement of pKa Value of 2.32 .....	192

## LIST OF TABLES

	Page
Table 3. 1 Quantum yield of photo-ODIBO under 351 nm and 320 nm .....	66
Table 3. 2 Lifetime of ODIBO-OH in different concentrations of oxygen .....	67
Table 3. 3 Conversion, absorbance change, and concentration change of PO under 350-nm laser irradiation .....	70
Table 3. 4 Conversion, absorbance change, and concentration change of PO under 321-nm laser irradiation .....	71
Table 3. 5 Conversion, absorbance change, and concentration change of 4-nitroveratrole under 350-nm laser irradiation .....	71
Table 3. 6 Conversion, absorbance change, and concentration change of 4-nitroveratrole under 321-nm laser irradiation .....	72
Table 4. 1 Concentration of photo-ODIBO nanosuspension .....	80
Table 4. 2 DLS data of Photo-ODIBO nanosuspension without surfactant .....	84
Table 4. 3 DLS data of Photo-ODIBO nanosuspension with 1 % PVP .....	84
Table 4. 4 Formula to prepare Photo-ODIBO using varying concentrations of PBS and methanol .....	86
Table 4. 5 Buffer preparation and pH value .....	87
Table 4. 6 Concentration change of Photo-ODIBO-OH nanosuspension .....	89
Table 5. 1 Concentration of solutions used in measurement of extinction coefficient .....	102
Table 5. 2 Absorbance change before and after irradiation in basic conditions .....	102

Table 5. 3 Absorbance change before and after irradiation in acidic conditions.....	102
Table 5. 4 Absorbance change before and after irradiation in acidic conditions.....	103

## LIST OF FIGURES

	Page
Figure 1. 1 Selective labeling of cells via photo triggered SPAAC reactions .....	24
Figure 1. 2 Preparation of ADIBO–photoDIBO cross-linker for sequential SPAAC reaction ....	24
Figure 1. 3 Photo-decarbonylation of CORM compounds .....	28
Figure 2. 1 Reaction rate of ADIBO-Acid with TEG-N <sub>3</sub> .....	40
Figure 3. 1 Three pathways of photodecarbonylation of cyclopropanone derivatives .....	63
Figure 3. 2 Photo-ODIBO spectra change in 350 nm and 321 nm .....	72
Figure 3. 3 4-Nitroveratrole spectra change in 350 nm and 321 nm .....	72
Figure 3. 4 Nanosecond transient absorption spectrometer set-up .....	73
Figure 3. 5 Set-up of gas purging system used in nanosecond transient spectroscopy .....	74
Figure 3. 6 Nanosecond transient spectroscopy of photo-ODIBO triplet in (a) Oxygen; (b) Air; (c) Argon.....	74
Figure 4. 1 DLS test result of Photo-ODIBO nanosuspension without surface surfactant.....	77
Figure 4. 2 DLS test result of photo-ODIBO nanosuspension with 1 % PVP .....	78
Figure 4. 3 Photo-ODIBO in varying methanol concentrations in water .....	79
Figure 4. 4 UV of photo-ODIBO-OH nanosuspension with and without PVP .....	80
Figure 4. 5 UV of supernatant of Photo-ODIBO-OH nanosuspension with and without PVP ....	81
Figure 4. 6 Spectra change of photo-ODIBO-OH solution before and after irradiation .....	82
Figure 4. 7 Spectra change of 4-nitroveratrole solution before and after irradiation .....	83
Figure 4. 8 UV spectra of Photo-ODIBO-OH in buffer with varying pH .....	87

Figure 4. 9 Boltzmann fitting of pKa value of Photo-ODIBO-OH .....	88
Figure 5. 1 UV spectra of Photo-ODIBO solution (a) and Extinction coefficient (b).....	93
Figure 5. 2 Irradiation of Photo-ODIBO-OH in basic conditions .....	93
Figure 5. 3 Irradiation of 4-nitroveratrole.....	93
Figure 5. 4 Irradiation of photo-ODIBO-OH in acidic conditions .....	94
Figure 5. 5 Measurement of extinction coefficient factor.....	95
Figure 5. 6 Spectra change of photo-ODIBO acid solution before and after irradiation.....	97
Figure 5. 7 UV spectra of quinine sulfate solutions used in measurement.....	98
Figure 5. 8 UV spectra of photo-ODIBO-OH methanol solutions used in measurement .....	99
Figure 5. 9 UV spectra of photo-ODIBO-OH Na <sub>3</sub> PO <sub>4</sub> solutions used in measurement .....	99
Figure 5. 10 Quinine sulfate fluorescence spectra (excitation wavelength: 345 nm).....	100
Figure 5. 1 UV spectra of Photo-ODIBO solution (a) and Extinction coefficient (b).....	93
Figure 5. 2 Irradiation of Photo-ODIBO-OH in basic conditions .....	93
Figure 5. 3 Irradiation of 4-nitroveratrole.....	93
Figure 5. 4 Irradiation of photo-ODIBO-OH in acidic conditions .....	94
Figure 5. 5 Measurement of extinction coefficient factor.....	95
Figure 5. 6 Spectra change of photo-ODIBO acid solution before and after irradiation.....	97
Figure 5. 7 UV spectra of quinine sulfate solutions used in measurement.....	98
Figure 5. 8 UV spectra of photo-ODIBO-OH methanol solutions used in measurement .....	99
Figure 5. 9 UV spectra of photo-ODIBO-OH Na <sub>3</sub> PO <sub>4</sub> solutions used in measurement .....	99
Figure 5. 10 Quinine sulfate fluorescence spectra (excitation wavelength: 345 nm).....	100

## LIST OF SCHEMES

	Page
Scheme 1. 1 Resonance structure of cyclopropenone.....	1
Scheme 1. 2 Synthesis of diphenylcyclopropenone by Breslow et al.....	2
Scheme 1. 3 Synthesis of diphenylcyclopropenone by Vol'pin et al. ....	2
Scheme 1. 4 Protonation of Diphenylcyclopropenone under HBr Gas .....	2
Scheme 1. 5 Synthesis of cyclopropenone derivatives using Favorskii reaction .....	3
Scheme 1. 6 Synthesis of cyclopropenone derivatives using LiCCl <sub>3</sub> .....	3
Scheme 1. 7 Preparation of cyclopropenone without any substituent groups .....	4
Scheme 1. 8 Preparation of cyclopropenone derivative via trichloroproepenium ion.....	5
Scheme 1. 9 Synthesis of hydroxy phenylcyclopropenone via $\alpha$ -elimination .....	5
Scheme 1. 10 Synthesis of hydroxy phenylcyclopropenone via Friedel-Crafts and hydrolysis.....	6
Scheme 1. 11 Synthesis of unsubstituted cyclopropenone .....	6
Scheme 1. 12 Preparation of cyclopropenone derivative via UV irradiation .....	7
Scheme 1. 13 The reaction of cyclopropenone derivatives with furan.....	8
Scheme 1. 14 Reaction between difluorocyclopropenone and benzofuran derivatives.....	9
Scheme 1. 15 Dimerization of cyclopropenone derivatives with copper catalyst .....	10
Scheme 1. 16 Proposed mechanism of dimerization of cyclopropenone derivatives.....	10
Scheme 1. 17 [3+2] Annulation of cyclopropenone and cyclopropanes .....	11

Scheme 1. 18 Proposed mechanism of [3+2] annulation reaction.....	11
Scheme 1. 19 Palladium-catalyzed ring-opening alkynylation of cyclopropenones .....	12
Scheme 1. 20 Proposed mechanism for the palladium-catalyzed ring-opening alkynylation. ....	12
Scheme 1. 21 Rhodium(III)-catalyzed C–C coupling of arenes and cyclopropenones .....	13
Scheme 1. 22 Proposed Mechanism of Rhodium-Catalyzed C-C Coupling .....	14
Scheme 1. 23 Reaction Scheme of CuBr <sub>2</sub> Catalyzed for Cascade Ring-Opening Dual Halogenation.....	15
Scheme 1. 24 Proposed Mechanism of CuBr <sub>2</sub> Catalyzed for Cascade Ring-Opening Dual Halogenation of Cyclopropenones.....	15
Scheme 1. 25 Reaction scheme of cyclopentadienone formation by [3+2] ring-opening addition with cyclopropenone derivatives without CO.....	16
Scheme 1. 26 Proposed mechanism of cyclopentadienone formation by [3+2] ring-opening addition with cyclopropenone derivatives .....	16
Scheme 1. 27 Nickel catalyzed ring-opening addition of cyclopropenone derivatives and $\alpha, \beta$ – unsaturated ketones.....	17
Scheme 1. 28 Palladium-catalyzed [3+2] addition of aniline and cyclopropenone derivatives ...	17
Scheme 1. 29 Reaction scheme and mechanism of cyclopropenone acting as nucleophilic attack catalyst .....	18
Scheme 1. 30 Reaction scheme of transformation of cyclopropenone derivatives under PPh <sub>3</sub> ...	18
Scheme 1. 31 Mechanism transformation of cyclopropenone derivatives under PPh <sub>3</sub> .....	19
Scheme 1. 32 Reaction scheme between cyclopropenone and thiourea derivatives .....	19

Scheme 1. 33 Reaction scheme between cyclopropenone and phosphine derivatives .....	20
Scheme 1. 34 Pyrolysis decarbonylation of diphenylcyclopropenone .....	20
Scheme 1. 35 Photo-decarbonylation of hydroxy-cyclopropenone .....	21
Scheme 1. 36 Photo-decarbonylation of hydroxy-cyclopropenone .....	22
Scheme 1. 37 Formation of zwitterionic intermediates .....	22
Scheme 1. 38 Preparation of ODIBO-PMSA conjugates through SPAAC reaction .....	27
Scheme 2. 1 Structure of Photo-ODIBO-NHS (2.01) and Photo-ADIBO-NHS (2.02) .....	38
Scheme 2. 2 Synthetic Route of Photo-ODIBO-NHS .....	39
Scheme 2. 3 Synthetic route of photo-ADIBO-NHS .....	39
Scheme 2. 4 Synthesis of photo-ODIBO-biotin .....	41
Scheme 2. 5 Synthetic route of photo-ADIBO-propargyl .....	44
Scheme 2. 6 Synthetic route of photo-ODIBO-propargyl .....	44
Scheme 2. 7 Irradiation of compound 2.08 and 2.32 with 420 nm light .....	45
Scheme 3. 1 Steps to synthesize photo-ODIBO-OMe .....	64

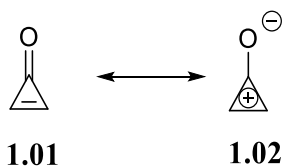
## CHAPTER 1

### INTRODUCTION

Cyclopropenone seems like a pebble in the brook of organic chemistry, with its simplicity in structure, stability under harsh conditions, and wide applications in biological environment. Cyclopropenone has the largest strain energy of any three-membered alicyclic compound,<sup>1</sup> and its three-membered ring accounts for its high reactivity.

#### 1.1 Cyclopropenone and Synthesis of Cyclopropenone Derivatives

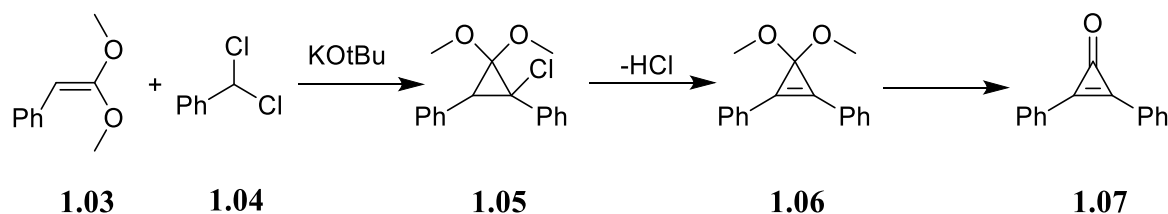
The cyclopropenone moiety consists of a three-carbon-based ring with a carbonyl group. The unsubstituted cyclopropenone can be represented as the zwitterionic resonance form **1.02** in which cyclopropenyl cation displays Hückel aromaticity. The aromaticity is still under argument for cyclopropenone itself, but a recent study suggests that oxygen in the carbonyl group polarizes the oxygen-carbon double bonds creating a pseudo  $2\pi$  system, which provided computational evidence on the aromaticity of cyclopropenone.<sup>2</sup> Due to this specific structure, cyclopropenone has amphiphilic properties with both nucleophilicity and electrophilicity.



#### *Scheme 1. 1 Resonance structure of cyclopropenone*

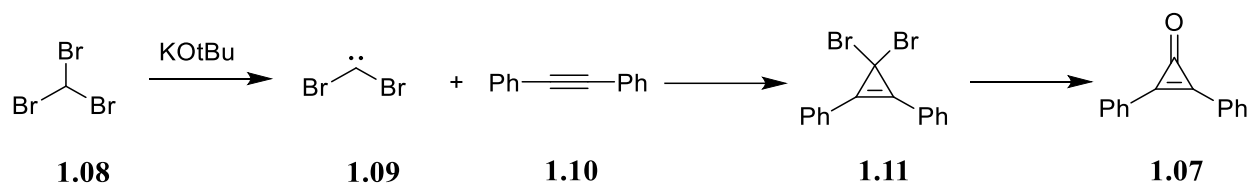
Dr. Breslow first synthesized cyclopropenone derivatives in 1959<sup>3</sup> where they used the reaction between benzal chloride and ketene dimethyl acetal in the presence of potassium t-

butoxide and reaction took only two steps to finish. In the first step, carbene will be added to the double bond of ketene acetal, which produces the cyclopropenone ketal product. In the second step,  $\beta$ -elimination will give cyclopropanone ketal followed by hydrolysis to afford a diphenylcyclopropenone product.

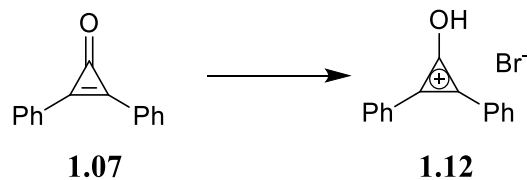


**Scheme 1. 2 Synthesis of diphenylcyclopropenone by Breslow et al.**

Vol'pin *et al.* synthesized diphenylcyclopropenone in the same year as Breslow. Their synthesis used dibromocarbene, formed by a reaction of bromoform and potassium tert-butoxide, and diphenylacetylene. They also found that with the adding of HBr gas, cyclopropenone will be protonated and produce the bromide product.<sup>4</sup>



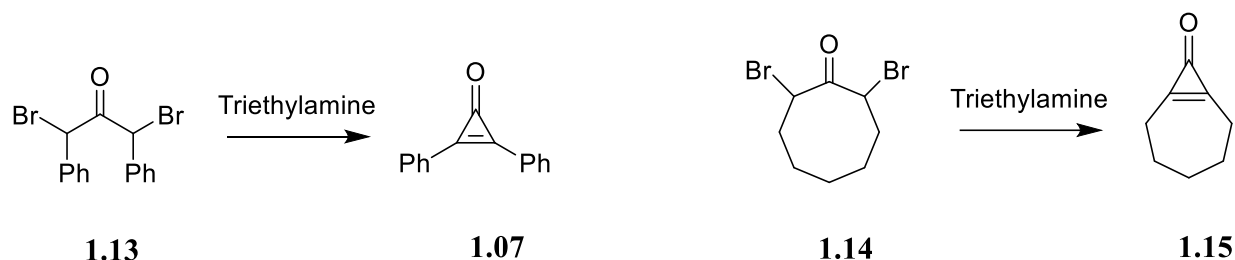
**Scheme 1. 3 Synthesis of diphenylcyclopropenone by Vol'pin et al.**



**Scheme 1. 4 Protonation of Diphenylcyclopropenone under HBr Gas**

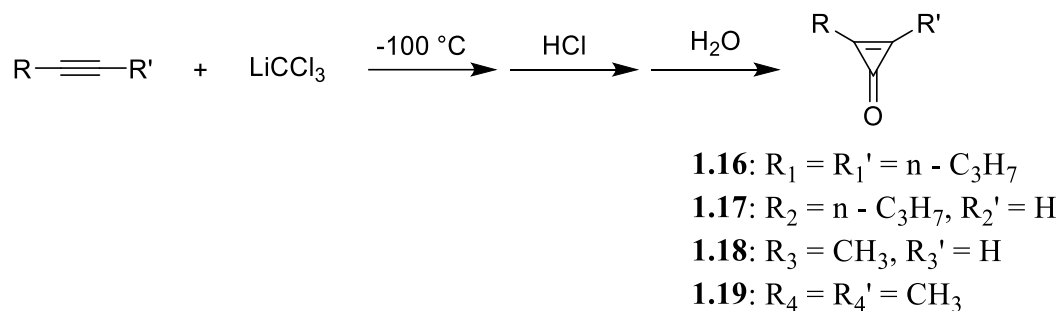
In 1963, Breslow *et al.* proposed a novel method for synthesizing cyclopropenone derivatives using the Favorskii reaction.<sup>5</sup> They started with  $\alpha,\alpha'$  – dibromodiphenylketone and triethylamine, and the percentage yield of the reaction can reach 50 % – 60 %. More interestingly,

if starting with cyclic compounds 2,8 – dibromo cyclooctenone, they can obtain the product cycloheptenocyclopropenone. However, this method could not produce unsubstituted cyclopropenone because the dihaloketone starting materials could not survive under the harsh reaction conditions.



***Scheme 1. 5 Synthesis of cyclopropenone derivatives using Favorskii reaction***

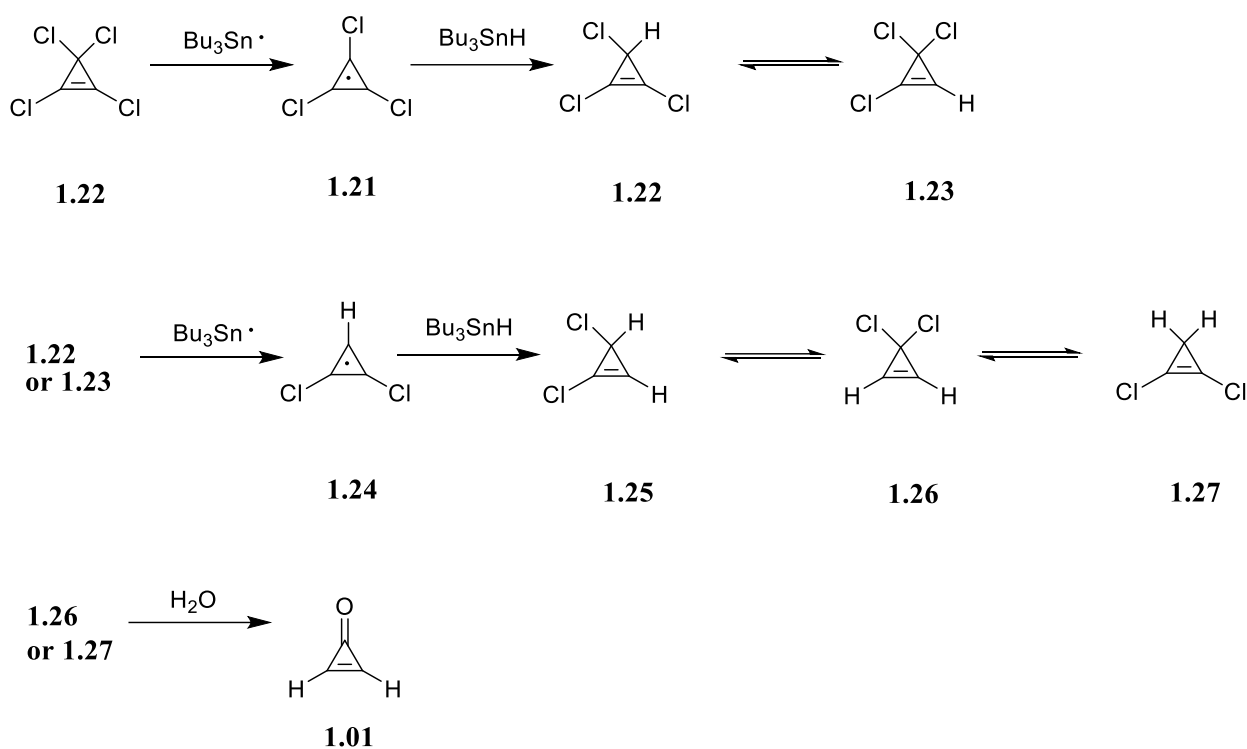
The first monosubstituted cyclopropenone derivatives were synthesized through carbene addition. In 1966, Breslow et al. synthesized monosubstituted cyclopropenone using lithium trichloromethane with different acetylene starting materials. Those reactions were expected to be conducted under low temperatures to prevent side reaction and evaporation of the alkyne derivatives.



***Scheme 1. 6 Synthesis of cyclopropenone derivatives using LiCCl<sub>3</sub>***

In 1970, Breslow et al. designed new synthetic route of unsubstituted cyclopropenone.<sup>8</sup> Starting with tetrachlorocyclopropene and tri-n-butyltin hydride, the pure product could then be separated through preparative liquid chromatography. The reaction mechanism could be the

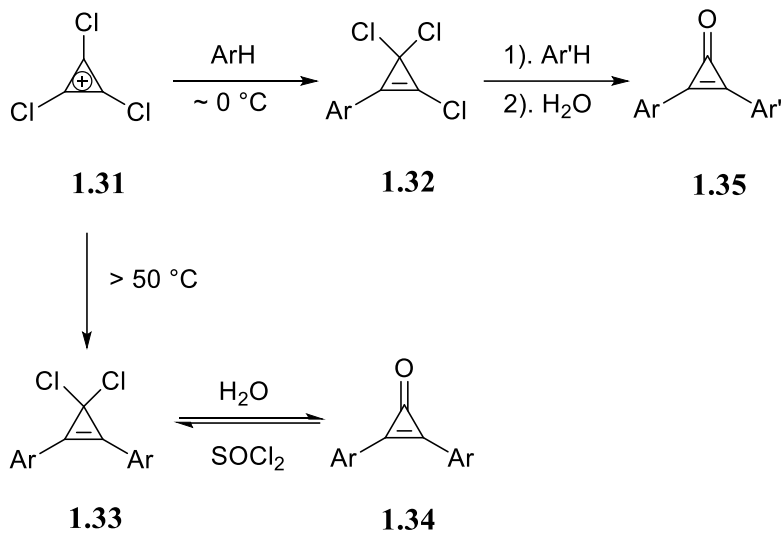
usual free-radical dichlorination mechanism. The radical compound could be the first intermediates since only allylic chloride was removable. Compound **1.22**, 1,2,3-trichlorocyclopropene would form and isomerize to compound **1.23** through the cyclopropenyl cation. Then, radical intermediates **1.24** would create via the removal of allylic chloride. By picking up hydrogen, compounds **1.25** and **1.26** could be quickly produced with isomerization to compound **1.27**.



**Scheme 1. 7 Preparation of cyclopropenone without any substituent groups**

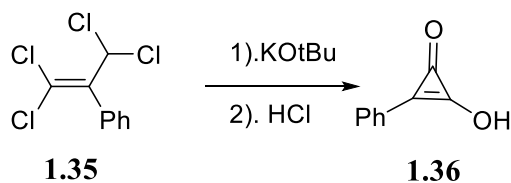
West et al. found that the trichlorocyclopropenium ion could react with benzene derivatives smoothly to provide either aryl-trichlorocyclopropenes or gem-dichloro-diaryl cyclopropenes.<sup>9,10</sup> When dichloro-compound is treated with iced water, corresponding cyclopropenone products were produced. More interestingly, aryl-trichlorocyclopropenes can

react with other equivalent aromatic compounds, forming cyclopropenone derivatives with different substituent groups.

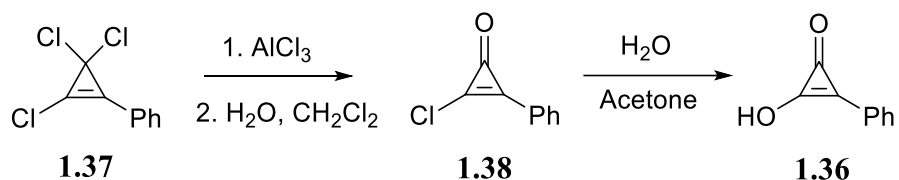


**Scheme 1. 8 Preparation of cyclopropenone derivative via trichloropropenium ion**

For the synthesis of hydroxy cyclopropenone derivatives, Farnum proposed using  $\alpha$ -elimination of tetrachloropropenes to synthesize cyclopropenones.<sup>11</sup> Once finished, the reaction was treated with dry HCl in ether, and the percentage yield of the reaction can reach 11 %. Then, Farnum and Thurston proposed the synthesis of compound **1.36** through Friedel-Crafts reaction of tetrachlorocyclopropene to the benzene and hydrolysis of compounds **1.37** and **1.38** with high yield.<sup>12</sup>

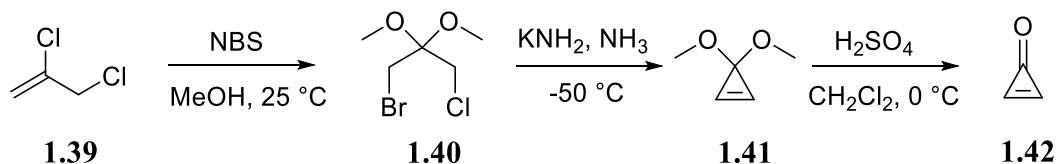


**Scheme 1. 9 Synthesis of hydroxy phenylcyclopropenone via  $\alpha$ -elimination**



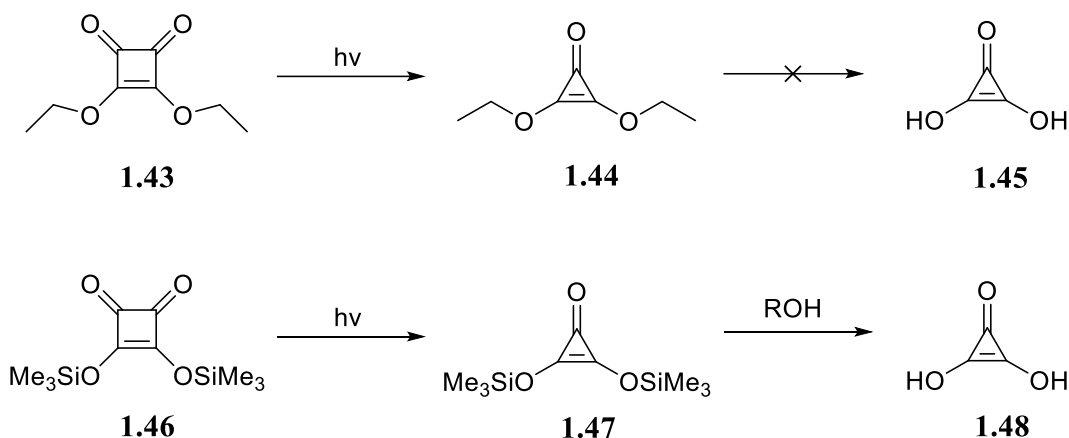
***Scheme 1. 10 Synthesis of hydroxy phenylcyclopropanone via Friedel-Crafts and hydrolysis***

Breslow et al. synthesized cyclopropanone compound without any substituent groups and acidified compound **1.41** with sulfuric acid.<sup>13</sup> The pure compound **1.42** can be obtained, and more than 60 % yield can be achieved via this three-step reaction. The work was inspired by Baucom and Butler, who invented the synthesis of dimethoxy cyclopropanone and found it can be hydrolyzed to cyclopropanone conveniently.<sup>14</sup>



***Scheme 1. 11 Synthesis of unsubstituted cyclopropanone***

West et al. synthesized deltic acid through a novel method with light irradiation.<sup>15</sup> In a previous study, Dehmlow et al. found that cyclopropanone derivatives can be prepared through the irradiation of squaric ester.<sup>16</sup> Unfortunately, deltic acid could not be prepared through the hydrolysis of deltic esters.<sup>16</sup> Based on that, West et al. reported a new way of using trimethylsilyl protected squaric acid for UV irradiation. Those groups can be easily deprotected by alcohol to yield deltic acid as a white solid.



**Scheme 1.12 Preparation of cyclopropenone derivative via UV irradiation**

## 1.2 Reactions of Cyclopropenone

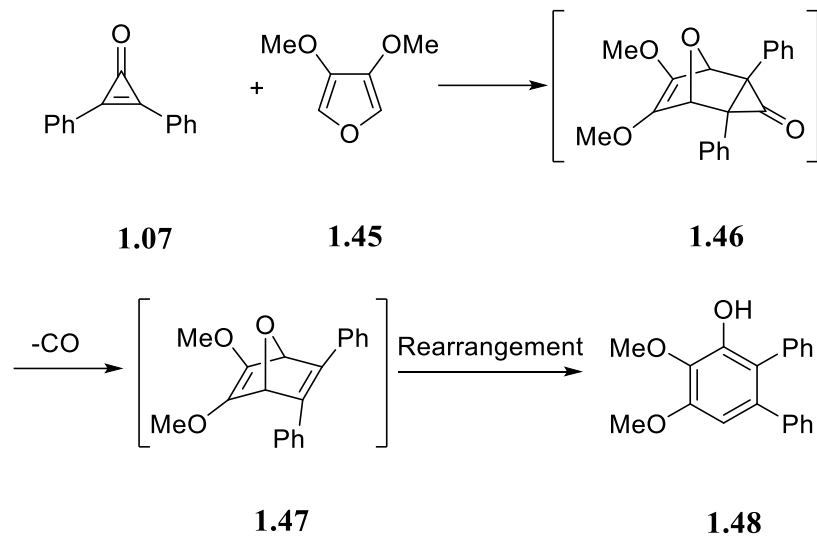
Due to the presence of carbonyl groups, cyclopropenone moiety has special amphiphilic properties with both nucleophilicity and electrophilicity. Thus, cyclopropenone derivatives can undergo a huge variety of reactions. Most reactions can be categorized into five different types: (a). Cycloaddition to carbon-carbon double bond; (b). Cycloaddition to carbonyl groups; (c). [3+m] cycloaddition reaction; (d). Nucleophilic Attack; (e). Decarbonylation

### 1.2.1 Cycloaddition of Carbon-Carbon Double Bond

Due to the strained carbon-carbon double bond in the structure, cyclopropenone tends to react much faster with dienes than maleic anhydride or other dienophiles. The reaction tends to take place under milder conditions to yield a stable 1:1 cycloaddition product.<sup>17</sup>

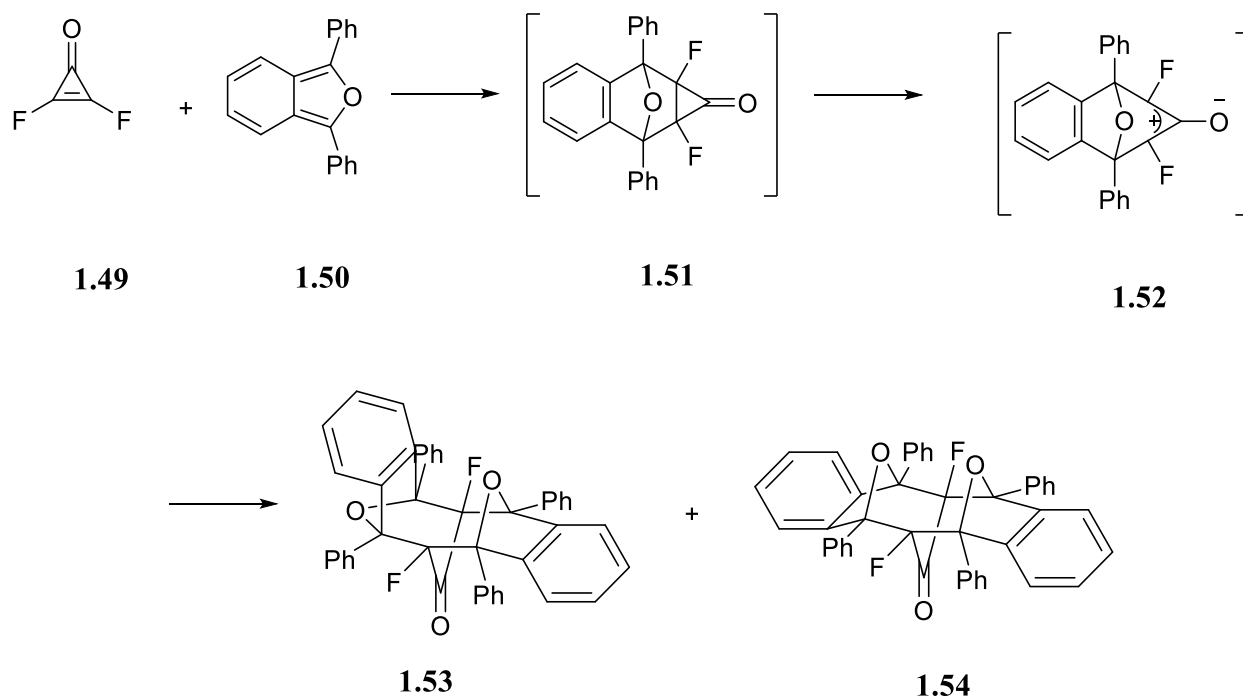
Not long after the synthesis of cyclopropenone by Dr. Breslow, scientists used cyclopropenone derivatives in Diels-Alder reactions. Okamoto et al. reported the reactions between highly reactive 3,4-dimethoxyfuran and diphenylcyclopropenone under high pressure (~10 kbar).<sup>17</sup> It was noted no reaction happened between furan and maleic acid under ten kbar pressure and the reaction required much higher pressure to accomplish the reaction (~22 kbar).

After forming the cycloaddition adduct, decarboxylation would happen at high pressure, followed by the rearrangement to produce compound **1.48**.



**Scheme 1.13** The reaction of cyclopropanone derivatives with furan

Dailey et al. studied reaction between difluorocyclopropanone **1.49** with benzofuran derivatives **1.50**, and it could proceed at room temperature. Unexpectedly, the reaction didn't stop at the Diels-Alder adduct compound **1.51**, producing compounds **1.53** and **1.54**. A further computational study found that it underwent oxyallyl intermediate **1.52**, which is consistent with the apparent high reactivity of cyclopropanone. It was also revealed that the increased reactivity of the fluorinated system is the consequence of the destabilization of the cyclopropanone by the two fluoride groups.



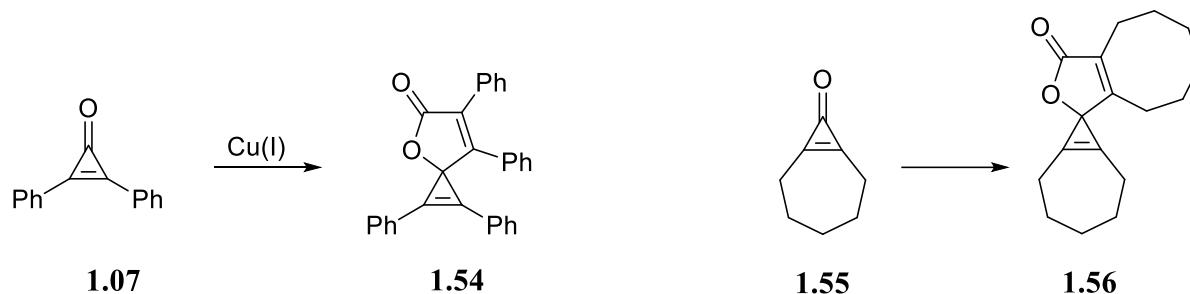
***Scheme 1.14 Reaction between difluorocyclopropenone and benzofuran derivatives***

While cyclopropenone derivatives can react smoothly with electron rich furan via IEDDA (inversed demand electron Diels Alder) reaction, they are unreactive with some other traditional IEDDA dienes, such as tetrazines.<sup>47-49</sup> Thus, there will be more field to be discovered with cycloaddition reactions to carbon-carbon double bond in cyclopropenone derivatives.

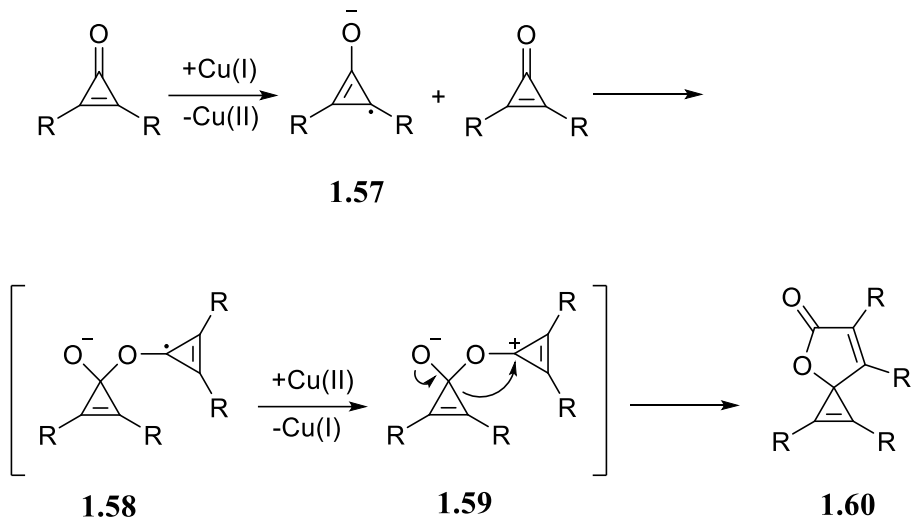
**1.2.2 Cycloaddition of Carbonyl Groups**

Gleiter et al. reported the dimerization of cyclopropenone derivatives using Cu(I) as a catalyst. Two molecules of cyclopropenone would react under heated conditions with a high yield. It is noted that the dimerization of cyclopropenone would have a 98 % yield when using diphenylcyclopropenone. Ascribing to ESR spectroscopy, they proposed a transition mechanism between the monomer and dimer of cyclopropenone derivatives. Cyclopropenone derivatives were reduced to radical anion intermediates **1.57** in the first step. In the second step, **1.57** reacted

with another cyclopropenone molecule, resulting in the formation of intermediates **1.58**, which were rapidly oxidized to **1.59**. The latter species underwent ring-opening in the following step:<sup>19</sup>



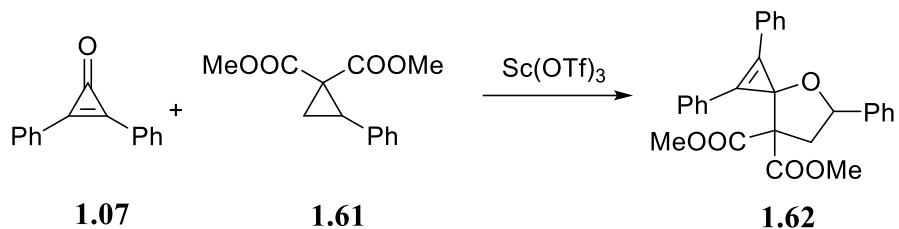
**Scheme 1.15** Dimerization of cyclopropenone derivatives with copper catalyst



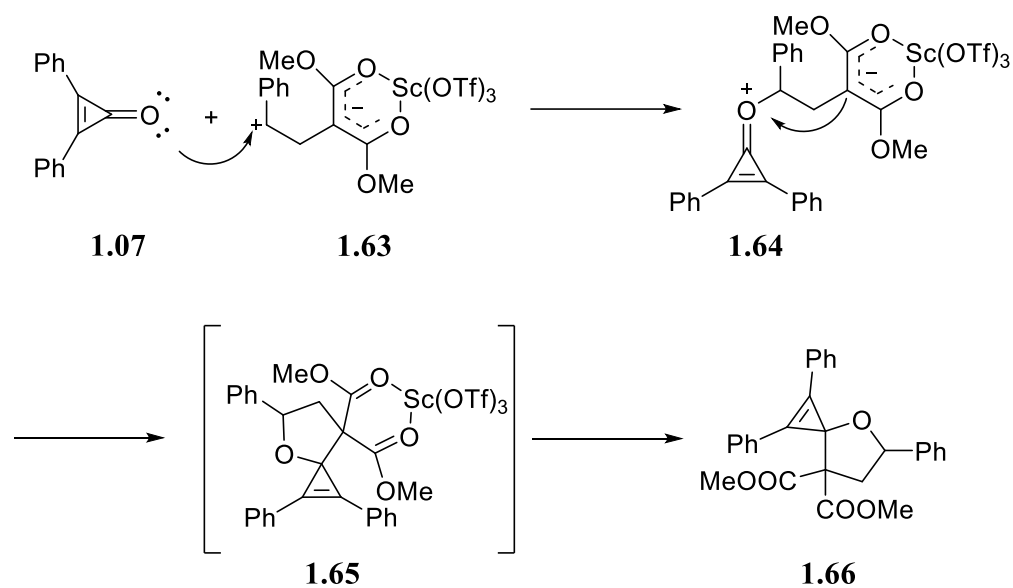
**Scheme 1.16** Proposed mechanism of dimerization of cyclopropenone derivatives

Sierra et al. synthesized oxaspiro compounds via the reaction of cyclopropanone and cyclopropanes with scandium catalyst.<sup>20</sup> This process allowed direct access to 4-oxaspiro[2,4]hept-1-ene derivatives through [3+2] annulation reaction with excellent yield. They also studied the mechanism of this reaction with DFT calculations. Following the ring-opening of cyclopropanes, the oxygen atom, which exhibits electrophilic property, would add to the positive charge carbon in **63**, resulting in intermediates **64**. Then annulation would occur, which ended with the formation of product **66**. This method is compatible with both the substituent's

reactants containing organometallic moieties that may be found in future applications in bioorganometallic chemistry.



**Scheme 1. 17** [3+2] Annulation of cyclopropenone and cyclopropanes



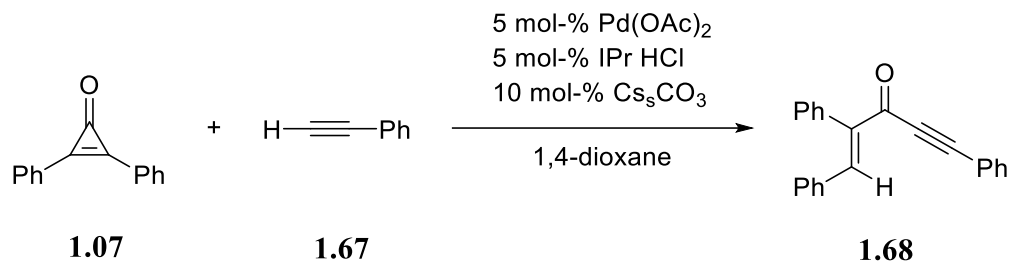
**Scheme 1. 18** Proposed mechanism of [3+2] annulation reaction

### 1.2.3 [3+m] Reaction of Cyclopropenone

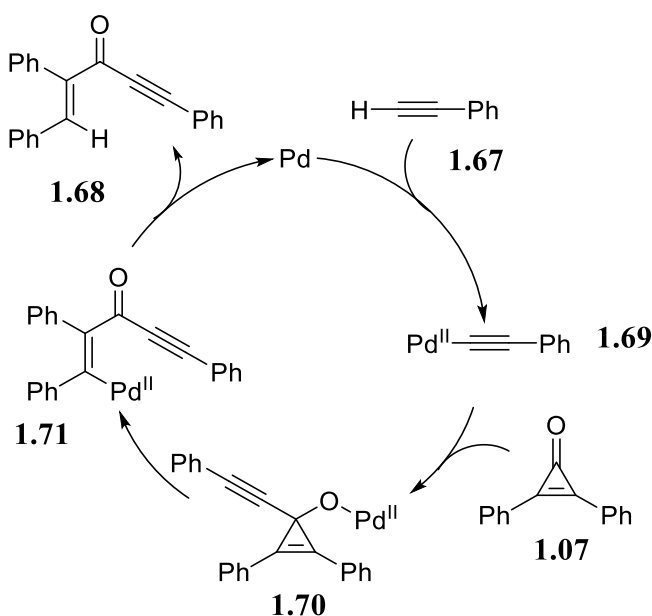
Due to the strain of cyclopropenone, the rings in cyclopropenone derivatives can be very easily broken. Therefore, cyclopropenone derivatives have a high potential for undergoing [3+m] annulation reaction. Most of the [3+m] reactions can be categorized into two different types:<sup>21</sup>

- (1). Metal-catalyzed ring-opening to  $\beta$ -carbon elimination;
- (2). Metal-catalyzed ring-opening to [3+2] addition.

Sakurai et al. reported the ring-opening of cyclopropenone derivatives by alkylation with palladium complex catalyst.<sup>22</sup> With the addition of bases such as Cs<sub>2</sub>CO<sub>3</sub>, the reaction can have high percentage yield (88 %). They also proposed a mechanism explaining how those palladium-catalyzed reactions happened. They mentioned that the reaction starts with a coordination of palladium and alkyne derivatives. Then, the alkynyl-palladium species can undergo alkynylpalladation to the C=O bond to generate palladium (II) cyclopropenolate. After this, ring-opening occurs to form the alkynylpalladium (II) species, which sequentially produces compound 68.

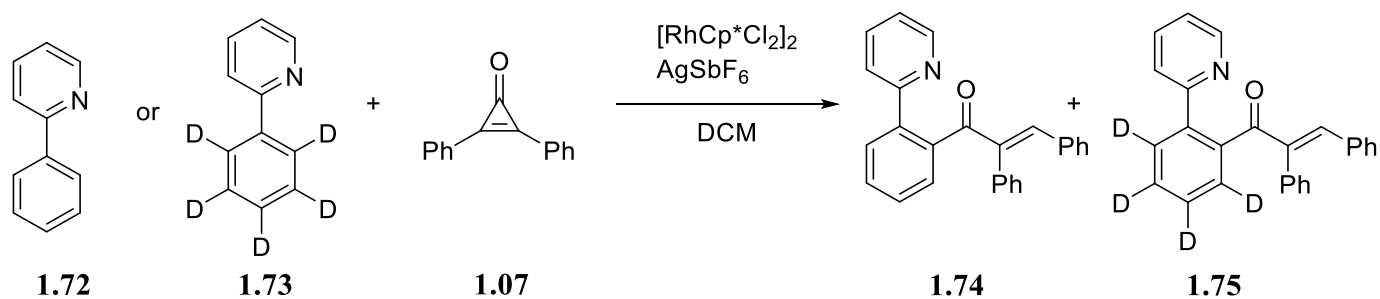


**Scheme 1. 19 Palladium-catalyzed ring-opening alkylation of cyclopropenones**

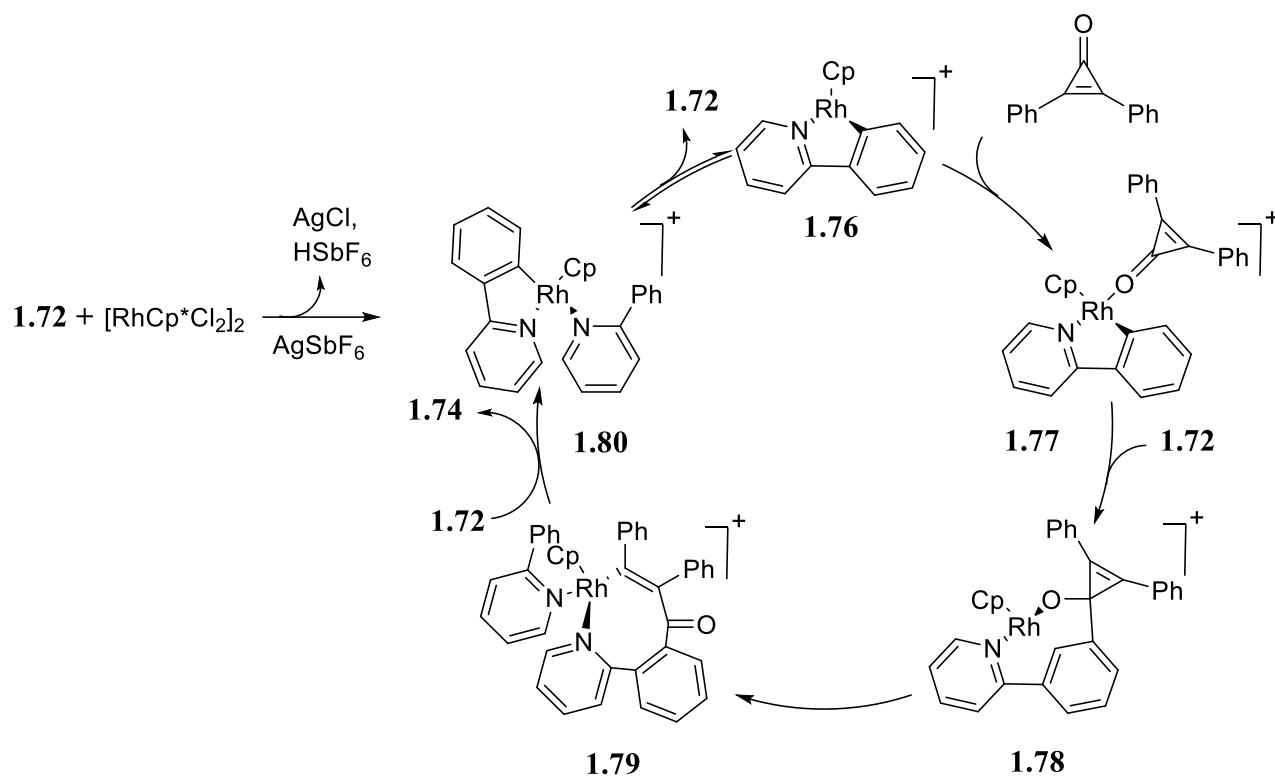


**Scheme 1. 20 Proposed mechanism for the palladium-catalyzed ring-opening alkylation.**

Li et al. reported a mild synthesis method of chalcones via Rhodium (III) – catalyzed C-C coupling of arenes and cyclopropenones.<sup>23</sup> These reactions can occur under mild conditions with a high yield and broad substrate scope. A plausible mechanism has been proposed to explain the reactions with the help of kinetic isotopic studies. Reaction rate of **1.72** is 1.7 times of reaction rate of **1.73**, which indicates the involvement of C-H activation. Complex **1.80** generated from  $[\text{Cp}^*\text{RhCl}_2]_2 / \text{AgSbF}_6$  and **1.72** undergoes ligand dissociation reaction to produce reactive intermediates **1.76**, which cyclopropenone derivatives would attack rapidly to provide adduct intermediates **1.77**. A ring-opening intermediates **1.78** is formed by migrating the aryl group into the carbonyl group of cyclopropenone and then removing the  $\beta$ -carbon. The final product was then released with another molecule joining the catalytic cycle.

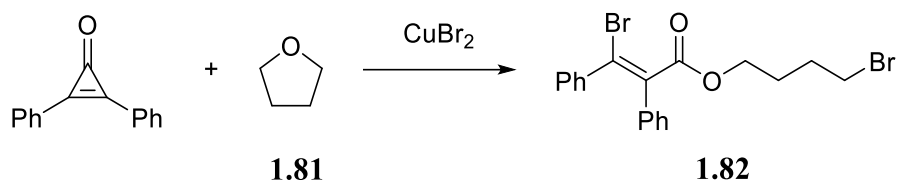


*Scheme 1.21 Rhodium(III)-catalyzed C–C coupling of arenes and cyclopropenones*

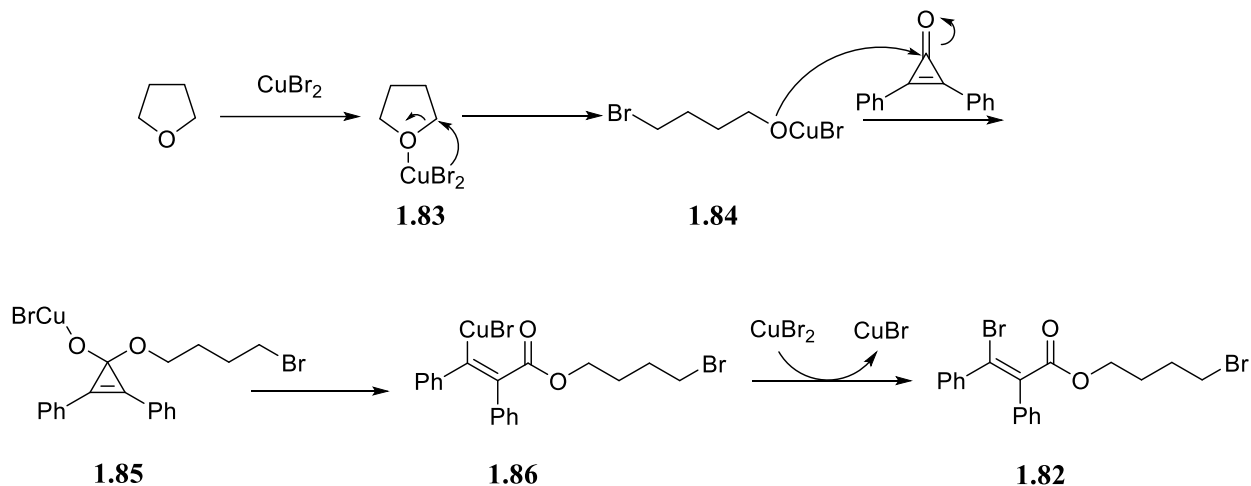


**Scheme 1.22 Proposed Mechanism of Rhodium-Catalyzed C-C Coupling**

Liu et al. reported the synthesis of a  $\beta$ -unsaturated ester using cyclopropenones and cyclic ethers.<sup>24</sup> Traditional methods, such as the hydrohalogenation of propargylic esters may yield the formation of different isomers. In this study,  $\text{CuBr}_2$  was used as a bromine source, promoting the ring-opening of cyclopropenone derivatives, stereospecifically producing product **1.82**. They also proposed a detailed mechanism of how the reaction happened. First, tetrahydrofuran was activated by coordination with  $\text{CuBr}_2$ , followed by a nucleophilic attack of the bromide ion and the ring-opening of five-membered rings. Then, oxygen would attack cyclopropenone derivatives with the generation of acetal derivatives. Subsequent bromination would then happen and result in the formation of intermediates **1.86**, which reacted with another molecule of  $\text{CuBr}_2$  to produce product **1.82**.

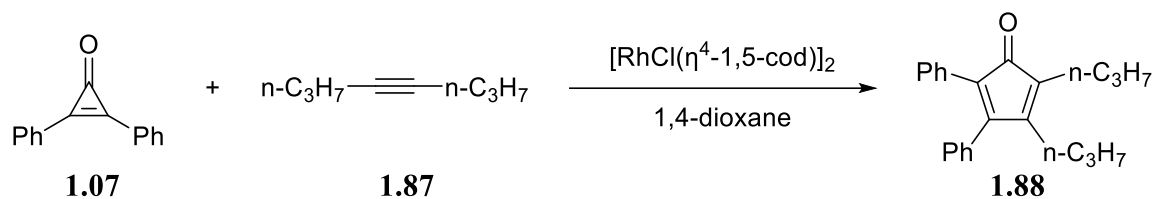


**Scheme 1. 23 Reaction Scheme of CuBr<sub>2</sub> Catalyzed for Cascade Ring-Opening Dual Halogenation**

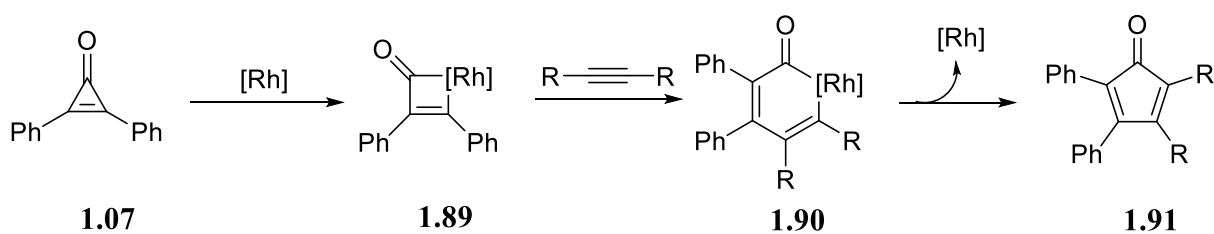


**Scheme 1. 24 Proposed Mechanism of CuBr<sub>2</sub> Catalyzed for Cascade Ring-Opening Dual Halogenation of Cyclopropanones**

Another essential type of the [3+m] reaction is the metal-catalyzed ring-opening to [3+2] addition. Kondo et al. proposed the synthesis of cyclopentadienone derivatives from the rhodium-catalyzed [3+2] addition of diphenyl cyclopropanone.<sup>25</sup> Under argon without CO, cyclopentanone derivatives could be obtained without decarbonylation. Besides, rhodium complexes showed high catalytic activities for expected cyclization reactions to give the corresponding products. A feasible mechanism has also been proposed starting with the coordination of rhodium to cyclopropanone. The four-membered ring would be easily opened and react with acetylene derivatives, followed by the leaving of rhodium to provide cyclopentadienone products.

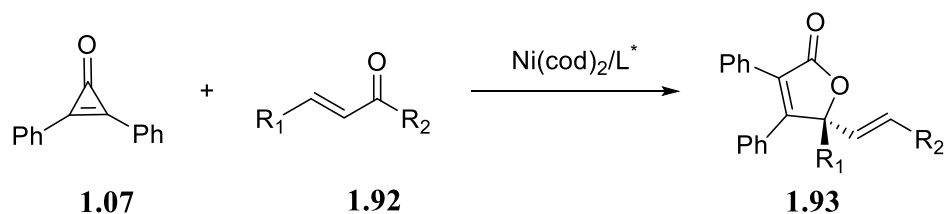


**Scheme 1. 25** Reaction scheme of cyclopentadienone formation by [3+2] ring-opening addition with cyclopropenone derivatives without CO

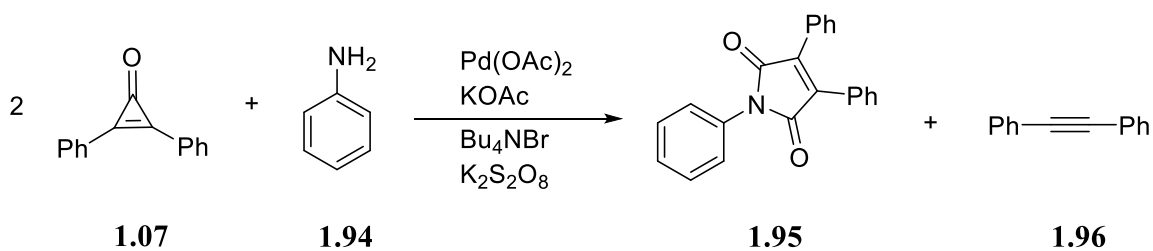


**Scheme 1. 26** Proposed mechanism of cyclopentadienone formation by [3+2] ring-opening addition with cyclopropenone derivatives

In addition to rhodium, scientists have also tried to use other metal catalysts in the [3+2] ring-opening addition with cyclopropenones. Li et al. proposed  $\text{Ni}^0$ -catalyzed chemo- and enantioselective cycloaddition between cyclopropenones and  $\alpha, \beta$ -unsaturated ketones/imines.<sup>26</sup> The reaction integrates C-C bond cleavage of cyclopropenones and enantioselective functionalization by carbonyl or imine groups, which provide a mild method for the synthesis of lactones in the future. Ravikumar et al. synthesized maleimide derivatives through palladium-catalyzed [3+2] cycloaddition reactions.<sup>27</sup> From isotopic study with  $^{18}\text{O}$ , they found that both carbonyl groups in the product were from diphenylcyclopropanone, which is an intriguing characteristic of this reaction.



**Scheme 1. 27 Nickel catalyzed ring-opening addition of cyclopropenone derivatives and  $\alpha$ ,  $\beta$  – unsaturated ketones**

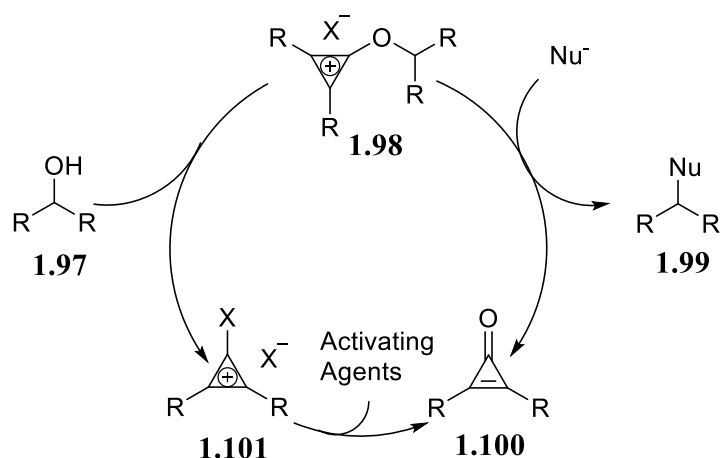


**Scheme 1. 28 Palladium-catalyzed [3+2] addition of aniline and cyclopropenone derivatives**

#### 1.2.4 Nucleophilic Attack

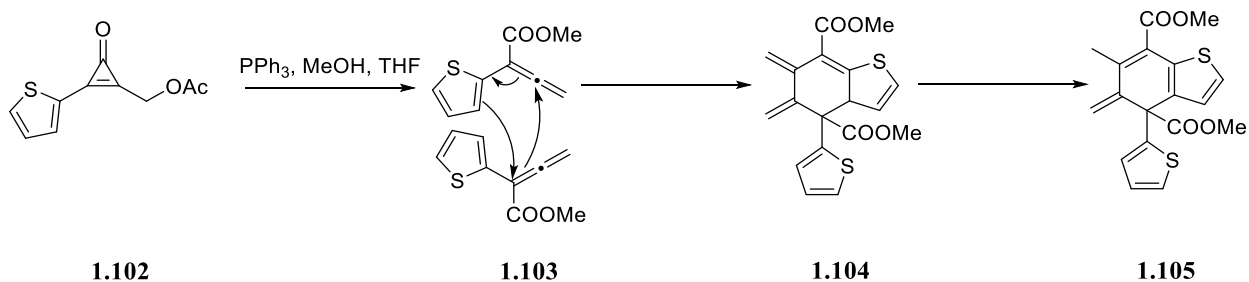
Due to the presence of the carbonyl group and electronegativity differences between carbon and oxygen, cyclopropenone can easily be attacked by various nucleophiles, such as alcohol, phosphine, or amines. Those reactions have been used in many fields such as total synthesis, cell labeling, and green chemistry.

Lambert et al. used cyclopropenone as a catalyst in nucleophilic attack reaction and successfully transformed alcohol into alkyl halide under mild conditions.<sup>28</sup> With oxalyl chloride as the activating agent, the reaction can proceed through the formation of cyclopropenium ions resulting in stereospecific products.

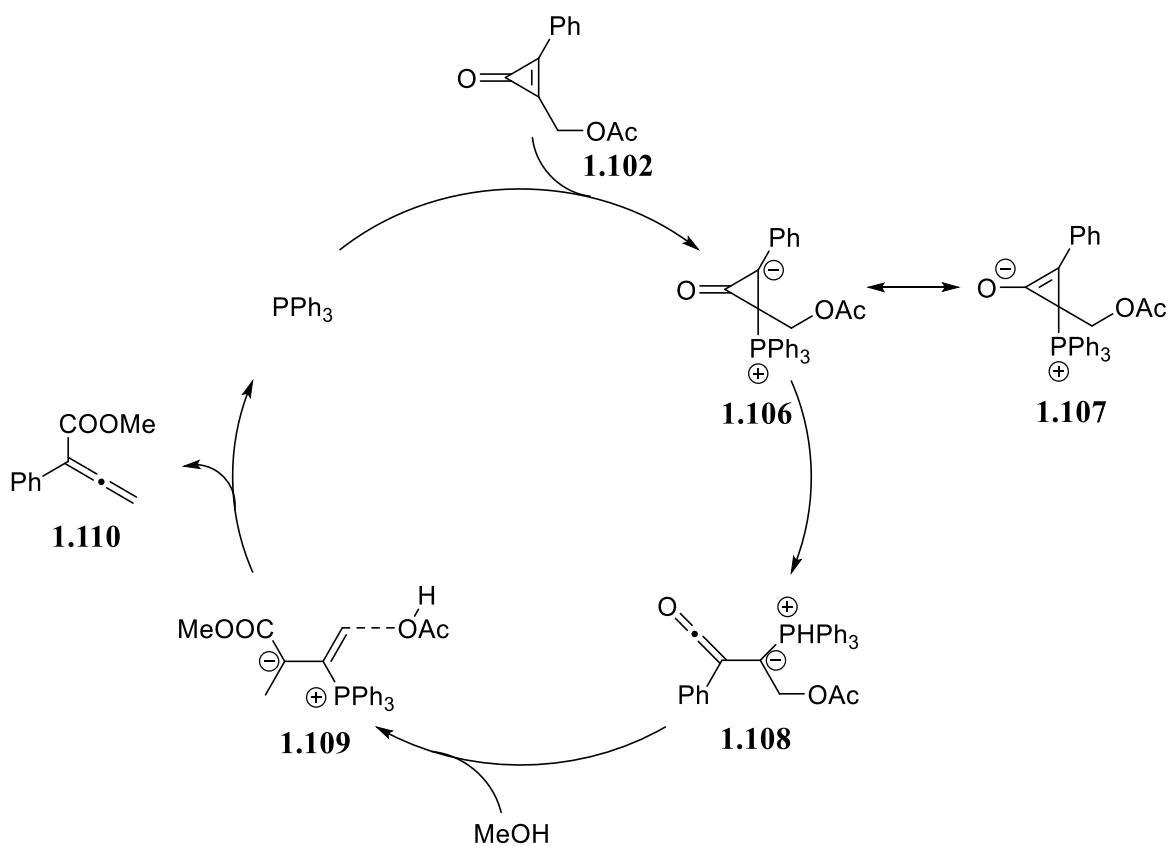


**Scheme 1.29** Reaction scheme and mechanism of cyclopropanone acting as nucleophilic attack catalyst

Shi et al. reported the formation of allene derivatives via reactions between  $\text{PPh}_3$ , methanol, and THF. The product **1.103** then reacts with itself to form six-membered rings of [4+2] cyclic reactions, followed by rearrangement driven by the aromaticity of thiophene. They also proposed a mechanism to explain the process. According to them,  $\text{PPh}_3$  is added to the double bond of cyclopropanone, resulting in zwitterionic intermediates **1.106**. Then, the cyclopropanone ring is opened with a positive charge transferred to the carbon adjacent to the Lewis base, forming ketene intermediates **1.108**. The ketene is attacked by methanol with the leaving of the OAc group, which provides the final allene product.

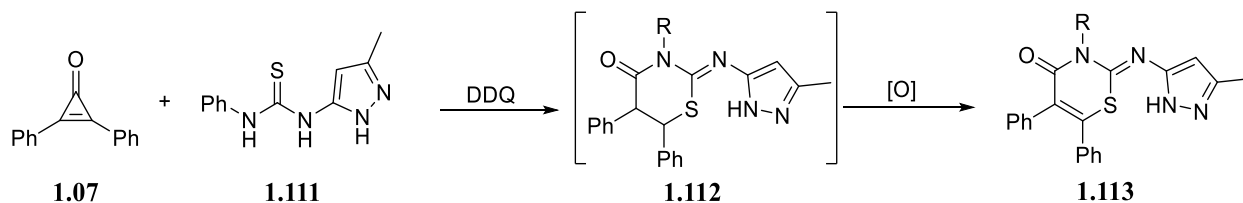


**Scheme 1.30** Reaction scheme of transformation of cyclopropanone derivatives under  $\text{PPh}_3$



**Scheme 1.31** Mechanism transformation of cyclopropenone derivatives under  $PPh_3$

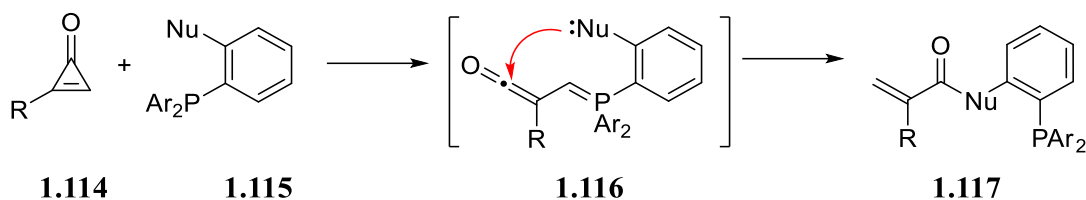
El-Sheref reported a new synthesis of 1,3-thiazine derivatives starting from cyclopropenone and thiourea derivatives.<sup>30</sup> The reaction started with a nucleophilic attack of the sulfur atom in thiourea to cyclopropenone and then resulted in formation of a new six-membered ring. DDQ served as an oxidation reagent in this fascinating reaction.



**Scheme 1.32** Reaction scheme between cyclopropenone and thiourea derivatives

Prescher et al. reported a novel bioorthogonal ligation between functionalized phosphine and cyclopropenone.<sup>50</sup> Triarylphosphine attacked the carbon-carbon double bond in

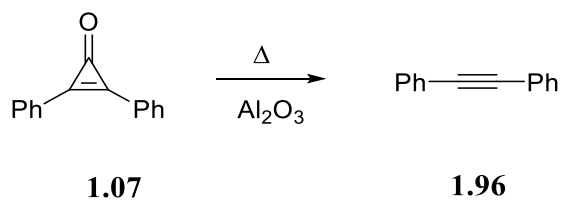
cyclopropenone derivatives to form the ketene intermedia **1.116** and the nucleophile attacked the center carbon in the ketene resulting in the formation of compound **1.117**. They also noticed that those components showed good stability in physiological buffer and fast reaction rate. All the reaction can finish within 2 hours with high concentration of phosphine components. Thus, those reaction should have great potential for utility in living systems.



*Scheme 1.33 Reaction scheme between cyclopropenone and phosphine derivatives*

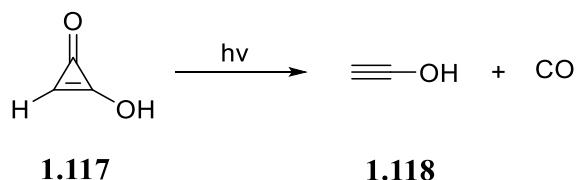
### 1.2.5 Decarbonylation

Decarbonylation of cyclopropenone derivatives can happen with transition metal catalyst, pyrolysis and under UV irradiation. In **1.2.2**, we discussed one example on using transition metal catalyst for dimerization of diphenylcyclopropenone and releasing of carbon monoxide. As early as 1981, Wardsworth et al. reported synthesis of diarylacetylene through pyrolysis of diphenylcyclopropenone.<sup>51</sup> In a typical pyrolysis of diphenylcyclopropenone, spiro side product **1.54** would always accompany the formation of acetylene.<sup>52,53</sup> In their study, they added aluminum oxide to the diphenylcyclopropenone o-dichlorobenzene solution and both symmetrical and unsymmetrical cyclopropenones produced clean diarylacetylene products.



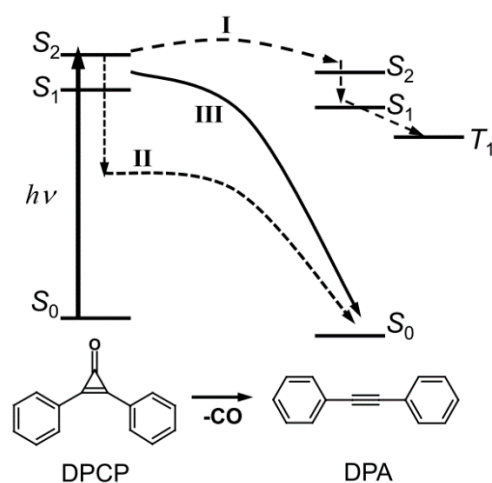
*Scheme 1.34 Pyrolysis decarbonylation of diphenylcyclopropenone*

Another unique property of cyclopropenone is that its derivatives are photolabile. This phenomenon was first reported by Breslow et al.,<sup>32</sup> but no structure characterization or spectra evidence was provided. Kresge and Popik reported the decarbonylation of hydroxy-cyclopropenone under UV irradiation, and products were confirmed by the comparison of authentic compounds.<sup>31</sup> Popik and his coworkers also explored photodecarbonylation of other cyclopropenone under UV irradiation and proposed the possible zwitterionic intermediates during the process.<sup>33-36</sup> They proposed photo-decarbonylation of different cyclopropenones under multi-photon irradiation.<sup>37-38</sup>



***Scheme 1. 35 Photo-decarbonylation of hydroxy-cyclopropenone***

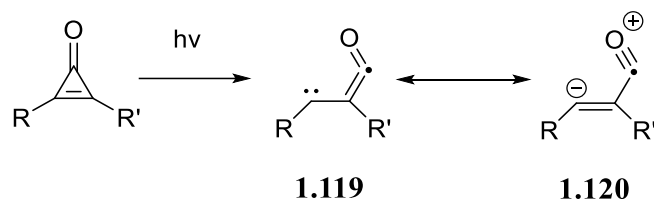
Various mechanisms have been proposed to explain the photo-decarbonylation of cyclopropenone. Currently, three different pathways have been widely acknowledged. Hirata and Mataga concluded that the photodissociation of diphenylcyclopropenone in the solution was considerably quicker than their experimental time resolution of several picoseconds, and the immediate result they saw was diphenylacetylene in the S<sub>2</sub> state<sup>40-41</sup>. Then, the S<sub>2</sub> excited state of diphenylacetylene decays to the S<sub>1</sub> excited state of diphenylacetylene under internal conversion. With that, the S<sub>1</sub> excited state of diphenylacetylene undergoes intersystem cross to the T<sub>1</sub> excited state of diphenylacetylene. Next, the excited state of diphenylacetylene relaxes to the ground state through internal conversion.



**Scheme 1. 36 Photo-decarbonylation of hydroxy-cyclopropenone<sup>54</sup>**

Nguyen and Geerlings proposed that photo-decarbonylation should happen in the ground state rather than the excited state through computational methods.<sup>42</sup> They claimed that ascribing to the high thermodynamic stability of carbon monoxide, most intermediates with properties of semi-carbene and semi-zwitterion lie higher in energy than the separated systems. This results in increasing energy to promote an electron to the lowest-lying excited states.

Our group also investigated the decarbonylation of several different cyclopropenone derivatives with femtosecond pump-probe transient absorption spectroscopy.<sup>43</sup> With the assistance of DFT calculation, we found that cyclopropenone decarbonylation takes place via a short-life intermediate in the excited state. We also determined that decarbonylation is a stepwise process happening in the excited-state energy surface.



**Scheme 1. 37 Formation of zwitterionic intermediates**

### **1.3 Application of Photo-Decarbonylation of Cyclopropenone**

For the photo-decarbonylation of cyclopropenone derivatives, two different products would form—one is an alkyne, and the other is CO. Both products would have their biological applications which make the photo-decarbonylation greatly intriguing. Thus, in this part of the thesis, we will discuss the two main applications of photo-decarbonylation of cyclopropenone: removing photolabile groups for photo-SPAAC reactions and releasing carbon monoxide.

#### **1.3.1 Photo-Decarbonylation to Remove Photolabile Groups**

In biorthogonal reactions, SPAAC (Strained-Promoted-Alkyne-Azide-Cycloaddition) reactions have become a rising star with their fast reaction rate, high specificity, low toxicity, accessible engineering, and chemical and biological inertness<sup>44</sup>. Those reactions, as indicated in the name, required one strained alkyne and one azide compound without any catalyst. However, alkyne could not survive several different harsh reaction conditions including an acidic environment or some transition metal catalyst. One way is to use cyclopropenone to protect alkynes use UV to remove carbonyl groups. With this method, we can achieve the photo-triggering of azide to alkyne easily.

Our group and Boons et al. first proposed the unmasking and deprotecting of cyclopropenone with UV light in 2009.<sup>34</sup> The masked cyclopropenone derivatives (photo-DIBO) didn't react with azide, but after irradiation, the triple bond would be exposed resulting in the linkage of alkyne and azide. Triazole products would form under ambient conditions and the biotin terminal could be successfully decorated to the surface of the cells. This would make it possible to label living cells expressing glycoproteins containing N-azidoacetyl-sialic acid.

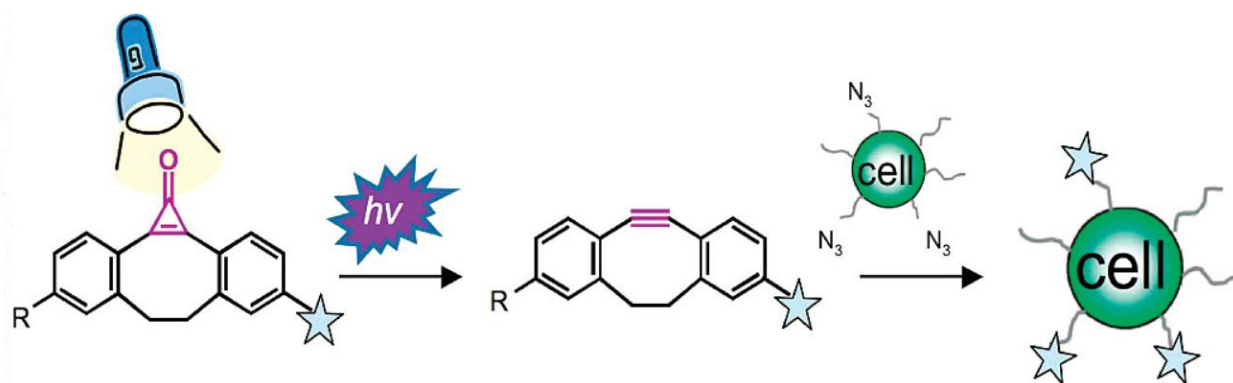


**Figure 1. 1 Selective labeling of cells via photo triggered SPAAC reactions**

The photo-decarbonylation of cyclopropenone can also be used in multi-functional click chemistry. Chemoselective sequential click ligation allows biological molecules, drug delivery vehicles, polymers, and surfaces to have various functions. Our group synthesized linkers with one part with ADIBO (Aza-Dibenzocyclooctyne) and the other part with photo-DIBO.<sup>45</sup> The compounds can successfully link with azide decorated biomacromolecules such as BSA-Azide, and once the first SPAAC is finished, the molecule can be irradiated by UV light to unmask the triple bond. The triple bond can then have a second SPAAC reaction with azide linked with silica beads. The molecule can release protein under the addition of diluted acid.

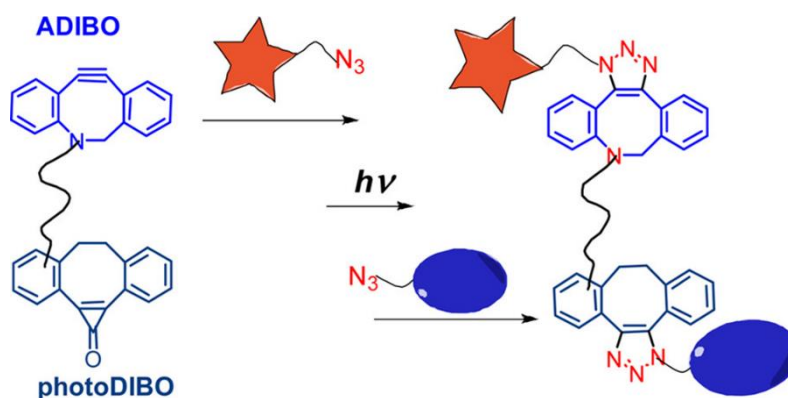


**Figure 1. 2 Preparation of ADIBO-photoDIBO cross-linker for sequential SPAAC reaction**

As one of the most popular imaging methods, molecular imaging is at leading edge of translational medicine.<sup>56</sup> Among various imaging methods, PET (Positron Emission Tomography) has increasing applications both preclinically and clinically. In all different isotopes, fluorine-18, with its high isotopic purity, simple and single decay process, moderate half-life, smallest positron range and highly chemical stability of C-F bond, is obliged to its widespread utility. One of the most distinguished application of <sup>18</sup>F-PET is clinical cancer diagnosis. To achieve that, macromolecules such as peptides and proteins are needed. Those molecules, however, cannot survive from harsh conditions of reactions that incorporate fluorine-18. Therefore, a prosthetic group is needed to conjugate fluorine-18 with demanded macromolecules. Due to the strain of lifetime of isotope, the conjugation reactions should have fast reaction rate. Those reactions are expected to be clean that few side products would be produced. SPAAC reactions perfectly fit the demand of PET probes.

In 2018, our group reported conjugation of ODIBO (oxadibenzocyclooctyne) to PET technology. In this work, ODIBO-TEG4-Tos (**1.122**) was synthesized and were linked with peptide PMSA. Compared with other SPAAC reagents, ODIBO has much faster reaction rate in aqueous solutions. The only preparation of ODIBO (oxadibenzocyclooctyne) now is by photo irradiation of photo-ODIBO derivatives. With that, researchers started with synthesis of **1.121** and irradiated the compound to afford compound **1.122**. Then they used SN2 reaction to link <sup>18</sup>F to ODIBO moiety. At last, they used SPAAC reaction between **1.123** and PMSA azide (**1.124**) to provide target PET probe **1.125**.

### **1.3.2 Photo-Decarbonylation to Release Carbon Monoxide**

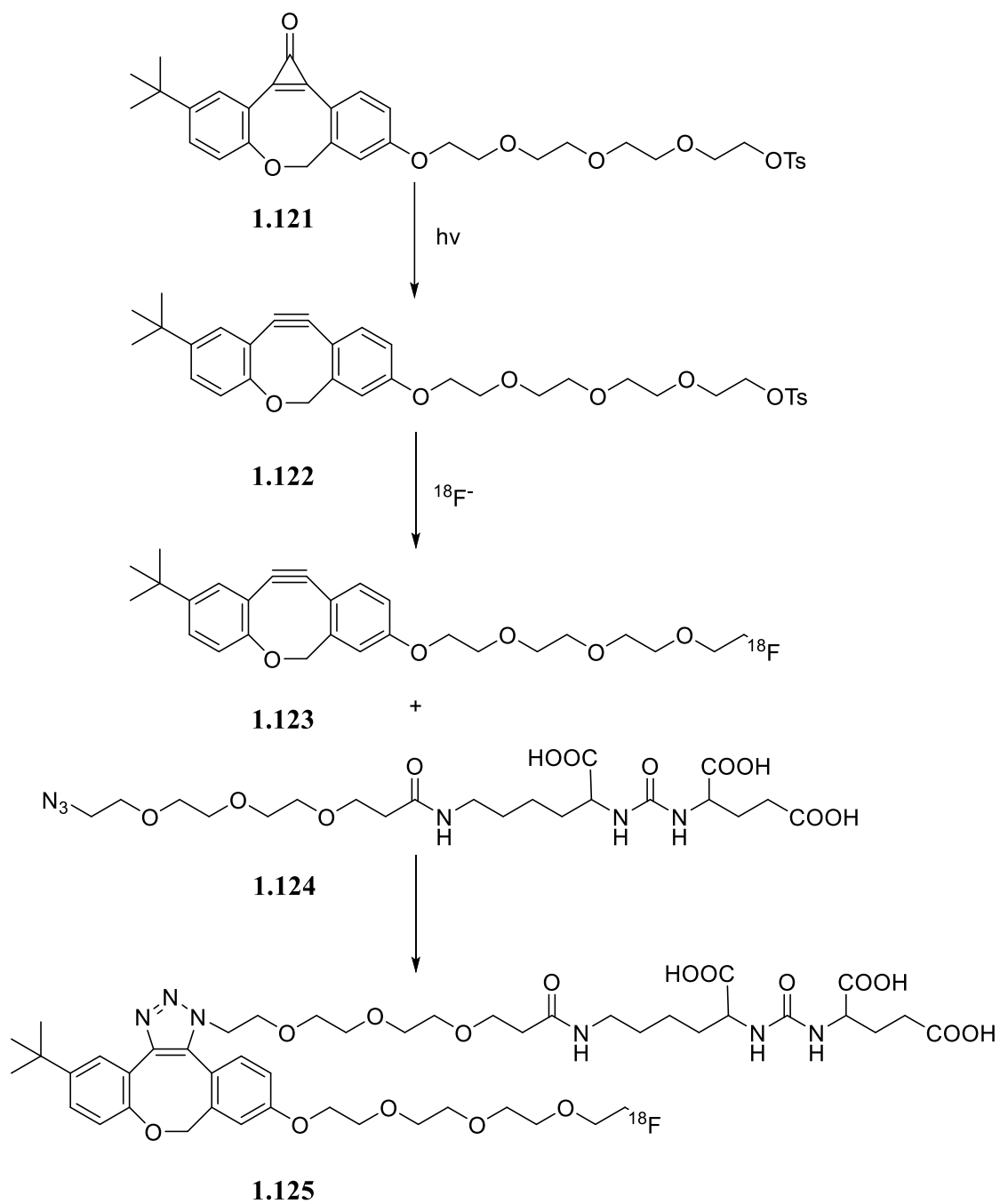
Given the significance of carbon monoxide in the control of ion channels and signaling pathways,<sup>55</sup> it has potential therapeutic uses, such as for the treatment of inflammation and

vascular malfunction.<sup>46</sup> UV is a common way for the controlled release of carbon monoxide. Cyclopropenone derivatives are excellent candidates for photo-CORM (carbon-monoxide releasing molecules) due to their clean release and easy control by UV light.

McConnell et al. reported a novel CO releasing molecule prepared with cyclopropenone derivatives and transition metal complexes.<sup>46</sup> The CORMs have good stability under a dark environment but undergo efficient decarbonylation and CO-release with the irradiation of UV light. Additionally, by altering the central metal ion, different monitoring methods would be applied from fluorometry to UV/Vis spectroscopy and NMR spectroscopy.

#### **1.4 Conclusion**

In this part, we started with the synthesis of different cyclopropenone derivatives. We also included the different reactions that cyclopropenone derivatives could undergo, including the cycloaddition of the carbon-carbon double bond, the cycloaddition of carbonyl groups, the [3+m] cycloaddition reaction, the nucleophilic attack, and photo-decarbonylation. In all the reactions, we picked up photo-decarbonylation as the center of our research with both applications and mechanistic studies. We see a bright future in the application of cyclopropenone photo-decarbonylation in other fields of research.



**Scheme 1. 38 Preparation of ODIBO-PMSA conjugates through SPAAC reaction**

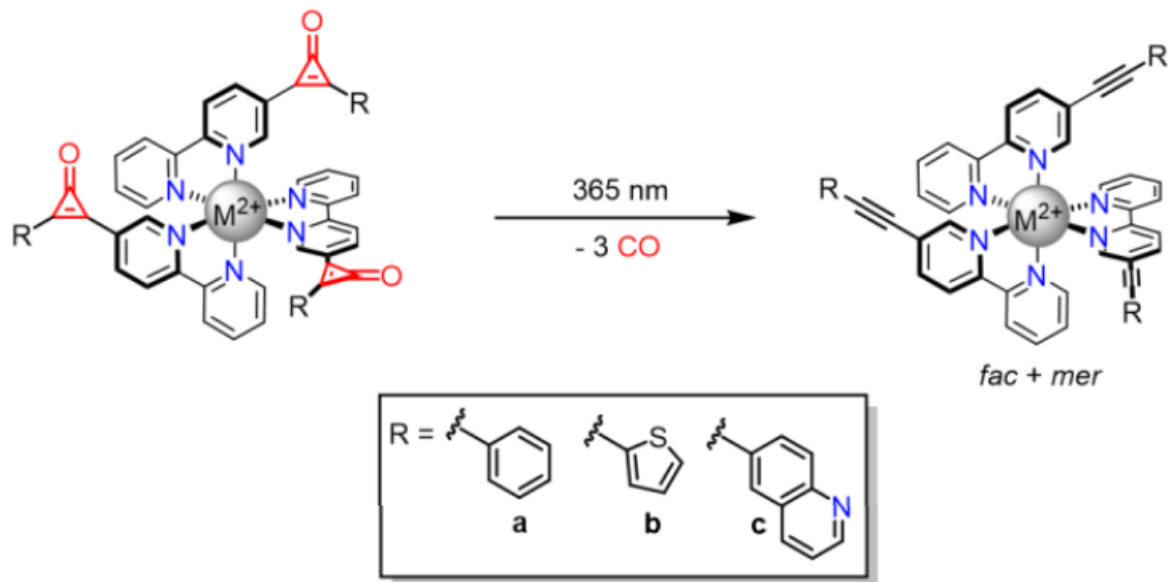


*Figure 1. 3 Photo-decarbonylation of CORM compounds*

## 1.5 Reference

1. Hopkins, H. P.; Bostwick, D.; Alexander, C. J., The thermochemistry of diphenylcyclopropanone. Strain vs. delocalization energy. *Journal of the American Chemical Society* 1976, 98 (6), 1355-1357.
2. Wang, H.-J.; Schleyer, P. v. R.; Wu, J. I.; Wang, Y.; Wang, H. J., A study of aromatic three membered rings. *International Journal of Quantum Chemistry* 2011, 111 (5), 1031-1038.
3. Breslow, R.; Haynie, R.; Mirra, J., The synthesis of diphenylcyclopropanone. *Journal of the American Chemical Society* 1959, 81 (1), 247-248.
4. Vol'pin, M. E.; Koreshkov, Y. D.; Kursanov, D. N., Diphenylcyclopropanone, a three-membered analog of tropone. *Bulletin of the Academy of Sciences of the USSR, Division of chemical science* 1959, 8 (3), 535-536.
5. Breslow, R.; Posner, J.; Krebs, A., Synthesis of Cyclopropanones by a Modified Favorskii Reaction. *Journal of the American Chemical Society* 1963, 85 (2), 234-234.
6. Quinkert, G.; Opitz, K.; Wiersdorff, W. W.; Weinlich, J., Lichtinduzierte decarbonylierung gelöster ketone bei raumtemperatur. *Tetrahedron Letters* 1963, 4 (27), 1863-1868.
7. Breslow, R.; Altman, L. J., Methylcyclopropanone and Related Compounds. *Journal of the American Chemical Society* 1966, 88 (3), 504-509.
8. Breslow, R.; Ryan, G.; Groves, J. T., Chlorocyclopropanes, chlorocyclopropenyl cations, and cyclopropanone. *Journal of the American Chemical Society* 1970, 92 (4), 988-993.

9. Tobey, S. W.; West, R., Diarylcyclopropenones via the Trichlorocyclopropenium Ion. *Journal of the American Chemical Society* 1964, 86 (19), 4215-4216.
10. West, R.; Zecher, D. C.; Tobey, S. W., 1-Aryl-2,3,3-trihalocyclopropenes and their reactions. *Journal of the American Chemical Society* 1970, 92 (1), 168-172.
11. Farnum, D. G.; Thurston, P. E.,  $\alpha$ -Elimination in 2-Phenyltetrachloropropene. Synthesis of Phenylhydroxycyclopropenone. *Journal of the American Chemical Society* 1964, 86 (19), 4206-4207.
12. West, R.; Chickos, J.; Osawa, E., Dichlorocyclopropenone. *Journal of the American Chemical Society* 1968, 90 (14), 3885-3886.
13. R. Breslow, J. Pecoraro, T. Sugimoto., Cyclopropenone. *Organic Synthesis*. 1977, vol. 57, pp. 41.
14. Baucom, K. B.; Butler, G. B. Synthesis and some reactions of 3,3-dimethoxycyclopropene. *The Journal of Organic Chemistry* 1972, 37 (11), 1730-1732.
15. Dehmlow, E. V. Diäthoxy-cyclopropenon (Dreiecksäurediäthylester). *Tetrahedron Letters* 1972, 13 (13), 1271-1274.
16. Eggerding, D.; West, R. Synthesis and properties of deltic acid (dihydroxycyclopropenone) and the deltate ion. *Journal of the American Chemical Society* 1976, 98 (12), 3641-3644.
17. Matsumoto, K.; Ikemi, Y.; Hashimoto, S.; Lee, H. S.; Okamoto, Y. High pressure [4 + 2] cycloaddition reactions of 3,4-dimethoxyfuran with dichloromaleic anhydride and with cyclopropane derivatives. *The Journal of Organic Chemistry* 1986, 51 (19), 3729-3730.
18. Jacobs, C. A.; Dailey, W. P. Why Is the Diels-Alder Adduct between Difluorocyclopropenone and 1,3-Diphenylisobenzofuran So Reactive? An ab Initio

- Molecular Orbital Study of the Ring-Opening of cis-2,3-Difluorocyclopropanone. *The Journal of Organic Chemistry* 1995, 60 (24), 7747-7750.
19. Körner, O.; Gleiter, R.; Rominger, F. Copper(I)-Promoted Synthesis of 4-Oxaspiro[2.4]hepta-1,6-dien-5-ones from Cyclopropanones. *Synthesis* 2009, (19), 3259-3262.
  20. Rivero, A. R.; Fernández, I.; Ramírez de Arellano, C.; Sierra, M. A. Synthesis of Oxaspiranic Compounds through [3 + 2] Annulation of Cyclopropanones and Donor–Acceptor Cyclopropanes. *The Journal of Organic Chemistry* 2015, 80 (2), 1207-1213.
  21. Sizhan Liu, M. C., Bowen Wang, Chunmei Hu, Yingying Zheng, Jing Li, Xuetao Xu, Zhen Wang, Shaohua Wang. Triethyl Amine-Promoted Cyclization Reaction between Cyclopropanone and  $\alpha$ -Halogenated Hydroxamate for the Synthesis of Polysubstituted 6H-1,3-Oxazin-6-one. *Chinese Journal of Organic Chemistry* 2021, 41 (4), 1622-1630.
  22. Matsuda, T.; Sakurai, Y. Palladium-Catalyzed Ring-Opening Alkynylation of Cyclopropanones. *European Journal of Organic Chemistry* 2013, (20), 4219-4222.
  23. Yu, S.; Li, X. Mild Synthesis of Chalcones via Rhodium(III)-Catalyzed C–C Coupling of Arenes and Cyclopropanones. *Organic Letters* 2014, 16 (4), 1220-1223.
  24. Miao, W.-H.; Gao, W.-X.; Huang, X.-B.; Liu, M.-C.; Zhou, Y.-B.; Wu, H.-Y. Cascade Ring-Opening Dual Halogenation of Cyclopropanones with Saturated Oxygen Heterocycles. *Organic Letters* 2021, 23 (24), 9425-9430.
  25. Kondo, T.; Taniguchi, R.; Kimura, Y. Ruthenium- and Rhodium-Catalyzed Ring-Opening Coupling Reactions of Cyclopropanones with Alkenes or Alkynes. *Synlett* 2018, 29 (06), 717-722.

26. Bai, D.; Yu, Y.; Guo, H.; Chang, J.; Li, X. Nickel(0)-Catalyzed Enantioselective [3+2] Annulation of Cyclopropanones and  $\alpha,\beta$ -Unsaturated Ketones/Imines. *Angewandte Chemie International Edition* 2020, 59 (7), 2740-2744.
27. Nanda, T.; Ravikumar, P. C. A Palladium-Catalyzed Cascade C–C Activation of Cyclopropanone and Carbonylative Amination: Easy Access to Highly Functionalized Maleimide Derivatives. *Organic Letters* 2020, 22 (4), 1368-1374.
28. Vanos, C. M.; Lambert, T. H. Development of a Catalytic Platform for Nucleophilic Substitution: Cyclopropanone-Catalyzed Chlorodehydration of Alcohols. *Angewandte Chemie International Edition* 2011, 50 (51), 12222-12226.
29. Wei, Y.; Zhao, W.-T.; Yang, Y.-L.; Zhang, Z.; Shi, M. Allenic Esters from Cyclopropanones by Lewis Base Catalysis: Substrate Scope, the Asymmetric Variant from the Dynamic Kinetic Asymmetric Transformation, and Mechanistic Studies. *ChemCatChem* 2015, 7 (20), 3340-3349.
30. El-Sheref, E. M. One-pot synthesis of 3-substituted-2-[(3-methyl-1H-pyrazol-5-yl)imino]-5,6-diphenyl-1,3-thiazin-4-ones. *Journal of Sulfur Chemistry* 2017, 38 (6), 625-634.
31. Chiang, Y.; Kresge, A. J.; Popik, V. V. Flash Photolytic Generation and Study of Ynolate Ions and the Corresponding Ketenes in Aqueous Solution. *Journal of the American Chemical Society* 1995, 117 (36), 9165-9171.
32. Breslow, R.; Oda, M.; Pecoraro, J. The chemistry of cyclopropanone. Reactions at the carbonyl group, and 1,2 cleavages. *Tetrahedron Letters* 1972, 13 (43), 4415-4417.

33. Poloukhine, A.; Popik, V. V. Highly Efficient Photochemical Generation of a Triple Bond: Synthesis, Properties, and Photodecarbonylation of Cyclopropenones. *The Journal of Organic Chemistry* 2003, 68 (20), 7833-7840.
34. Poloukhine, A. A.; Mbua, N. E.; Wolfert, M. A.; Boons, G.-J.; Popik, V. V. Selective Labeling of Living Cells by a Photo-Triggered Click Reaction. *Journal of the American Chemical Society* 2009, 131 (43), 15769-15776.
35. McNitt, C. D.; Popik, V. V. Photochemical generation of oxa-dibenzocyclooctyne (ODIBO) for metal-free click ligations. *Organic & Biomolecular Chemistry* 2012, 10 (41), 8200-8202.
36. Sutton, D. A.; Yu, S.-H.; Steet, R.; Popik, V. V. Cyclopropenone-caged Sondheimer diyne (dibenzo[a,e]cyclooctadiyne): a photoactivatable linchpin for efficient SPAAC crosslinking. *Chemical Communications* 2016, 52 (3), 553-556.
37. Urdabayev, N. K.; Poloukhine, A.; Popik, V. V. Two-photon induced photodecarbonylation reaction of cyclopropenones. *Chemical Communications* 2006, (4), 454-456.
38. McNitt, C. D.; Cheng, H.; Ullrich, S.; Popik, V. V.; Bjerknes, M. Multiphoton Activation of Photo-Strain-Promoted Azide Alkyne Cycloaddition “Click” Reagents Enables in Situ Labeling with Submicrometer Resolution. *Journal of the American Chemical Society* 2017, 139 (40), 14029-14032.
39. Vennekate, H. Photodecarbonylation of Diphenylcyclopropenone – a Direct Pathway to Electronically Excited Diphenylacetylene? *Zeitschrift für Physikalische Chemie* 2011, 225 (9-10), 1089-1104.

40. Hirata, Y.; Mataga, N. Picosecond dye laser photolysis study of diphenylcyclopropanone in solution: formation of the electronically excited states of diphenylacetylene. *Chemical Physics Letters* 1992, 193 (4), 287-291.
41. Takeuchi, S.; Tahara, T. Femtosecond absorption study of photodissociation of diphenylcyclopropanone in solution: Reaction dynamics and coherent nuclear motion. *The Journal of Chemical Physics* 2004, 120 (10), 4768-4776.
42. Nguyen, L. T.; De Proft, F.; Nguyen, M. T.; Geerlings, P. Theoretical study of cyclopropanones and cyclopropanethiones: decomposition via intermediates. *Journal of the Chemical Society, Perkin Transactions 2* 2001, (6), 898-905.
43. Poloukhine, A.; Popik, V. V. Mechanism of the Cyclopropanone Decarbonylation Reaction. A Density Functional Theory and Transient Spectroscopy Study. *The Journal of Physical Chemistry A* 2006, 110 (5), 1749-1757.
44. Sletten, E. M.; Bertozzi, C. R. From Mechanism to Mouse: A Tale of Two Bioorthogonal Reactions. *Accounts of Chemical Research* 2011, 44 (9), 666-676.
45. Arumugam, S.; Popik, V. V. Sequential “Click” – “Photo-Click” Cross-Linker for Catalyst-Free Ligation of Azide-Tagged Substrates. *The Journal of Organic Chemistry* 2014, 79 (6), 2702-2708.
46. Lehr, M.; Neumann, T.; Näther, C.; McConnell, A. J. M-CPOnes: transition metal complexes with cyclopropanone-based ligands for light-triggered carbon monoxide release. *Dalton Transactions* 2022, 51 (17), 6936-6943.

47. Mayer, S. V.; Murnauer, A.; von Wrisberg, M.-K.; Jokisch, M.-L.; Lang, K. Photo-induced and Rapid Labeling of Tetrazine-Bearing Proteins via Cyclopropenone-Caged Bicyclononynes. *Angewandte Chemie International Edition* 2019, 58 (44), 15876-15882.
48. Row, R. D.; Prescher, J. A. Constructing New Bioorthogonal Reagents and Reactions. *Accounts of Chemical Research* 2018, 51 (5), 1073-1081.
49. Heiss, T. K.; Dorn, R. S.; Ferreira, A. J.; Love, A. C.; Prescher, J. A. Fluorogenic Cyclopropenones for Multicomponent, Real-Time Imaging. *Journal of the American Chemical Society* 2022, 144 (17), 7871-7880.
50. Shih, H.-W.; Prescher, J. A. A Bioorthogonal Ligation of Cyclopropenones Mediated by Triarylphosphines. *Journal of the American Chemical Society* 2015, 137 (32), 10036-10039.
51. Wadsworth, D. H.; Donatelli, B. A. Preparation of Diarylacetylenes via Cyclopropenones. *Synthesis* 1981, 1981 (04), 285-286.
52. Breslow, R.; Eicher, T.; Krebs, A.; Peterson, R. A.; Posner, J. Diphenylcyclopropenone<sup>1,2</sup>. *Journal of the American Chemical Society* 1965, (6), 87.
53. Krebs, A. W. Cyclopropenylium Compounds and Cyclopropenones. *Angewandte Chemie International Edition in English* 1965, 4 (1), 10-22.
54. Vennekate, H. Photodecarbonylation of Diphenylcyclopropenone – a Direct Pathway to Electronically Excited Diphenylacetylene? *Zeitschrift für Physikalische Chemie* 2011, 225 (9-10), 1089-1104.

55. Kapetanaki, S. M.; Burton, M. J.; Basran, J.; Uragami, C.; Moody, P. C. E.; Mitcheson, J. S.; Schmid, R.; Davies, N. W.; Dorlet, P.; Vos, M. H.; et al. A mechanism for CO regulation of ion channels. *Nature Communications* 2018, 9 (1), 907.
56. Liu, Z.; Radtke, M. A.; Wong, M. Q.; Lin, K.-S.; Yapp, D. T.; Perrin, D. M., Dual Mode Fluorescent <sup>18</sup>F-PET Tracers: Efficient Modular Synthesis of Rhodamine-[cRGD]<sub>2</sub>-[<sup>18</sup>F]-Organotrifluoroborate, Rapid, and High Yielding One-Step <sup>18</sup>F-Labeling at High Specific Activity and Correlated in Vivo PET Imaging and ex Vivo Fluorescence. *Bioconjugate Chemistry* 2014, 25, 1951-1962.
57. Wang, M.; McNitt, C. D.; Wang, H.; Ma, X.; Scarry, S. M.; Wu, Z.; Popik, V. V.; Li, Z. The efficiency of <sup>18</sup>F labelling of a prostate specific membrane antigen ligand via strain-promoted azide-alkyne reaction: reaction speed versus hydrophilicity. *Chemical Communications* 2018, 54 (56), 7810-7813.

## CHAPTER 2

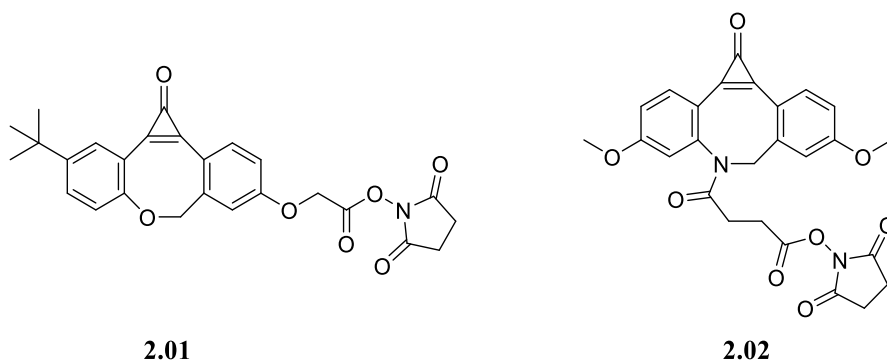
### CYCLOPROPENONES IN THE SYNTHESIS OF MULTIPLE FUNCTIONALIZED TERMINAL SPAAC REAGENTS

#### 2.1 Introduction

Due to its mild condition, selectivity, and suitable reaction rate, SPAAC (Strained-Promoted-Alkyne-Azide-Cycloaddition) has gained popularity in the research field of labeling<sup>1,2</sup> and generating novel pharmaceuticals<sup>3,4</sup>. The current chapter discusses specific findings regarding cyclopropenone as photolabile groups in SPAAC reactions, which are categorized by different functional groups and methods of linkages.

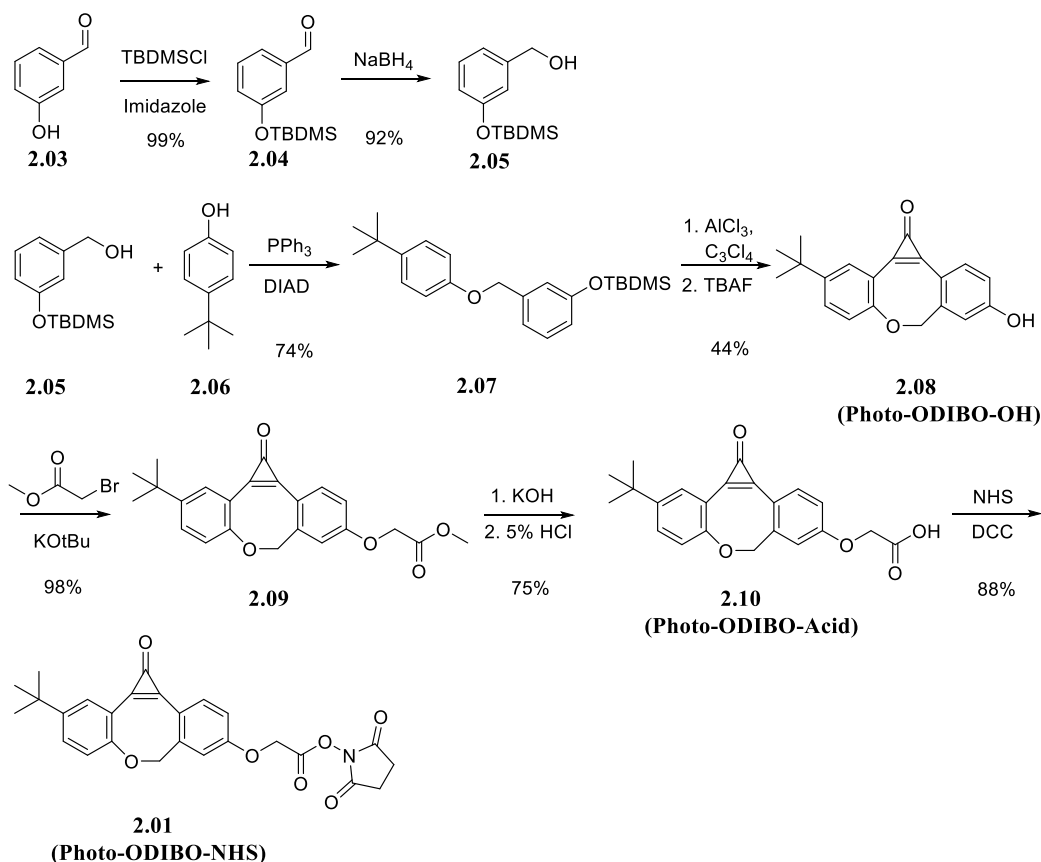
#### 2.2 Synthesis of NHS-ester terminal SPAAC reagents

Coupling between activated acids, such as NHS ester, and amines has characterized a widely used method for linkages of small molecules with bio-macromolecules. With the introduction of SPAAC chemistry, two bio-macromolecules could be easily crosslinked via tandem reactions of NHS coupling and cycloaddition. Given these techniques, we successfully designed the compounds, **2.01** and **2.02**, as in the figure below.



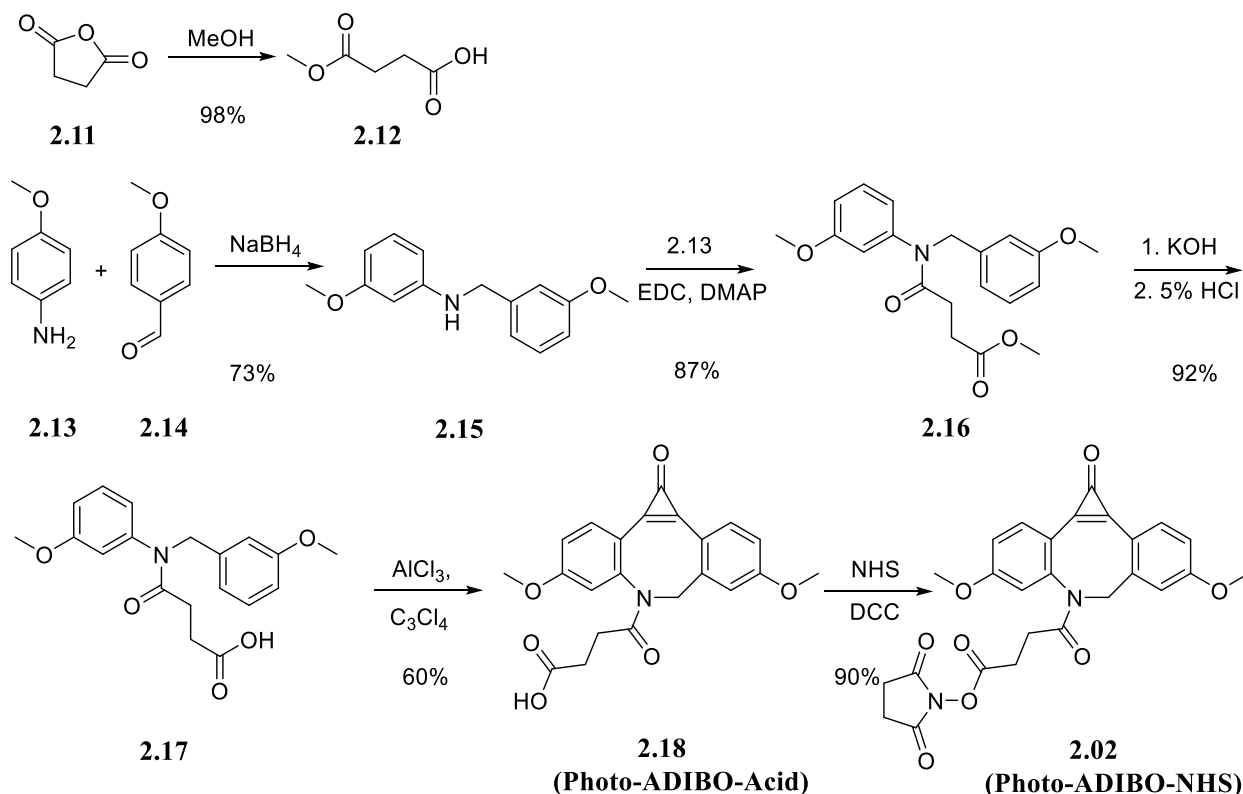
**Scheme 2. 1 Structure of Photo-ODIBO-NHS (2.01) and Photo-ADIBO-NHS (2.02)**

To synthesize compound **2.01**, we started with 3-hydroxybenzaldehyde (**2.03** in Figure **2.02**) and protected it using TBDMSCl. This was followed by a reduction in the compound from **2.04** to **2.05** using NaBH<sub>4</sub> before applying the Mitsunobu reaction between compound **2.05** and **2.06** to obtain compound **2.07**. Then we used Friedel-Crafts reactions between **2.07**, AlCl<sub>3</sub>, and tetrachlorocyclopropene, to obtain TBDMS protected photo-ODIBO. As the separation of the compound was considered inconvenient and unnecessary, TBAF was used to deprotect it, thereby affording **2.08** as photo-ODIBO-OH. We then employed the SN<sub>2</sub> reaction between **2.08** and methyl 2-bromoacetate to obtain the ester compound, **2.09**, which was then deprotected to obtain compound **2.10** as photo-ODIBO-Acid. This compound was then modified to afford compound **2.11** as photo-ODIBO-NHS.



### Scheme 2. 2 Synthetic Route of Photo-ODIBO-NHS

To obtain photo-ADIBO-NHS, we started with the synthesis of linker **2.13** by refluxing succinic anhydride **2.11** in methanol. Aniline derivative **2.14** and aldehyde **2.15** were mixed and reduced by sodium borohydride to afford compound **2.16**. Then, we deployed EDC coupling between **2.13** and **2.16** to obtain compound **2.17** followed by deprotection to provide compound **2.18**. After that, we applied Friedel-Crafts reaction to obtain compound **2.19** and use DCC and NHS to get compound **2.20** as photo-ADIBO-NHS.



### Scheme 2. 3 Synthetic route of photo-ADIBO-NHS

Since NHS ester derivatives, **2.01** and **2.02**, were found to be unstable in the aqueous environment, the reaction rates of ODIBO-Acid and ADIBO-Acid with azide were investigated. Both compounds were irradiated under 350 nm light in situ, following which kinetic studies were

immediately conducted. As expected, the rate of ODIBO-Acid with TEG-N<sub>3</sub> (**2.21**) is  $3.62 \pm 0.01 \text{ M}^{-1}\text{s}^{-1}$  while that of ADIBO-Acid with TEG-N<sub>3</sub> is  $0.96 \pm 0.01 \text{ M}^{-1}\text{s}^{-1}$ .

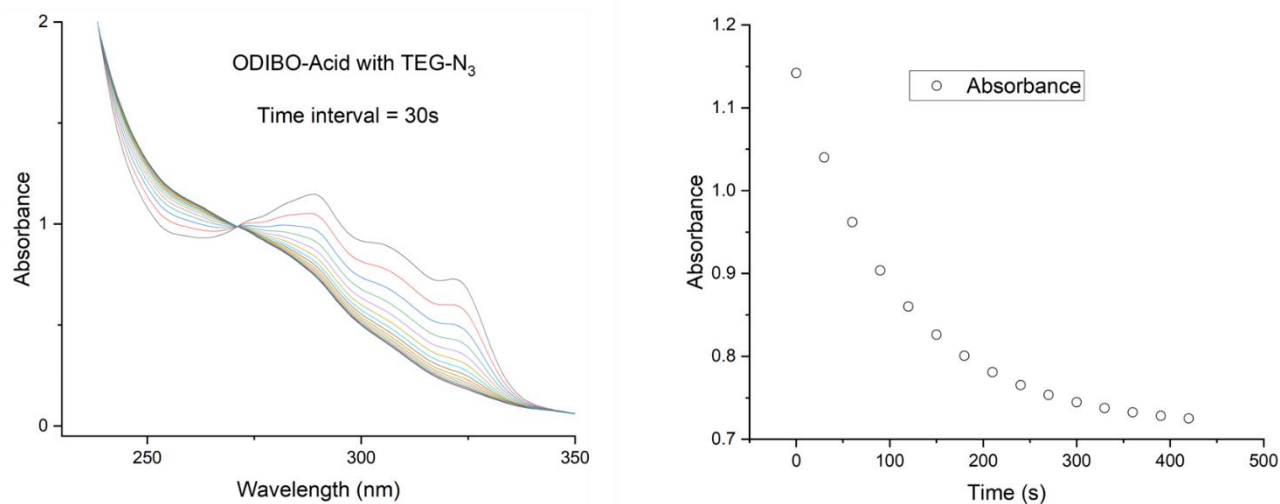


**Figure 2.03 Reaction Rate of ODIBO-Acid with TEG-N<sub>3</sub>**

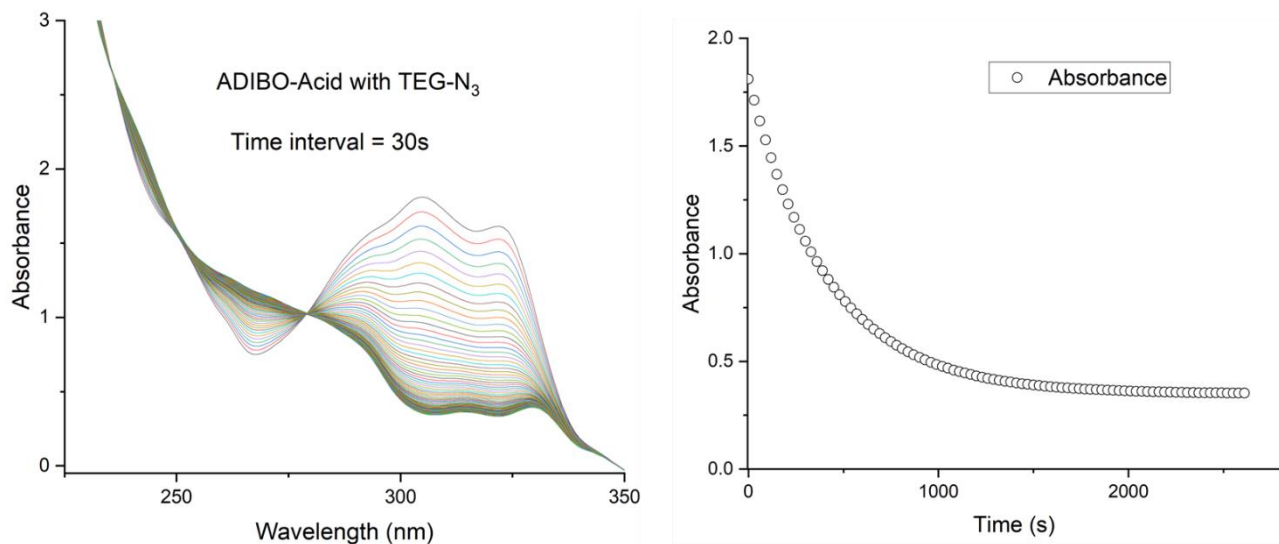


**Figure 2. 1 Reaction rate of ADIBO-Acid with TEG-N<sub>3</sub>**

### 2.3 Synthesis of SPAAC Regents with Biotin

Many protein and nucleic acid detection and purification techniques have employed the interaction between biotin and avidin or streptavidin.<sup>5-6</sup> The very strong binding between avidin



SN2 reaction to alter the tosyl group to the azido group, subsequently modifying the other part to the OTs group. After this, the SN2 reaction was used to link azido groups to the terminal of photo-ODIBO while the CuAAC reaction was used to link propargyl-decorated biotin to the terminal of photo-ODIBO.

#### **2.4 Synthesis of SPAAC Reagents with Propargyl Terminal**

The copper-catalyzed azide-alkyne cycloaddition reaction was significantly useful and promising in terms of its application in various biorthogonal fields. Aside from the use of peptide bonds in linking small cyclopropanone molecules with bio-macromolecules, we were invested in the use of CuAAC reactions in the same. Thus, we proposed the synthesis of compounds **2.27** and **2.36** in addition to their synthetic routes.

The synthesis of **2.27** began with the generation of the linker **2.28**, followed by EDC coupling with **2.13** to obtain the compound, **2.30**. This was followed by the use of Friedel-Crafts reaction to obtain compound **2.27** as photo-ADIBO-Propargyl. To increase the hydrophilicity of Photo-ADIBO, we introduced two hydroxy groups to the side of the structure. We initially planned to synthesize compound **2.33** from the deprotection of **2.27**; however, as the reaction failed, we turned to EDC coupling between propargyl amine and acid compound **2.32**. Thus, the hydrophilic photo-ADIBO with propargyl terminal has been prepared.

For photo-ODIBO derivatives, the synthesis of **2.36** starts with the synthesis of linker **2.35**, with the simple reaction between the propargyl alcohol and tosyl chloride. After this, the SN2 reaction is used between **2.35** and **2.08** to obtain compound **2.36**.

#### **2.5 Water Solubility of Photo-ODIBO-OH and Photo-ADIBO-Bis-OH**

To gain a general understanding of how target compounds can be dissolved in water, we tested the water solubility of photo-ODIBO-OH (**2.08**) and photo-ADIBO-Bis-OH (**2.32**). Both

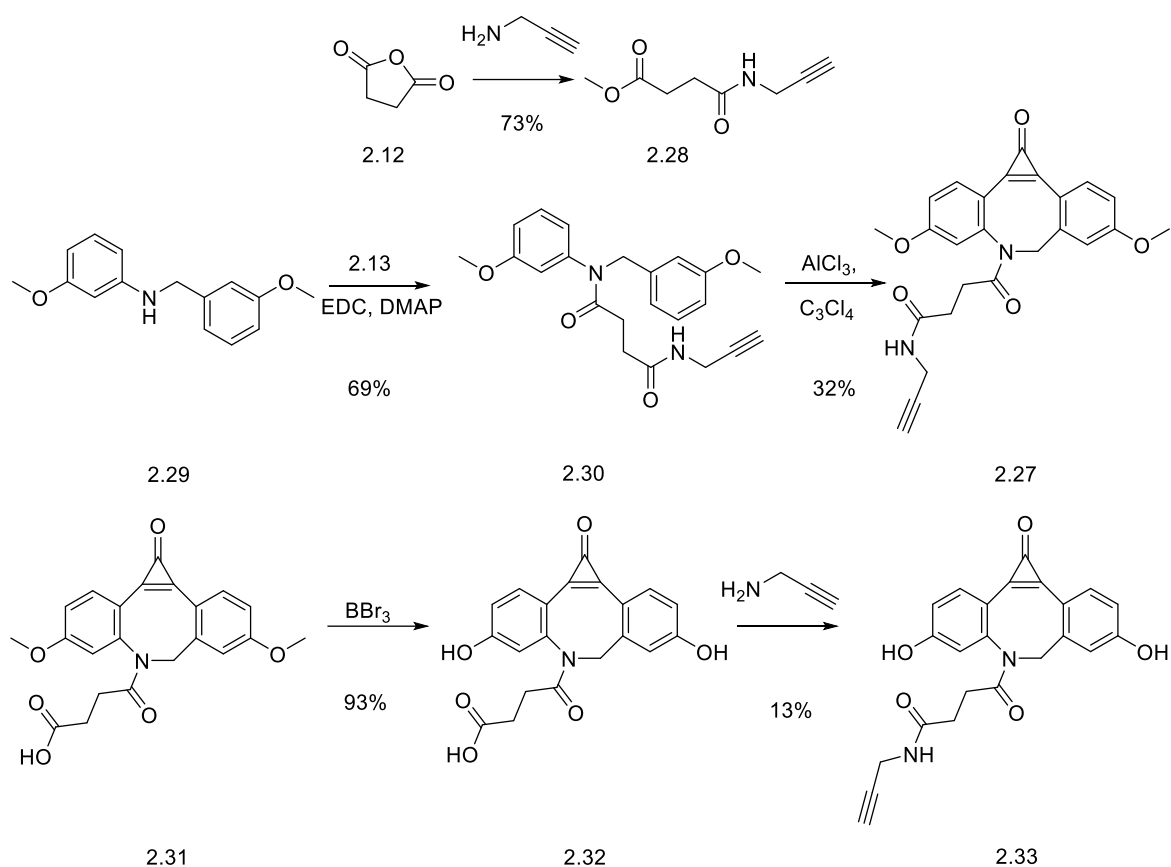
compounds were first dispersed in phosphate buffer, sonicated, and filtered through a syringe filter. The solution was collected, and the absorbance of both compounds was measured to determine the concentration change.

From UV spectra of photo-ODIBO-OH (**2.08**), the absorbance change at 345 nm can be calculated as  $\text{Abs}(\lambda=345 \text{ nm}) = 0.03699$ . The extinction coefficient factor of photo-ODIBO-OH at 345 nm is  $17594 \text{ M}^{-1}\text{cm}^{-1}$ .<sup>9</sup> Thus, the concentration of photo-ODIBO-OH in the phosphate buffer (pH = 7.4) is calculated to be less than 10  $\mu\text{M}$ . For compound **2.32**, since we observed that the concentration of pure saturated solution would be too high for UV measurement, the solution was diluted 9 times to ensure adequate dilution in line with the Beer-Lambert Law. From the UV spectra, the absorbance change at 345 nm can be calculated as  $\text{Abs}(\lambda=345 \text{ nm}) = 1.36872$ . Thus, the concentration of solution diluted 9 times can be calculated as 86.7  $\mu\text{M}$ , and hence, that of the saturated solution can be calculated as 780  $\mu\text{M}$ .

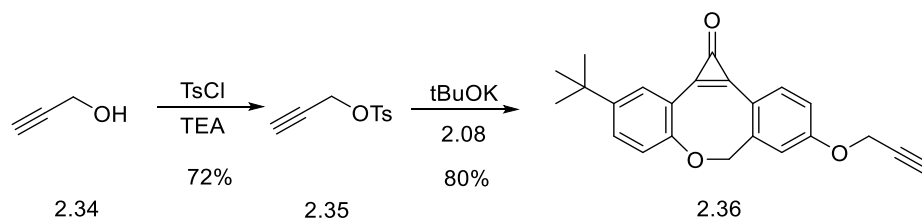
The solubility data indicate that compound **2.32** showed excellent water solubility, while for compound **2.08**, no notable water solubility was observed. The ionization of **2.32** may be attributed to the greater water solubility of **2.32**, relative to **2.08**. Further, the hydrophobicity of tert-butyl groups in **2.08** may also have resulted in the low water solubility of **2.08**.

## **2.6 Visible Light Irradiation for Transforming Photo-XDIBO Derivatives into XDIBO SPAAC Reagents**

While UV can very easily remove carbonyl groups in cyclopropanone derivatives, it cannot penetrate tissue in living organisms.<sup>8</sup> This problem may be resolved by using visible light to irradiate photo-XDIBO (X = N and O) compounds in situ. To verify the ability of visible light to induce photodecarbonylation, photo-XDIBO (X = N and O) derivatives were used for a visible light irradiation test.



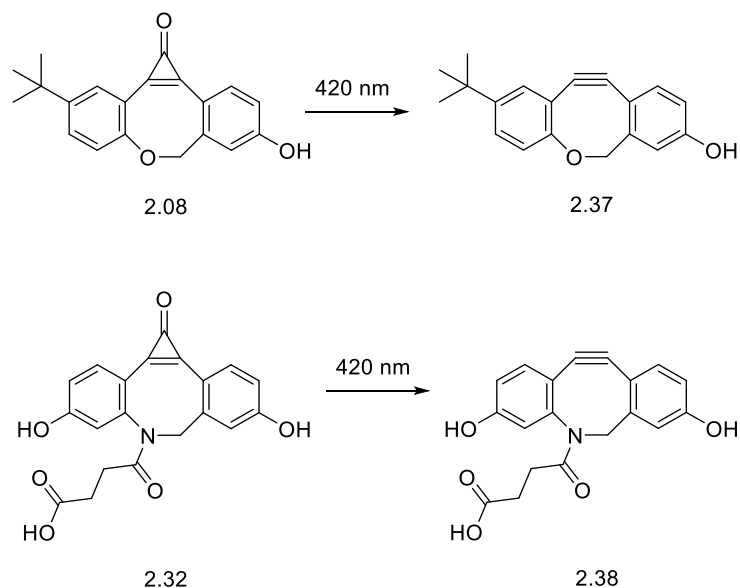
**Scheme 2. 5 Synthetic route of photo-ADIBO-propargyl**



**Scheme 2. 6 Synthetic route of photo-ODIBO-propargyl**

Under 420 nm light irradiation, derivatives of both photo-ODIBO (compound 2.08) and photo-ADIBO (compound 2.32) can smoothly transform to ODIBO and ADIBO derivatives, respectively. Under 350 nm irradiation, compound **2.32** was unable to transform into **2.38** or the mixed products cannot be separated. We assumed that this occurred due to the strong absorption of ADIBO derivatives at 350 nm and ADIBO derivatives are not stable at 350 nm irradiation.

However, compound **2.38** is characterized by low absorption at 420 nm. Thus, the irradiation with 420 nm light would not result in the photo reaction of **2.38**, which explains the clean products formation under 420 nm irradiation of compounds **2.08** and **2.35**.



***Scheme 2. 7 Irradiation of compound 2.08 and 2.32 with 420 nm light***

Lastly, to evaluate the efficiency of photodecarbonylation under 420 nm light, the quantum yield of the photoreactions was measured. During the three min time span, the average concentration change of photo-ODIBO-OH in methanol solution was found to be  $4.01 \pm 0.05$   $\mu\text{M}$ . For the actinometer, we chose 4-nitroveratrole (chemical quantum yield as 0.116). Its concentration change was  $27.4 \pm 2$   $\mu\text{M}$ . The quantum yield can then be calculated as  $1.7 \pm 0.2$  %.

**2.07 Conclusion**

In conclusion, we have synthesized a series of SPAAC reagents based on the photo-irradiation of cyclopropanone derivatives with NHS ester, biotin, and propargyl terminal. To confirm whether these compounds could be used in the biological environment, the water solubility of photo-ODIBO and ADIBO derivatives was measured. Photo-ADIBO derivatives

demonstrated significant water solubility while photo-ODIBO can only be moderately soluble in water. Lastly, visible light was used to irradiate photo-ODIBO and photo-ADIBO derivatives, resulting in the formation of both alkyne products. We hope that these compounds can be successfully used in in-vivo and in-situ labeling.

## **2.08 Experimental Section**

### **Materials and Method**

All organic solvents were dried and freshly distilled before use. While THF, DMF, and DCM were dried over the MBraun SPS solvent purification system, other reagents were purchased through Aldrich, VMR, Fisher, or Oakwood Chemical. Chromatography was performed with 40-63  $\mu\text{m}$  silica gel powder. All NMR spectra were recorded using a 400 MHz instrument. The absorption spectra were recorded on CARY 5000 Bio UV-Visible Spectrometer, while the quantum yield was determined using 4-nitroveratrole as an actinometer. Photo-irradiation was carried out in the Rayonet photo reactor with 1–16 8 W 350 nm or 420 nm fluorescent lamps.

### **Kinetics**

The rate of the reaction was measured using CARY 5000 Bio UV-Visible Spectrometer. Both ODIBO-Acid and ADIBO-Acid were prepared freshly before use. The temperature was set to 25 °C and controlled to 0.1 °C accuracies. The reaction between ODIBO-Acid and excess azide was monitored following the absorption decay at 290 nm and ADIBO-Acid while excess azide was monitored at 305nm. The experimental data were fitted with the first exponential decay while the  $\tau$  value from the fitting was used to calculate the rate constant between strained alkynes and azide.

## Synthesis of Compounds

Synthesis of Compounds 2.03 – 2.08, was in line with the previous report.<sup>9, 10</sup>

### **Methyl 2-((3-(tert-butyl)-1-oxo-1,7-dihydrodibenzo[b,f]cyclopropa[d]oxocin-9-yl)oxy)acetate (2.09).**

3-(tert-butyl)-9-hydroxydibenzo[b,f]cyclopropa[d]oxocin-1(7H)-one(250mg, 0.82mmol) was dissolved in 50 mL THF. Potassium carbonate (0.340 g, 2.46 mmol) was added to the solution portion-wise. Methyl bromoacetate (0.249 g, 1.63 mmol) was added to the solution before the reaction mixture was refluxed for 5 hours. The mixture was quenched using saturated ammonium chloride and diluted with 100 mL ethyl acetate. Subsequently, the organic layer was concentrated in vacuo and the mixture was purified through column chromatography (DCM : methanol = 30:1) to provide Methyl 2-((3-(tert-butyl)-1-oxo-1,7-dihydrodibenzo[b,f]cyclopropa[d]oxocin-9-yl)oxy)acetate as a pale yellow and gradually solidifying oil (287 mg, 93 %). <sup>1</sup>H NMR (400 MHz, CDCl<sub>3</sub>) δ 8.00(m, 3H), 7.53(d, 1H), 7.23(d, 1H), 7.10(s, 1H), 7.04(d, 1H), 5.37(d, 1H), 4.81(d, 1d), 4.77(s, 2H), 3.86(s, 3H), 1.38(s, 9H) <sup>13</sup>C NMR (101 MHz, DMSO-d<sub>6</sub>) δ 177.5, 168.5, 160.8, 160.4, 150.7 148.1, 143.6, 142.8, 140.8, 135.6, 131.2, 131.0, 122.1, 117.6, 116.9, 114.4, 78.8, 65.2, 52.7, 34.7, 31.4 MS found at 755.3 (2M-H<sup>+</sup>) (Calcd C<sub>46</sub>H<sub>43</sub>O<sub>10</sub><sup>-</sup> as 755.3)

### **2-((3-(Tert-butyl)-1-oxo-1,7-dihydrodibenzo[b,f]cyclopropa[d]oxocin-9-yl)oxy)acetic acid (2.10).**

Methyl 2-((3-(tert-butyl)-1-oxo-1,7-dihydrodibenzo[b,f]cyclopropa[d]oxocin-9-yl)oxy)acetate (2.71 g, 7.16 mmol) was dissolved in 100 mL of THF. 1M KOH (14 mL) solution was added dropwise to the mixture. The reaction was stirred in an ice bath for 30 mins before quenching with 1M HCl until the pH of the aqueous layer was under 7. The white solid was collected through suction filtration as the product (2.24 g, 86 %). <sup>1</sup>H NMR (400 MHz, DMSO-d<sub>6</sub>) δ

7.90(s,1H), 7.81(m, 1H), 7.68(m, 1H), 7.42-7.32(m, 2H), 7.21(s, 1H), 5.42(d, 1H), 4.92(m, 3H), 1.39(s, 9H); <sup>13</sup>C NMR (101 MHz, DMSO-d<sub>6</sub>) δ 170.5, 167.3, 157.9, 153.7, 145.0, 141.3, 138.3, 132.5, 129.8, 129.0, 127.9, 127.7, 127.3, 127.1, 121.7, 114.1, 114.0, 74.7, 64.8, 52.7, 31.7  
HRMS found at 363.0002 (M-H<sup>+</sup>) (Calcd C<sub>22</sub>H<sub>19</sub>O<sub>5</sub><sup>-</sup> as 363.1232)

**2,5-Dioxopyrrolidin-1-yl 2-((3-(tert-butyl)-1-oxo-1,7-dihydrodibenzo[b,f]cyclopropa[d]oxocin-9-yl)oxy)acetate (2.01):**

2-((3-(tert-butyl)-1-oxo-1,7-dihydrodibenzo[b,f]cyclopropa[d]oxocin-9-yl)oxy)acetic acid (1eq, 200 mg, 0.549 mmol), N-hydroxy succinimide (1.1 eq, 69.5 mg, 0.604 mmol) and DCC(1.1eq, 124.6 mg, 0.604 mmol) were dissolved in 10 mL of degassed DMF. The mixture was stirred at room temperature overnight. Then the mixture was set to cool under 4°C. The insoluble solid was filtered out before the rest of the solution was concentrated in to provide 2,5-dioxopyrrolidin-1-yl 2-((3-(tert-butyl)-1-oxo-1,7-dihydrodibenzo[b,f]cyclopropa[d]oxocin-9-yl)oxy)acetate(210 mg, 83 %) as a slightly pink solid. <sup>1</sup>H NMR (400 MHz, DMSO-d<sub>6</sub>) δ 7.87(d, 1H), 7.79(d, 1H), 7.66(m, 1H), 7.35(d, 1H), 7.29(d, 1H), 7.16(m, 1H), 5.38(d, 1H), 4.89(m, 3H), 2.59(s, 4H), 1.33(s, 9H) <sup>13</sup>C NMR (101 MHz, DMSO-d<sub>6</sub>) δ 173.3, 170.1, 161.7, 160.4, 151.6, 147.8, 144.5, 142.4, 141.5, 135.2, 131.5, 130.1, 122.4, 118.0, 117.9, 117.2, 115.4, 78.3, 65.1, 34.7, 31.5, 25.7

**4-Methoxy-4-oxobutanoic acid (2.12) <sup>13</sup>:**

Succinic acid (20 g, 200 mmol) was dissolved in 200 mL of methanol and refluxed overnight. The mixture was then concentrated in vacuo to provide 4-methoxy-4-oxobutanoic acid (26.0 g, 98 %) as a white solid. <sup>1</sup>H NMR (400 MHz, CDCl<sub>3</sub>) δ 10.12(s, 1H), 3.66(m, 3H), 3.00(m, 4H)

**3-Methoxy-N-(3-methoxybenzyl) aniline (2.15) <sup>12</sup>.**

3-Methoxybenzaldehyde (10 g, 73.4 mmol) was added to a solution of 3-methoxyaniline (9.95 g, 80.7 mmol) in 250 mL of anhydrous methanol. After stirring for 3 hours at room temperature, the yellow solution was treated with NaBH<sub>4</sub> (8.33 g, 220 mmol) and stirred for another 30 minutes. The reaction mixture was then quenched with ammonium chloride, extracted with diethyl ether (3 x 200 mL), dried over MgSO<sub>4</sub>, and concentrated in vacuo. Subsequently, the mixture was purified through column chromatography to provide 3-methoxy-N-(3-methoxybenzyl) aniline as colorless oil (15.6 g, 79 %) <sup>1</sup>H NMR (400 MHz, CDCl<sub>3</sub>) δ 7.29(1H, t), 7.11(1H, t), 6.97(2H, m), 6.84(1H, d), 6.29(2H, t), 6.22(1H, s), 4.32(2H, s), 4.13(1H, m), 3.82(3H, s), 3.78(3H, s)

**Methyl 4-((3-methoxybenzyl) (3-methoxyphenyl) amino)-4-oxobutanoate (2.16) <sup>12</sup>:**

4-methoxy-4-oxobutanoic acid chloride (22.4 g, 149 mmol) was added to a solution of 200 mL methylene chloride, triethylamine (10.24 g, 101.2 mmol), and 3-methoxy-N-(3-methoxybenzyl) aniline (12.3 g, 50.6 mmol), set in an ice bath and stirred overnight. The reaction was quenched with saturated sodium bicarbonate and washed with 100\*3 mL water and 100 mL brine. This was followed by an in-vacuo concentration of the mixture and subsequent purification through column chromatography (hexane: ethyl acetate=3:1) to provide methyl 4-((3-methoxybenzyl) (3-methoxyphenyl) amino)-4-oxobutanoate (12.8 g, 71.6 mmol) as orange oil. <sup>1</sup>H NMR (400 MHz, CDCl<sub>3</sub>) δ 7.27(m, 1H), 7.18(d, 1H), 6.86(d, 1H), 6.79(m, 3H), 6.66(d, 1H), 6.59(m, 1H), 4.86(s, 2H), 2.66(t, 2H), 2.46(t, 2H).

**4-((3-Methoxybenzyl)(3-methoxyphenyl)amino)-4-oxobutanoic acid (2.17) <sup>12</sup>:**

Methyl 4-((3-methoxybenzyl)(4-methoxyphenyl)amino)-4-oxobutanoate (23.0g, 64.4mmol) was dissolved in 100 mL THF. 2 mL water was added to the resulting solution before adding potassium hydroxide (3.61 g, 129 mmol, 2 eq) in 130 mL and stirring the mixture at room temperature for 12 hours. The mixture was concentrated in vacuo and re-dissolved in 15 mL 10 % NaOH. The organic layer was then separated and kept extracted by 15 mL\*3 10 % NaOH. The aqueous layer was combined, chilled in an ice bath, and acidified by concentrated HCl until the pH of the solution reached 2. The mixture was extracted by 100 mL\*3 ethyl acetate and concentrated in vacuo. The crude product was then concentrated through column chromatography to provide 4-((3-methoxybenzyl)(4-methoxyphenyl)amino)-4-oxobutanoic acid as a colorless oil(17.1 g, 77 %). <sup>1</sup>H NMR (400 MHz, CDCl<sub>3</sub>) δ 7.23(m, 2H), 6.89(m, 1H), 6.79(m, 3H), 6.64(d, 1H), 6.56(s, 1H), 4.87(s, 2H), 3.75(d, 6H), 2.69(t, 2H), 2.43(t, 2H)

**4-(4,9-Dimethoxy-1-oxo-1,7-dihydro-6H-dibenzo[b,f]cyclopropa[d]azocin-6-yl)-4-oxobutanoic acid (2): 4-(4,9-dimethoxy-1-oxo-1,7-dihydro-6H-dibenzo[b,f]cyclopropa[d]azocin-6-yl)-4-oxobutanoic acid (2.18).**

AlCl<sub>3</sub>(16.7 g 125 mmol 3.5 eq) and tetrachloro-cyclopropene(6.35 g, 35.7 mmol) were added to 500 mL of anhydrous DCM at room temperature. The solution mixture was stirred at room temperature for 10 minutes and then removed to -78 °C and stirred for another 5 minutes. 4-((3-methoxybenzyl)(3-methoxyphenyl)amino)-4-oxobutanoic acid (12.3 g, 35.7 mmol) was then added to the reaction at -78 °C. Then, the reaction mixture was stirred at -78 °C for 4 hours and stirred for another 1 hour at room temperature. The reaction mixture was quenched with 5 % HCl (100 mL), diluted with 150 mL DCM, and washed with water and brine. The mixture was then purified through the silica gel column (from hexane:acetone = 1:1 to acetone) to provide a brown

oil. The mixture was then purified via recrystallization in 10 % methanol, in ethyl acetate (30 mL), to obtain a purified yellow solid (5.87 g, 42 %).

<sup>1</sup>H NMR (400 MHz, DMSO-d<sub>6</sub>) δ 12.0(s, 1H), 7.92(d, 1H), 7.75(d, 1H), 7.38(d, 1H), 7.26(d, 1H), 7.20(m, 1H), 7.07(m, 1H), 5.04(d, 1H), 4.24(d, 1H), 3.89(d, 6H), 2.27(m, 2H), 1.88(m, 2H)  
<sup>13</sup>C NMR (101 MHz, DMSO-d<sub>6</sub>) δ 201.81, 174.23, 163.29, 162.31, 151.38, 146.35, 143.28, 140.13, 135.41, 134.66, 118.69, 116.08, 115.85, 115.40, 114.96, 114.64, 113.75, 56.50, 56.08, 29.50, 29.40 HRMS found at 392.1138 (M-H<sup>+</sup>) (Calcd C<sub>22</sub>H<sub>18</sub>NO<sub>6</sub> as 362.1134)

**2,5-Dioxopyrrolidin-1-yl 4-(4,9-dimethoxy-1-oxo-1,7-dihydro-6H-dibenzo[b,f]cyclopropa[d]azocin-6-yl)-4-oxobutanoate (2.02).**

4-((3-methoxybenzyl)(3-methoxyphenyl)amino)-4-oxobutanoic acid(393 mg, 1.00 mmol) was dissolved in 10 mL DMF. DCC(227 mg, 1.1 mmol) and NHS(127 mg, 1.10 mmol) were then added to the solution. The mixture was stirred at room temperature overnight. The mixture was cooled in fridge under 5 °C overnight and filtered out the solid. The solution was then concentrated in vacuo to provide 2,5-dioxopyrrolidin-1-yl 4-(4,9-dimethoxy-1-oxo-1,7-dihydro-6H-dibenzo[b,f] cyclopropa[d]azocin-6-yl)-4-oxobutanoate as yellow solid(276 mg, 56 %). <sup>1</sup>H NMR (400 MHz, DMSO-d<sub>6</sub>) δ 7.93(m, 1H), 7.36(d, 1H), 7.34(d, 1H). 7.28(d, 1H), 7.20(m, 1H), 7.06(m, 1H), 5.06(d, 1H), 4.27(d, 1H), 3.89(d, 6H), 2.89(s, 4H), 2.67(m, 2H), 2.06(m, 2H) <sup>13</sup>C NMR (101 MHz, DMSO-d<sub>6</sub>) δ 170.5, 168.9, 163.1, 162.8, 162.4, 151.5, 145.9, 143.1, 142.6, 135.3, 134.9, 118.9, 116.0, 115.9, 115.2, 114.9, 113.8, 113.7, 36.3, 33.8, 31.3, 29.0, 26.4, 25.8, 24.0 ESI-MS found at 513.1228 (M+Na<sup>+</sup>) (Calcd C<sub>26</sub>H<sub>22</sub>N<sub>2</sub>O<sub>8</sub>Na as 513.1273)

**2-(2-(2-(2-Hydroxyethoxy)ethoxy)ethoxy)ethyl 4-methylbenzenesulfonate (2.20) <sup>14</sup>.**

A solution of tetra ethylene glycol(51.0 g, 262 mmol, 10 eq) in methylene chloride was added to Tosyl chloride (5.01 g, 26.2 mmol), followed by 6 mL TEA at 0 °C. The mixture was stirred at

room temperature overnight before being washed with water. The combined organic layers were dried with sodium sulfate and concentrated in vacuo to provide 2-(2-(2-(2-hydroxyethoxy)ethoxy)ethoxy)ethyl 4-methyl benzenesulfonate as a colorless oil (9.10 g, 99.7 %).  $^1\text{H}$  NMR (400 MHz,  $\text{CDCl}_3$ )  $\delta$  7.81(2H, d), 7.35(2H, d), 4.17(2H, m), 3.66(14H, m), 2.62(3H, s)

**2-(2-(2-(2-Azidoethoxy)ethoxy)ethoxy)ethan-1-ol (2.21) <sup>14</sup>.**

Mono-Tosyl tetraethylene glycol and sodium azide were dissolved in 40 mL ethanol. The mixture was refluxed overnight at 80 °C. The mixture was concentrated in vacuo and re-dissolved in 200 mL of ethyl acetate. The mixture was washed with 100 mL \* 3 sodium bicarbonate, 100 mL water, and 100mL brine. The mixture was then concentrated in vacuo to provide 2-(2-(2-(2-azidoethoxy)ethoxy)ethoxy)ethan-1-ol as a colorless liquid (2.19 g, 38 %).  $^1\text{H}$  NMR (400 MHz,  $\text{CDCl}_3$ )  $\delta$  3.72-3.67 (t, 2H), 3.66-3.61 (m, 10H), 3.59-3.55 (m, 2H), 2.94-2.84 (m, 1H)  $^{13}\text{C}$  NMR (101 MHz,  $\text{CDCl}_3$ )  $\delta$  72.55, 70.57, 70.26, 69.93, 66.62, 61.58, 50.59.

**2-(2-(2-(2-Azidoethoxy)ethoxy)ethoxy)ethyl 4-methylbenzenesulfonate (2.22) <sup>14</sup>.**

Triethylamine (0.72 g, 7.12 mmol) was added to a solution of 2-(2-(2-azidoethoxy)ethoxy)ethan-1-ol (1.56 g, 7.12 mmol) and p-toluenesulfonyl chloride (2.04 g, 10.7 mmol) in  $\text{CH}_2\text{Cl}_2$  (50 mL). The reaction was then stirred overnight, concentrated in vacuum, and purified by flash chromatography (1:1 to 2:3 hexane: ethyl acetate) to afford 2-(2-(2-(2-azidoethoxy)ethoxy)ethoxy)ethyl 4-methylbenzenesulfonate (2.63 g, 99 %) as a colorless oil.  $^1\text{H}$  NMR (400 MHz,  $\text{CDCl}_3$ )  $\delta$  7.84 – 7.78 (d, 2H, J = 8Hz), 7.39 – 7.32 (d, 2H, J = 8Hz), 3.73 – 3.58 (m, 12H), 3.44 – 3.36 (m, 2H), 2.46 (s, 3H)  $^{13}\text{C}$  NMR (101 MHz,  $\text{CDCl}_3$ )  $\delta$  171.14, 144.81, 133.04, 129.83, 127.98, 70.76, 70.72, 70.68, 70.61, 70.04, 69.25, 68.69, 60.39, 50.69, 21.64, 21.05, 14.20.

**9-(2-(2-(2-(2-Azidoethoxy)ethoxy)ethoxy)ethoxy)-3-(tert-butyl)dibenzo[b,f]cyclopropa  
[d]oxocin-1(7H)-one (2.23)**

K<sub>2</sub>CO<sub>3</sub> (1.27 g, 9.20 mmol) was added to a solution of photo-ODIBO-OH (1.88 g, 6.13 mmol) and a Tos-EG<sub>4</sub>-N<sub>3</sub> linker (2.63 g, 7.36 mmol) in DMF (21 mL). The solution was stirred and heated at 80 °C for 5 hours. The reaction mixture was diluted with ethyl acetate (200 mL), washed with water (5x50 mL), brine (100 mL), and dried over MgSO<sub>4</sub>. The organic layer was then filtered, concentrated in vacuum, and purified via flash chromatography (20:1 DCM: MeOH) to afford photo-ODIBO-EG<sub>3</sub>-Azide (1.50 g, 47 % yield) of a slightly yellow oil. <sup>1</sup>H NMR (400 MHz, CDCl<sub>3</sub>) δ 7.99-7.93 (m, 2H), 7.55 – 7.52 (m, 1H), 7.26-7.18 (m, 1H), 7.13-7.03 (m, 2H), 5.32-5.29 (d, 1H, J = 12Hz), 4.85-4.77 (d, 1H, J=12Hz), 4.28-4.24 (m, 2H), 3.95-3.89 (m, 2H), 3.74-3.64 (m, 10H), 3.42-3.34 (m, 2H), 1.37 (s, 9H) <sup>13</sup>C NMR (101 MHz, CDCl<sub>3</sub>) 162.04, 160.44, 152.74, 148.01, 144.01, 142.23, 140.69, 135.50, 131.10, 130.73, 122.05, 117.87, 117.41, 117.05, 114.66, 78.78, 71.00, 70.81, 70.79, 70.76, 70.14, 69.53, 67.99, 50.75, 34.66, 31.44. HRMS: 508.2440 (M+H<sup>+</sup>) (calcd. for C<sub>28</sub>H<sub>34</sub>N<sub>3</sub>O<sub>6</sub> 508.2442)

**3-(D-Biotinylamido)-1-propyne (2.25)**

1-Ethyl-3-(3-dimethylaminopropyl)carbodiimide hydrochloride (EDC·HCl) (1.01 g, 5.32 mmol) was added to a solution of D-biotin (1.00 g, 4.09 mmol) and propargylamine (0.270 g, 4.91 mmol) in CH<sub>3</sub>CN:MeOH (3:1, 16 mL). The reaction was stirred at room temperature for 6.5 hours and then concentrated in vacuo. Then, MeOH was added to the crude residue and the solution was filtered through celite. The filtrate was concentrated in vacuo and purified via flash chromatography (10:1, CHCl<sub>3</sub>:MeOH) to afford 3-(D-Biotinylamido)-1-propyne (0.89g, 77

yield) as a white solid.  $^1\text{H}$  NMR (400 MHz,  $\text{CDCl}_3$ )  $\delta$  8.28-8.20 (m, 1H), 6.47-6.35 (d, 2H,  $J = 27\text{Hz}$ ), 4.34-4.37 (m, 1H), 4.16-4.10 (m, 1H), 3.86-3.82 (m, 2H), 3.35 (s, 1H), 3.14-3.06 (m, 2H), 2.86-2.79 (m, 1H), 2.62-2.48 (m, 3H), 2.11-2.05 (t, 2H), 1.68-1.23 (m, 6H)  $^{13}\text{C}$  NMR (101 MHz,  $\text{CDCl}_3$ )  $\delta$  172.26, 163.17, 81.84, 73.30, 61.49, 59.64, 55.86, 35.32, 28.65, 28.49, 28.17, 25.60. HRMS: 282.1198  $[\text{M} + \text{H}]^+$  (Calcd for  $\text{C}_{13}\text{H}_{19}\text{N}_3\text{O}_2\text{S}$  281.1198)

**Photo-ODIBO-EG4-Biotin (2.26)** <sup>15</sup>.

$\text{CuI}$  (0.021 g, 0.114 mmol) was added to a solution of photo-ODIBO-EG4-N3 (0.530 g, 1.14 mmol), 3-(D-Biotinylamido)-1-propyne (0.481 g, 1.71 mmol), and triethylamine (0.231 g, 2.28 mmol) in DMF (8 mL). The solution was stirred overnight, diluted with ethyl acetate (100 mL), washed with a saturated solution of  $\text{NH}_4\text{Cl}$  (2x50 mL), washed with brine (50 mL), and dried over  $\text{MgSO}_4$ . The crude solution was then concentrated in vacuo and purified via flash chromatography (10:1 to 10:2 DCM: MeOH) to afford photo-ODIBO-EG4-Biotin (0.276 g, 31 % yield) as an off-white solid.  $^1\text{H}$  NMR (400 MHz,  $\text{CDCl}_3$ )  $\delta$  8.31-8.22 (m, 1H), 7.89-7.81 (m, 2H), 7.79 (s, 1H), 7.67-7.62 (d, 1H,  $J = 8\text{Hz}$ ), 7.37 -7.28 (m, 1H), 6.43-6.32 (m, 3H), 5.40-5.32 (d, 1H,  $J = 12\text{Hz}$ ), 4.91-4.84 (d, 1H,  $J = 12\text{Hz}$ ), 4.53 -4.43 (m, 2H), 4.31-4.21 (m, 6H), 4.13 (m, 1H), 3.81 -3.75 (m, 4H), 3.63-3.56 (m, 2H), 3.55-3.46 (m, 6H), 3.08 (s, 1H), 2.93 (s, 1H), 2.86-2.77 (m, 1H), 2.59 (s, 1H), 1.64-1.39 (m, 6H), 1.35 (s, 9H)  $^{13}\text{C}$  NMR (101 MHz,  $\text{CDCl}_3$ )  $\delta$  172.41, 163.16, 162.16, 160.39, 147.75, 145.36, 144.41, 141.53, 135.24, 131.41, 130.07, 123.55, 122.73, 117.63, 117.25, 115.36, 78.40, 70.39, 70.25, 70.13, 70.03, 69.23, 69.16, 68.29, 61.48, 59.66, 55.86, 49.74, 35.46, 34.70, 34.56, 31.50, 31.17, 28.69, 28.49, 25.66 ESI-HRMS: 789.3640 ( $\text{M} + \text{Na}^+$ ) (Calcd. for  $\text{C}_{41}\text{H}_{53}\text{N}_6\text{O}_8\text{S}^+$  789.3646)

**4-Oxo-4-(prop-2-yn-1-ylamino)butanoic acid (2.28).**

A solution of succinic anhydride (300 mg, 3 mmol) in 3 mL of THF was added to propargylamine (198 mg, 3.6 mmol). The mixture was stirred at room temperature for 20 h and before adding CH<sub>2</sub>Cl<sub>2</sub> (20 mL) to it. The resulting precipitate was filtered to give the desired product (338 mg, 73 %) as a yellow solid. <sup>1</sup>H NMR (400 MHz, DMSO-d<sub>6</sub>) δ 12.09(s, 1H), 8.31(t, 1H), 3.85(m, 2H), 3.10(t, 1H), 2.52(s, 1H), 2.42(t, 2H), 2.32(t, 2H) <sup>13</sup>C NMR (101 MHz, DMSO-d<sub>6</sub>) δ 174.0, 171.4, 81.8, 75.3, 30.3, 29.4, 28.5

**N1-(3-methoxybenzyl)-N1-(3-methoxyphenyl)-N4-(prop-2-yn-1-yl)succinimide (2.30)**

3-methoxy-N-(3-methoxybenzyl)aniline (1.00 g, 4.11 mmol), EDC (1.28 g, 12.3 mmol) and DMAP (50.0 mg, 1 mmol), were dissolved in DCM. 4-oxo-4-(prop-2-yn-1-ylamino)butanoic acid (1.91 g, 12.3 mmol) was added to the solution. The mixture was stirred overnight at room temperature and then quenched by sat. NH<sub>4</sub>-Cl before washing with brine. The mixture was then concentrated in vacuo and further purified by column chromatography to provide N1-(3-hydroxybenzyl)-N1-(3-methoxyphenyl)-N4-(prop-2-yn-1-yl)succinimide as a colorless oil (1.08 g, 69 %). <sup>1</sup>H NMR (400 MHz, CDCl<sub>3</sub>) δ 7.32-7.16 (m, 2H), 6.89-6.75 (m, 3H), 6.67-6.55 (m, 3H), 4.85 (s, 2H), 4.03 (m, 2H), 3.82-3.67 (d, 6H), 2.59-2.41 (m, 4H), 2.24-2.22 (m, 1H) <sup>13</sup>C NMR (101 MHz, CDCl<sub>3</sub>) δ 172.06, 160.42, 159.63, 142.88, 138.80, 130.37, 129.40, 128.65, 127.78, 120.96, 120.48, 114.14, 114.04, 113.82, 113.00, 112.96, 79.71, 77.38, 77.27, 77.07, 76.75, 71.35, 60.42, 55.37, 55.22, 53.16, 31.37, 30.04, 29.17, 21.07, 14.21.

**4-(4,9-Dimethoxy-1-oxo-1,7-dihydro-6H-dibenzo[b,f]cyclopropa[d]azocin-6-yl)-4-oxo-N-(prop-2-yn-1-yl)butanamide (2.27) <sup>12</sup>.**

AlCl<sub>3</sub>(1.23 g, 9.20 mmol, 3.5 eq) and tetrachloro-cyclopropene(0.468 g, 2.62 mmol) were added to 100 mL anhydrous DCM at room temperature. The solution mixture was stirred at room

temperature for 10 minutes and then removed to -78 °C and stirred for another 5 minutes. N1-(3-methoxybenzyl)-N1-(3-methoxyphenyl)-N4-(prop-2-yn-1-yl)succinamide (1.00 g, 2.63 mmol) was then added to the reaction at -78 °C. The reaction mixture was then stirred at -78 °C for 4 hours and stirred for another hour at room temperature. The reaction mixture was quenched with 5 % HCl (100 mL), diluted with 150 mL DCM, and washed with water and brine. The mixture was then purified through the silica gel column (from DCM to DCM : methanol = 30:1) to provide brown oil. The mixture was then recrystallized from ethyl acetate : methanol (10/1) to provide 4-(4,9-dimethoxy-1-oxo-1,7-dihydro-6H-dibenzo[b,f]cyclopropa[d]azocin-6-yl)-4-oxo-N-(prop-2-yn-1-yl)butanamide as a yellowish solid (0.358 g , 32 %) <sup>1</sup>H NMR (400 MHz, DMSO-d<sub>6</sub>) δ 7.92-7.88 (d, 1H), 7.77-7.70 (d, 1H), 7.57-7.39 (m, 1H), 7.29-7.21 (m, 1H), 7.22-7.13 (m, 1H), 7.07-7.00 (m, 1H), 5.08-4.98 (d, 1H, J=12 Hz), 4.26-4.17 (d, 1H, J=12 Hz), 3.96-3.85 (d, 6H), 3.34 (s, 2H), 2.83 (s, 1H), 2.70 (s, 1H), 2.69-2.55 (m, 1H), 2.30-2.18 (m, 1H), 2.10-1.98 (m, 1H), 1.89-1.71 (m, 1H)

**4-(4,9-Dihydroxy-1-oxo-1,7-dihydro-6H-dibenzo[b,f]cyclopropa[d]azocin-6-yl)-4-oxobutanoic acid (2.32).**

BBr<sub>3</sub>(7.77 g, 31.0 mmol) was added to the solution of 4-(4,9-dimethoxy-1-oxo-1,7-dihydro-6H-dibenzo[b,f]cyclopropa[d]azocin-6-yl)-4-oxobutanoic acid (1.22 g, 3.0 mmol) and 25 mL methylene chloride dropwise in -78 °C and stirred for 168 hours. The mixture was then quenched with 50 mL water and concentrated in vacuo. Subsequently, the residue was suspended in 10 mL of ethanol and stirred for 15mins. The solid was filtered out to provide 4-(4,9-dihydroxy-1-oxo-1,7-dihydro-6H-dibenzo[b,f]cyclopropa[d]azocin-6-yl)-4-oxobutanoic acid as a yellow solid (1.05 g, 93 %) <sup>1</sup>H NMR (400 MHz, DMSO-d<sub>6</sub>) δ 10.94-10.33 (m, 2H), 7.85-7.75 (d, 1H), 7.66-

7.56 (d, 1H), 7.12-6.95 (m, 3H), 6.91-6.80 (d, 1H), 5.03-4.86 (d, 1H), 4.27-4.10 (d, 1H), 2.50-2.12 (m, 3H), 1.98-1.73 (m, 1H) <sup>13</sup>C NMR (101 MHz, DMSO-d<sub>6</sub>) δ 173.98, 171.46, 161.96, 161.08, 151.42, 146.33, 142.86, 142.15, 138.80, 135.40, 134.91, 119.91, 117.16, 116.22, 115.36, 114.48, 113.77, 55.82, 40.58, 40.37, 40.17, 39.96, 39.75, 39.54, 39.33, 29.61, 29.38. HRMS: 368.0824 (M-H<sup>+</sup>) (calcd. for C<sub>20</sub>H<sub>14</sub>NO<sub>6</sub><sup>-</sup> 365.0821)

**Prop-2-yn-1-yl 4-(4,9-dihydroxy-1-oxo-1,7-dihydro-6H-dibenzo[b,f]cyclopropa[d]azocin-6-yl)-4-oxobutanoate (2.33) <sup>12</sup>.**

4-(4,9-dimethoxy-1-oxo-1,7-dihydro-6H-dibenzo[b,f]cyclopropa[d]azocin-6-yl)-4-oxobutanoic acid (460 mg, 1.17 mmol) was dissolved in 50 mL of DCM. EDC (193 mg, 3.51 mmol) and DMAP (14.3 mg, 0.117 mmol) were added to the solution. Propargyl amine (193 mg, 3.51 mmol) was then added to the mixture before stirring the solution overnight at room temperature. The mixture was quenched by saturated NH<sub>4</sub>Cl, washed with brine, and concentrated in vacuo. The mixture was then further separated by column chromatography (Acetone) to provide 4-(4,9-dimethoxy-1-oxo-1,7-dihydro-6H-dibenzo[b,f]cyclopropa[d]azocin-6-yl)-4-oxo-N-(prop-2-yn-1-yl)butanamide as white solid (65 mg, 13 %). <sup>1</sup>H NMR (400 MHz, DMSO-d<sub>6</sub>) δ 10.80 (s, 1H), 10.46 (s, 1H), 8.27-8.10 (m, 1H), 7.83-7.56 (d, 1H), 7.68-7.58 (d, 1H), 7.14-6.96 (m, 3H), 6.91-6.81 (d, 1H), 5.00-4.90 (d, 1H), 4.27-4.08 (d, 1H), 3.80-3.67 (m, 2H), 3.05 (s, 1H), 2.68-2.56 (m, 1H), 2.30-2.16 (m, 1H), 2.10-1.99 (m, 1H), 1.91-1.77 (m, 1H) <sup>13</sup>C NMR (101 MHz, DMSO-d<sub>6</sub>) δ 171.63, 171.18, 162.00, 161.11, 151.42, 146.42, 142.85, 142.12, 138.88, 135.34, 134.89, 120.02, 117.13, 116.23, 115.41, 114.49, 113.75, 81.60, 73.33, 55.83, 40.69, 40.48, 40.28, 40.07, 39.86, 39.65, 39.44, 30.51, 29.78, 28.22.

**Prop-2-yn-1-yl 4-methylbenzenesulfonate (2.35) <sup>16</sup>.**

NaH (0.257 g, 10.7 mmol) and propargyl alcohol (0.500 g, 10.7 mmol) were added to 40 mL of DCM in an ice bath. Tosyl chloride (2.04 g, 10.7 mmol) was then added to the solution in an ice bath. The mixture was stirred overnight at room temperature and quenched with saturated ammonium chloride. Subsequently, it was washed with water and brine before the separation of the organic layer. The solution was then concentrated in vacuo and further purified with a column chromatograph (hexane: ethyl acetate=1:1) to provide prop-2-yn-1-yl 4-methyl benzenesulfonate as a colorless oil (1.36 g, 72 %). <sup>1</sup>H NMR (400 MHz, DMSO-d<sub>6</sub>) δ 7.84-7.74 (d, 2H), 7.38-7.31 (d, 2H), 4.74-4.63 (d, 2H), 2.53-2.41 (m, 4H) <sup>13</sup>C NMR (101 MHz, DMSO-d<sub>6</sub>) δ 145.29, 132.90, 130.21, 127.73, 77.40, 75.40, 57.39, 21.61

**3-(Tert-butyl)-9-(prop-2-yn-1-yloxy)dibenzo[b,f]cyclopropa[d]oxocin-1(7H)-one (2.36).**

3-(tert-butyl)-9-hydroxydibenzo[b,f]cyclopropa[d]oxocin-1(7H)-one and potassium t-butoxide was added to 25 mL THF. Prop-2-yn-1-yl 4-methylbenzenesulfonate was added to the solution and the mixture was refluxed overnight. The mixture was then quenched with sat. NH<sub>4</sub>Cl and extracted with ethyl acetate. The organic layer was then washed with brine and concentrated on vacuo. The crude product was then separated through silica gel column chromatography to provide 3-(tert-butyl)-9-(prop-2-yn-1-yloxy)dibenzo[b,f]cyclopropa[d]oxocin-1(7H)-one as white solid (179 mg, 80 %). <sup>1</sup>H NMR (400 MHz, DMSO-d<sub>6</sub>) δ 7.92-7.89 (d, J = 12 Hz, 1H), 7.82-7.79 (m, 1H), 7.69-64 (m, 1H), 7.40-7.37 (m, 1H), 6.56-6.41 (d, J = 9 Hz, 1H), 7.25-7.20 (m, 1H), 5.40-5.36 (d, J = 12 Hz, 1H), 5.00-4.96 (m, 2H), 4.94-4.88(d, J =12 Hz, 1H), 3.19-3.14 (m, 1H) <sup>13</sup>C NMR (101 MHz, DMSO-d<sub>6</sub>) δ 160.73, 160.41, 151.39, 147.79, 144.35, 142.67, 141.43, 135.12, 131.46, 130.12, 122.73, 118.33, 118.19, 117.21, 115.79, 79.40, 78.99, 78.35,

56.48, 34.69, 31.50, 23.56, 13.94. 2.09 HRMS: 345.1485 (M+H<sup>+</sup>) (calcd. for C<sub>23</sub>H<sub>21</sub>O<sub>3</sub><sup>+</sup>  
345.1491)

## 2.09 References

- Kim, E.; Koo, H. Biomedical applications of copper-free click chemistry: in vitro, in vivo, and ex vivo. *Chemical Science* 2019, 10 (34), 7835-7851.
1. Morey, T. M.; Esmaeili, M. A.; Duennwald, M. L.; Rylett, R. J. SPAAC Pulse-Chase: A Novel click chemistry-based method to determine the half-life of cellular proteins. *Frontiers in Cell and Developmental Biology* 2021, 9, Methods.
  2. Farrer, N. J.; Griffith, D. M. Exploiting azide-alkyne click chemistry in the synthesis, tracking and targeting of platinum anticancer complexes. *Current Opinion in Chemical Biology* 2020, 55, 59-68.
  3. Thirumurugan, P.; Matosiuk, D.; Jozwiak, K. Click Chemistry for Drug Development and Diverse Chemical–Biology Applications. *Chemical Reviews* 2013, 113 (7), 4905-4979.
  4. Green, N.; Avidin. 3. The Nature of the Biotin-Binding Site. *Biochemical Journal* 1963, 89 (3), 599-609.
  5. Livnah, O.; Bayer, E. A.; Wilchek, M.; Sussman, J. L. Three-dimensional structures of avidin and the avidin-biotin complex. *Proceedings of the National Academy of Sciences* 1993, 90 (11), 5076-5080.
  6. Castro, V.; Rodríguez, H.; Albericio, F. CuAAC: An efficient click chemistry reaction on solid phase. *ACS Combinatorial Science* 2016, 18 (1), 1-14.

7. Meinhardt, M.; Krebs, R.; Anders, A.; Heinrich, U.; Tronnier, H. Wavelength-dependent penetration depths of ultraviolet radiation in human skin. *Journal of Biomedical Optics* 2008, 13 (4), 044030.
8. McNitt, C. D.; Popik, V. V. Photochemical generation of oxa-dibenzocyclooctyne (ODIBO) for metal-free click ligations. *Organic & Biomolecular Chemistry* 2012, 10 (41), 8200-8202.
9. Durie, K.; Yatvin, J.; McNitt, C. D.; Reese, R. A.; Jung, C.; Popik, V. V.; Locklin, J. Multifunctional surface manipulation using orthogonal click chemistry. *Langmuir* 2016, 32 (26), 6600-6605.
10. Pavlickova, L.; Kuzmic, P.; Soucek, M. Chemical actinometry in the UV range based on the photohydrolysis of 3,4-dimethoxynitrobenzene. *Collect. Czech. Chem. Commun.* 1986, 51, 368.
11. Li, Z.; Kosuri, S.; Foster, H.; Cohen, J.; Jumeaux, C.; Stevens, M. M.; Chapman, R.; Gormley, A. J. A Dual Wavelength Polymerization and Bioconjugation Strategy for High Throughput Synthesis of Multivalent Ligands. *Journal of the American Chemical Society* 2019, 141 (50), 19823-19830.
12. Wheatley, B. M. M.; Keay, B. A. Use of Deuterium Labeling Studies to Determine the Stereochemical Outcome of Palladium Migrations during an Asymmetric Intermolecular Heck Reaction. *The Journal of Organic Chemistry* 2007, 72 (19).
13. Yang, J.; Wang, Y.; Rassat, A.; Zhang, Y.; Sinaÿ, P. Synthesis of novel highly water-soluble 2:1 cyclodextrin/fullerene conjugates involving the secondary rim of  $\beta$ -cyclodextrin. *Tetrahedron* 2004, 60 (52), 12163-12168.

14. Nainar, S.; Kubota, M.; McNitt, C.; Tran, C.; Popik, V. V.; Spitale, R. C. Temporal Labeling of Nascent RNA Using Photoclick Chemistry in Live Cells. *Journal of the American Chemical Society* 2017, 139 (24), 8090-8093.
15. Soltani Rad, Mohammad N.; Behrouz, S.; Mohammadtaghi-Nezhad, J.; Zarenezhad, E.; Agholi, M. Silica-tethered cuprous acetophenone thiosemicarbazone (STCATSC) as a novel hybrid nano-catalyst for highly efficient synthesis of new 1,2,3-triazolyl-based metronidazole hybrid analogues having potent anti-giardial activity. *Applied Organometallic Chemistry* 2019, 33 (4), 4799.

## CHAPTER 3

### ULTRAFAST TRANSIENT ABSORPTION SPECTROSCOPY OF PHOTODECARBONYLATION OF PHOTOOXADIBENZOCYCLOOCTYNE

#### 3.1 Introduction

In the first chapter, we mentioned that there are three different mechanisms to explain the photodecarbonylation of cyclopropenone derivatives, with no solid conclusion. Recently, with the help of femtosecond ultrafast transient absorption spectroscopy, our collaborator Dr. Learnmore Shenje found that photo-ODIBO under 321 nm and 350 nm may undergo a different mechanism.<sup>1</sup> Based on their discovery, we found that photo-ODIBO under 321 nm exhibits fast decarbonylation in 250 fs, while photo-ODIBO under 350 nm took longer for the reaction to finish.

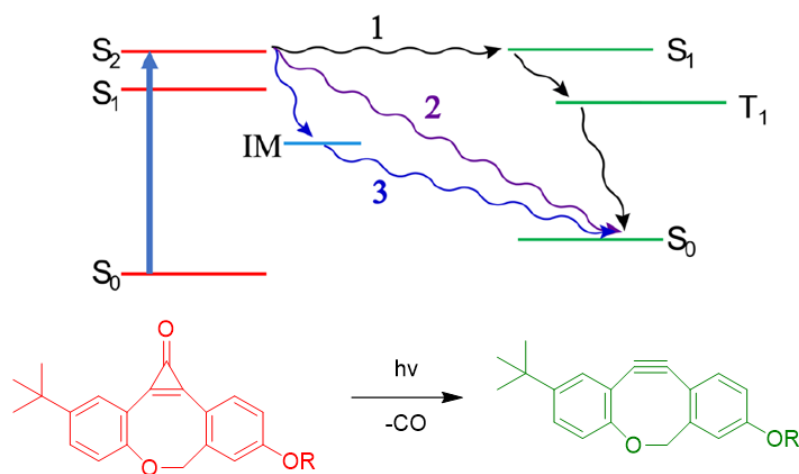
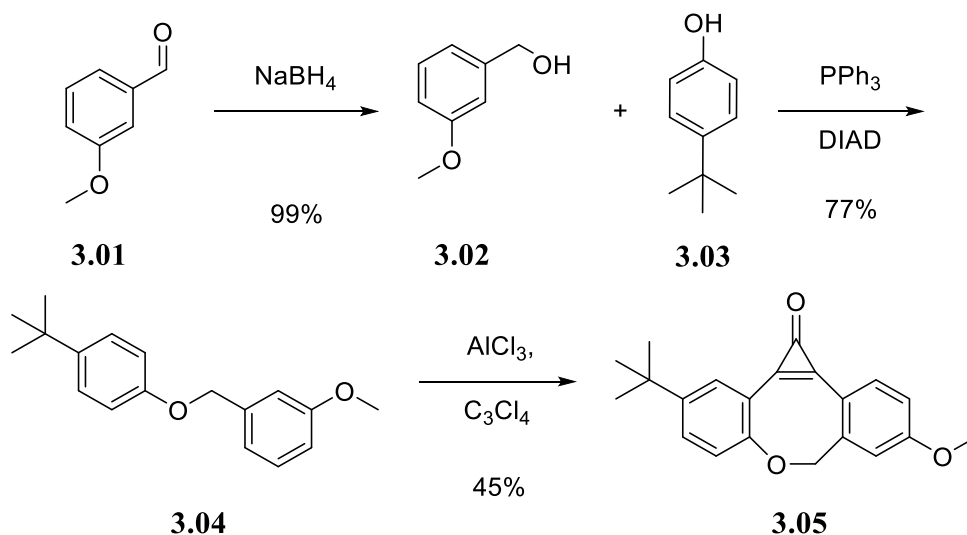


*Figure 3. 1 Three pathways of photodecarbonylation of cyclopropenone derivatives*

In this chapter, we discuss the synthesis of photo-ODIBO-OMe and the quantum yield of its solution in methanol solution under 321 nm and 350 nm. By comparing the quantum yields, we noticed the difference between irradiation under 321 nm and 350 nm. Then, to explain the difference, we used nanosecond transient absorption spectroscopy to study the formation of the triplet state of photo-ODIBO under 266 nm and 355 nm irradiation.

### 3.2 Synthesis of Photo-ODIBO-OMe

The synthesis of photo-ODIBO-OMe started with the reduction of 3-methoxy benzaldehyde (**3.01**). Then we subjected **3.02** and **3.03** to the Mitsunobu reaction, which produced **3.04**. Lastly, using  $\text{AlCl}_3$  as a catalyst, we can get compound **3.05**, which is a white powder. During the second step of the reaction, to get a pure product, 5%  $\text{H}_2\text{O}_2$  in water was added to quench the reaction, and the precipitated white solid was separated so that  $\text{PPh}_3$  could be removed to avoid any contamination during the next step.



*Scheme 3.1 Steps to synthesize photo-ODIBO-OMe*

### 3.3 Measurement of Quantum Yield of Photo-ODIBO under 321 nm and 350 nm

To prove the difference in the mechanism of photo-ODIBO decarbonylation under 321 nm and 350 nm, we measured the quantum yields of the reaction under these two conditions. To make sure the condition of irradiation was suitable, these experiments were conducted in the physics department of UGA.

Changes in the concentration of photo-ODIBO solution and actinometer were determined using a UV-Vis spectrometer. Calculation of quantum yield is performed using the following equations:

$$\Phi = \frac{n_s}{I_{abs}} \quad (1)$$

where  $n_s$  (mol) is the number of starting materials converted at the final irradiation time,  $I_{abs}$  (mole, quanta) is the integrated light intensity absorbed. When under the same condition (temperature, same vial for irradiation, same irradiation time etc.),

$$I_{abs}(PO) = I_{abs}(4 - NV) \quad (2)$$

where  $I_{abs}(PO)$  is the integrated light intensity absorbed by PO when irradiated, and  $I_{abs}(4-NV)$  is the integrated light intensity absorbed by 4-nitroveratrole. Combining Equations (1) and (2), we get

$$\Phi(PO) = \frac{n_s(PO)}{n_s(4-NV)} * \Phi(4 - NV) \quad (3)$$

where  $\Phi(PO)$  is the quantum efficiency of PO and  $\Phi(4-NV)$  is the quantum efficiency of 4-nitroveratrole, the value of which has been reported to be  $0.116 \pm 0.002$ .<sup>2</sup> Using this, we calculated  $\Phi(PO)$  under 321 nm to be  $14 \pm 1 \%$  and  $\Phi(PO)$  under 350 nm to be  $18 \pm 2 \%$ .

In other words, photo-ODIBO under the two wavelengths showed very similar quantum efficiency and produced same product. We noticed that the quantum yield of photo-ODIBO

under 350 nm is slightly higher than the quantum yield under 321 nm. Also, according to the mechanism proposed by Dr. Shenje <sup>1</sup>, the T<sub>1</sub> excited state of ODIBO-OH can be one of the intermediates in the mechanism. To prove this, we used nanosecond transient absorption spectroscopy to find a trace of the triplet state of ODIBO.

	Conversion of PO (μM)	Conversion of 4-NV (μM)	Quantum Yield
Under 350 nm	5.9 ± 0.1	3.7 ± 0.3	0.18 ± 0.02
Under 321 nm	6.4 ± 0.3	4.7 ± 0.1	0.14 ± 0.01

**Table 3. 1 Quantum yield of photo-ODIBO under 350 nm and 321 nm**

### **3.4 Study of Triplet-State Photo-ODIBO-OMe using Nanosecond Transient Spectroscopy**

There is a long history of using nanosecond transient spectroscopy to study the said mechanism. Due to the forbidden transformation between T<sub>1</sub> to S<sub>0</sub>, the lifetime of triplet-state molecules is much longer than those of a singlet state, which makes it suitable for study using nanosecond transient spectroscopy.

Another characteristic of the triplet-state molecules is that they can be influenced by ground-state oxygen. According to Hund's rule, in the LUMO of O<sub>2</sub>, there are two unpaired electrons in two different orbitals. This arrangement of electrons makes ground-state O<sub>2</sub> triplet. Due to the unpaired electrons on their frontier orbitals, triplet oxygen can interact with triplet state molecules. Thus, the presence of ground-state O<sub>2</sub> affects the lifetime of triplet-state ODIBO molecules.

Hence, measurements were conducted under different oxygen concentrations, from 0% to 100%. With that, we compared the lifetime of ODIBO triplet states under atmosphere of nitrogen, air, and pure oxygen; we found that the lifetime decreased with the increasing concentration of oxygen.

We irradiated the ODIBO solution with 266 nm. When pure argon was purged in the solution and used for the atmosphere of the measurement (Figure 3.5), the triplet-state molecules exhibited the longest lifetime of 290  $\mu$ s. Since there was no oxygen in this environment, no interaction between ground-state oxygen and triplet-state molecules existed. When pure oxygen was used, the triplet molecules exhibited the shortest lifetime of only 190  $\mu$ s. When oxygen was replaced with air, the lifetime value fell between the two abovementioned values. This proves that the species we observed using the nanosecond transient absorption spectroscopy were the triplet-state of ODIBO.

Oxygen content of the purge gas	Lifetime ( $\mu$ s)
0% (Argon)	290 $\pm$ 10 $\mu$ s
20% (Air)	238 $\pm$ 15 $\mu$ s
100%	190 $\pm$ 10 $\mu$ s

**Table 3. 2 Lifetime of ODIBO-OH in different concentrations of oxygen**

### 3.5 Conclusion

In this project, we synthesized photo-ODIBO-OMe and studied the mechanism of photo-ODIBO-OMe decarbonylation with 321 nm and 350 nm irradiation. We measured the quantum yield of photo decarbonylation of photo-ODIBO-OMe under 321 nm and 350 nm and found that the quantum yields of the reaction under two wavelengths are very similar which revealed that the mechanism of the photoreaction under these two wavelengths are very similar. To investigate the participation of the potential the in the proposed mechanism,<sup>1</sup> we used nano-second laser photolysis to study the triplet state of ODIBO-OH and found the triplet state molecules under 266 nm irradiation. With 355 nm irradiation, we didn't find any transient species. We hope those

findings could provide new insights in understanding the mechanism of photo-decarbonylation of cyclopropenone derivatives.

### **3.6 Experimental Section**

#### **3.6.1 Material and instrument information:**

For the measurement of quantum yield of photo-ODIBO under 350 nm and 321 nm, we used 4-nitroveratrole as an actinometer, and absorption data were collected using Agilent Cary 60 Spectrophotometer. For the stock solution of photo-ODIBO-OH, the compound (26.2 mg) was dissolved in 1000 mL methanol. For the stock solution of 4-nitroveratrole, the compound (13.2 mg) was dissolved in 500 mL 0.5M KOH. All the stock solutions were purged with nitrogen and were used within 6 h. Nanosecond laser flash photolysis was conducted using LKS.50 kinetic spectrometer (Applied Photo-physics) equipped with an Nd:YAG laser.

#### **3.6.2 Synthesis of Photo-ODIBO-OMe**

##### **1(1-((4-(tert-butyl) phenoxy) methyl)-3-methoxybenzene):**

DIAD (6.26 g 33.4 mmol) was added to a solution of 3-methoxy benzyl alcohol (4.62 g, 33.4 mmol), 4-(tert-butyl) phenol (5.02 g 33.4 mmol), and triphenylphosphine (8.26 g, 33.4 mmol) in THF (100 mL) at 0°C, and the solution was stirred for 30 mins at room temperature. The reaction mixture was diluted with 100 mL hexane. H<sub>2</sub>O<sub>2</sub> (30%, 10 mL) was then added to the solution, and the reaction mixture was refluxed at 80°C. The mixture was filtered and concentrated in a vacuum. The reaction mixture was then diluted with ethyl acetate, washed with water, and purified with column chromatography (hexane: ethyl acetate = 10:1) to provide (1-((4-(tert-butyl) phenoxy) methyl)-3-methoxybenzene) as a colorless oil (8.28 g, 77.4%) [7.30-7.32 (d, J = 9.2 Hz, 2H), 7.28 (s, 1H), 6.99-7.02 (m, 2H), 6.99-6.93 (d, J = 8.8 Hz, 2H), 6.85-6.87 (dd, J = 8, 2 Hz, 1H), 5.02 (s, 2H), 3.81(s,3H), 1.30 (s, 9H)].

## **2 (3-(tert-butyl)-9-methoxydibenzo[b,f]cyclopropa[d]oxocin-1(7H)-one):**

$\text{AlCl}_3$  (0.493 g 3.7 mmol) and tetrachloro-cyclopropene (0.658 g, 3.7 mmol) were added to 100 mL of anhydrous DCM at room temperature. The solution was stirred at room temperature for 10 mins and then removed to  $-78^\circ\text{C}$  and stirred for another 5 minutes. Following this, (1-((4-(tert-butyl) phenoxy) methyl)-3-methoxybenzene) (1.00 g, 3.7mmol) was added to the solution at  $-78^\circ\text{C}$ . The reaction mixture was then stirred at  $-78^\circ\text{C}$  for 4 h and stirred for another 1 hour at room temperature. The reaction mixture was quenched with 5% HCl (70 mL) diluted with 150 mL DCM and washed with water and brine. The mixture was then purified using a silica gel column (DCM: methanol = 70:1) to obtain a brown-colored oil. The mixture was then recrystallized from ethyl acetate and hexanes (ethyl acetate: hexane = 1:1) to obtain 3-(tert-butyl)-9-methoxydibenzo[b,f]cyclopropa[d]oxocin-1(7H)-one(0.53g, 45%) as a yellow solid.  $^1\text{H-NMR}$ : 7. -7.93 (m, 2H), 7.49-7.51 (dd, 1H), 7.21-7.19 (d, J = 8.4 Hz, 1H), 7.01-7.02 (m, 2H), 5.27-5.29 (d, 1H), 4.78-4.81 (d, 1H), 3.91 (s, 3H), 1.35 (s, 9H).

### **3.6.3 Measurement of Quantum Yield**

To measure the quantum yield, 2.5 mL of photo-ODIBO-OH was irradiated under 350 nm with a power of 130 nJ and under 321 nm with a power of 180 nJ. To get measurable and accurate results of absorbance change in 4-nitroveratrole, the irradiation time was 450 s under 350 nm irradiation and 360 s under 321 nm irradiation. All the measurements were conducted thrice.

The absorbance under the same irradiation time is calculated using the following equations:

$$Abs_{Average} = Abs_{Actual} * \frac{t_{ODIBO}}{t_{4-NV}} \quad (1)$$

where  $t_{ODIBO}$  is the irradiation time of PO,  $t_{4-NV}$  is the irradiation time of 4-nitroveratrole,  $Abs_{Average}$  is the average absorbance change of 4-nitroveratrole under  $t_{ODIBO}$ , and  $Abs_{Actual}$  is the  $t_{4-NV}$ .

For irradiation of PO under 350 nm, the average conversion is  $7.3 \pm 0.1\%$ . The average change in absorbance is  $0.104 \pm 0.002$ , and the average change in concentration is  $5.92 \pm 0.09$   $\mu\text{M}$ .

	Conversion %	Absorbance Change	Concentration Change ( $\mu\text{M}$ )
1	7.2	0.103	5.86
2	7.4	0.106	6.05
3	7.2	0.103	5.86
Average	$7.3 \pm 0.1$	$0.104 \pm 0.002$	$5.92 \pm 0.09$

**Table 3. 3 Conversion, absorbance change, and concentration change of PO under 350-nm laser irradiation**

For irradiation of PO under 321nm, the average conversion is  $7.8 \pm 0.3\%$ . The average change of absorbance is  $0.1128 \pm 0.005$ , and the average change in concentration is  $6.41 \pm 0.3$   $\mu\text{M}$ .

	Conversion %	Absorbance Change	Concentration Change ( $\mu\text{M}$ )
1	7.6	0.109	6.09
2	8.2	0.119	6.79
3	7.3	0.110	6.24

Average	$7.8 \pm 0.3$	$0.113 \pm 0.005$	$6.41 \pm 0.3$
---------	---------------	-------------------	----------------

**Table 3. 4 Conversion, absorbance change, and concentration change of PO under 321-nm laser irradiation**

For irradiation of 4-nitroveratrole under 350 nm, the average conversion is  $97.4 \pm 0.2\%$ . The average change of absorbance is  $0.01116 \pm 0.0009$ , and the average change of concentration is  $3.69 \pm 0.3 \mu\text{M}$ .

	Conversion %	Absorbance Change	Concentration Change ( $\mu\text{M}$ )
1	97.6	0.0104	3.52
2	97.6	0.0104	3.46
3	97.2	0.0114	4.09
Average	$97.4 \pm 0.2$	$0.0112 \pm 0.0009$	$3.69 \pm 0.3$

**Table 3. 5 Conversion, absorbance change, and concentration change of 4-nitroveratrole under 350-nm laser irradiation**

For irradiation of 4-nitroveratrole under 321 nm, the average conversion is  $97.8 \pm 0.1$ . The average change of absorbance is  $0.01418 \pm 0.0003$ , and the average change in concentration is  $4.71 \pm 0.09 \mu\text{M}$ .

	Conversion %	Absorbance Change	Concentration Change ( $\mu\text{M}$ )
1	97.8	0.0145	4.80
2	97.8	0.0143	4.75
3	97.9	0.0138	4.58

Average	$97.8 \pm 0.1$	$0.0142 \pm 0.0003$	$4.71 \pm 0.09$
---------	----------------	---------------------	-----------------

**Table 3. 6 Conversion, absorbance change, and concentration change of 4-nitroveratrole under 321-nm laser irradiation**

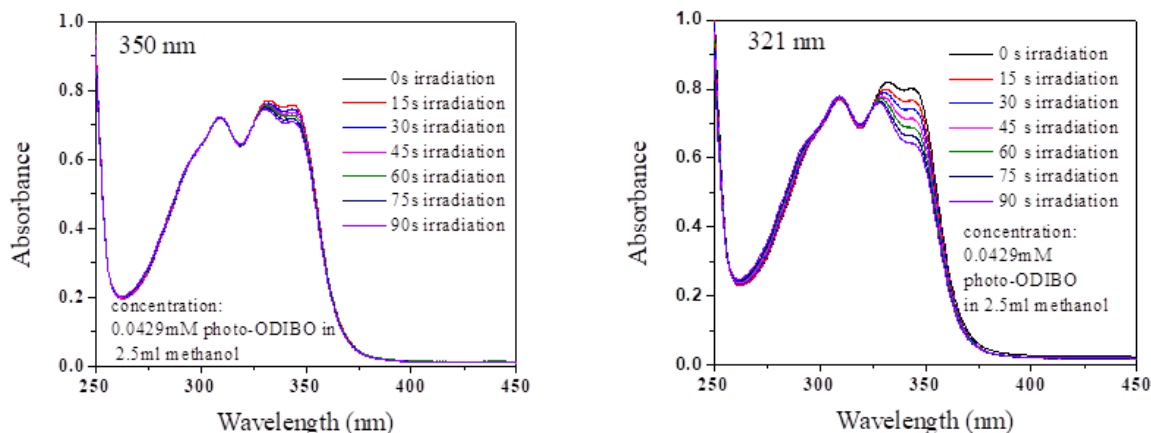


**Figure 3. 2 Photo-ODIBO spectra change in 350 nm and 321 nm (labeled on each spectra)**

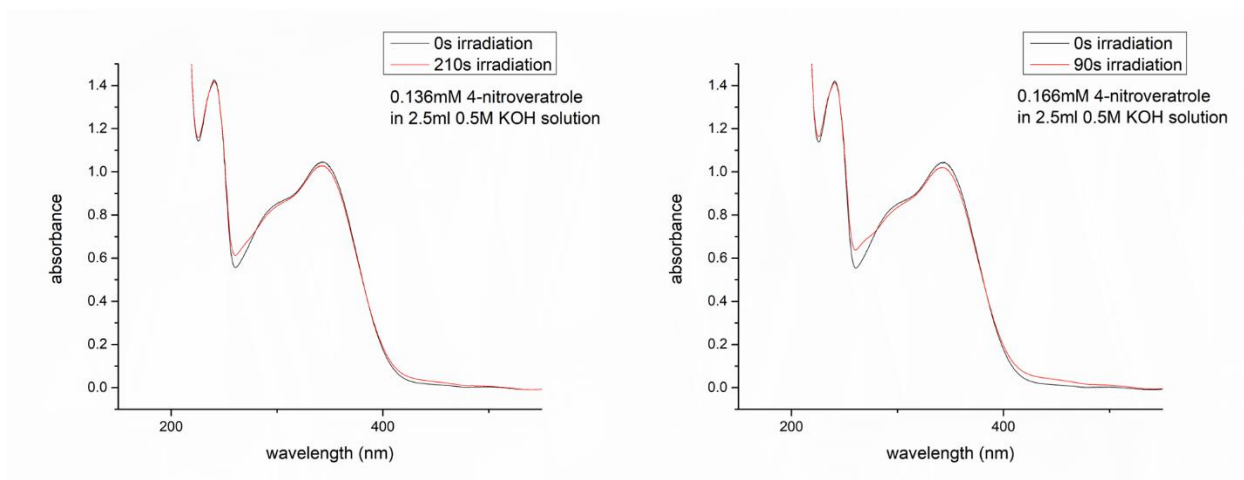


**Figure 3. 3 4-Nitroveratrole spectra change in 350 nm (210s irradiation) and 321 nm (90s irradiation)**

### 3.6.4 Measurement of Triplet-State ODIBO

A graph of the nanosecond transient absorption set-up is presented below. The Nd:YAG laser irradiates the samples in sample housing. The wavelength of the laser can be tuned using

harmonic modules to 266 nm, 355 nm, 523 nm, with 1024 nm original light. The absorbance change and time was recorded by photomultiplier tube detector.

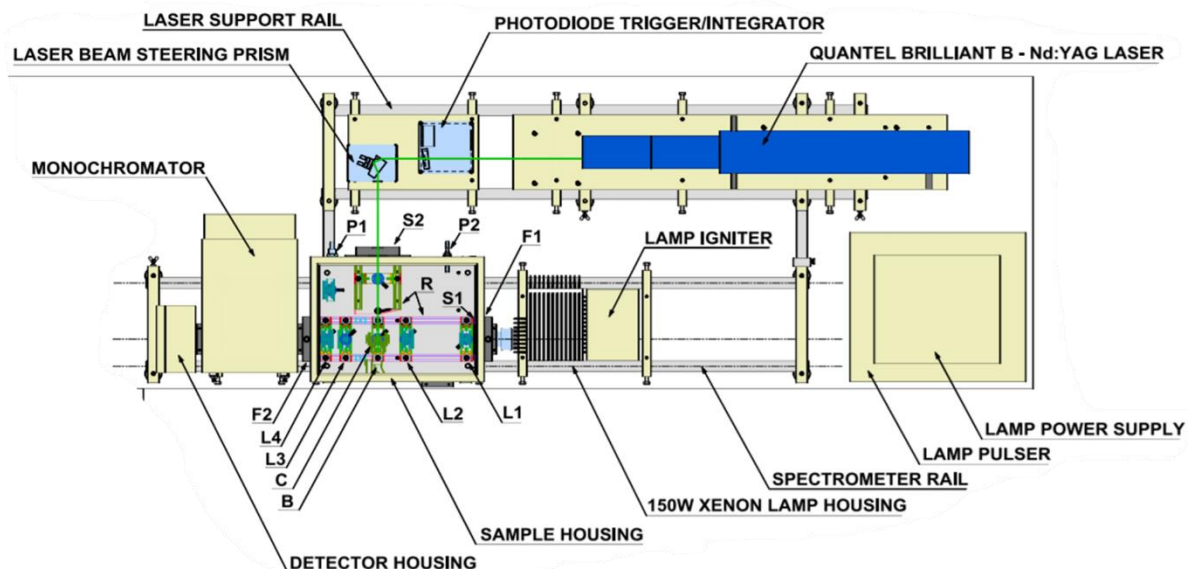


**Figure 3. 4 Nanosecond transient absorption spectrometer set-up**

To test whether oxygen affects the lifetime of the triplet state, we built an easy set-up that enabled us to perform nanosecond transient spectroscopy using the laser kinetic system.

Different gases can be used to fill the yellow balloon, as shown in the graph. The yellow balloon was connected to a part of a syringe head so that the needle can be equipped for the set-up. This needle connected to the balloon has to be dipped under the surface of the solution so that the gas can purge the solution easily. The other needle connected to the air must be placed above the surface of the solution.

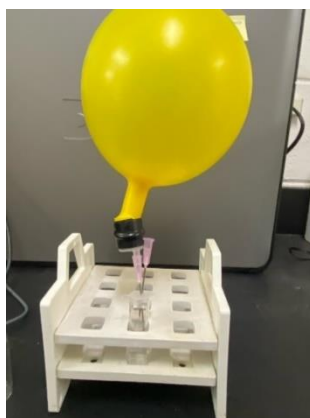


**Figure 3. 5** Set-up of gas purging system used in nanosecond transient spectroscopy

The relationship between absorbance and time was recorded under 390 nm. First, exponential decay was applied to calculate the rate of decay and the lifetime of the triplet. The spectra are depicted below.

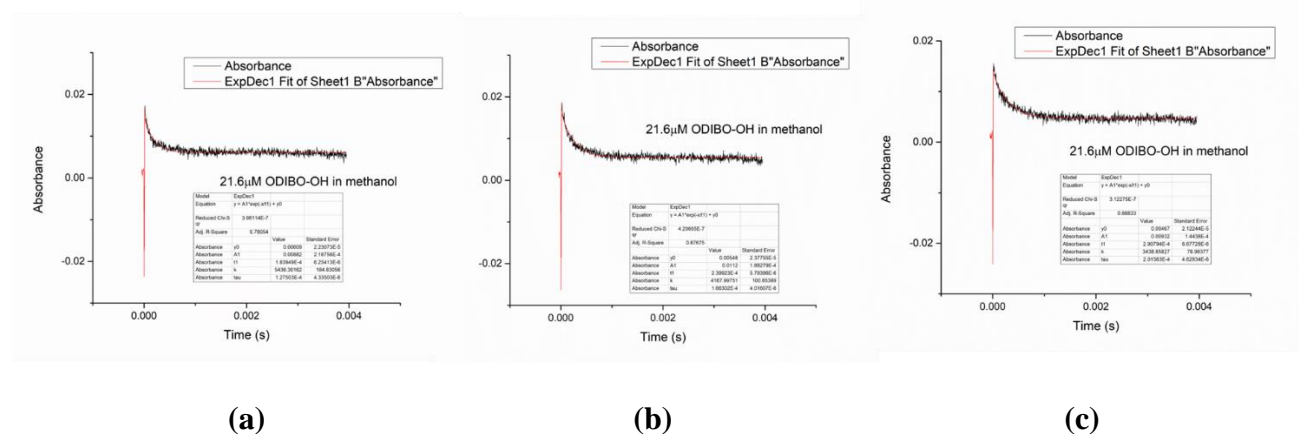


**Figure 3. 6** Nanosecond transient spectroscopy of photo-ODIBO triplet in (a) Oxygen; (b) Air; (c) Argon.

### 3.7 References

1. Shenje, L.; Thompson, W.; Ren, Z.; Lin, N.; Popik, V.; Ullrich, S. Ultrafast Transient Absorption Spectroscopy of the Photodecarbonylation of Photo-oxadibenzocyclooctyne (photo-ODIBO). *The Journal of Chemical Physics* 2021, 154 (7), 074302.
2. Pavlíčková, L.; Kuzmic, P.; Soucek, M. Chemical Actinometry in the UV Range Based on the Photohydrolysis of 3,4-dimethoxynitrobenzene. *Collection of Czechoslovak Chemical Communications* 1986, 51 (2), 368–374.

## CHAPTER 4

### PHOTONIC AMPLIFICATION EFFECT OF PHOTOOXADIBENZYL CYCLOOCTYNE

#### 4.1 Introduction

Most SPAAC reagents contain benzene rings in their structures, because of which most of the compounds are hydrophobic. One strategy to overcome this is to directly irradiate cyclopropenone derivatives in their nanocrystalline state and finish the SPAAC reaction in situ. Thus, it is vital to study the feasibility of cyclopropenone irradiation in the nanocrystalline state.

Garcia-Garibay and his coworkers reported that diphenyl cyclopropenone nanocrystalline suspension showed an enhancement of quantum yield as compared with the solution, which they called ‘photonic amplification’ effect. In a later study, they found that this phenomenon was induced by a quantum chain reaction in which one photon initiates more than one photo reaction<sup>1-5</sup>. Thus, we aimed to observe the photonic amplification effect in photo-ODIBO derivatives.

In this project, we designed a new method using UV-Vis spectrometry to study the photonic amplification effect of photo-ODIBO nanocrystalline in both the acidic environment and neutral environment. Compared to NMR analysis, this would be a more convenient and efficient method, with less waste on deuterated solvents. We hope these findings would facilitate the studies on using nanocrystal strained alkynes for SPAAC linkages.

#### 4.2 Preparation of Nanocrystalline Suspension and Particle Size Measurement

The preparation of nanocrystalline of photo-ODIBO was done in accordance with the steps suggested by our group<sup>6</sup>. First, 5 mL of 2.5 mM photo-ODIBO-OH in methanol was

injected into a stirred 15 mL phosphate buffer solution (stir rate ~ 480rpm) over one minute. The mixture was then sonicated (without stirring) at 60°C for 30 mins to remove methanol. The resulting concentration of nanosuspension was found to be 0.833 mM in phosphate buffer (pH = 7.4). The size of the nanoparticle was determined by the DLS test. We noticed that, if the SDS is not added to the solution, the size of the nanoparticle was inconsistent. With that, we were afraid that the quantum yield of the solution may vary a lot.

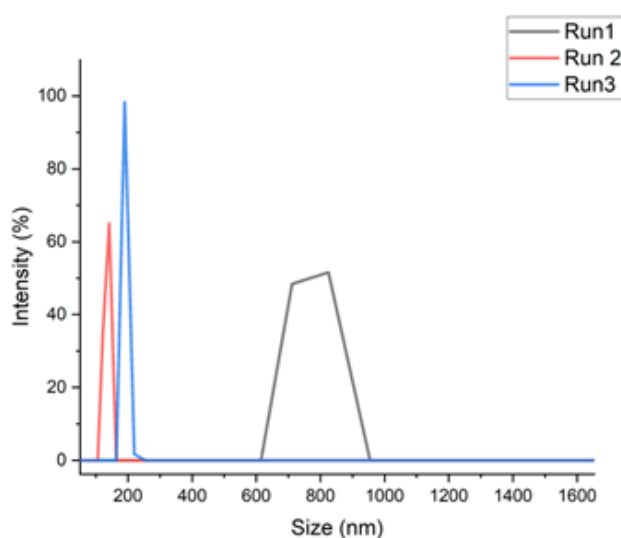


**Figure 4. 1 DLS test result of Photo-ODIBO nanosuspension without surfactant**

Hence, we decided to add 1% surfactant to the solution. Several different surfactants were chosen as candidates. For SDS (sodium dodecyl sulfate) and CTAB (Cetyltrimethyl Ammonium Bromide), the solubility of photo-ODIBO was so high that a solution rather than nanosuspension was formed. For PVP (Polyvinylpyrrolidone), we were able to obtain a constant distribution of photo-ODIBO-OH in phosphate buffer and decent formation of nanocrystals. The size distribution can be determined by the DLS test within a range of 300–600 nm.

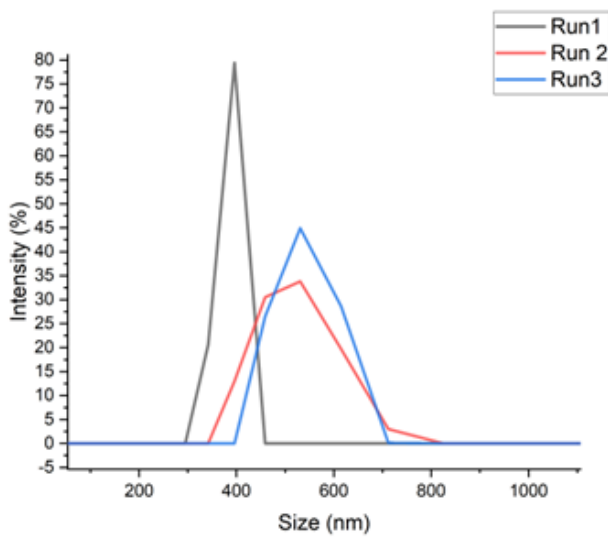


**Figure 4. 2 DLS test result of photo-ODIBO nanosuspension with 1% PVP**

#### **4.3 Measurement of Quantum Yield of Photo-ODIBO Nanosuspension in Neutral Buffer**

After obtaining the nanosuspension, we used a 350-nm light to irradiate the photo-ODIBO nanosuspension. Since concentrated solutions and crystals do not follow the Lambert-Beer law,<sup>8</sup> the nanosuspension must be diluted before UV spectra measurement. For that, we tested the UV spectra of photo-ODIBO using different concentrations of methanol in water. Solvents play a key role in affecting both the extinction coefficient and spectra shape of photo-ODIBO-OH. When photo-ODIBO is dissolved in neat methanol, a peak ( $\lambda = 330-350$  nm) of cyclopropanone could be clearly identified. However, when photo-ODIBO was dissolved in methanol consisting of 10% phosphate buffer, the peak of cyclopropanone was transformed to a broad singlet peak ( $\lambda = 330 - 400$  nm). More interestingly, when the phosphate buffer concentration was increased, the peak ( $\lambda = 330-350$  nm) could be observed again. Thus, we decided to use methanol to dilute the solution ten times.

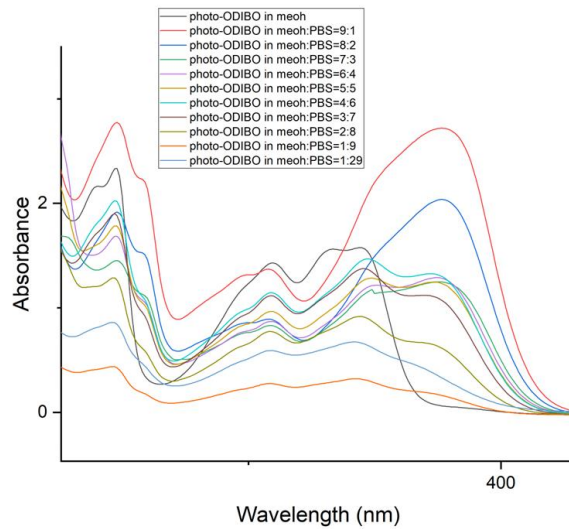


**Figure 4. 3 Photo-ODIBO in varying methanol concentrations in water ( 83  $\mu$ M photo-ODIBO in solvents)**

With the varying of solvent chosen, we needed to remeasure the extinction coefficient of photo-ODIBO-OH in 10% PBS in methanol with PVP. About 1.8 mL methanol and 0.2 mL phosphate buffer solution were mixed and sonicated for 10 mins to obtain a 10% phosphate buffer methanol solution (Solution A). Then, 1 mL of 2.5 mM photo-ODIBO stock solution was injected into a 9 mL solution A with 1% PVP. The resulting suspension was sonicated for 10 mins. Following this, 100  $\mu$ L of the suspension was fully dissolved in solution A each time, and the extinction coefficient was calculated based on the absorbance data ( $\lambda$  Max = 345 nm) taken from UV spectra.

We then irradiated the photo-ODIBO-OH nanosuspension with a 350 nm light for 10 s. About 300  $\mu$ L of nanosuspension was then diluted in 3 mL methanol. The obtained solution was then subjected to UV spectrometry. Thus, we can conclude that the change in the concentration of photo-ODIBO-OH in the solution is  $5.37 \pm 0.1 \mu$ M. Thus, the concentration change of nanosuspension should be  $59.1 \pm 1 \mu$ M.

	0s	10s	Absorbance Change	Concentration Change
Test 1	1.16	1.08	0.0824	5.24E-06
Test 2	1.19	1.10	0.0864	5.49E-06
Test 3	1.24	1.15	0.0850	5.40E-06

**Table 4. 1 Concentration of photo-ODIBO nanosuspension**

For the actinometer, the changes in concentration of 4-veratrole in 10 s were  $44.2 \pm 4 \mu\text{L}$ . We calculated the quantum yield of photo-ODIBO to be  $15.5 \pm 1\%$ . This value is quite close to what we observed from the solution, and no photonic amplification effect was observed. From the experimental design view, we proposed several reasons to explain why no amplification effect can be observed: 1) ionization of photo-ODIBO-OH may affect the decarbonylation of cyclopropanone; 2) high concentration of photo-ODIBO-OH in phosphate buffer. To solve this problem, we measured the quantum of photo-ODIBO-OH in pH under the pKa value of the compound.

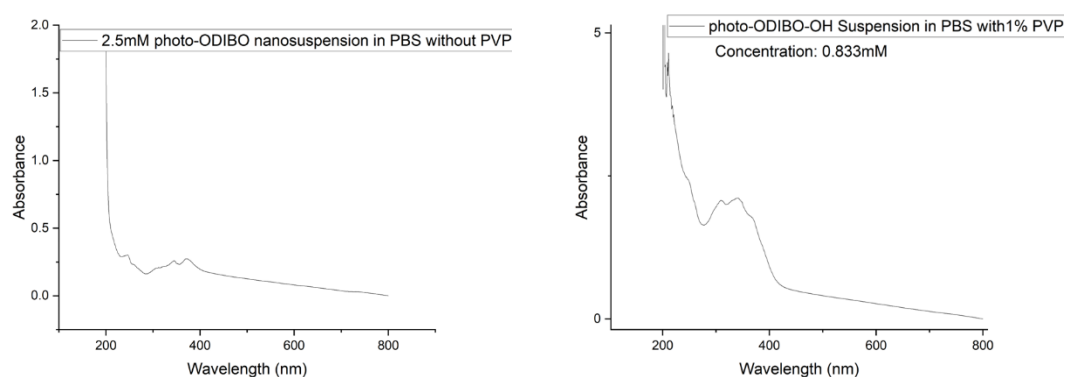


**Figure 4. 4 UV of photo-ODIBO-OH nanosuspension with and without PVP**

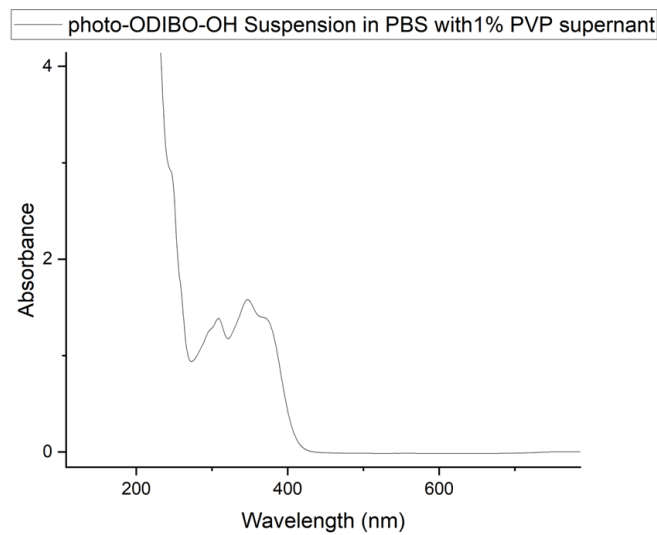


***Figure 4. 5 UV of supernatant of Photo-ODIBO-OH nanosuspension with PVP***

#### **4.4 Measurement of pKa Value of Photo-ODIBO-OH**

To measure the pKa of photo-ODIBO-OH, we prepared a series of buffer solutions with pH ranging from 1 to 12. About 100  $\mu$ L 0.22 mM Photo-ODIBO-OH solution was added to 3.0 mL of the abovementioned solutions to provide a 7.3- $\mu$ M solution. The UV-Vis spectra were taken immediately after solution preparation. The isosbestic point was observed at  $\sim$ 347 nm, except for the solutions with pH values of 1.02 and 2.11. Due to the presence of benzyl groups, photo-ODIBO is not stable in strongly acidic environment and ring opening product would form under this conditions. The Boltzmann fit was then applied to obtain the approximate pKa value, which was expected to be  $7.16 \pm 0.08$ .

#### **4.5 Measurement of Quantum Yield of Photo-ODIBO Nanosuspension in Acidic Buffer**

With a pKa value of around 7, we measured the quantum yield of photo-ODIBO nanosuspension in an acidic environment.

#### 4.5.1 Preparation of Nanosuspension of Photo-ODIBO-OH in Acidic Environment

About 0.167 mL of 2.20 mM photo-ODIBO-OH methanol solution was added to 1 mL phosphate buffer with a pH value of 4.48, through micropipette at a stirring rate of 400 rounds per minute. The solution was then sonicated at 60°C for 5 mins to remove methanol (0.367 mM).

#### 4.5.2 Irradiation of Nanosuspension

The resulting nanosuspension was placed into a photoreactor at a stirring rate of 200 rounds per minute. The nanosuspension was irradiated for 60 s at a wavelength of 350 nm.

#### 4.5.3 Collection of the Spectra

To use the extinction coefficient factor to calculate concentration, a diluted solution is needed. Hence, before the collection of spectra, we used methanol to dilute the nanosuspension. About 5.0 mL of methanol was added to the nanosuspension after irradiation to fully dissolve photo-ODIBO-OH, resulting in the formation of 6 mL of solution (0.612 mM). Following this, the UV spectra were taken for the solutions. Absorbance change was recorded at 345 nm. The extinction coefficient was found to be  $17594 \text{ M}^{-1}\text{cm}^{-1}$  from the previous report. The concentration was then calculated using the extinction coefficient value.

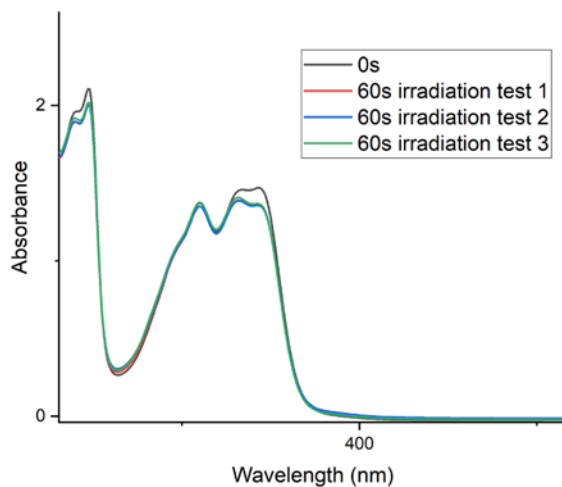


*Figure 4. 6 Spectra change of photo-ODIBO-OH solution before and after irradiation*

#### 4.5.4 Irradiation of 4-Nitroveratrole

To a 20 ml scintillation vial, 1 ml of solution (0.134 mM) was added using a micropipette. A stir bar (20 mm L\* 8mm W) was added, and the stirring rate was controlled at 200 rounds per minute. The sample was then irradiated for 60 s under 350 nm. The experiment was conducted three times to make sure that the results are repeatable. The average absorbance change of 4-nitroveratrole can be calculated as  $0.077 \pm 0.02$ . The concentration change can therefore be calculated as  $25.4 \pm 0.6 \mu\text{M}$ . After correction based on the absorbance differences in irradiation wavelengths of actinometer (Abs = 1.02 at 350 nm) and photo-ODIBO-OH (Abs = 1.28 at 350 nm), the quantum yield was calculated to be  $14.2 \pm 0.7\%$ .

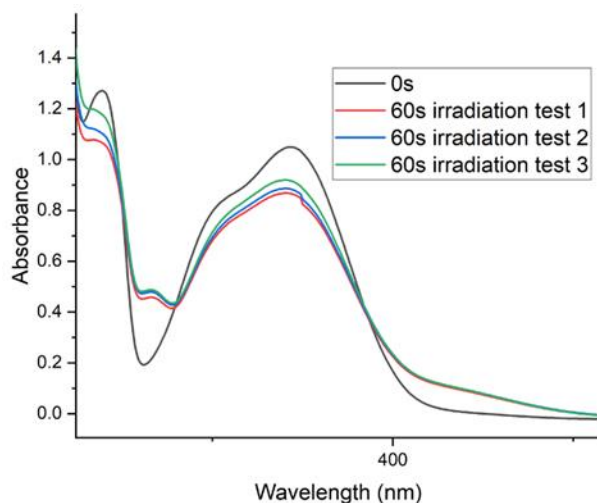


*Figure 4. 7 Spectra change of 4-nitroveratrole solution before and after irradiation*

#### 4.6 Conclusion and Future Work

Interestingly, we did not observe any photonic amplification in the photo-ODIBO-OH compound. One potential explanation of the lack of quantum yield enhancement is that the difference in crystal lattice structure of photo-ODIBO-OH in our study and the nanocrystals in previous reports. We planned to employ single crystal and powder diffractometry to explore

structure of these nanocrystals. We hope these studies can offer new insight into the mechanism of photo-decarbonylation of cyclopropanone derivatives.

## 4.7 Experimental Section

### 4.7.1 Detailed Procedure of Preparation of Nanosuspension:

To a 100 mL round bottom flask, 15 mL phosphate buffer (or 0.1 M NaH<sub>2</sub>PO<sub>4</sub> solution) was added using a micropipette. The solution was then stirred at room temperature at a stirring rate of 480–500 rounds per minute. To the solution, 5 mL of photo-ODIBO-OH methanol stock solution (2.4 mM) was added using a 1 mL syringe (1 mL Norm-Ject) (with 18G1½ needle, 1.2 mm\*40 mm, PrecisionGlide Inc., pink). The stock solution was added dropwise to phosphate buffer, 1.0 mL at a time (5 times to form a total volume of 5.0 mL) at an adding rate of 4–5 drops per second. The mixture was then sonicated at 60°C for 30 mins to remove methanol. The sonicated suspension's concentration was calculated to be 0.833 mM.

### 4.7.2 DLS Data of Photo-ODIBO Nanosuspension without Surfactant

	Run 1	Run 2	Run 3
Test	190	714	282

*Table 4. 2 DLS data of Photo-ODIBO nanosuspension without surfactant*

### 4.7.3 DLS Data of Photo-ODIBO Nanosuspension with 1% PVP

	Run 1	Run 2	Run 3
Test	309	385	567

*Table 4. 3 DLS data of Photo-ODIBO nanosuspension with 1% PVP*

### 4.7.4 UV Spectra Measurement for Different Ratios of Solvent

About 100 µL of 2.5 mM photo-ODIBO-OH in methanol was added to the solvent mixture. The mixture's ratios are provided below. The mixture was then sonicated for 10 mins

until clear solutions were obtained. Then UV spectra were taken immediately after each sonication.

	2.5 mM photo-ODIBO-OH solution (10 <sup>-2</sup> mL)	PBS (10 <sup>-2</sup> mL)	Methanol (10 <sup>-2</sup> mL)	Concentration (μM)
96.6% PBS in Methanol	1	29	0	83.3
90% PBS in Methanol	1	27	2	
80% PBS in Methanol	1	24	5	
70% PBS in Methanol	1	21	8	
60% PBS in Methanol	1	18	11	
50% PBS in Methanol	1	15	14	
40% PBS in Methanol	1	12	17	
30% PBS in Methanol	1	9	20	
20% PBS in Methanol	1	6	23	

10% PBS in Methanol	1	3	26	
------------------------	---	---	----	--

**Table 4. 4 Formula to prepare Photo-ODIBO using varying concentrations of PBS and methanol**

#### 4.7.5 Detailed Procedure of Measurement on UV Spectra of Supernatant

After sonication at 60°C for 30 mins, the suspension was separated into 15 centrifuge tubes evenly using a micropipette (1 mL at a time). Then, six of them were placed properly in a centrifuge (placed while ensuring the rotors were balanced). The tubes were centrifuged for 10 mins at 20000 rcf. The upper clear solutions (0.9 mL) were separated and placed in another six 1.5 mL centrifuge tubes and centrifuged for another 10 mins at 20000 rcf. From each centrifuge tube, the upper clear solutions (0.8 mL) were collected and placed into another six 1.5 mL centrifuge tubes and centrifuged for another 10 mins at 20000 rcf. Then the upper clear solution (0.7 mL) was collected and combined. Then the UV-Vis experiment was conducted to record the spectrum.

#### 4.7.6 Buffer Preparation for pKa Value Determination

0.1 M HClO <sub>4</sub>	0.1 M HClO <sub>4</sub>	1.02
0.01 M HClO <sub>4</sub>	10 mL 0.1 M HClO <sub>4</sub> + 90 mL 0.1 M NaCl	2.11
0.001 M HClO <sub>4</sub>	1 mL 0.1 M HClO <sub>4</sub> + 99 mL 0.1 M NaCl	3.14
Acetic Buffer (BR = 4)	10 mL 0.1 M NaOAc + 40 mL 0.1 M HOAc+ 40 mL 0.2 M NaCl	3.7
Acetic Buffer (BR = 1)	25 mL 0.1 M NaOAc + 25 mL 0.1 M HOAc+ 25 mL 0.2 M NaCl	4.34

Acetic Buffer (BR = 0.25)	40 mL 0.1 M NaOAc + 10 mL 0.1 M HOAc+ 10 mL 0.2 M NaCl	5.04
BP Buffer (BR = 4)	40 mL 0.1 M NaH <sub>2</sub> PO <sub>4</sub> + 30 mL 0.0333 M Na <sub>2</sub> HPO <sub>4</sub>	6.57
BP Buffer (BR = 1)	20 mL 0.1 M NaH <sub>2</sub> PO <sub>4</sub> + 60 mL 0.0333 M Na <sub>2</sub> HPO <sub>4</sub>	7.02
BP Buffer (BR = 0.25)	5 mL 0.1 M NaH <sub>2</sub> PO <sub>4</sub> + 60 mL 0.0333 M Na <sub>2</sub> HPO <sub>4</sub>	7.72
BP Buffer (BR = 0.20)	5 mL 0.1 M NaH <sub>2</sub> PO <sub>4</sub> + 75 mL 0.0333 M Na <sub>2</sub> HPO <sub>4</sub>	7.91
BP Buffer (BR = 0.15)	5 mL 0.1 M NaH <sub>2</sub> PO <sub>4</sub> + 100 mL 0.0333 M Na <sub>2</sub> HPO <sub>4</sub>	8.03
BP Buffer (BR = 0.10)	3 mL 0.1 M NaH <sub>2</sub> PO <sub>4</sub> + 90 mL 0.0333 M Na <sub>2</sub> HPO <sub>4</sub>	8.12
BP Buffer (BR = 0.033)	1 mL 0.1 M NaH <sub>2</sub> PO <sub>4</sub> + 90 mL 0.0333 M Na <sub>2</sub> HPO <sub>4</sub>	8.76

**Table 4. 5 Buffer preparation and pH value**

#### 4.7.7 UV Spectra of Determination of pKa Value of Photo-ODIBO-OH

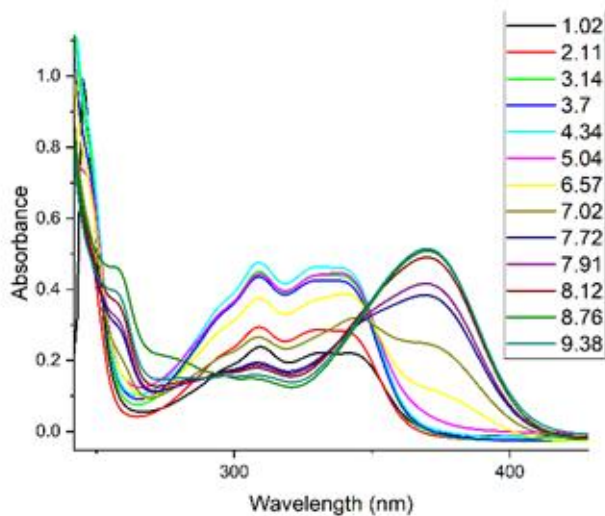


**Figure 4. 8 UV spectra of Photo-ODIBO-OH in buffer with varying pH**

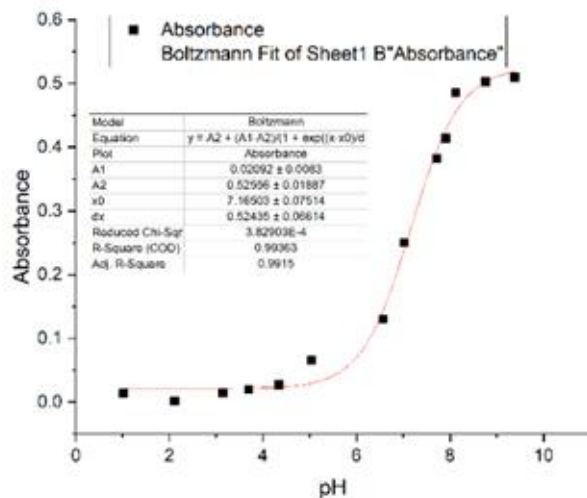


**Figure 4. 9 Boltzmann fitting of pKa value of Photo-ODIBO-OH**

#### 4.7.8 Nanosuspension Irradiation

For creating the nanosuspension in a neutral environment, the following procedure was followed. To a 20 mL scintillation vial, 3 mL of the solution was added using a micropipette (1 mL at a time). A stir bar (20 mm L\*8 mm W) was added, and the stirring rate was controlled at 240 rounds per minute. The sample was then irradiated for 10 s (nanosuspension) or 5 s (actinometer).

#### 4.7.9 Concentration Change of Photo-ODIBO-OH Nanosuspension

	0s Abs	60s Abs	Abs Change	Concentration Change	Average Concentration Change (μM)	Average Concentration Change in Nanosuspension (μM)
Test 1	1.46	1.35	0.11	6.15	6.17 ± 0.2	32.6 ± 1

Test 2		1.35	0.11	6.42		
Test 3		1.36	0.10	5.92		

***Table 4. 6 Concentration change of Photo-ODIBO-OH nanosuspension***

#### 4.8 References:

1. Kuzmanich, G.; Gard, M. N.; Garcia-Garibay, M. A. Photonic Amplification by a Single-State Quantum Chain Reaction in the Photodecarbonylation of Crystalline Diarylcyclopropanones. *Journal of the American Chemical Society* 2009, 131 (32), 11606-11614.
2. Kuzmanich, G.; Natarajan, A.; Chin, K. K.; Veerman, M.; Mortko, C. J.; Garcia-Garibay, M. A. Solid-State Photodecarbonylation of Diphenylcyclopropanone: A Quantum Chain Process Made Possible by Ultrafast Energy Transfer. *Journal of the American Chemical Society* 2008, 130 (4), 1140-1144.
3. Doan, S. C.; Kuzmanich, G.; Gard, M. N.; Garcia-Garibay, M. A.; Schwartz, B. J. Ultrafast Spectroscopic Observation of a Quantum Chain Reaction: The Photodecarbonylation of Nanocrystalline Diphenylcyclopropanone. *The Journal of Physical Chemistry Letters* 2012, 3 (1), 81-86.
4. Nielsen, A.; Kuzmanich, G.; Garcia-Garibay, M. A. Quantum Chain Reaction of Tethered Diarylcyclopropanones in the Solid State and Their Distance-Dependence in Solution Reveal a Dexter S<sub>2</sub>-S<sub>2</sub> Energy-Transfer Mechanism. *The Journal of Physical Chemistry A* 2014, 118 (10), 1858-1863.
5. Hernández-Linares, M. G.; Guerrero-Luna, G.; Pérez-Estrada, S.; Ellison, M.; Ortin, M.-M.; Garcia-Garibay, M. A. Large-Scale Green Chemical Synthesis of Adjacent Quaternary Chiral Centers by Continuous Flow Photodecarbonylation of Aqueous

6. Suspensions of Nanocrystalline Ketones. *Journal of the American Chemical Society* 2015, 137 (4), 1679-1684.
7. Sutton, D. A.; Yu, S.-H.; Steet, R.; Popik, V. V. Cyclopropenone-Caged Sondheimer diyne (dibenzo[a,e]cyclooctadiyne): A Photoactivatable Linchpin for Efficient SPAAC Crosslinking. *Chemical Communications* 2016, 52 (3), 553-556.
8. Oshina, I.; Spigulis, J. Beer-Lambert law for optical tissue diagnostics: current state of the art and the main limitations. *Journal of biomedical optics* 2021, 26 (10), 100901.

## CHAPTER 5

### MEASUREMENT OF QUANTUM YIELD OF PHOTO-ODIBO-OH IN DIFFERENT PH ENVIRONMENT

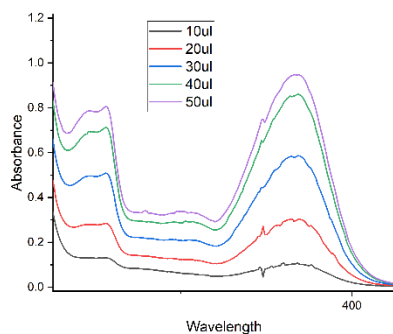
#### 5.1 Introduction

UV light is a common agent used to remove the carbonyl groups from cyclopropenone derivatives. Usually, UV irradiation is sufficient, with a quantum yield of 20–60 %<sup>1-6</sup>. Occasionally, we have found that it is difficult to remove carbonyl groups in a basic condition. In this chapter, we describe how we discovered the quantum yield of photochemistry on photo-ODIBO-OH in a basic environment and used a fluorometer to explain the reason behind it.

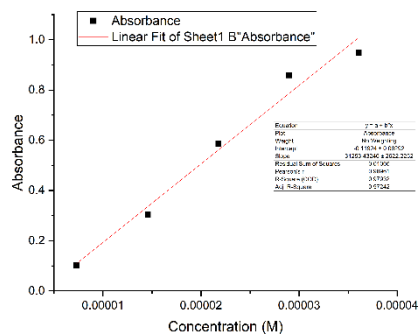
#### 5.2 Measurement of Quantum Yield of Photo-ODIBO-OH in Basic Condition

##### 5.2.1 Measurement of Extinction Coefficient of Photo-ODIBO in Basic Environment

About 10  $\mu\text{L}$  of the resulting stock solution was added to 3 mL of 0.0167 mM  $\text{Na}_3\text{PO}_4$  solution (pH = 12.3). The UV spectra were measured and absorbance was calculated at 346 nm. The extinction coefficient was calculated to be  $31000 \pm 3000 \text{ M}^{-1}\text{cm}^{-1}$ .



(a)



(b)

**Figure 5. 1 UV spectra of Photo-ODIBO solution (a) and Extinction coefficient (b)**

### 5.2.2 Irradiation of Photo-ODIBO-OH in Basic Conditions

For the solution to be irradiated, 50  $\mu\text{L}$  of 2.20 mM photo-ODIBO-OH methanol solution was added to 3 mL of buffer solution (pH = 12.3) (36  $\mu\text{M}$ ). The samples were irradiated for 600 s, and UV spectra were collected before and after irradiation. The experiments were repeated thrice. Absorbance changes were observed at 368 nm. Average concentration changes were calculated to be  $2.6 \pm 0.4 \mu\text{M}$  in 600 s.

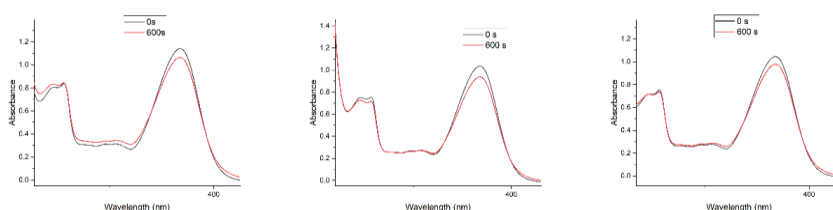


**Figure 5. 2 Irradiation of Photo-ODIBO-OH in basic conditions**

### 5.3 Measurement of Irradiation of Actinometer

About 3.0 mL of 4-nitroveratrole was irradiated for 30 s at 350 nm. The experiments were repeated thrice. Average concentration changes were calculated to be  $21.3 \pm 0.5 \mu\text{M}$  in 60 s. Average concentration changes could be calculated as  $213 \pm 5 \mu\text{M}$  in 600 s. Based on the values of absorbance of photo-ODIBO and 4-NV at 350 nm into consideration, we calculated the quantum yield of photo-ODIBO-OH in basic conditions to be  $0.14 \pm 0.02\%$ .

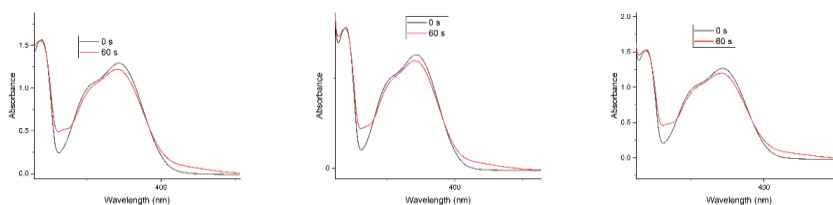


**Figure 5. 3 Irradiation of 4-nitroveratrole**

## 5.4 Irradiation of Photo-ODIBO-OH in Acidic Conditions

### 5.4.1 Preparation of Stock Solution

About 4 mL of 2.2 mM photo-ODIBO-OH methanol solution was diluted in 12 mL methanol (0.55 mM).

### 5.4.2 Measurement of Concentration Change

About 300  $\mu\text{L}$  stock solution was dissolved in 2 mL of buffer ( $\text{pH} = 4.48$ ) ( $71.7 \mu\text{M}$ ) (13% methanol in buffer). Samples were irradiated for 60 s, and UV spectra were taken before and after irradiation. Average concentration changes were found to be  $8.8 \pm 0.6 \mu\text{M}$  in 60 s. After calculating the absorbance of photo-ODIBO and 4-NV at 350 nm, we calculated the quantum yield of photo-ODIBO-OH in acidic conditions to be  $4.8 \pm 0.4\%$ . The quantum yield in acidic conditions was around 35 times the quantum yield in basic conditions. The results exhibit that ionization of photo-ODIBO-OH would greatly affect the quantum yield of photo-decarbonylation reaction of the compound. The negative charged phenolate compound showed much less reactivity than neutral phenol photo-ODIBO-OH compounds.

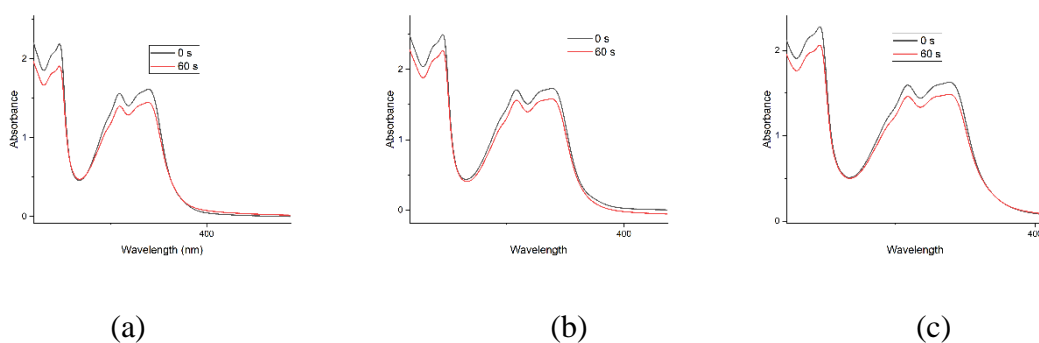


**Figure 5. 4 Irradiation of photo-ODIBO-OH in acidic conditions**

## 5.4 Measurement of Quantum Yield of Photo-ODIBO-Acid in Basic Conditions

To verify whether negative charge carried by photo-ODIBO-OH in basic solution is the key factor that affects the quantum yield of photo-ODIBO irradiation in solution, we measured the quantum yield of photo-ODIBO-Acid in basic conditions.

### 5.4 1 Preparation of Stock Solution of Photo-ODIBO Acid in Methanol and DMF Mixture

Due to the limited solubility of photo-ODIBO-Acid in methanol, the stock solution was prepared in a methanol and DMF mixture. About 22.3 mg photo-ODIBO-Acid was dissolved in 50 mL of methanol and DMF (1:1) and sonicated for 10 mins. The solution concentration was found to be 1.22 mM.

### 5.4 2 Measurement of Extinction Coefficient Factor of Photo-ODIBO-Acid

About 20  $\mu\text{L}$  of Photo-ODIBO-Acid stock solution was added to 3 mL of 0.0167 mM  $\text{Na}_3\text{PO}_4$  solution each time. UV-Vis spectrometer was used to determine absorbance. The extinction coefficient factor of photo-ODIBO-Acid was found to be  $14900 \pm 500 \text{ cm}^{-1} \text{ M}^{-1}$ .

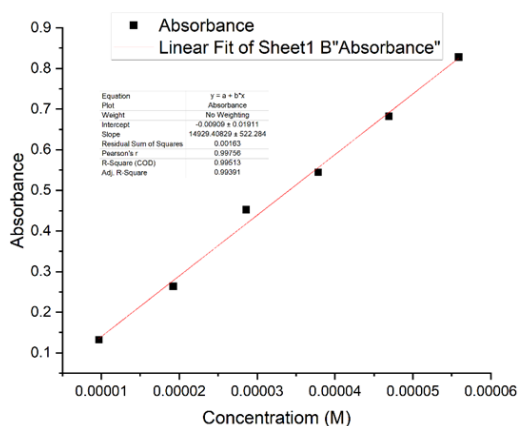


*Figure 5. 5 Measurement of extinction coefficient factor*

### **5.4.3 Preparation of Photo-ODIBO-Acid Solution in Basic Environment**

About 0.334 mL of 1.22 mM photo-ODIBO acid stock solution was added to 1 mL (pH = 12.26)  $\text{Na}_3\text{PO}_4$  through a micropipette at a stirring rate of 400 rounds per minute. The solution was then sonicated at 60°C for 5 mins to remove methanol (0.407 mM).

### **5.4.4 Irradiation of Photo-ODIBO-Acid Solution in Basic Environment**

The resulting solution was placed inside a photoreactor at a stirring rate of 200 rounds per minute. The solution was irradiated for 60 s at a wavelength of 350 nm. About 10 ml of  $\text{Na}_3\text{PO}_4$  (pH = 12.26) was added to the solution after irradiation to fully dissolved photo-ODIBO-OH, finally obtaining 11 ml of the solution. Then UV spectra were taken for the solutions.

Absorbance change was recorded at 345 nm. The average absorbance change of the solution can be calculated as  $0.021 \pm 0.001$ . The average concentration of the solution can be calculated as  $1.5 \pm 0.1 \mu\text{M}$ . Since we used methanol to dilute the solution, the average concentration change of the solution before the dilution can be calculated as  $17 \pm 1 \mu\text{M}$ . The quantum yield of photo-ODIBO-Acid was found to be  $7 \pm 1\%$ . The quantum yield of photo-ODIBO-Acid in basic conditions showed a higher quantum yield than the photo-ODIBO-OH solution in basic conditions, which excludes the reason for negative-charged depression in the quantum yield.

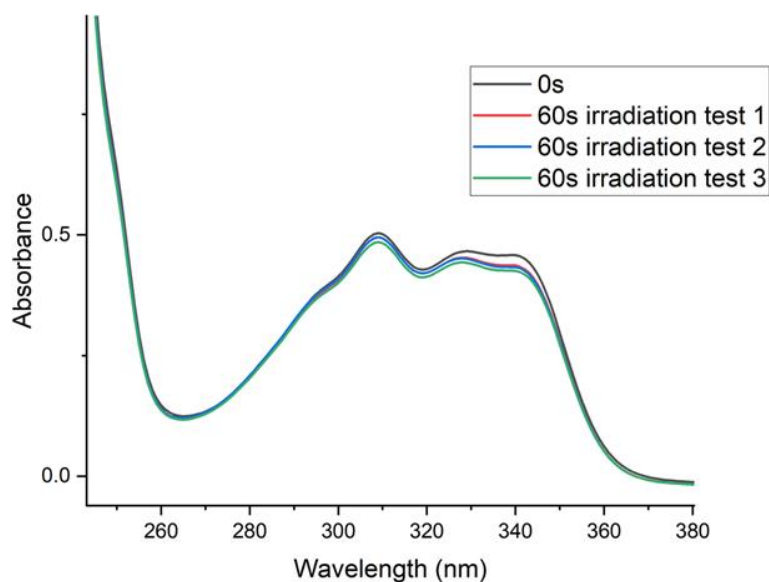


***Figure 5. 6 Spectra change of photo-ODIBO acid solution before and after irradiation***

### **5.5 Fluorescence Spectra Measurement**

When a molecule gets excited, it undergoes radiative decay, also known as fluorescence or phosphorescence emission, or a chemical reaction. Thus, fluorescence emission and photochemical pathways are actually competitive relationships concerning the use of photons. For our compound, if the photons were not used in a chemical reaction, one possible reason could be that our compound exhibits high fluorescence emission in basic solutions. We measured the fluorescence quantum yield for photo-ODIBO-OH in both basic conditions and acidic conditions. The quantum yield measurement followed the previous report<sup>7</sup>. We used quinine sulfate as the actinometer, which has a known quantum yield value of 0.54.

### 5.5.1 UV Spectra of Quinine Sulfate and Photo-ODIBO-OH with Gradient Concentrations

**Quinine Sulfate:** 0.1, 0.2, 0.3, 0.4, and 0.5 mL of stock solution were added to 3 mL of 0.5 M H<sub>2</sub>SO<sub>4</sub>, and UV spectra were taken for each mixture. The same quinine sulfate was used for 345-nm irradiation and 368-nm irradiation. Thus, only one set of UV data was collected.

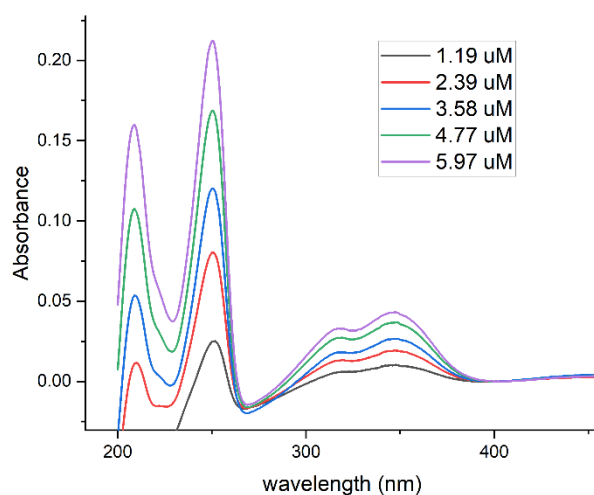


*Figure 5. 7 UV spectra of quinine sulfate solutions used in measurement*

**Photo-ODIBO-OH in Methanol:** 0.1, 0.2, 0.3, and 0.4 mL of stock solution was added to 3 mL of methanol with 0.1 mL 1.1 mM sodium azide in water. UV spectra were taken each time.

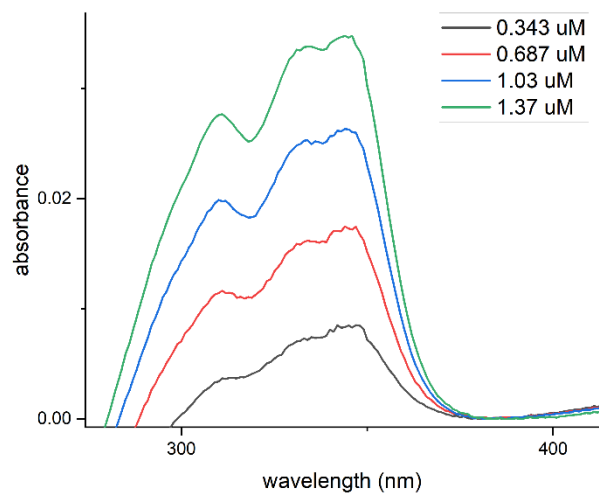


**Figure 5. 8 UV spectra of photo-ODIBO-OH methanol solutions used in measurement**

**Photo-ODIBO-OH in Basic:** 0.01, 0.02, 0.03, 0.04, and 0.05 mL of stock solution was added to 3 mL of 0.0167 M  $\text{Na}_3\text{PO}_4$ , and UV spectra were taken for each mixture.

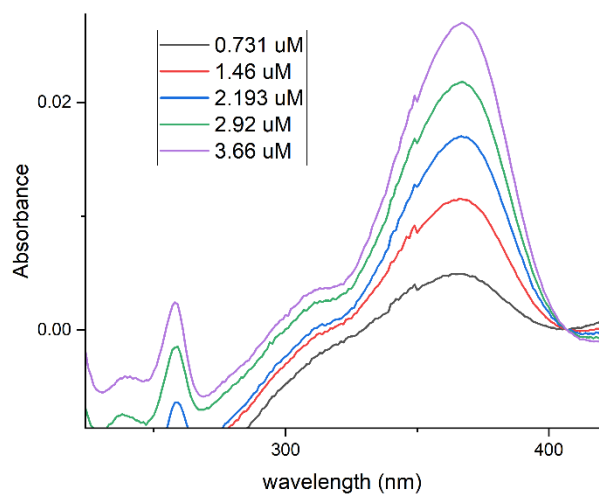


**Figure 5. 9 UV spectra of photo-ODIBO-OH  $\text{Na}_3\text{PO}_4$  solutions used in measurement**

## 5.5.2 Fluorescence Spectra of Quinine Sulfate and Photo-ODIBO-OH with Gradient Concentrations

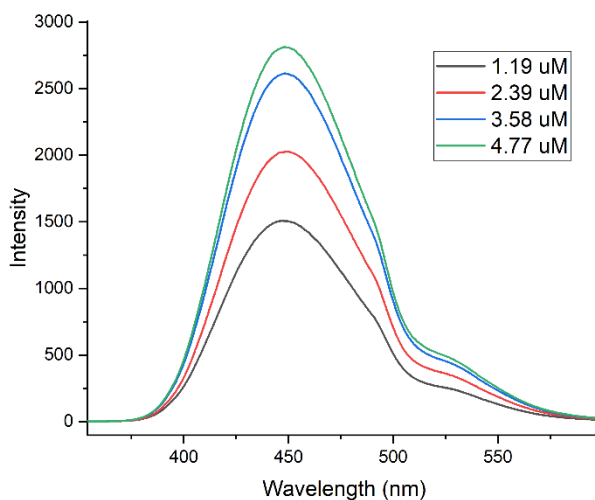


**Figure 5. 10 Quinine sulfate fluorescence spectra (excitation wavelength: 345 nm)**

Using the information above, we developed a relationship between the absorbance of the solution and the fluorescence intensity area. The slope value was found to be  $6.2 * 10^6 \pm 2 * 10^5$ . For the photo-ODIBO-OH solution in methanol, the slope value was calculated as  $1.4 * 10^5 \pm 1 * 10^4$ . For photo-ODIBO-OH in  $\text{Na}_3\text{PO}_4$  solution, the slope value was  $2.55 * 10^6 \pm 8 * 10^4$ .

Fluorescence quantum yield can be calculated using the following equation:

$$Q = Q_{Act} \left( \frac{Grad}{Grad_R} \right) \left( \frac{n^2}{n_R^2} \right)$$

where  $Q_{Act}$  is the quantum yield of actinometer, Grad is the slope value between absorbance and fluorescence intensity in photo-ODIBO solution,  $Grad_R$  is the slope value between absorbance and fluorescence intensity in the actinometer solution, n is the reflective index value of solvent of photo-ODIBO, and  $n_R$  is the reflective index value of solvent of actinometer. If it is methanol,  $n = 1.33$ . If it is 0.5 M  $\text{H}_2\text{SO}_4$ ,  $n = 1.35$ . If it is  $\text{Na}_3\text{PO}_4$ ,  $n = 1.48$ <sup>8</sup>.

Thus, the fluorescence quantum yield of photo-ODIBO-OH methanol solution was calculated to be  $1.2 \pm 0.1\%$ ; the fluorescence quantum yield of photo-ODIBO-OH in  $\text{Na}_3\text{PO}_4$  was  $22 \pm 3\%$ .

## 5.6 Conclusion

In this chapter, we discussed the recent findings regarding the difference in the quantum yield of photo-ODIBO-OH in basic conditions. For quantum yield of photo-ODIBO-OH in acidic condition, the quantum yield is  $4.8 \pm 0.4\%$ , while for the quantum yield in basic condition, it is  $0.14 \pm 0.02\%$ . Photo-ODIBO-OH showed much less reactivity under basic condition than acidic conditions, concerning photo-decarbonylation reactions. With the measurement of quantum yield of photo-decarbonylation of photo-ODIBO-Acid, we proved that the difference was not because of a negative charge. Further investigation into fluorescence quantum yield proved that most of the photons in the photo-ODIBO-OH basic solution was consumed in fluorescence emission. The fluorescence quantum yield results revealed that in photo-ODIBO-OH methanol solution, most of the photons were used in the photo-chemical reaction; in photo-ODIBO-OH in a basic environment, most of the photons were consumed in fluorescence radiative decay. This explains why photo-ODIBO-OH was unreactive during photo-decarbonylation under 350 nm.

## 5.7 Experimental Section

### 5.7.1 Concentration of Solutions Used in Measurement of Extinction Coefficient of Photo-ODIBO-OH in Basic Conditions

	10 $\mu\text{L}$	20 $\mu\text{L}$	30 $\mu\text{L}$	40 $\mu\text{L}$	50 $\mu\text{L}$
--	------------------	------------------	------------------	------------------	------------------

Solution	3.01	3.02	3.03	3.04	3.05
Volume (mL)					
Solution Concentration (M)	7.32E-06	1.46E-05	2.18E-05	2.89E-05	3.61E-05

**Table 5. 1 Concentration of solutions used in measurement of extinction coefficient**

### 5.7.2 Data of Concentration Change of Photo-ODIBO-OH in Basic Conditions

	Test 1	Test 2	Test 3
Before Irradiation	1.14	1.04	1.04
After Irradiation	1.06	0.938	0.978
Absorbance Change	0.0767	0.0976	0.0678

**Table 5. 2 Absorbance change before and after irradiation in basic conditions**

### 5.7.3 Data of Concentration Change of Photo-ODIBO-OH in Acidic Condition

	Test 1	Test 2	Test 3
Before Irradiation	1.61	1.73	1.63
After Irradiation	1.45	1.58	1.48
Absorbance Change	0.168	0.151	0.143

**Table 5. 3 Absorbance change before and after irradiation in acidic conditions**

**5.7.4 Concentration of Solutions Used in Measurement of Extinction Coefficient of Photo-ODIBO-Acid in Basic Conditions**

	20 $\mu$ L	40 $\mu$ L	60 $\mu$ L	80 $\mu$ L	100 $\mu$ L	120 $\mu$ L
Solution	2.52	2.54	2.56	2.58	2.60	2.62
Volume (mL)						
Solution	9.68 E-06	1.92 E-05	2.86 E-05	3.78 E-05	4.69 E-05	5.59 E-
Concentration (M)						05

*Table 5. 4 Absorbance change before and after irradiation in acidic conditions*

**5.7.5 Preparation of Stock Solution for Fluorescence Spectra Measurement**

**Quinine Sulfate:** 2.9 mg of quinine sulfate was dissolved in 100 mL of 0.5 M H<sub>2</sub>SO<sub>4</sub>.

The solution was sonicated for 30 mins before use (37.0  $\mu$ L).

**Photo-ODIBO-OH in Methanol:** 1 mL of 0.22 mM photo-ODIBO-OH was dissolved in 19 mL of methanol to provide 11  $\mu$ M of stock solution.

**Photo-ODIBO-OH in Na<sub>3</sub>PO<sub>4</sub>:** 1 mL of 2.2 mM photo-ODIBO-OH methanol solution was dissolved in 9 mL of Na<sub>3</sub>PO<sub>4</sub> to provide 0.22 mM stock solution.

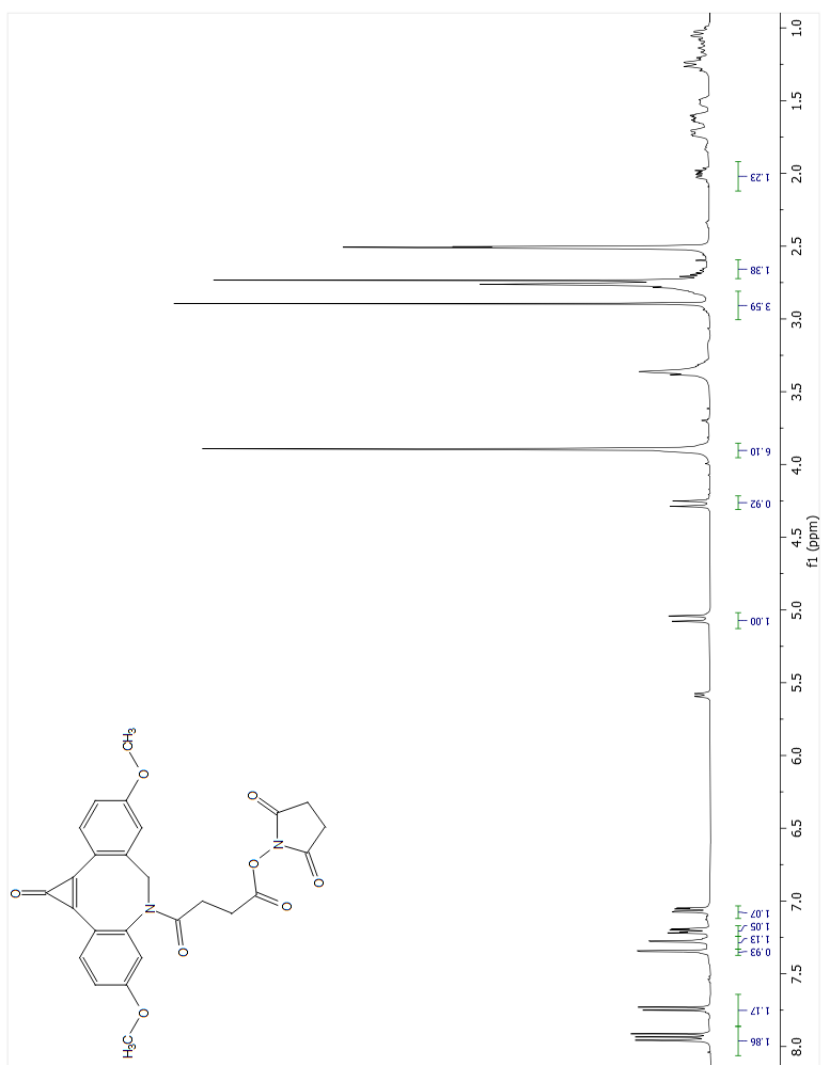
## 5.8 References

1. Poloukhine, A.; Popik, V. V. Highly Efficient Photochemical Generation of a Triple Bond: Synthesis, Properties, and Photodecarbonylation of Cyclopropenones. *The Journal of Organic Chemistry* 2003, 68 (20), 7833-7840.
2. Kuzmin, A. V.; Popik, V. V. Dual Reactivity of a Photochemically-generated Cyclic Enyne–allene. *Chemical Communications* 2009, (38), 5707-5709.
3. Zhu, Z.-B.; Wei, Y.; Shi, M. Recent Developments of Cyclopropene Chemistry. *Chemical Society Reviews* 2011, 40 (11), 5534-5563.
4. McNitt, C. D.; Popik, V. V. Photochemical Generation of Oxa-dibenzocyclooctyne (ODIBO) for Metal-free Click Ligations. *Organic & Biomolecular Chemistry* 2012, 10 (41), 8200-8202.
5. Arumugam, S.; Orski, S. V.; Mbua, N. E.; McNitt, C.; Boons, G.-J.; Locklin, J.; Popik, V. V. Photo-click Chemistry Strategies for Spatiotemporal Control of Metal-free Ligation, Labeling, and Surface Derivatization. *Pure and Applied Chemistry* 2013, 85 (7), 1499-1513.
6. Sutton, D. A.; Yu, S.-H.; Steet, R.; Popik, V. V. Cyclopropenone-caged Sondheimer diyne (dibenzo[a,e]cyclooctadiyne): A Photoactivatable Linchpin for Efficient SPAAC Crosslinking. *Chemical Communications* 2016, 52 (3), 553-556.
7. Dhimi, S.; Mello, A. J. D.; Rumbles, G.; Bishop, S. M.; Phillips, D.; Beeby, A. Phthalocyanine Fluorescence at High Concentration: Dimers or Reabsorption Effect? *Photochemistry and Photobiology* 1995, 61 (4), 341-346.

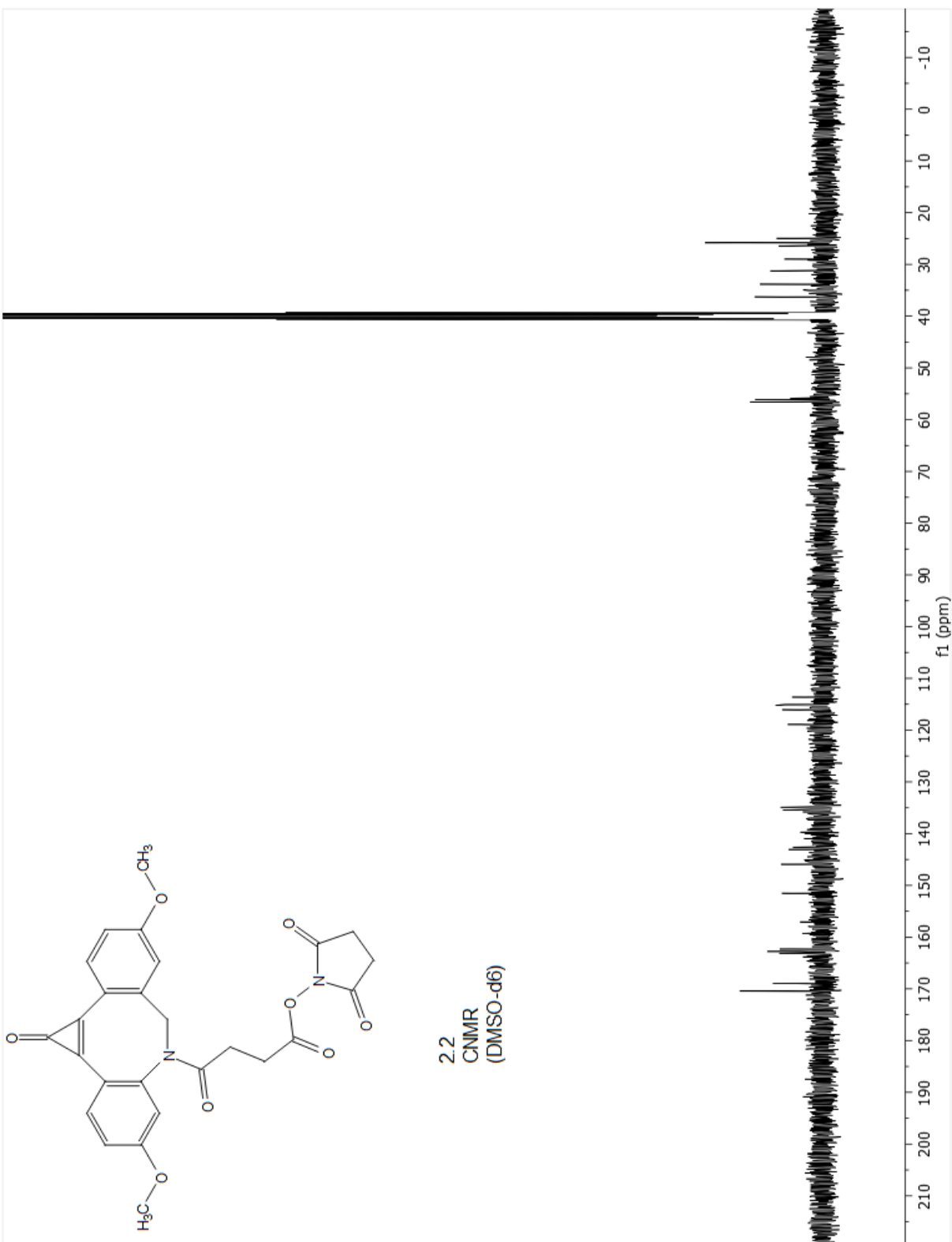
8. CRC Handbook of Chemistry and Physics, Robert Weast (ed.), CRC Press, Boca Raton, Florida, v. 61, 1980

## APPENDICES

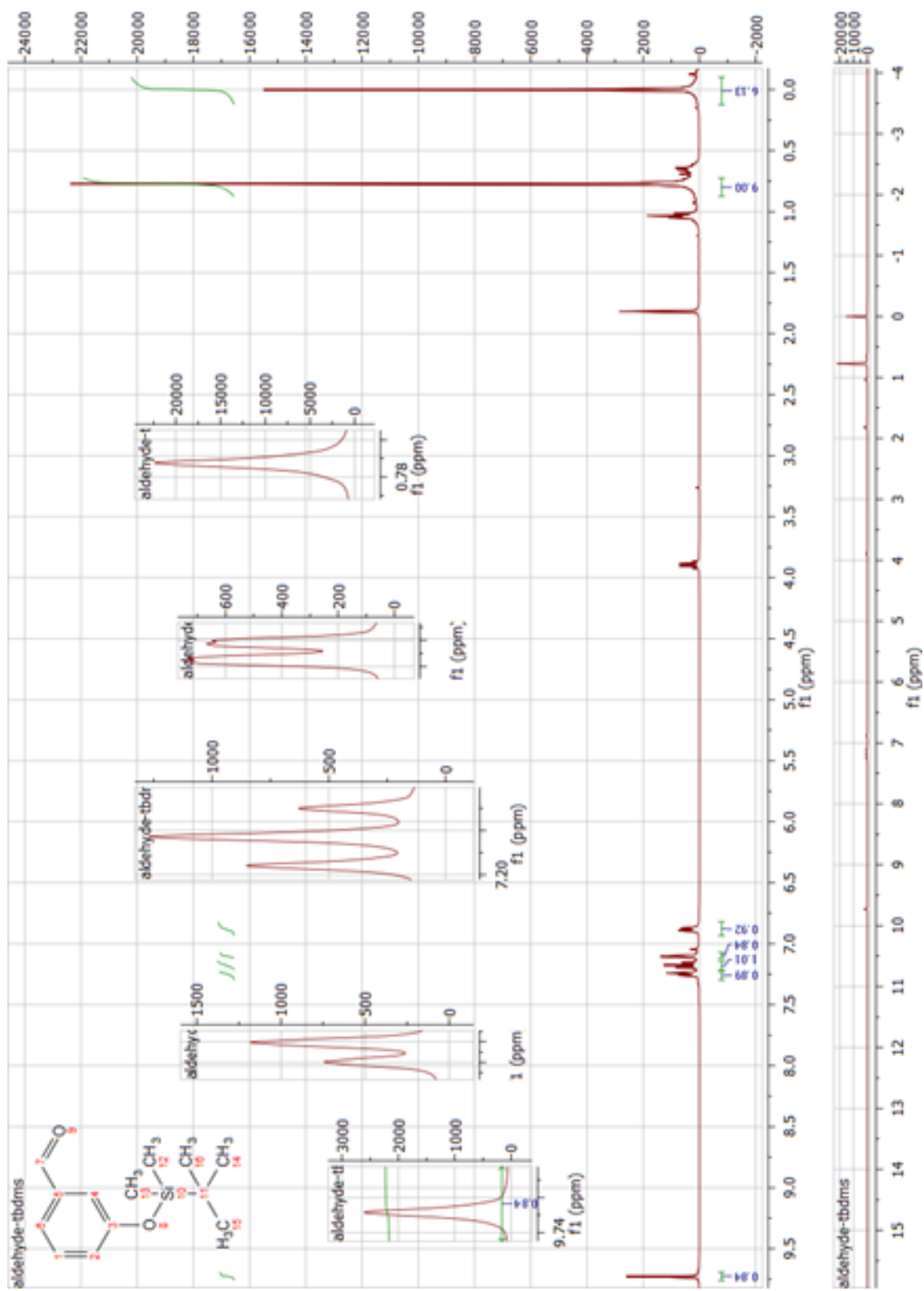
### 1. $^1\text{H}$ NMR and $^{13}\text{C}$ NMR



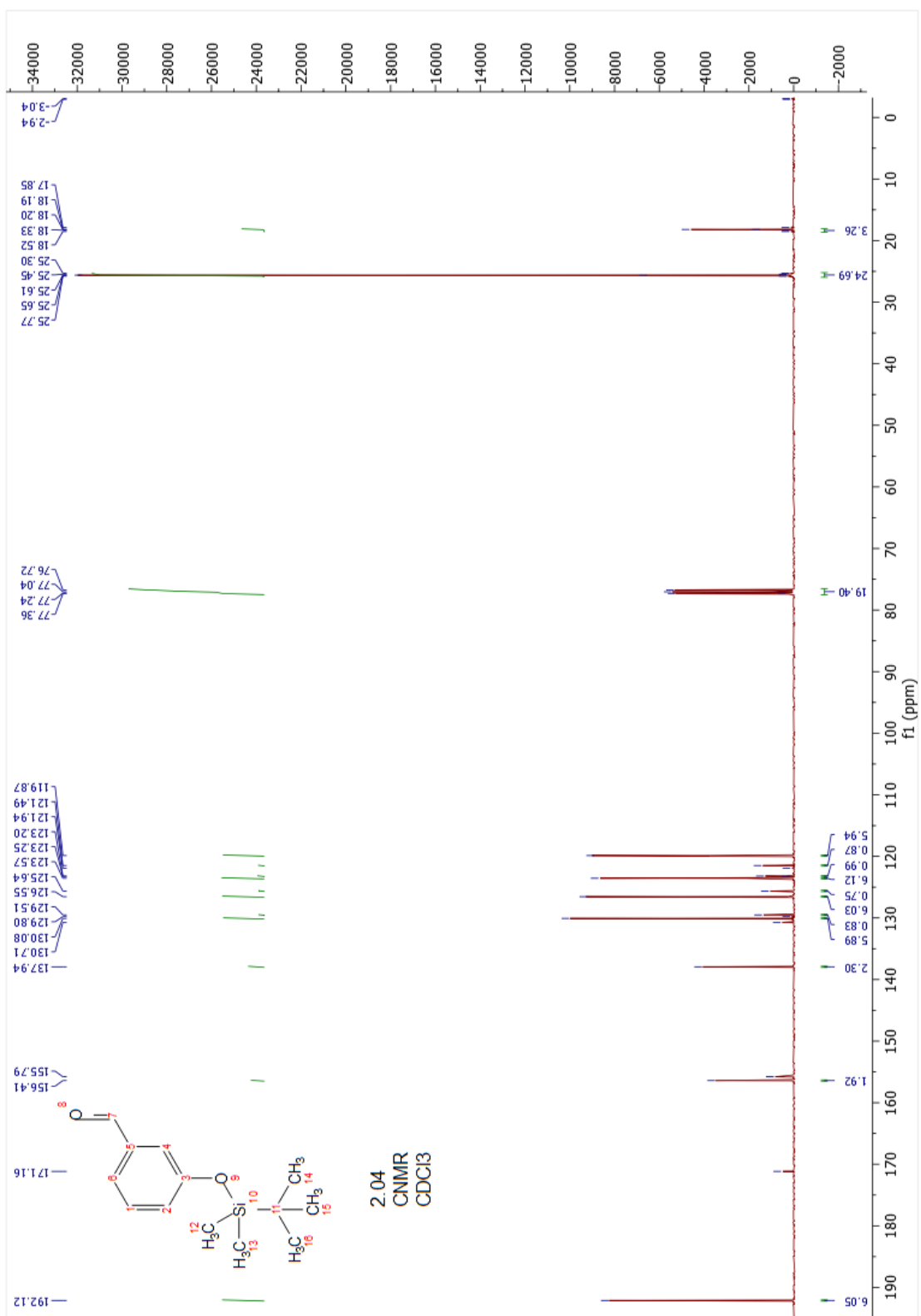
### 2.02 HNMR



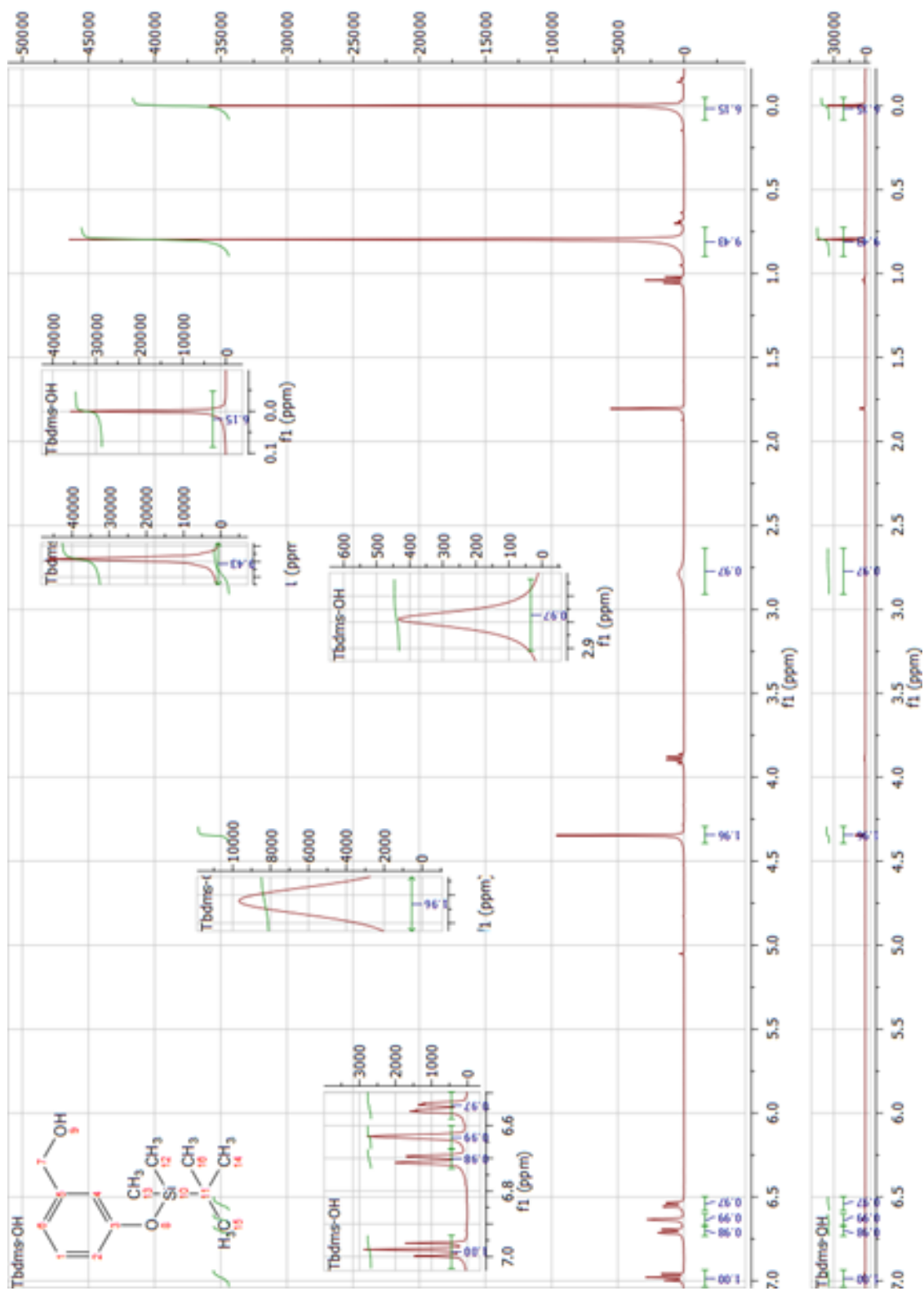
## 2.02 CNMR



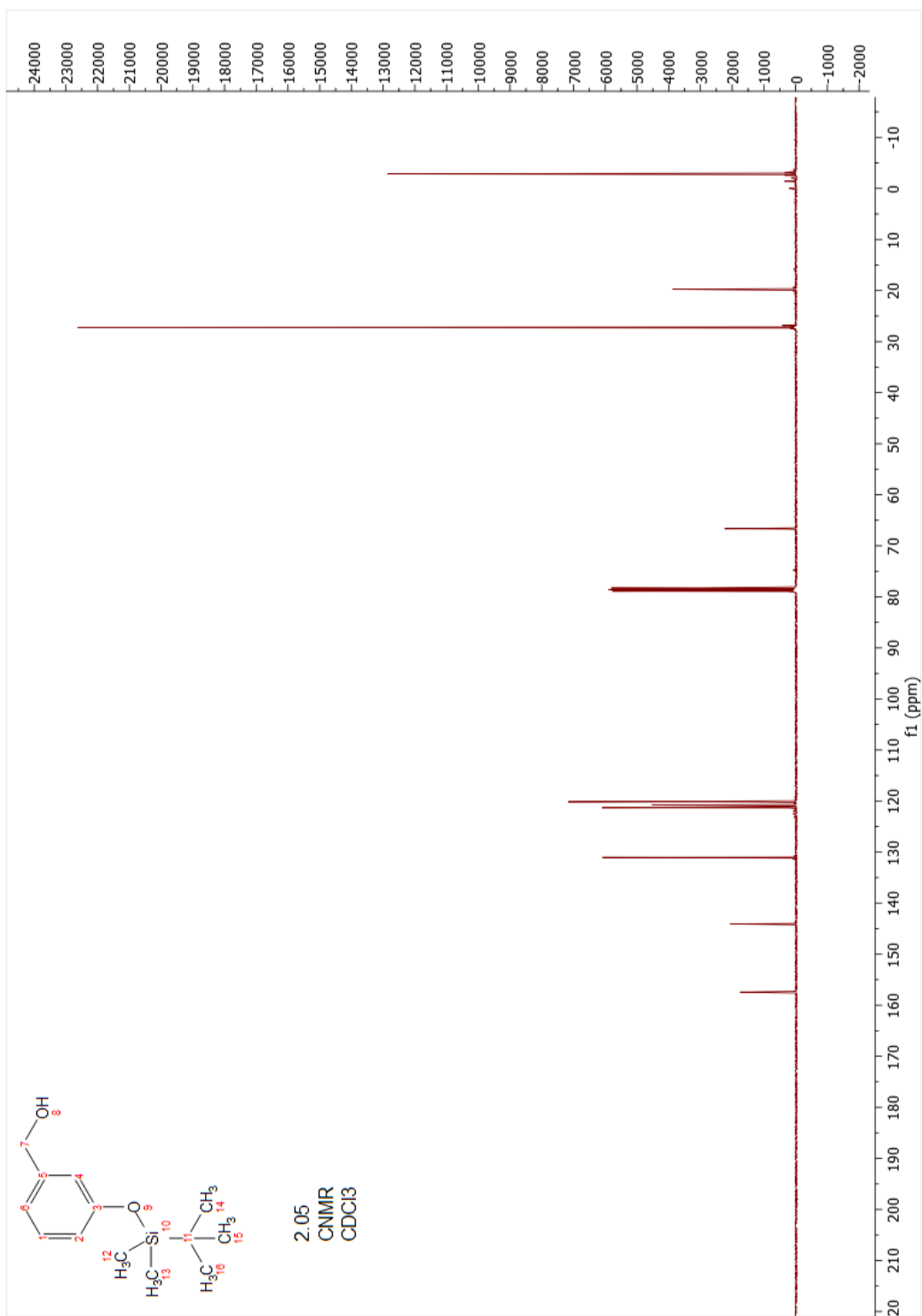
## 2.04 HNMR

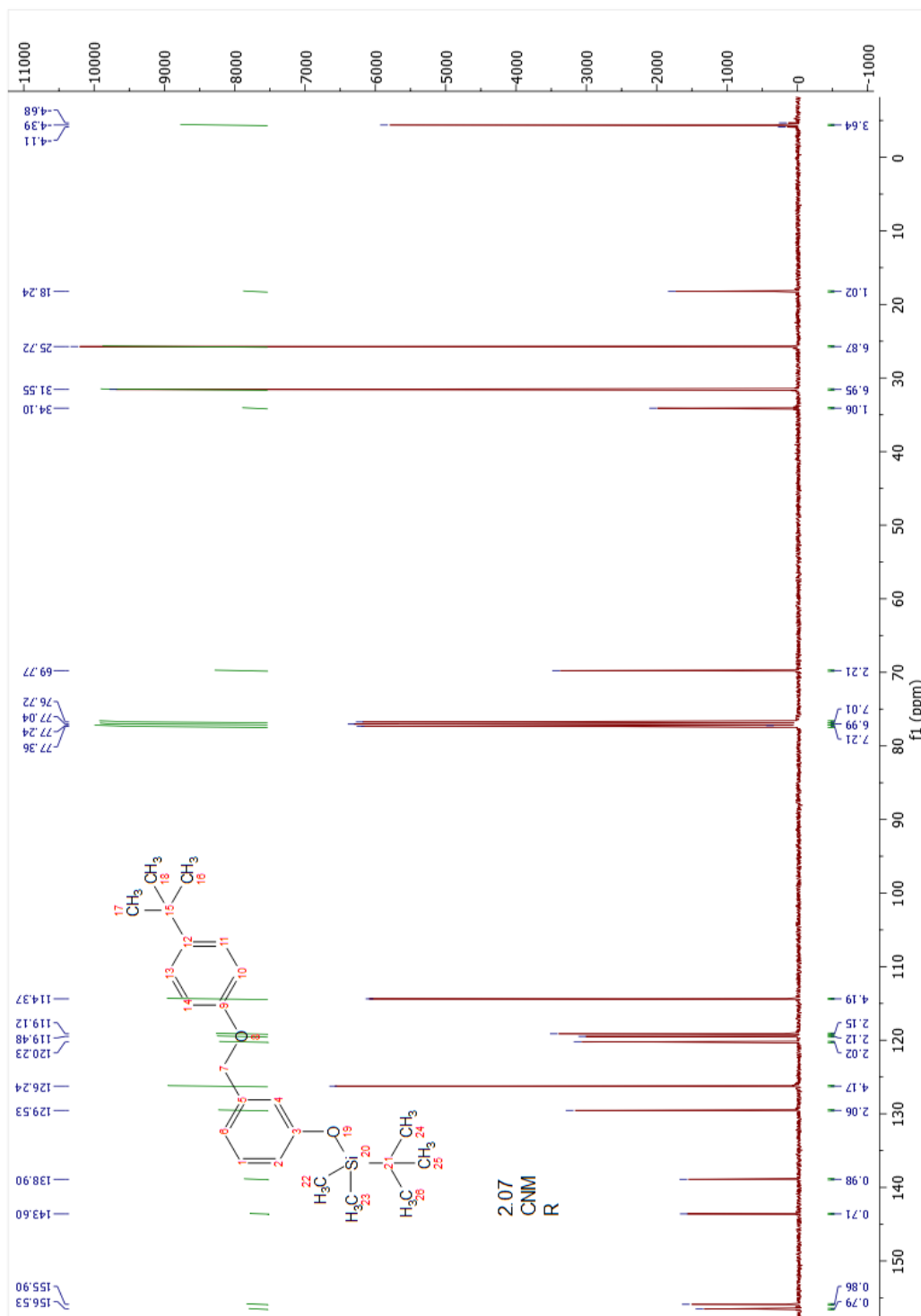


2.04 CNMR



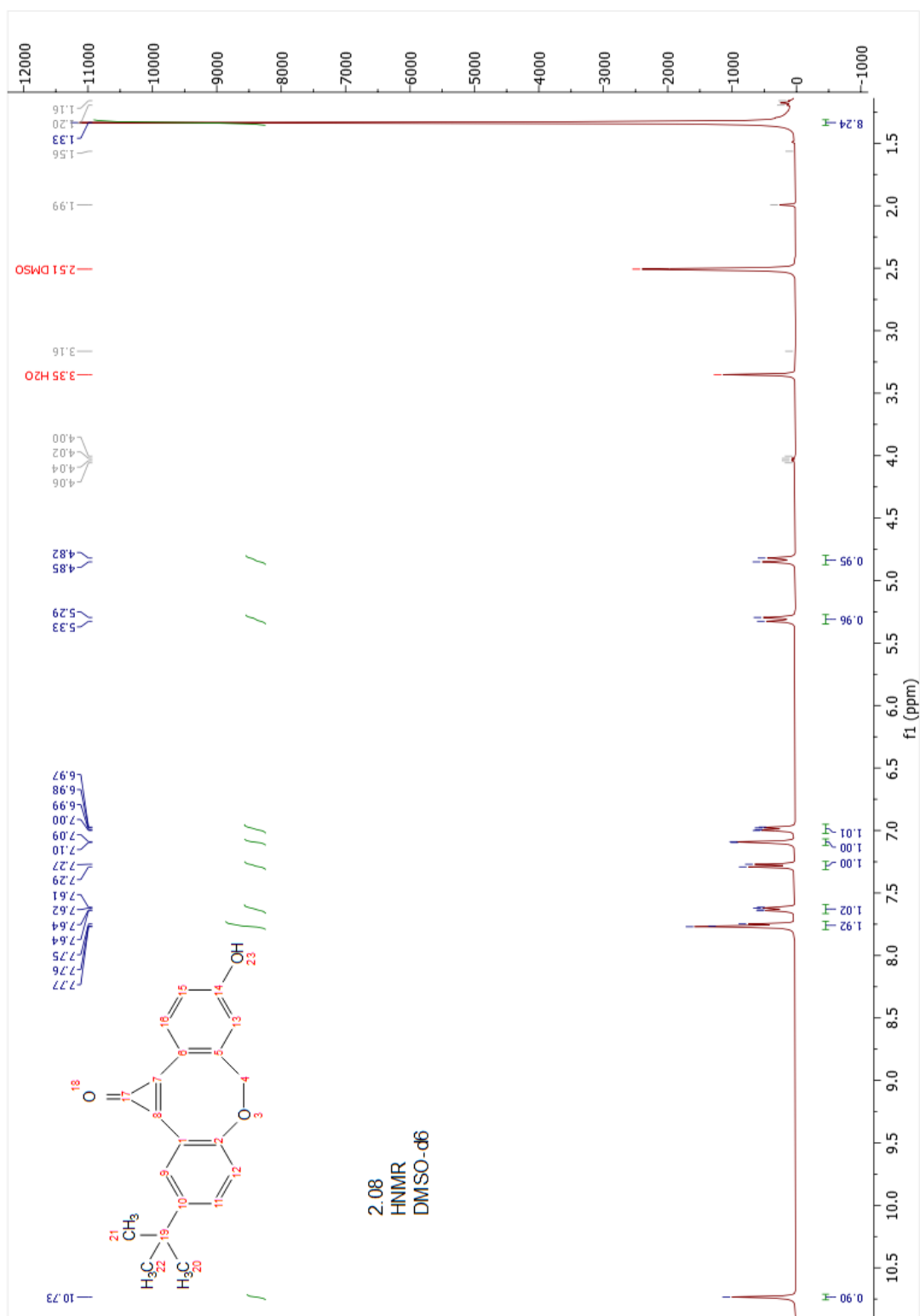
## 2.05 HNMR



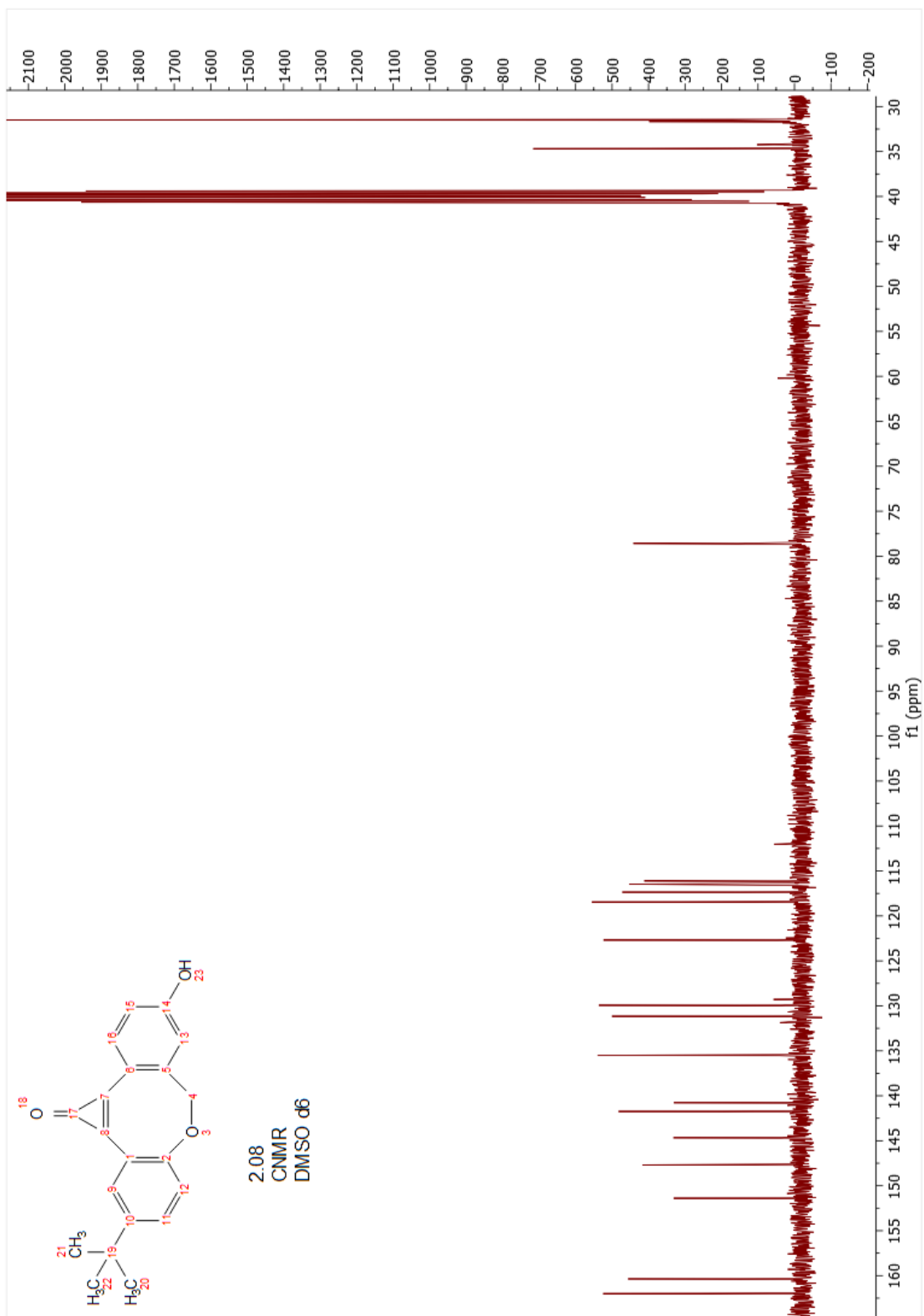


2.07 CNMR

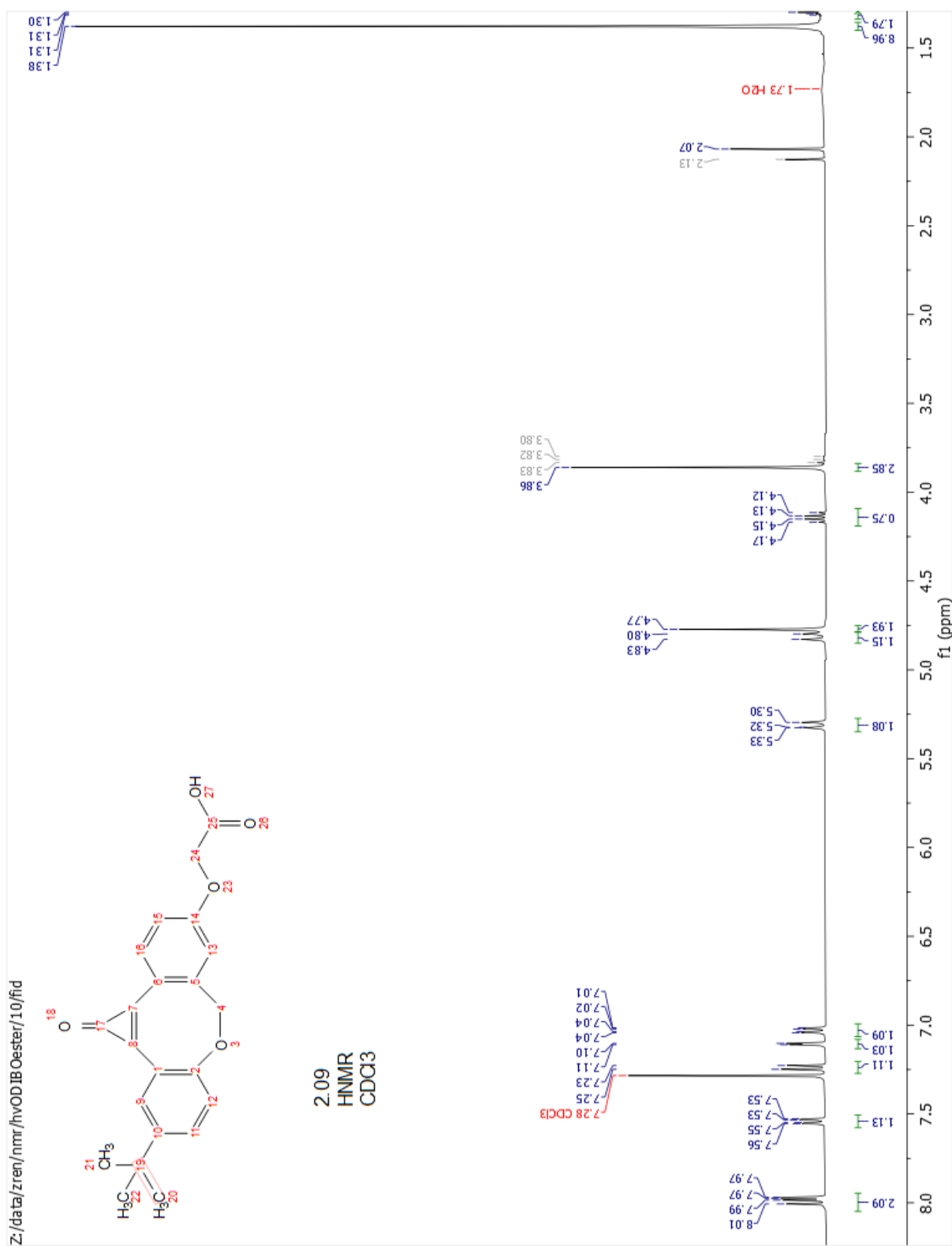




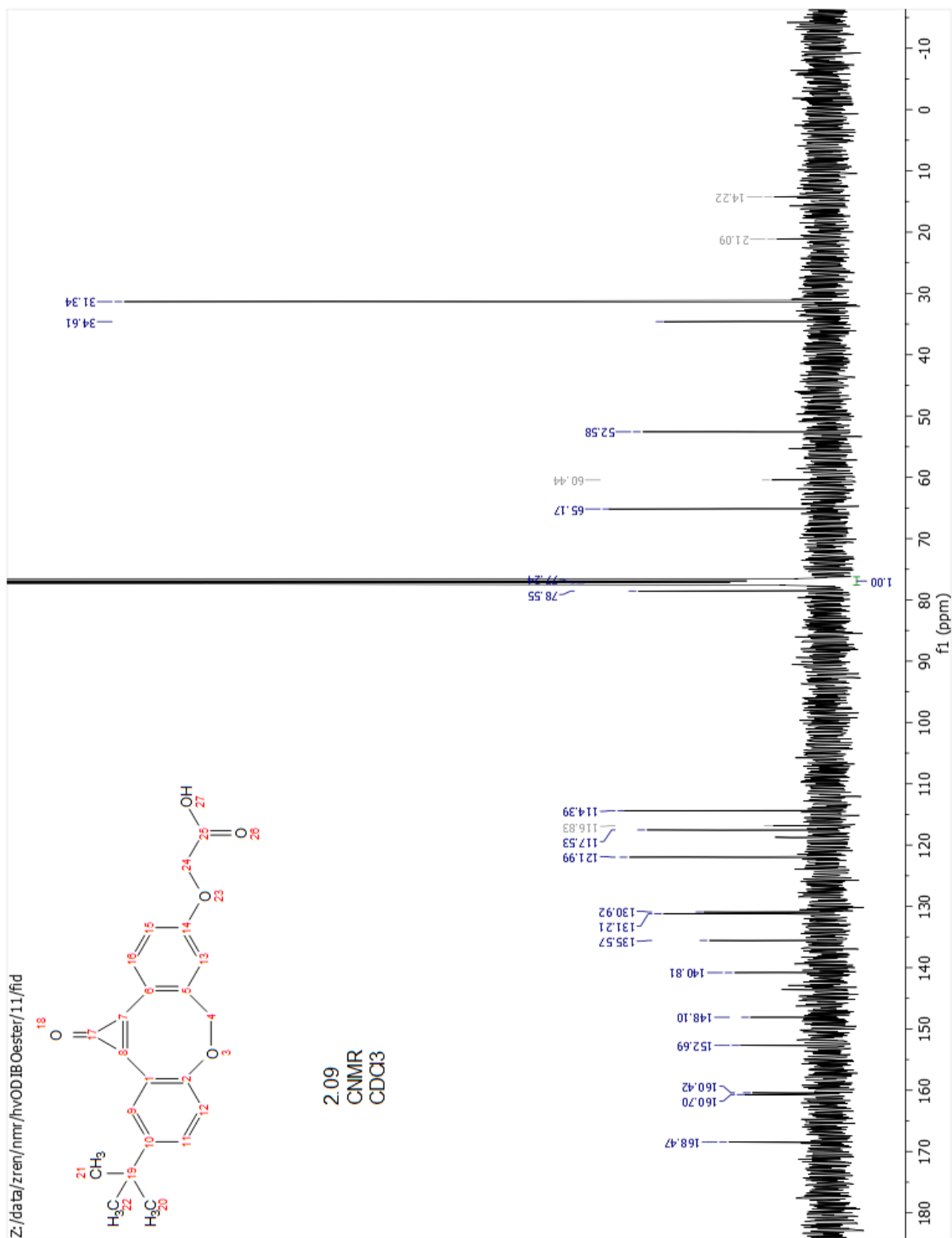
2.08 HNMR



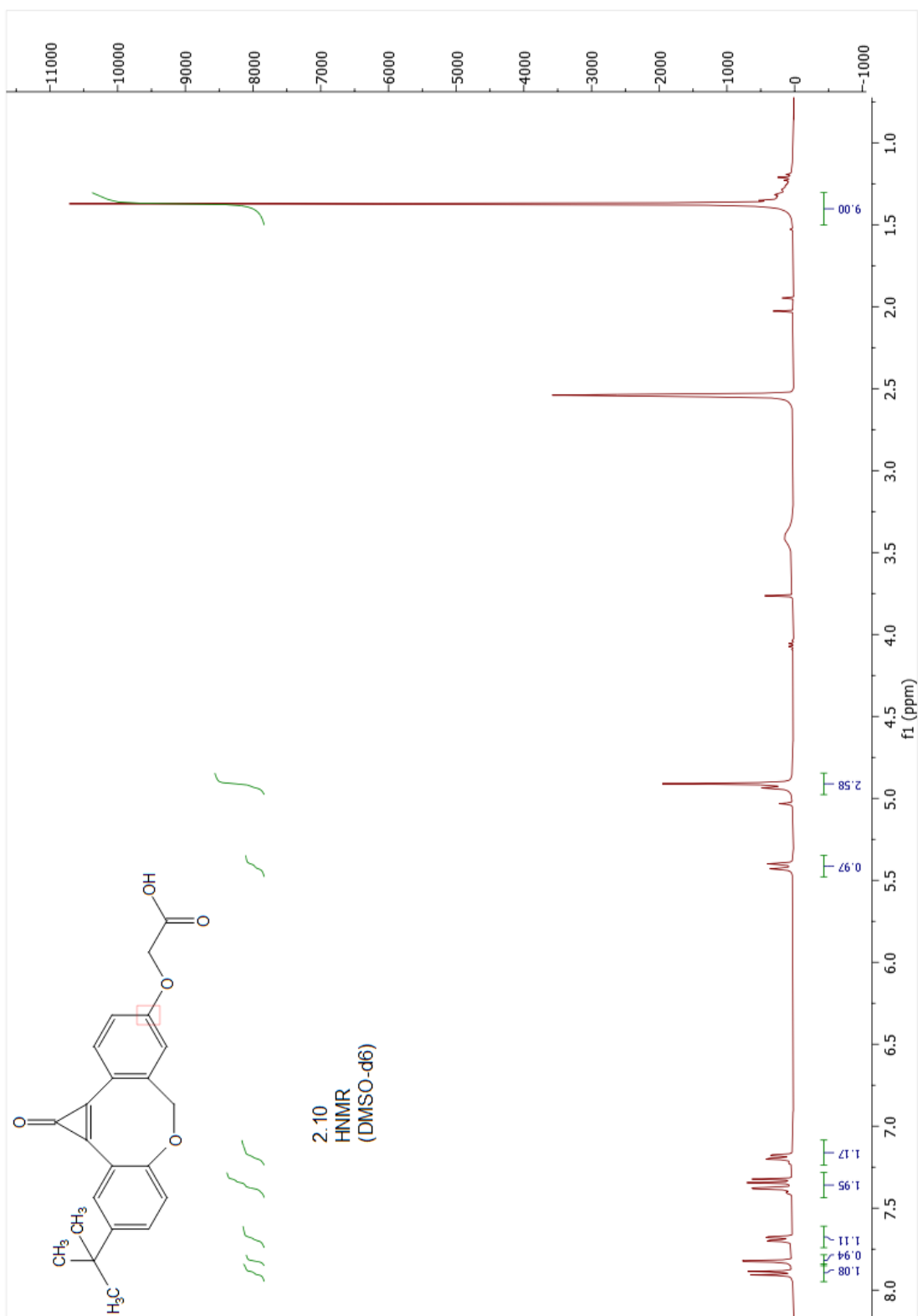
2.08 CNMR



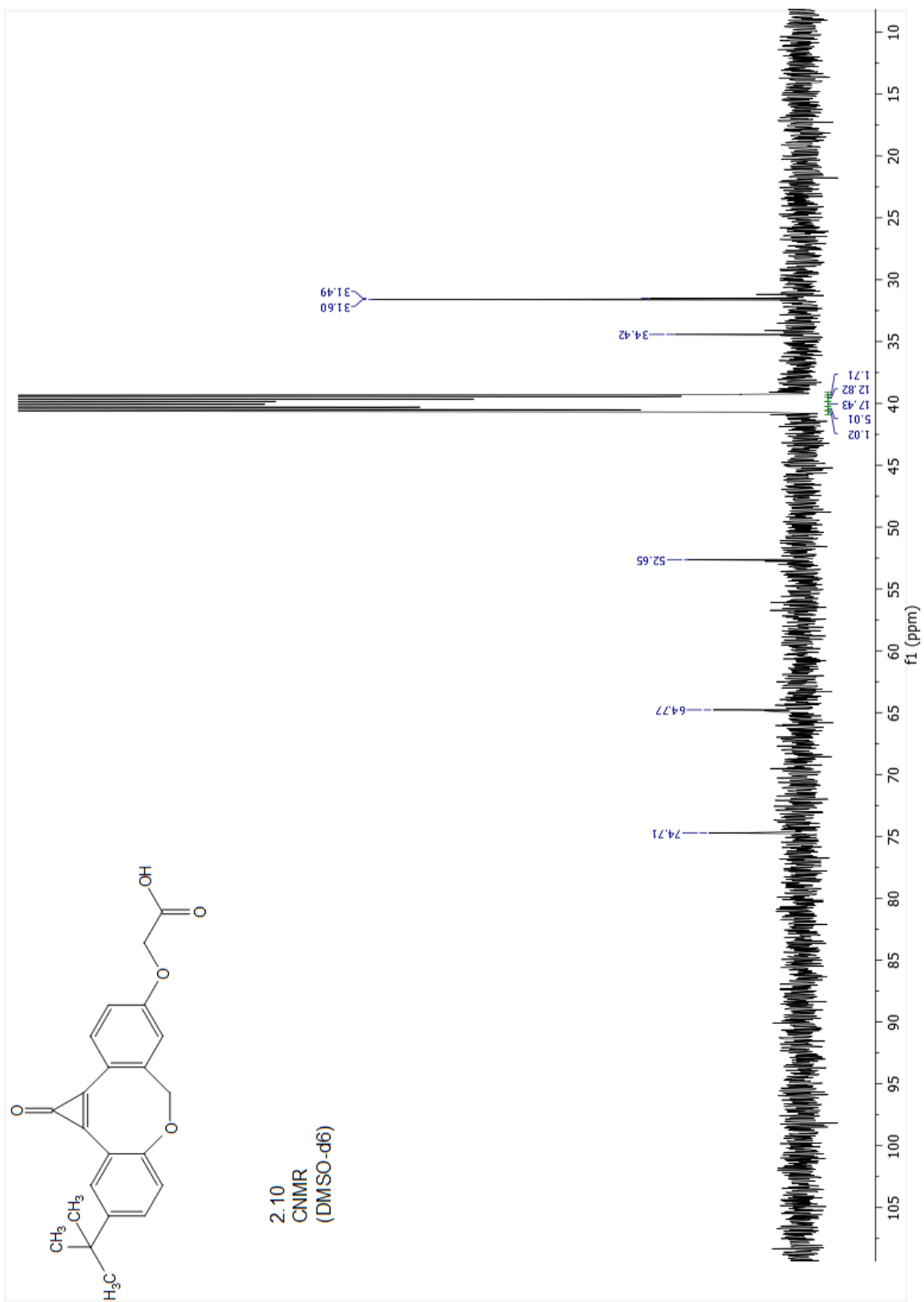
2.09 HNMR



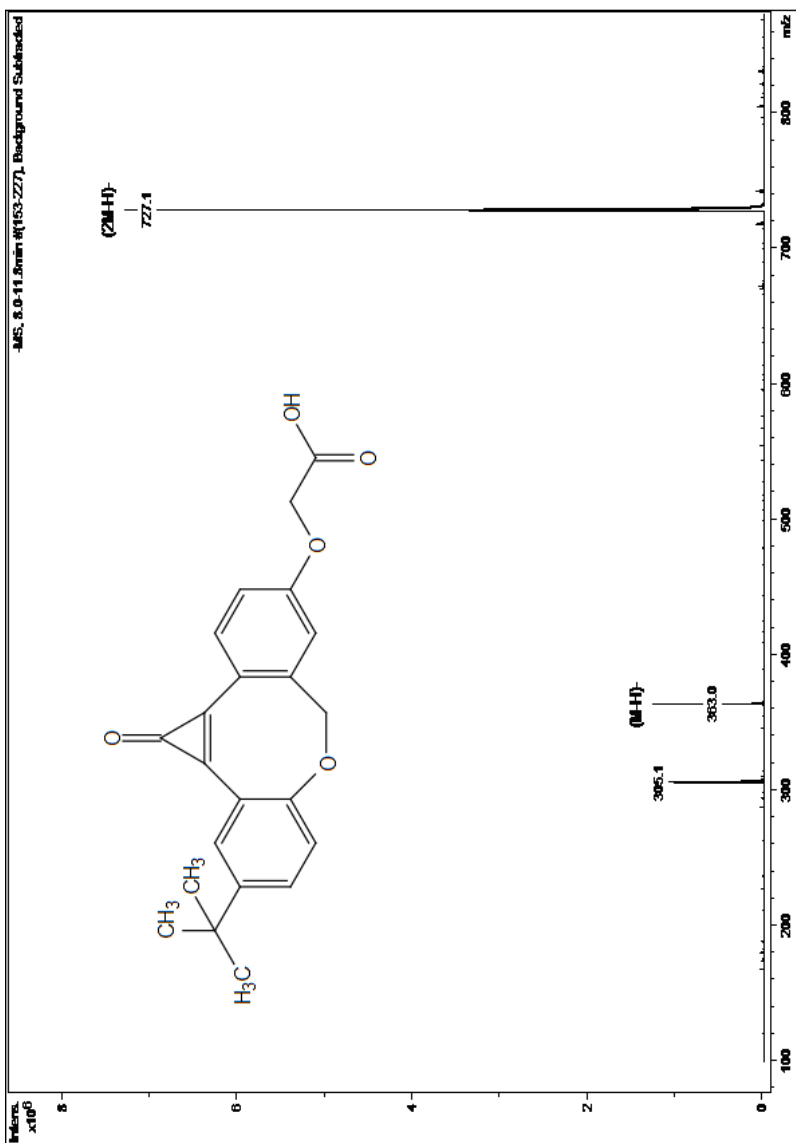
## 2.09 CNMR



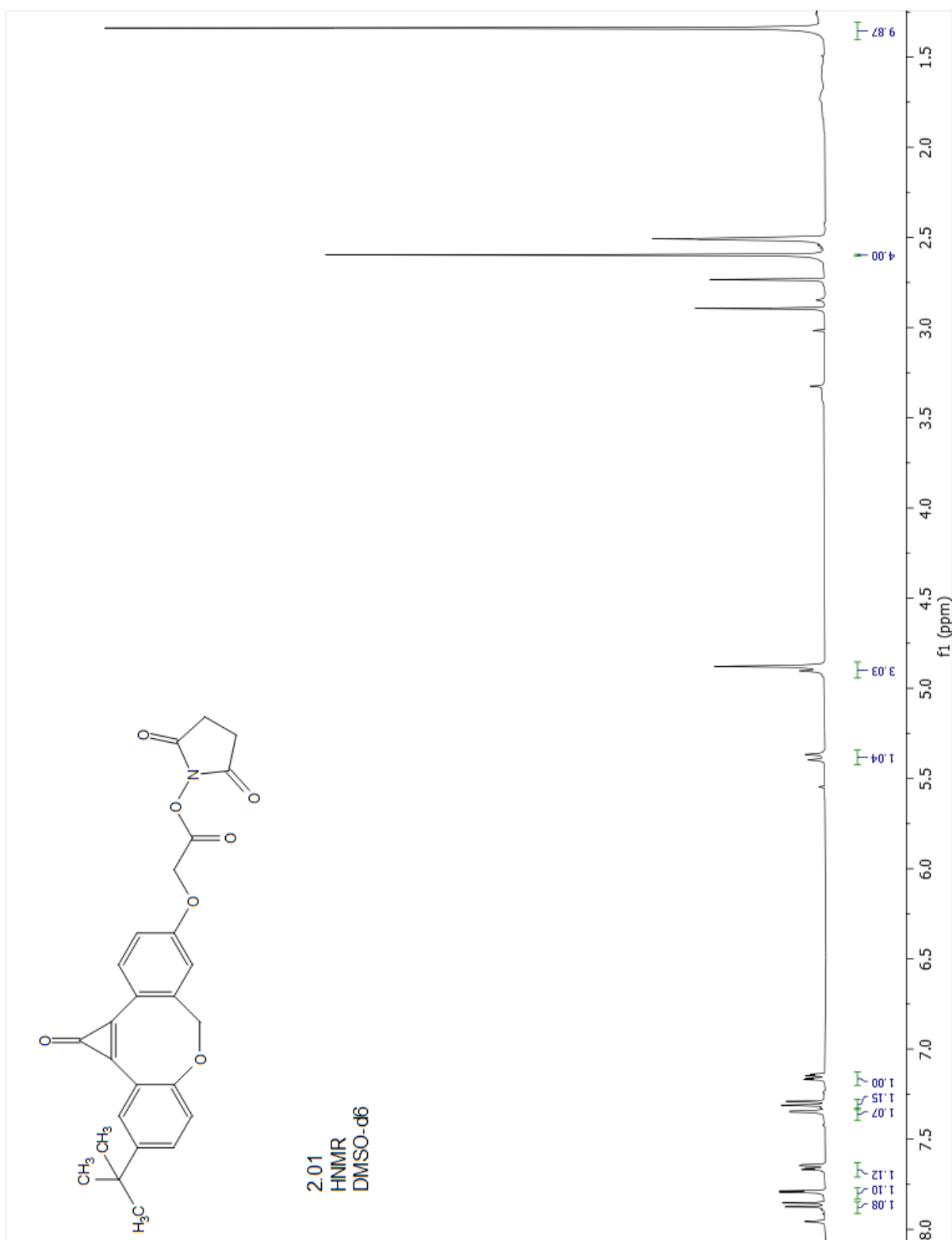
2.10 HNMR



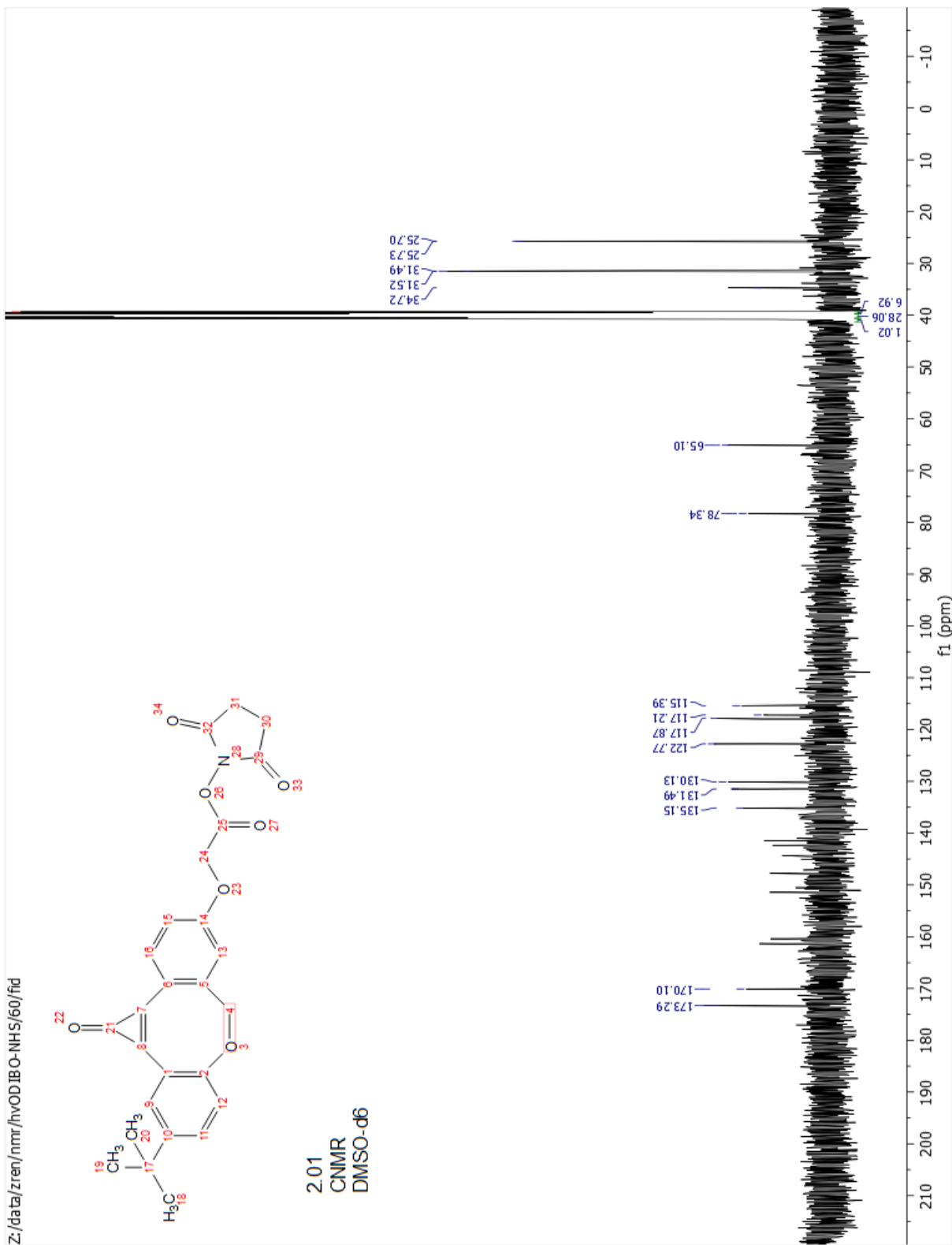
**2.10 CNMR**



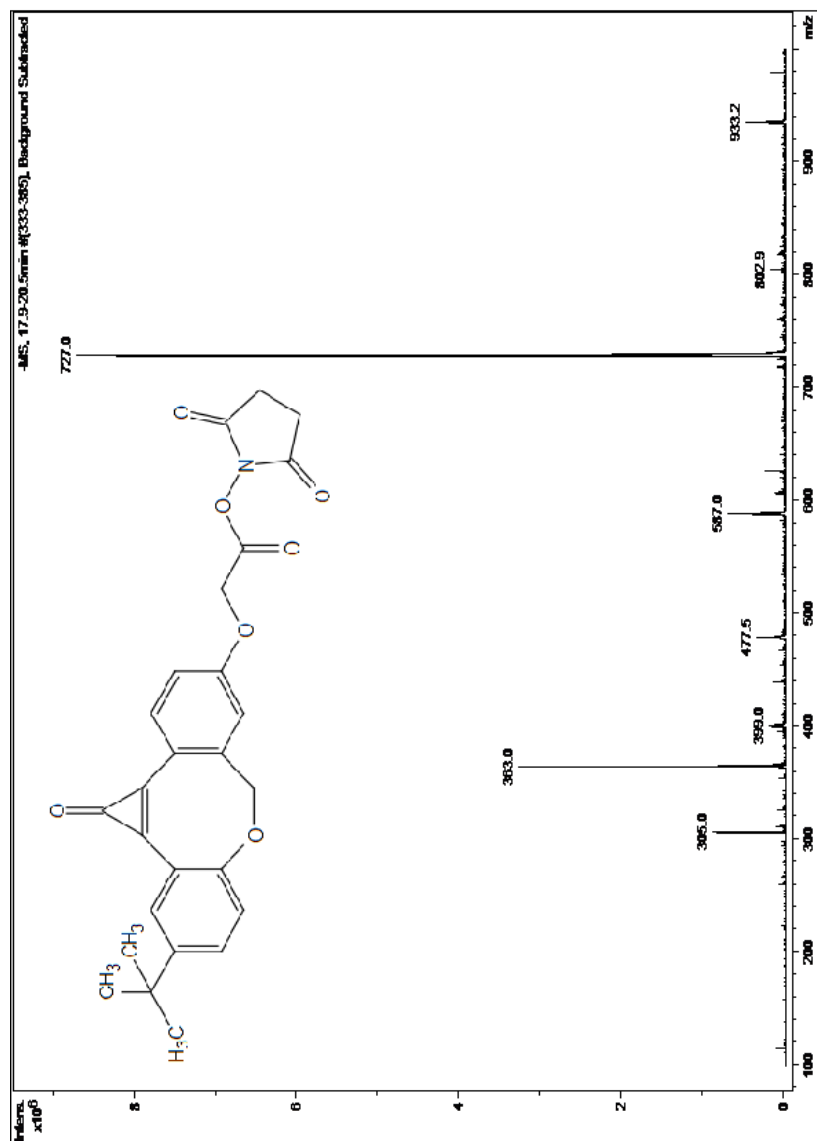
## 2.10 ESI-MS



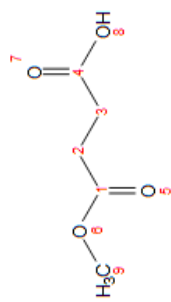
## 2.01 HNMR



## 2.01 CNMR

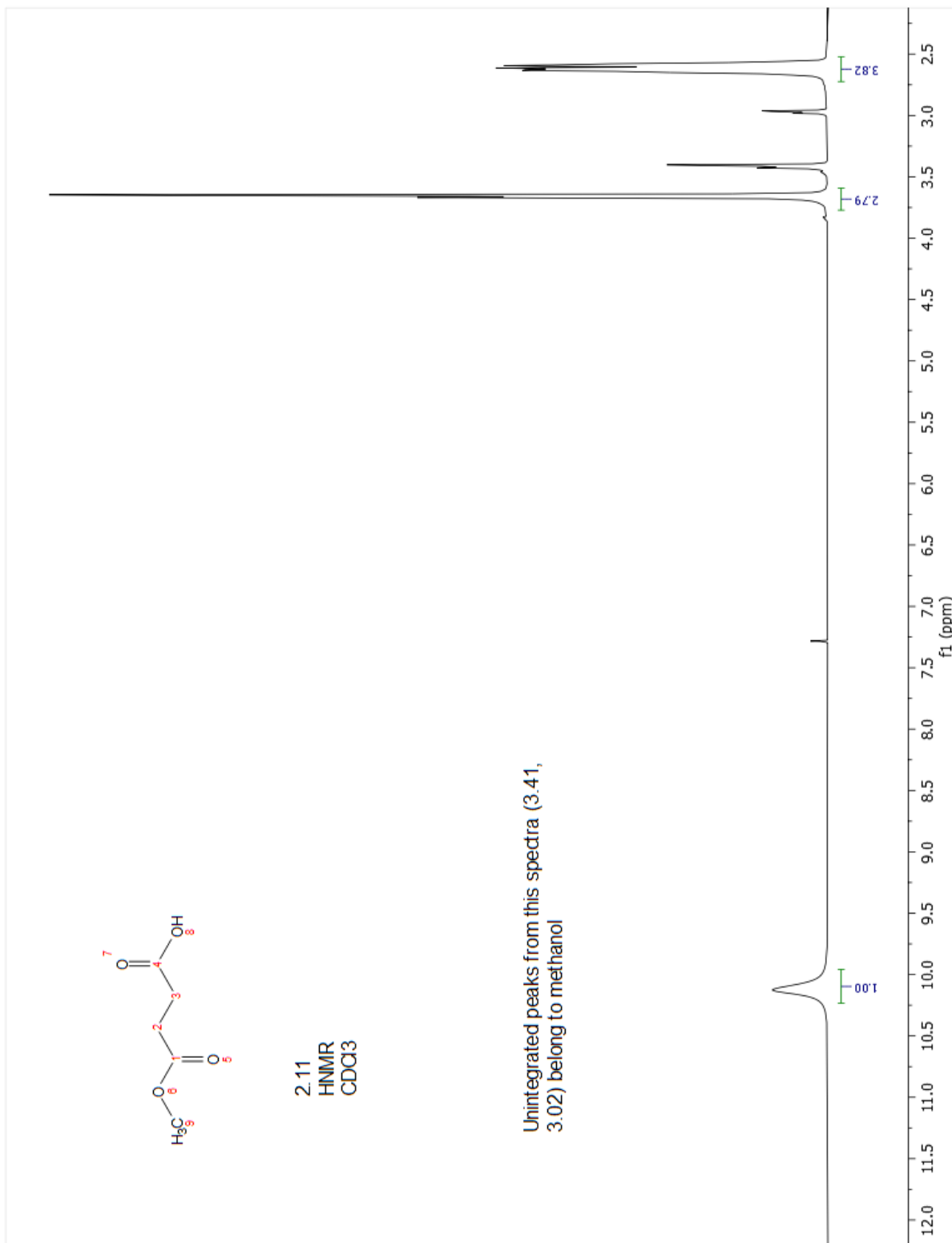


2.01 MS

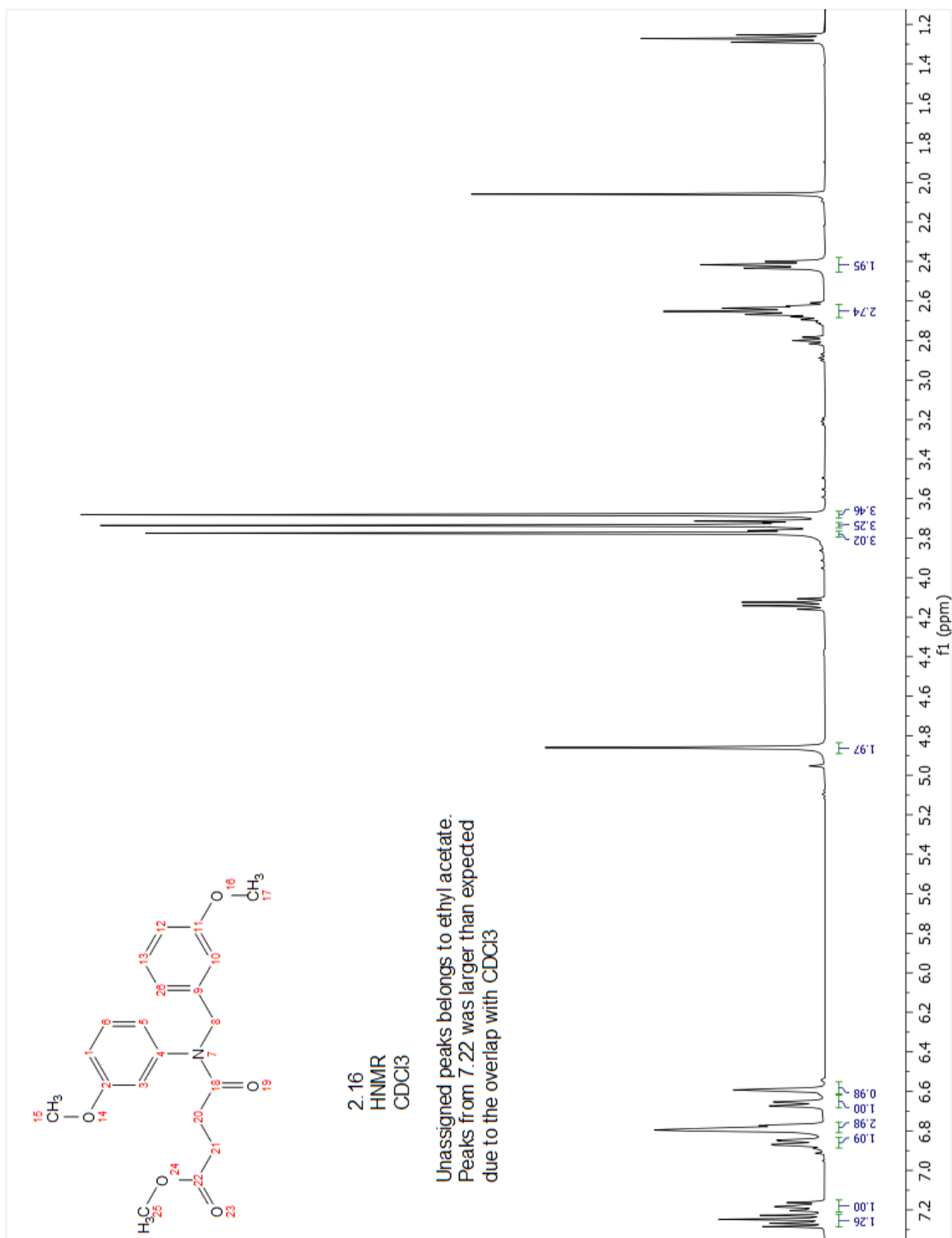


2.11  
HNMR  
CDCl3

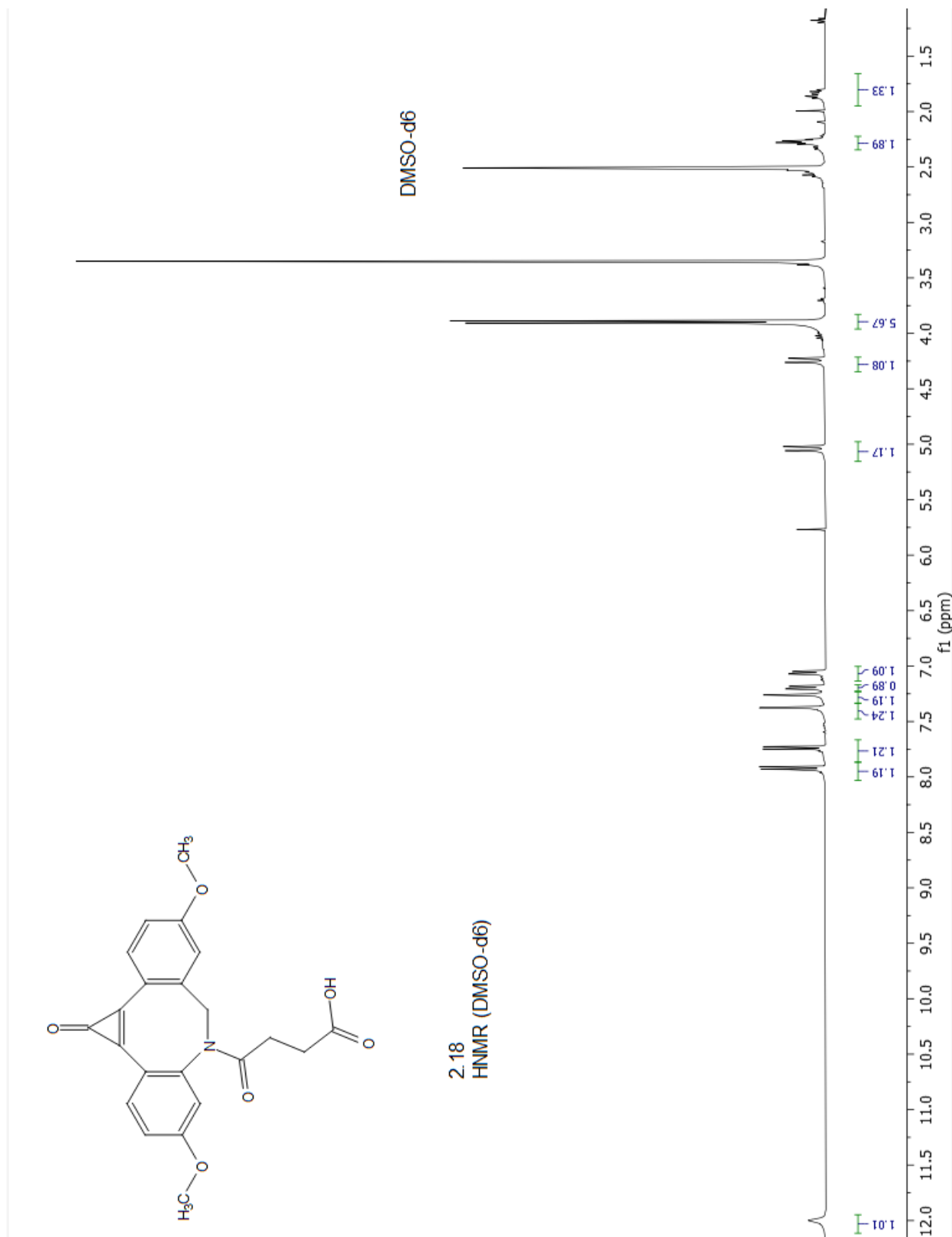
Unintegrated peaks from this spectra (3.41, 3.02) belong to methanol



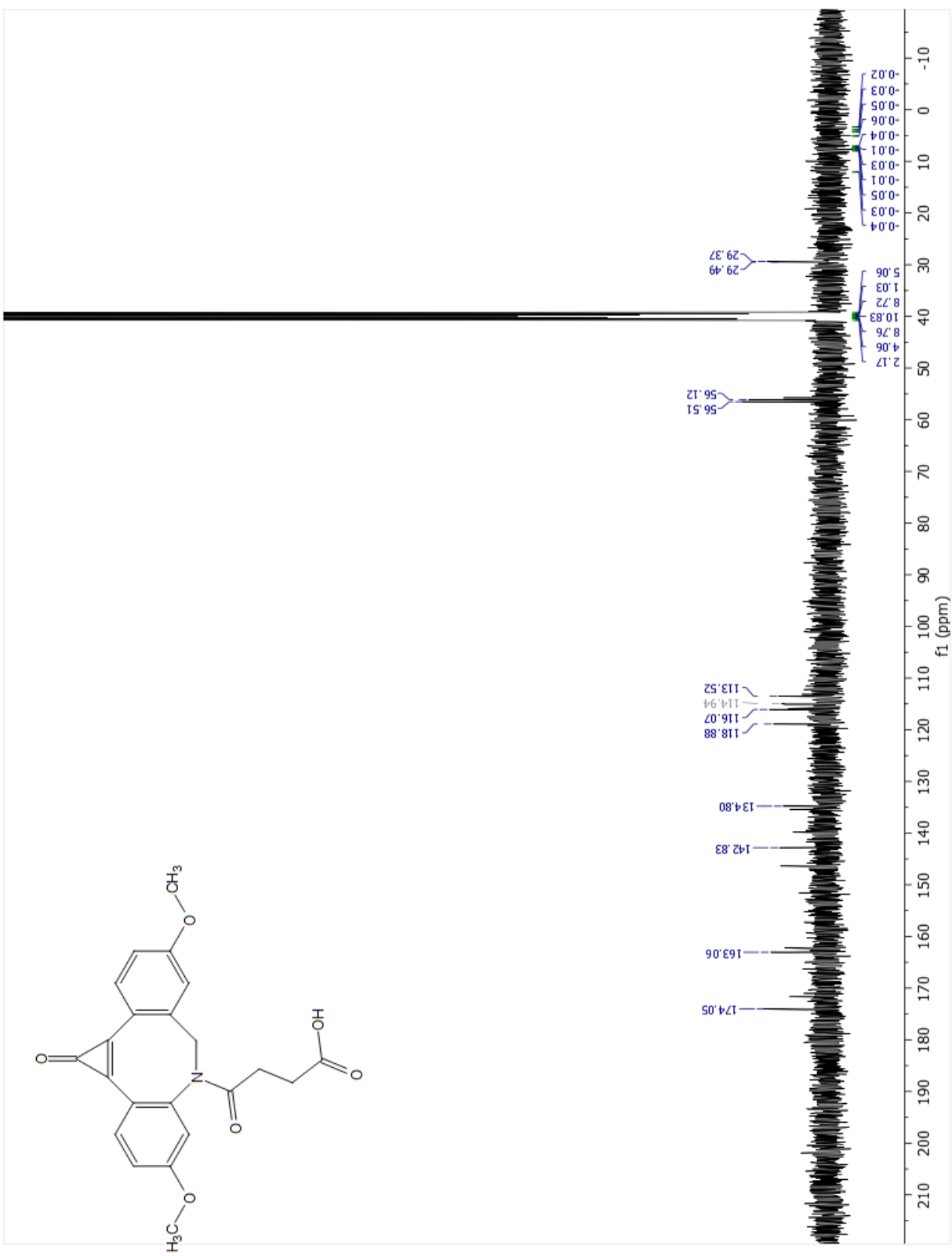
## 2.12 HNMR



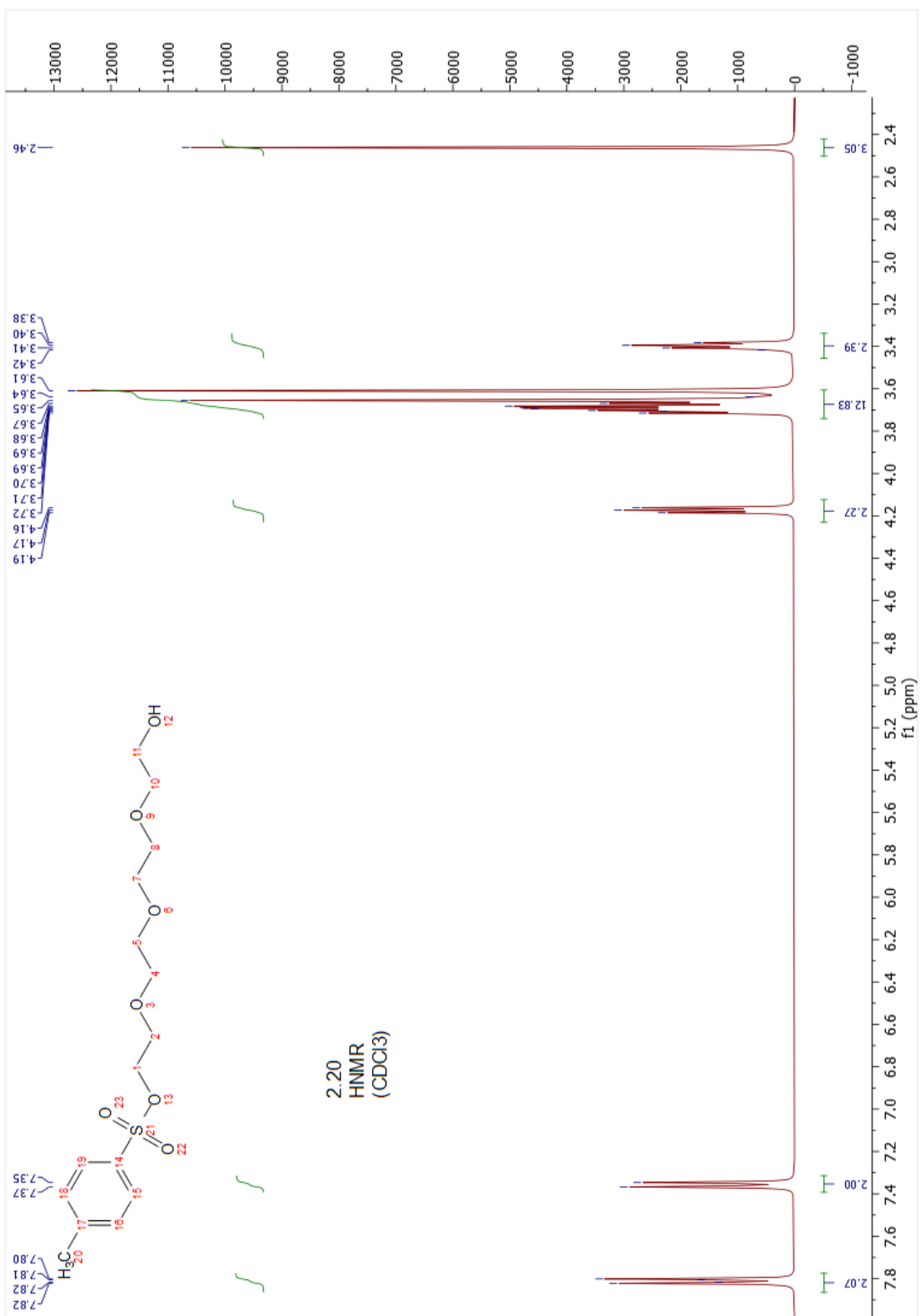
## 2.16 HNMR



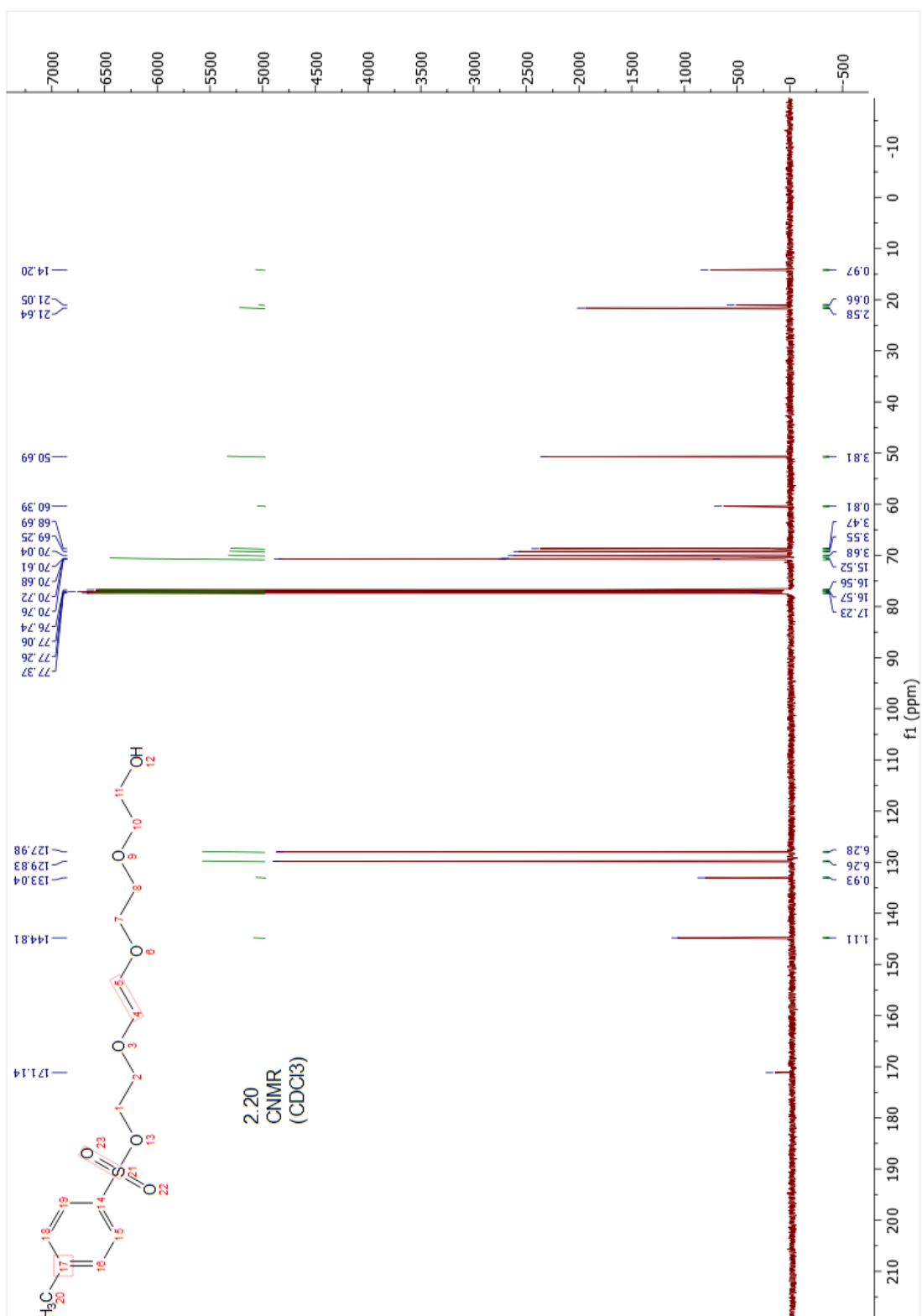
2.18 HNMR



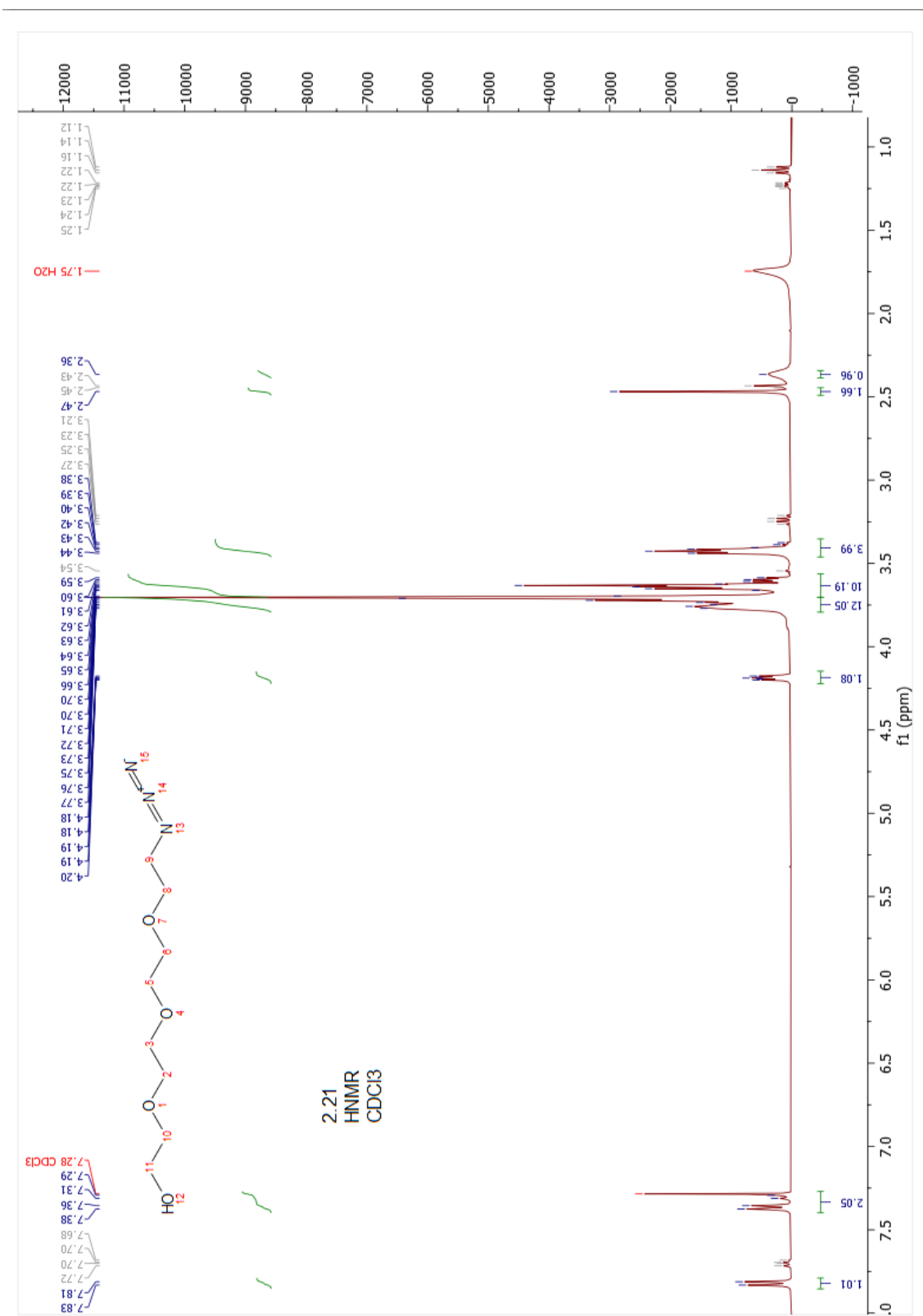
## 2.18 CNMR



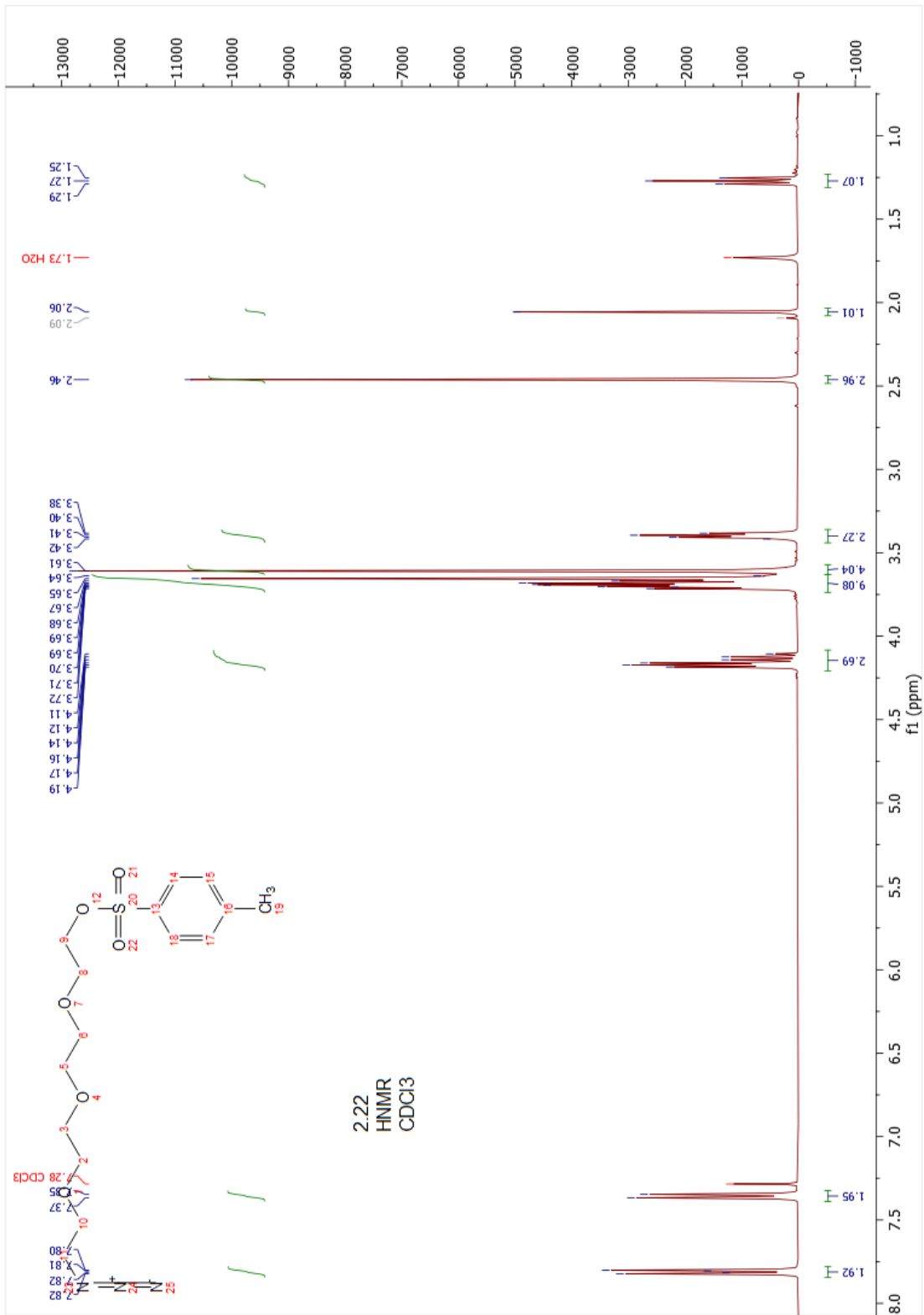
2.20 HNMR



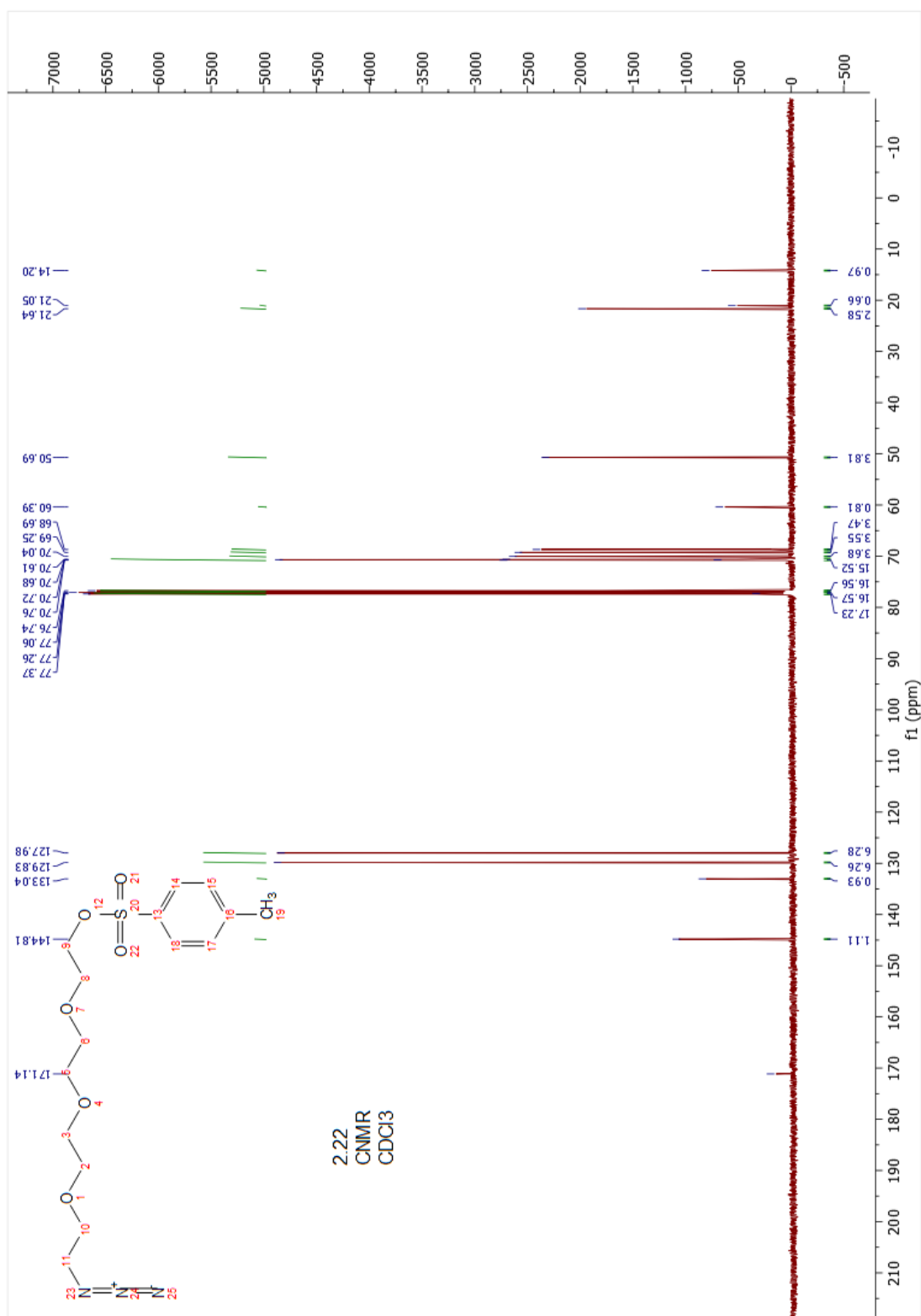
## 2.20 CNMR



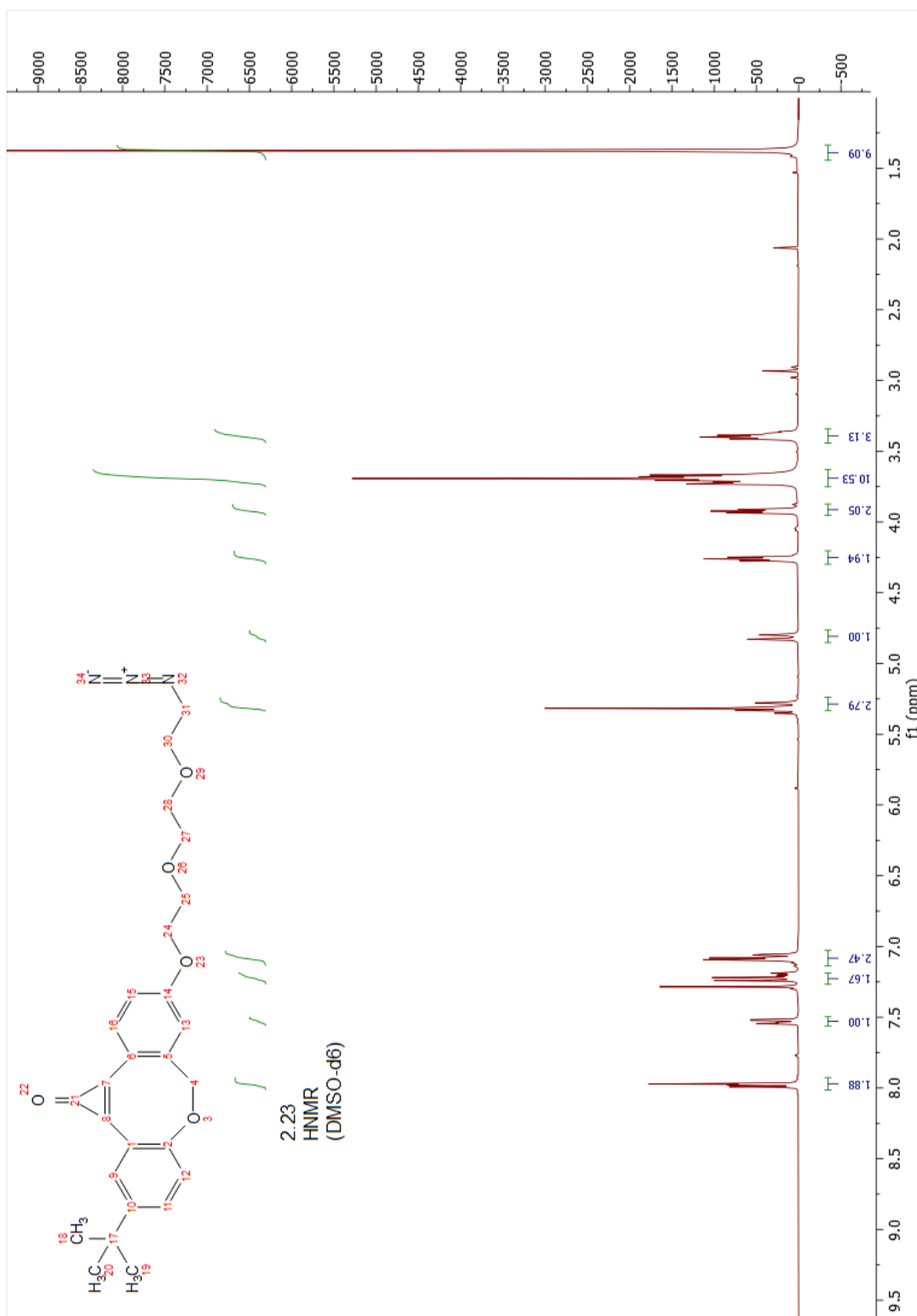
2.21 HNMR



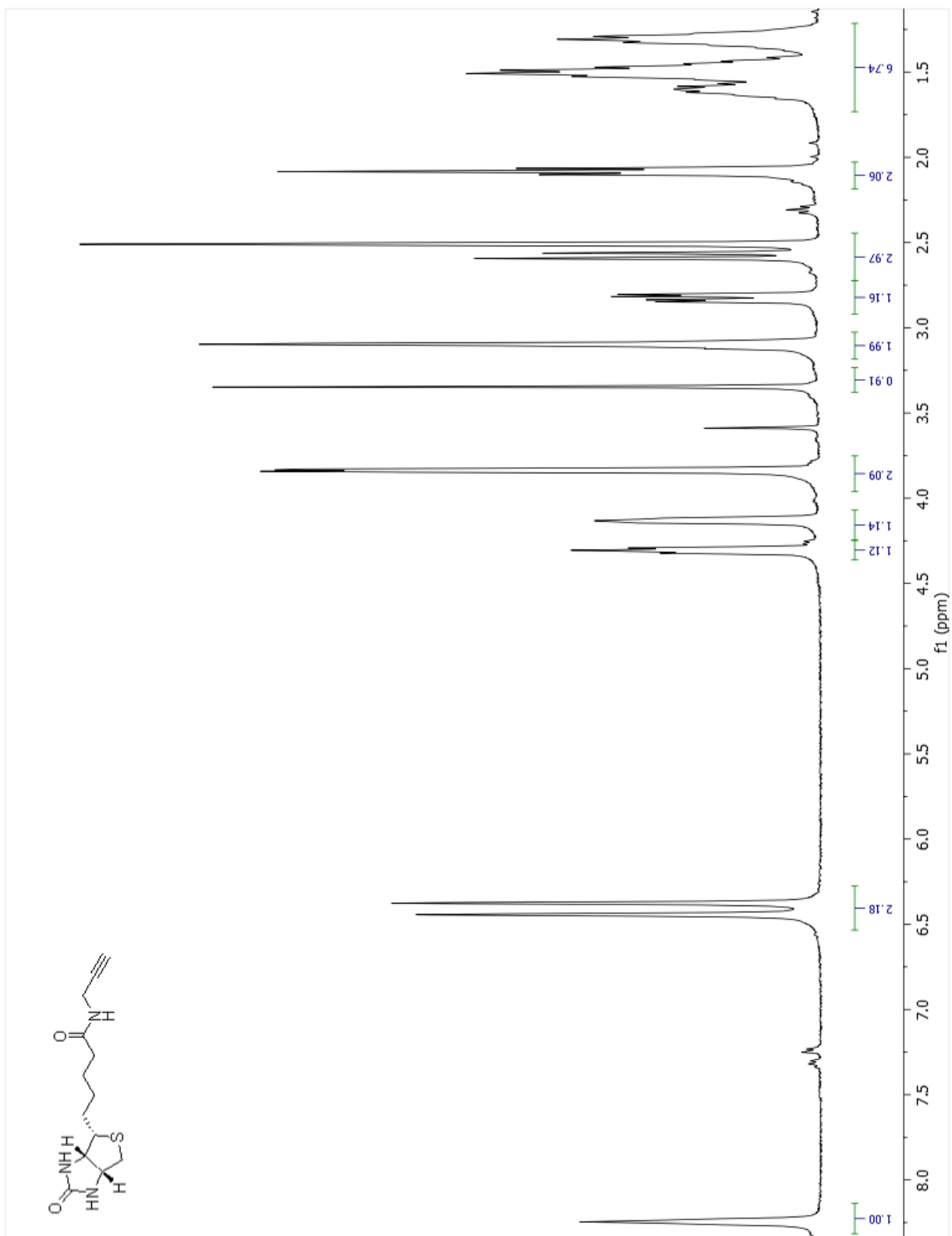
2.22 HNMR



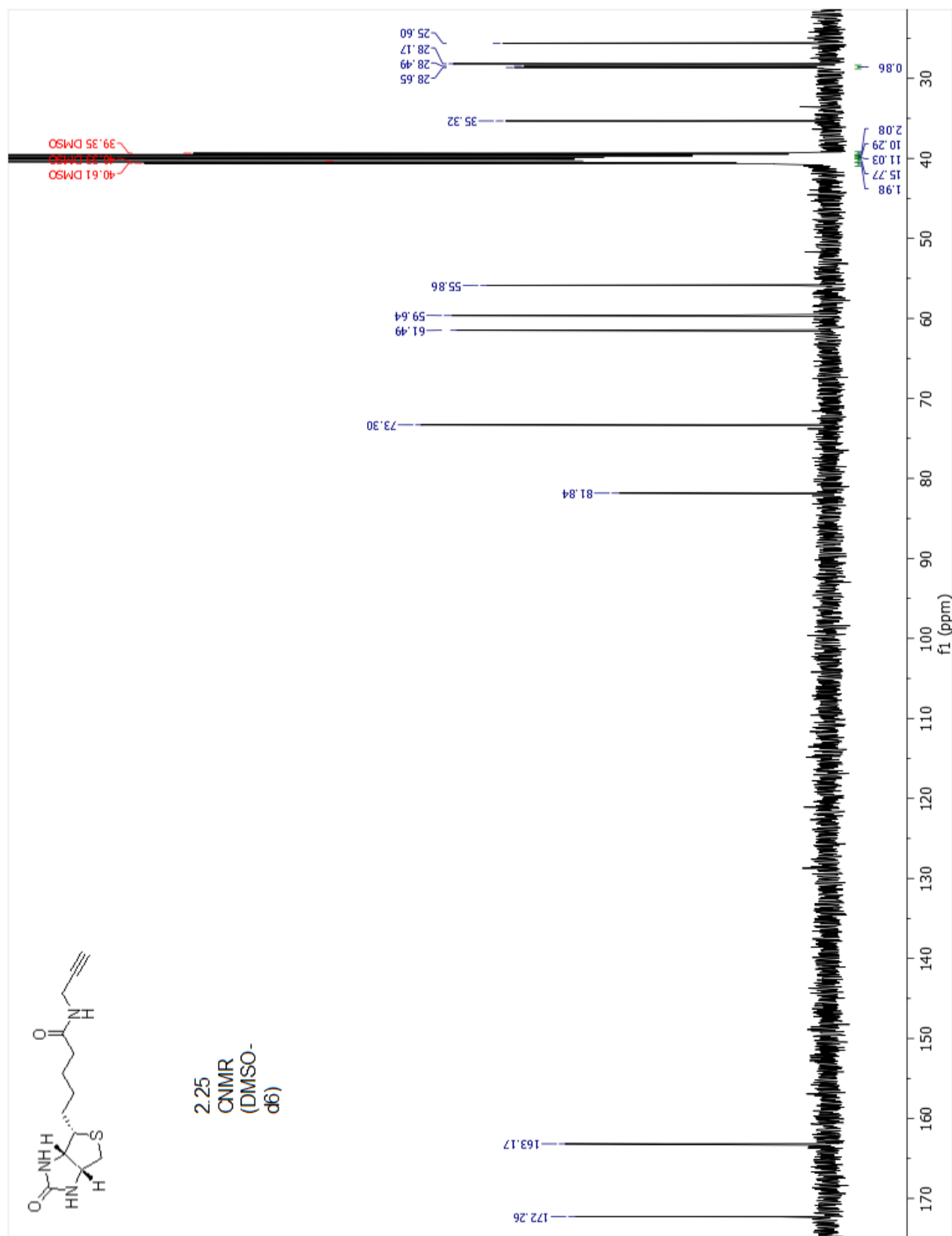
2.22 CNMR



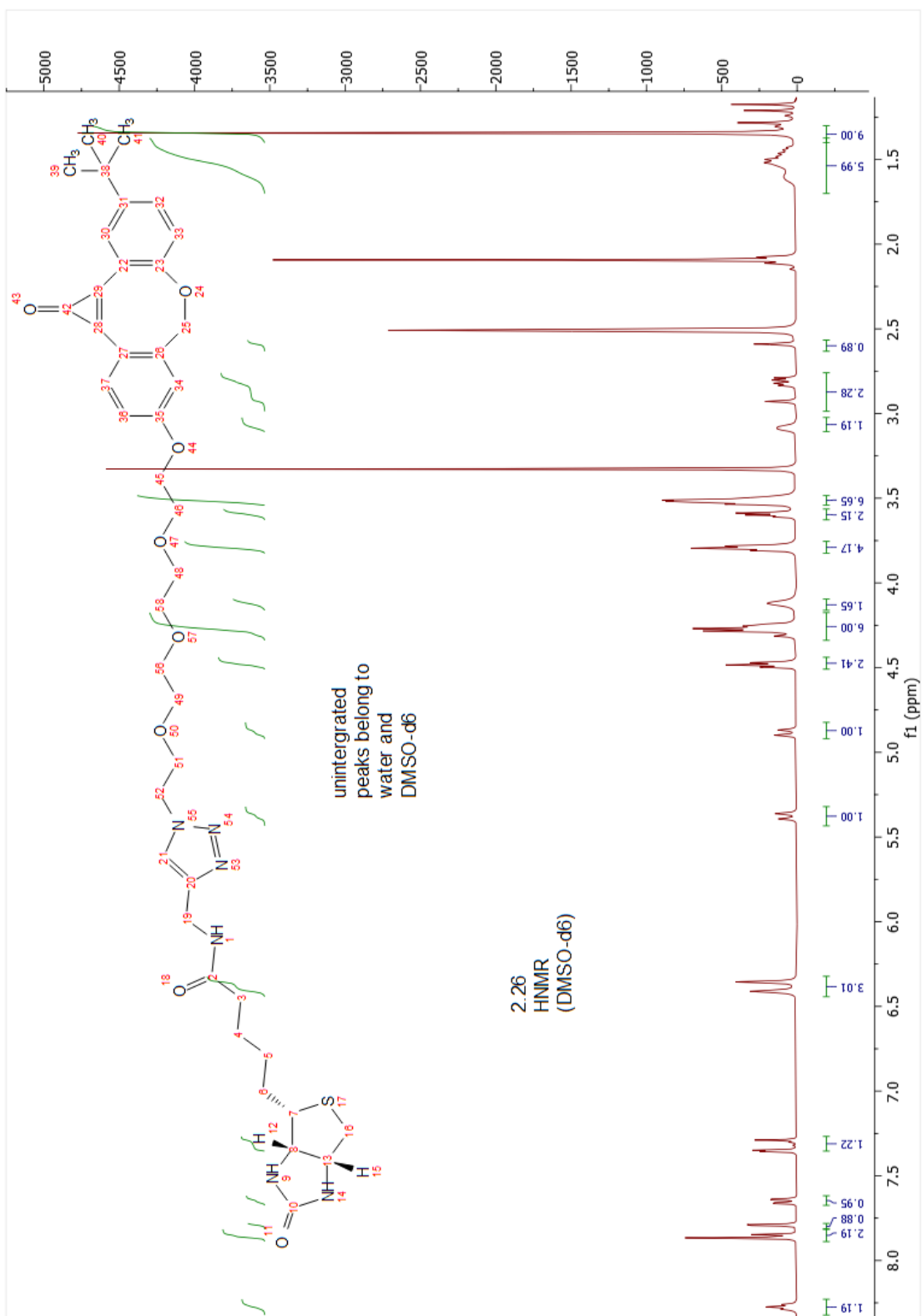
2.23 HNMR



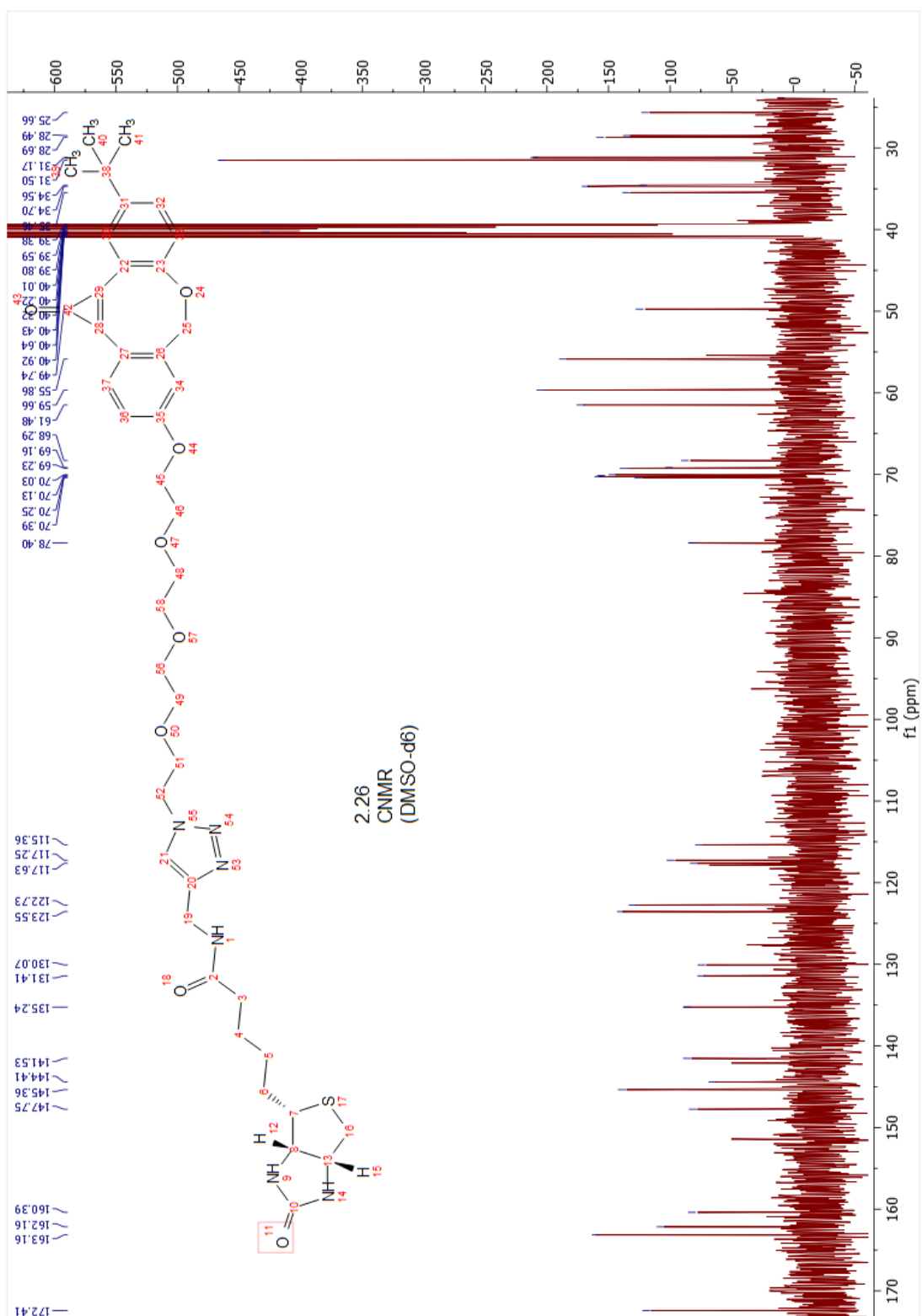
2.25 HNMR



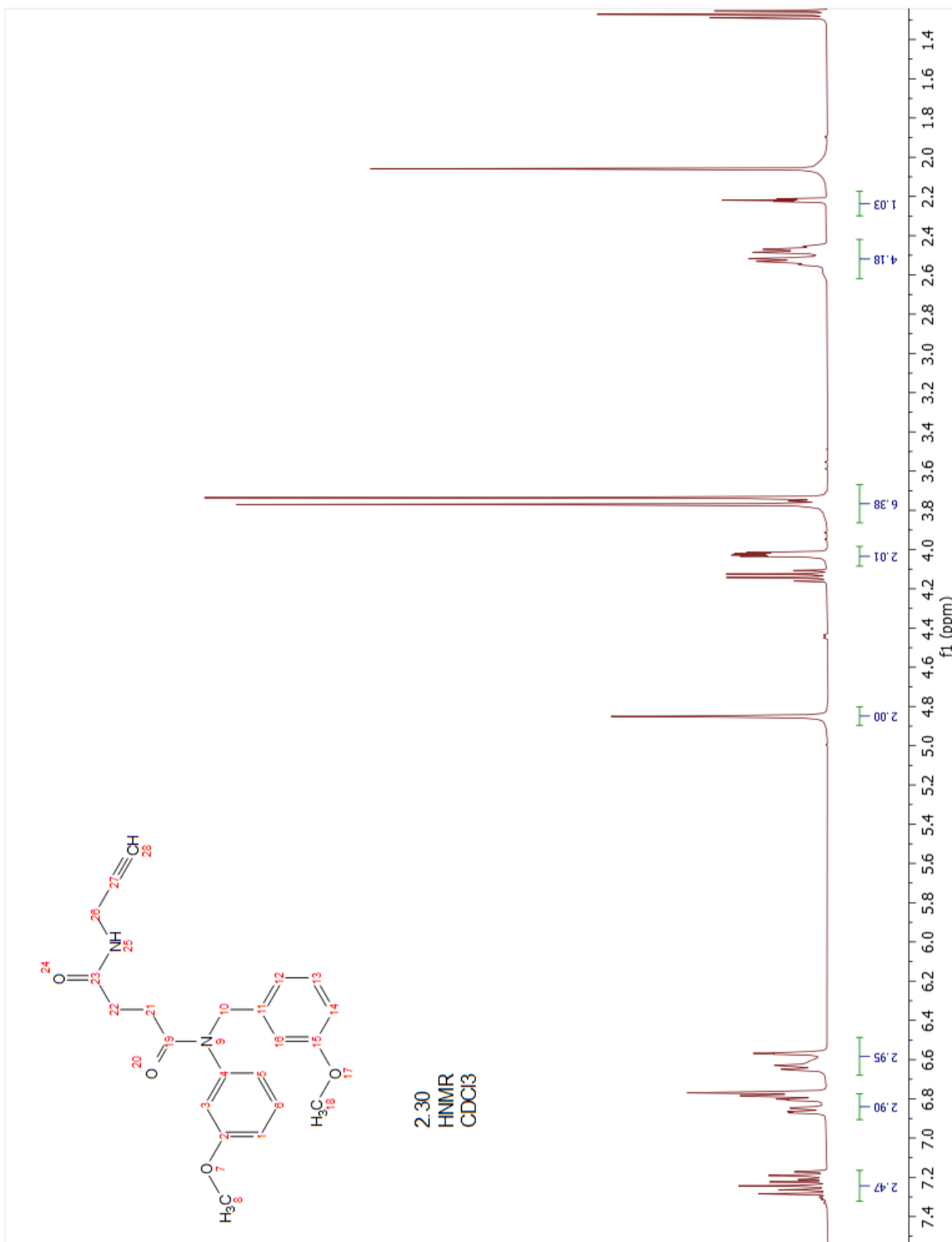
**2.25 CNMR**



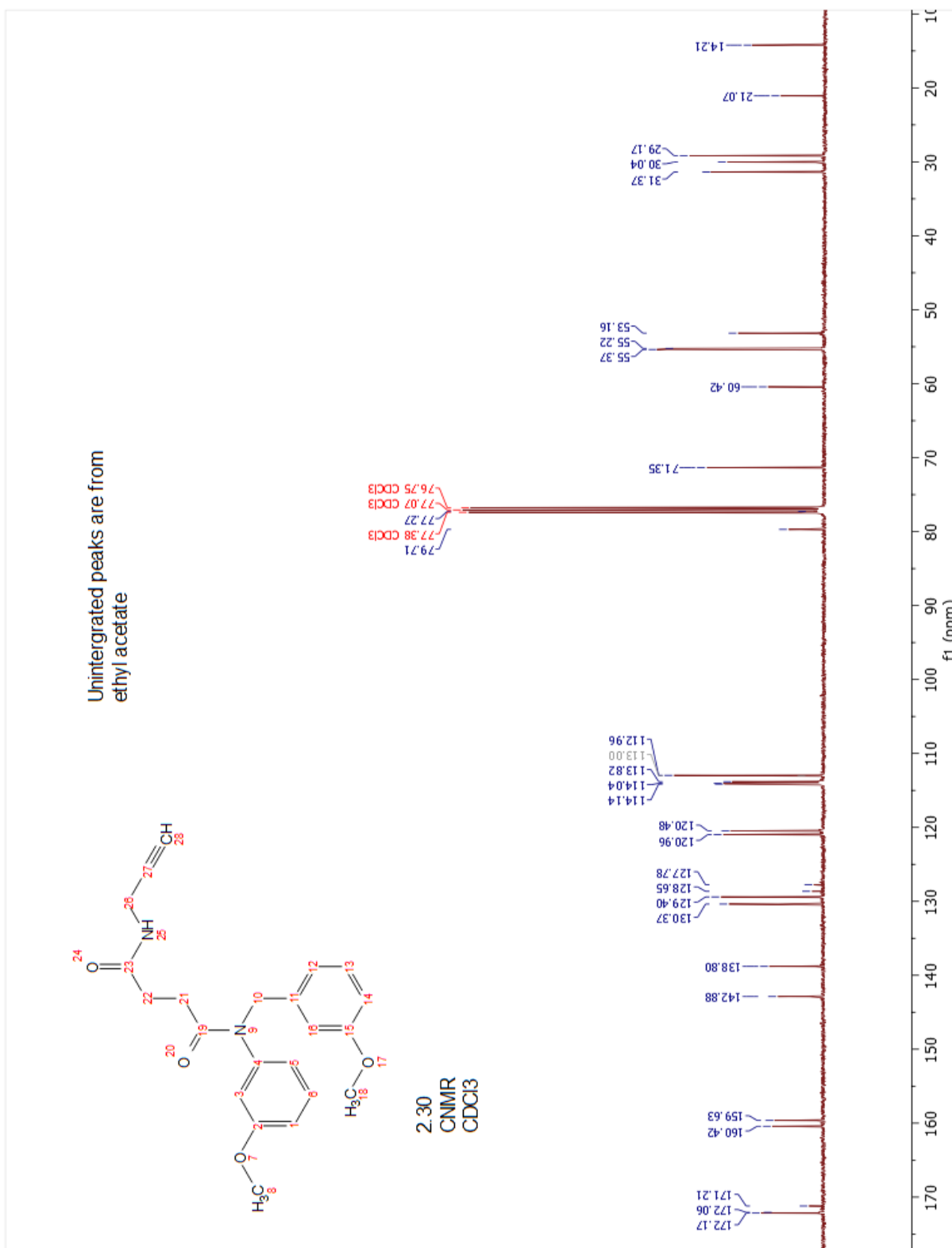
2.26 HNMR



2.26 CNMR

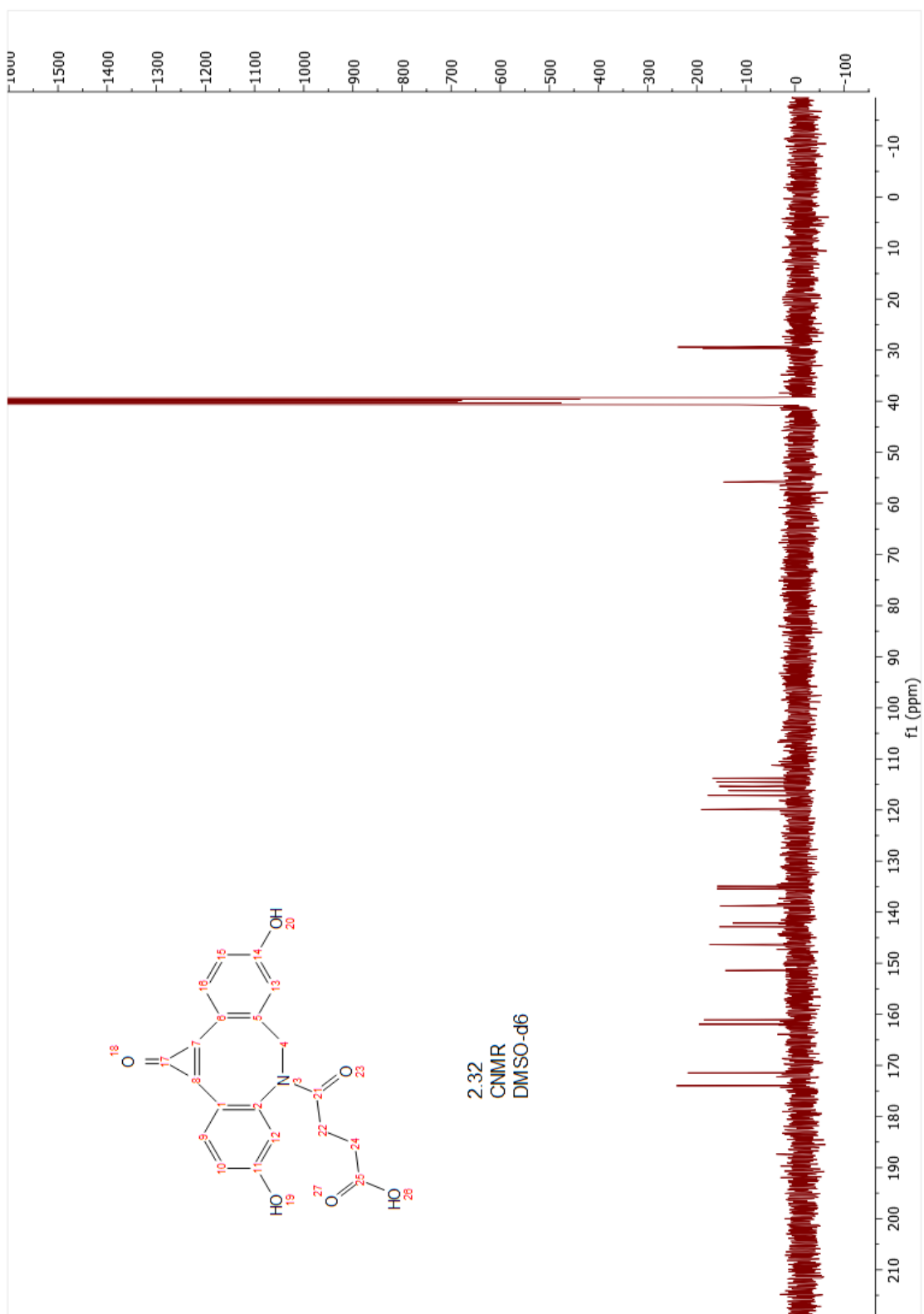


**2.30 <sup>1</sup>H NMR**

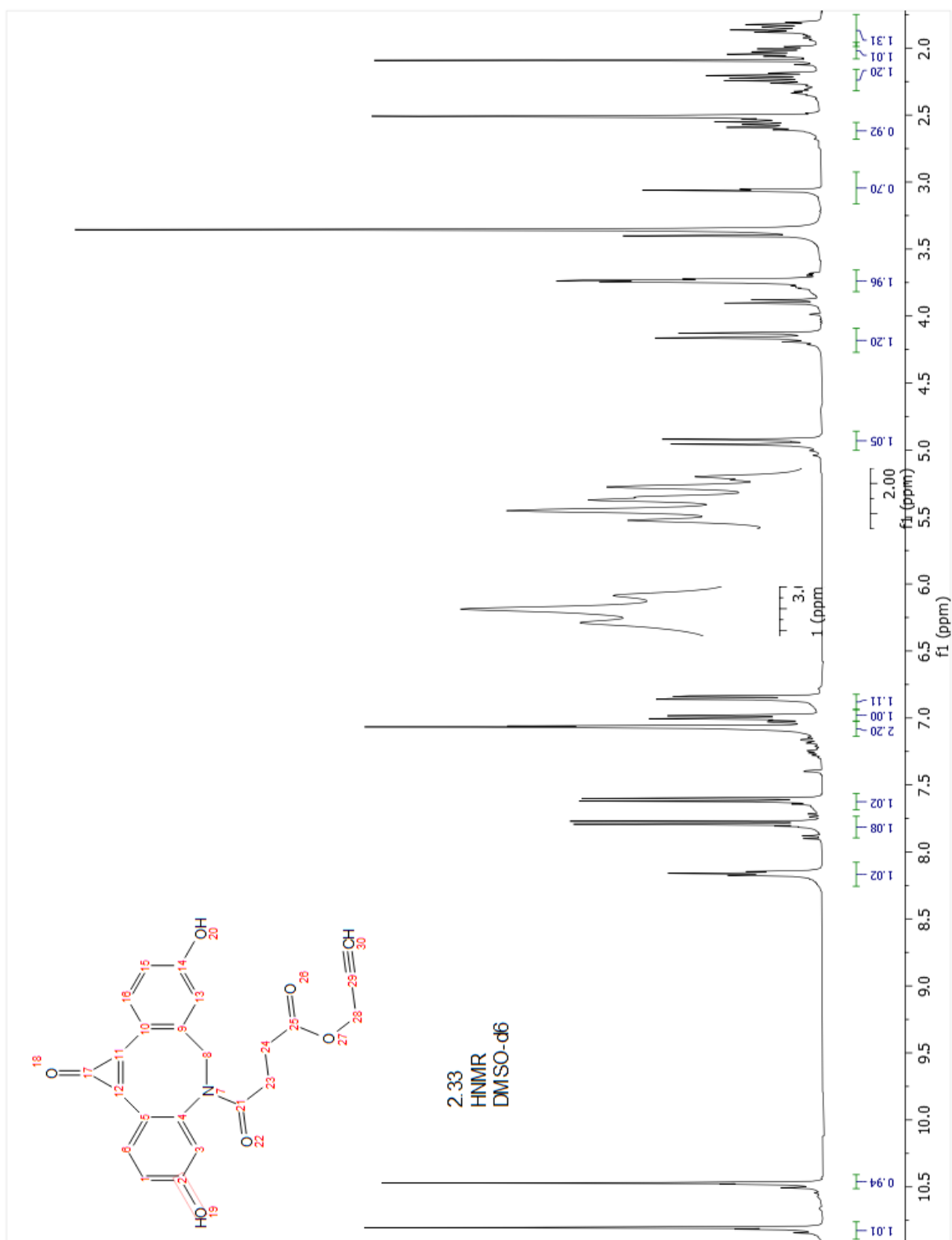


### 2.30 CNMR

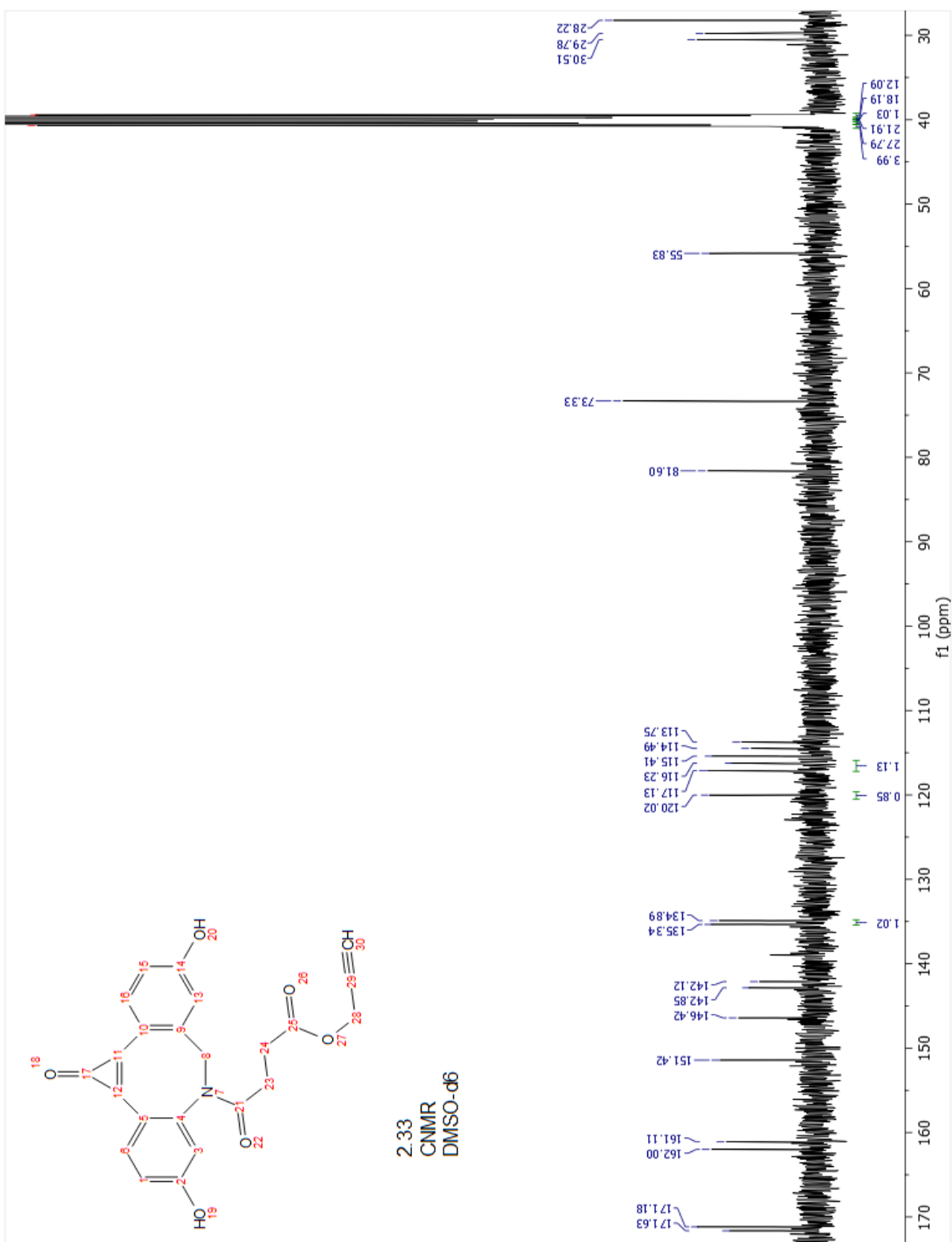




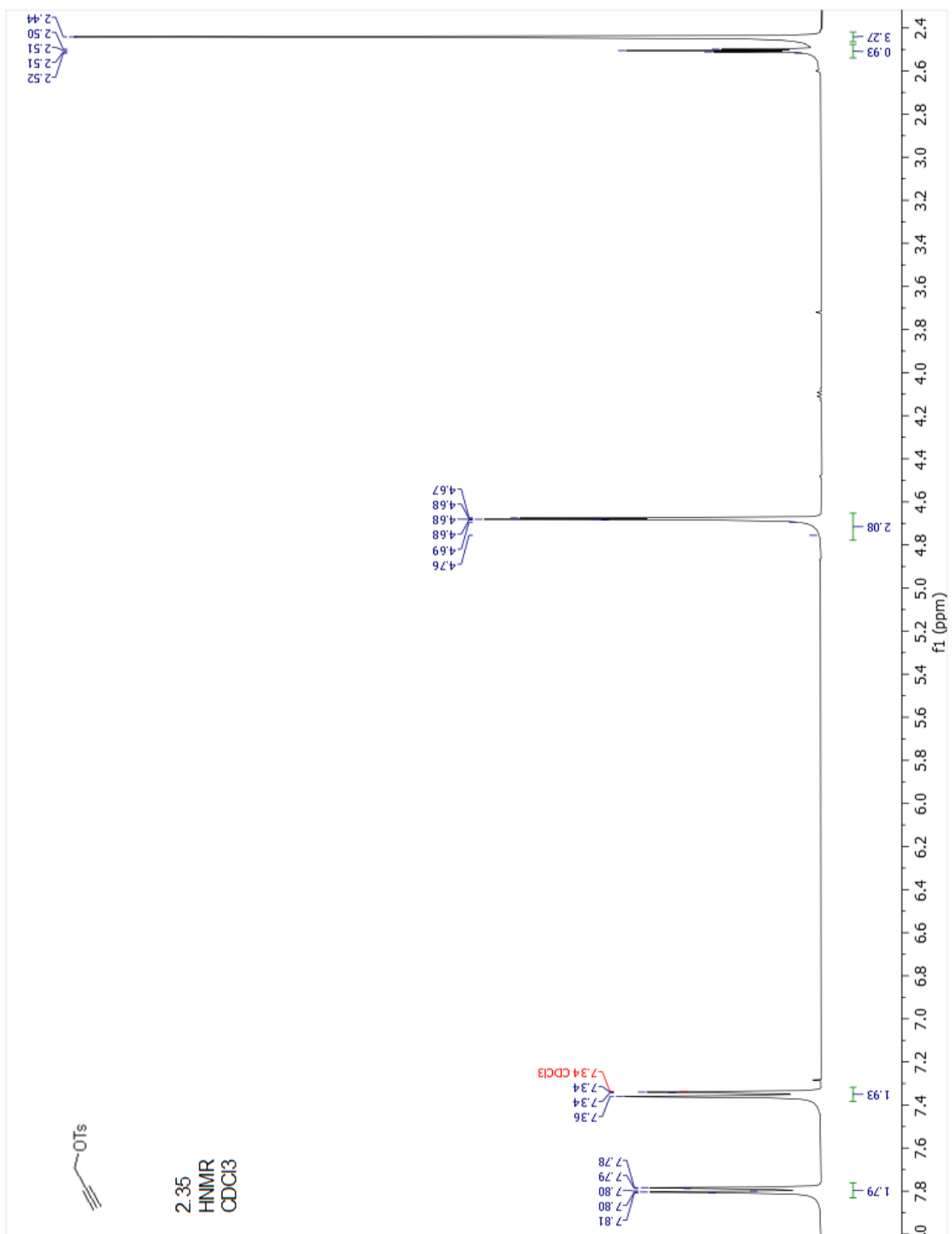
## 2.32 CNMR



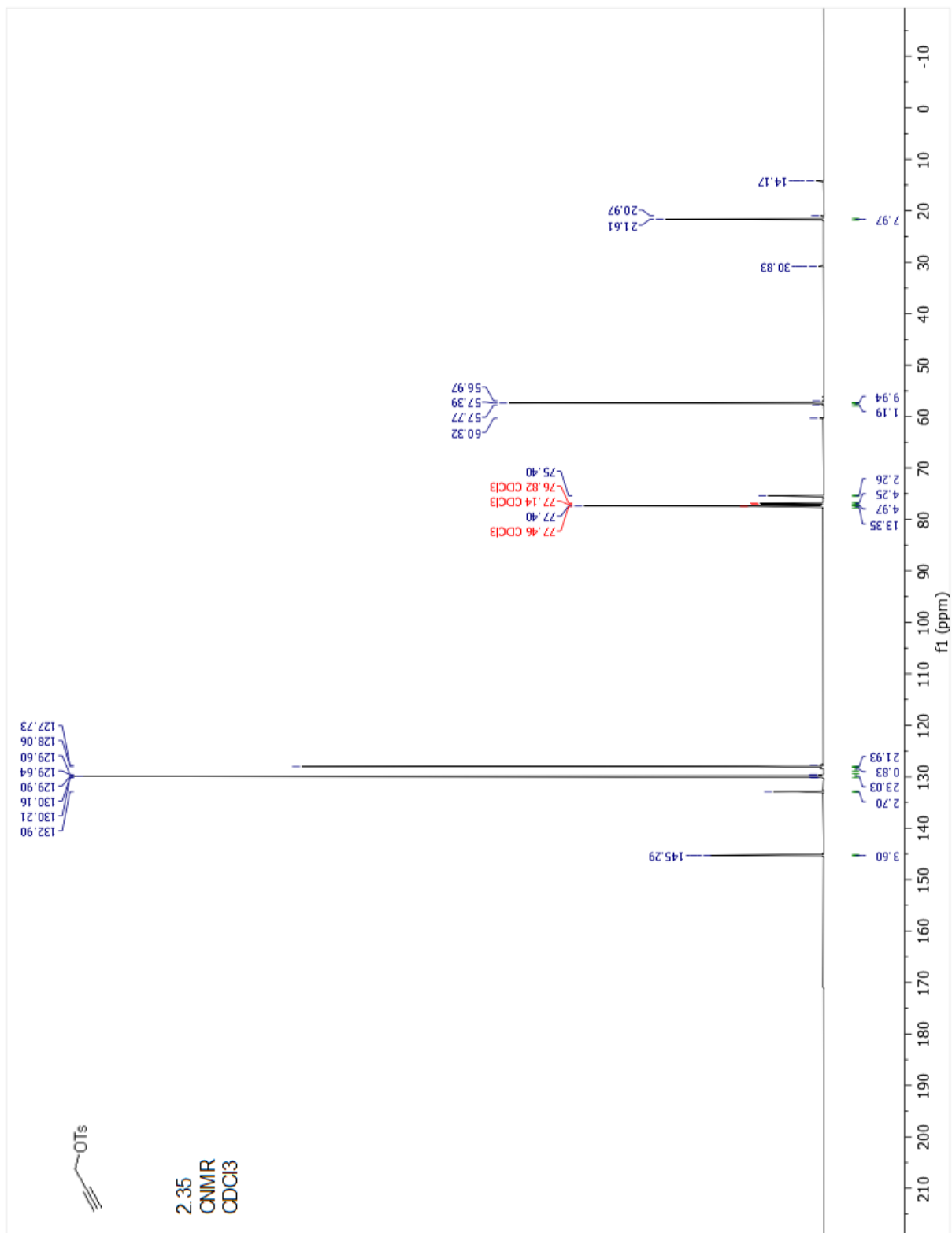
### 2.33 <sup>1</sup>H NMR



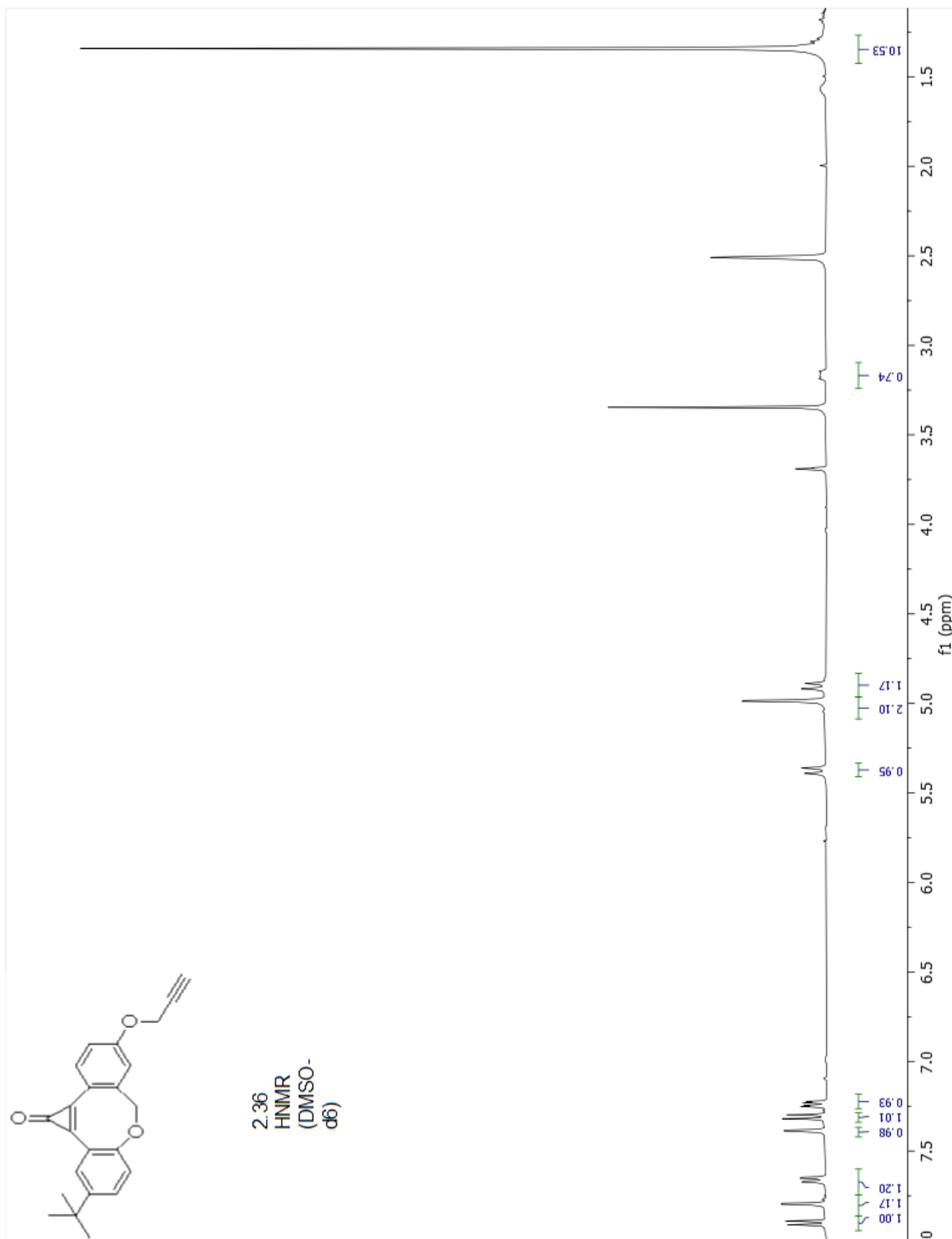
### 2.33 CNMR



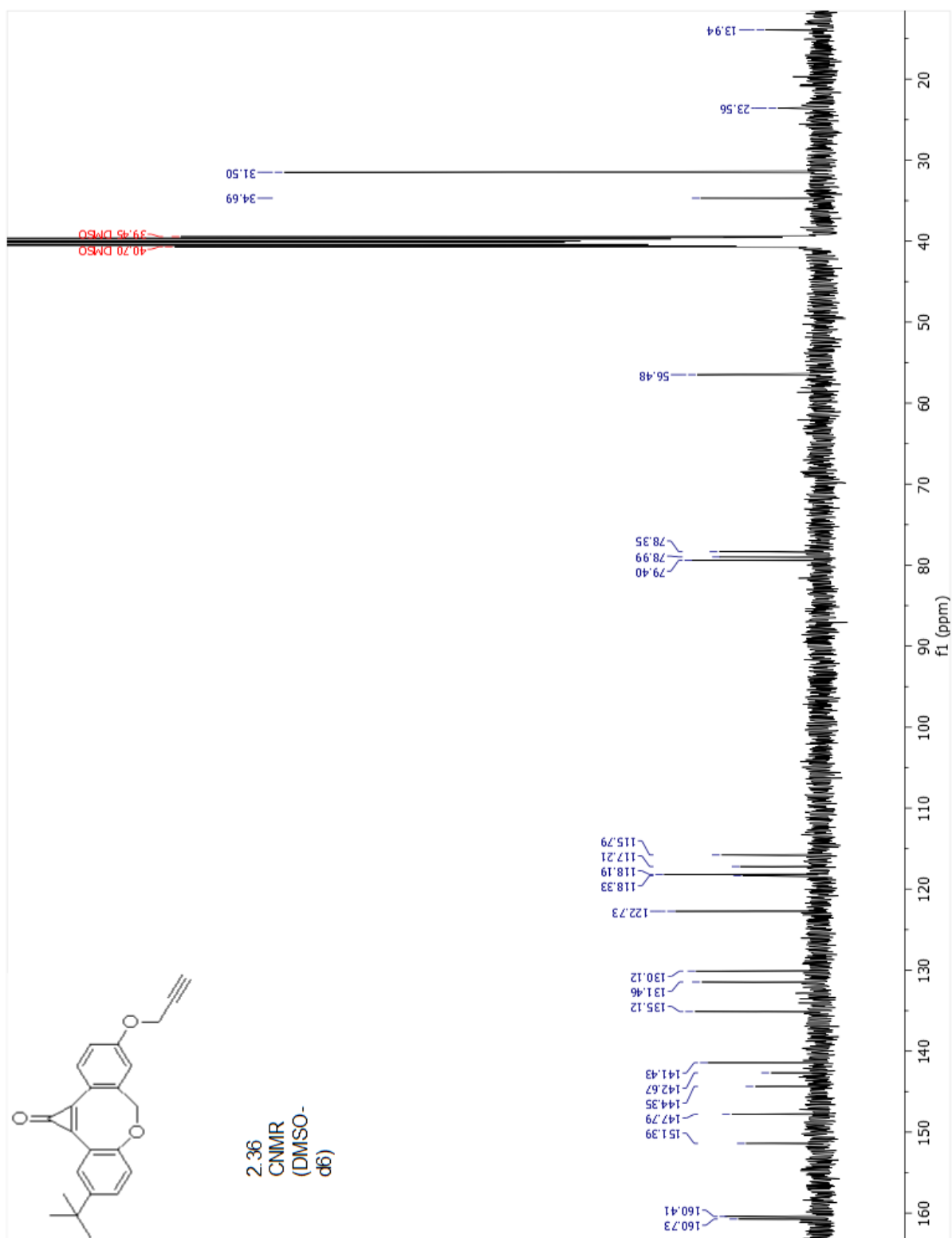
2.35 HNMR



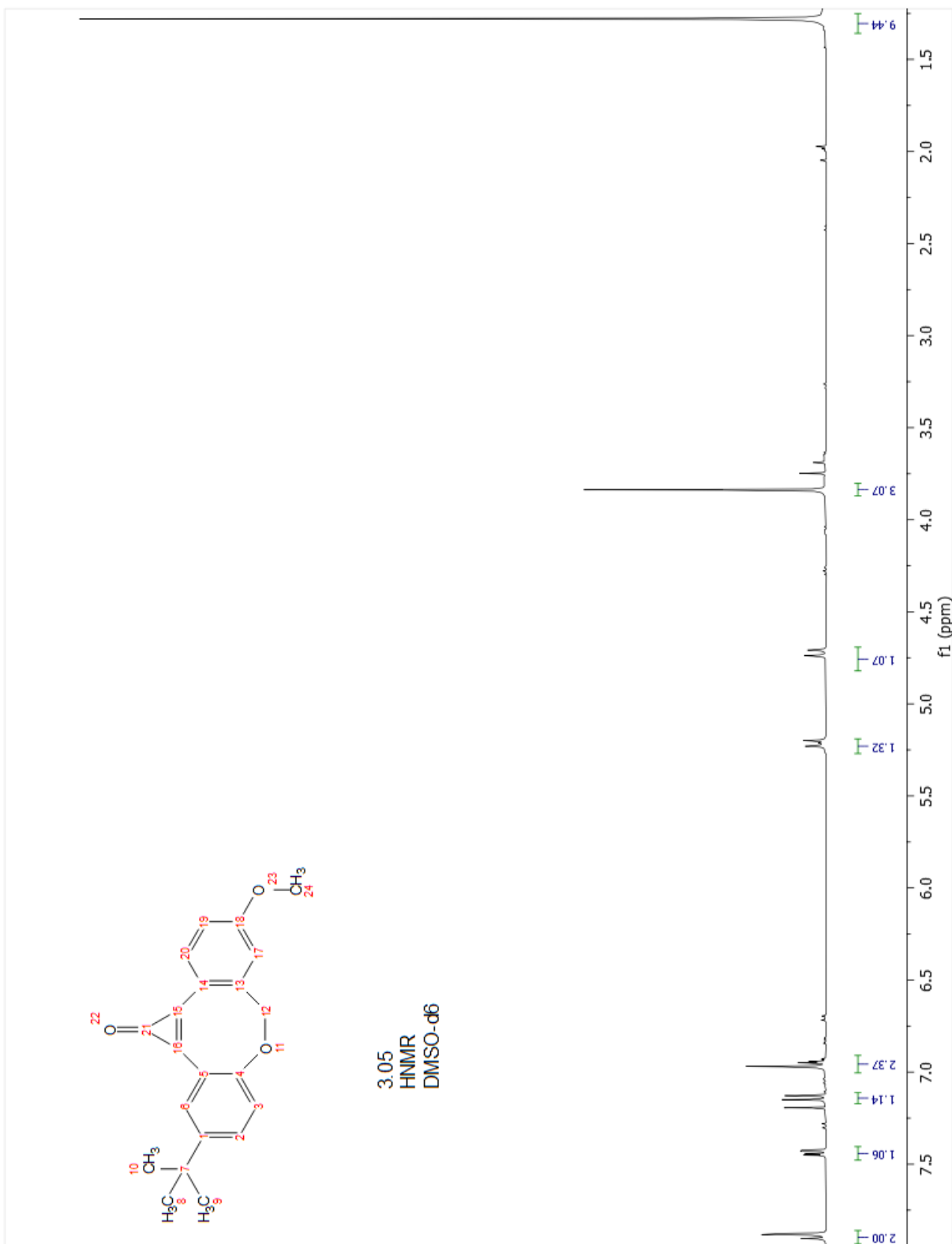
### 2.35 CNMR



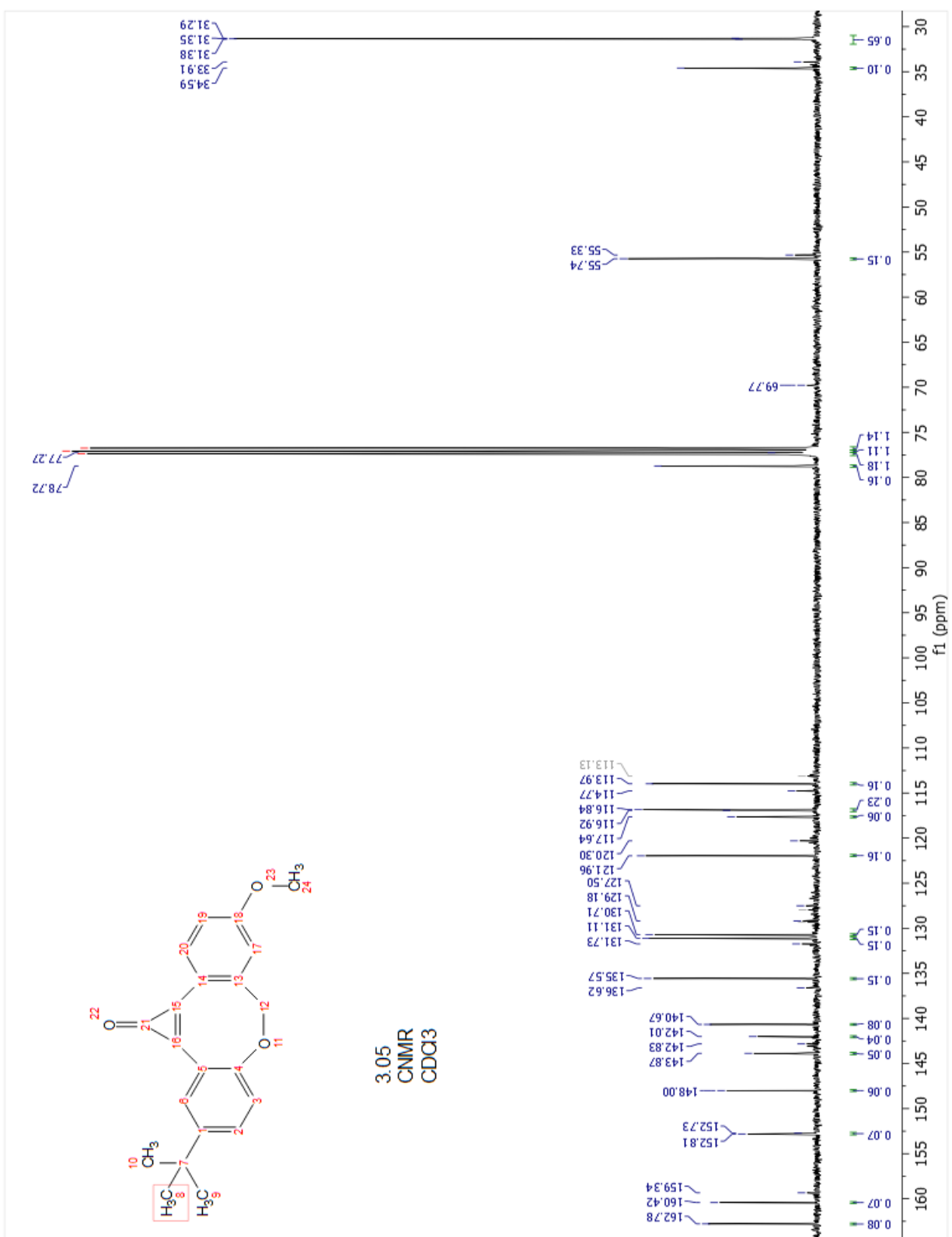
**2.36 HNMR**



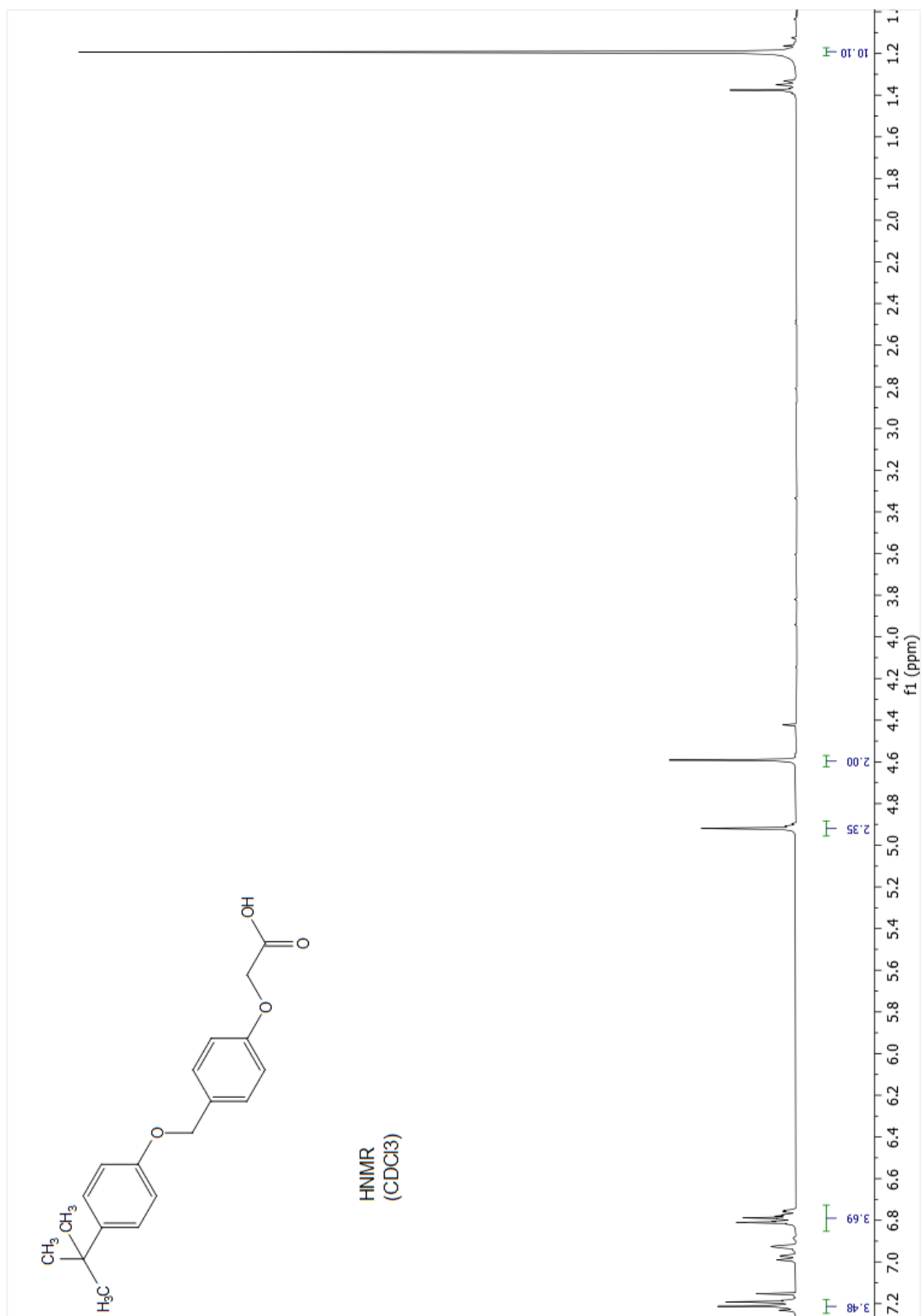
2.36 CNMR

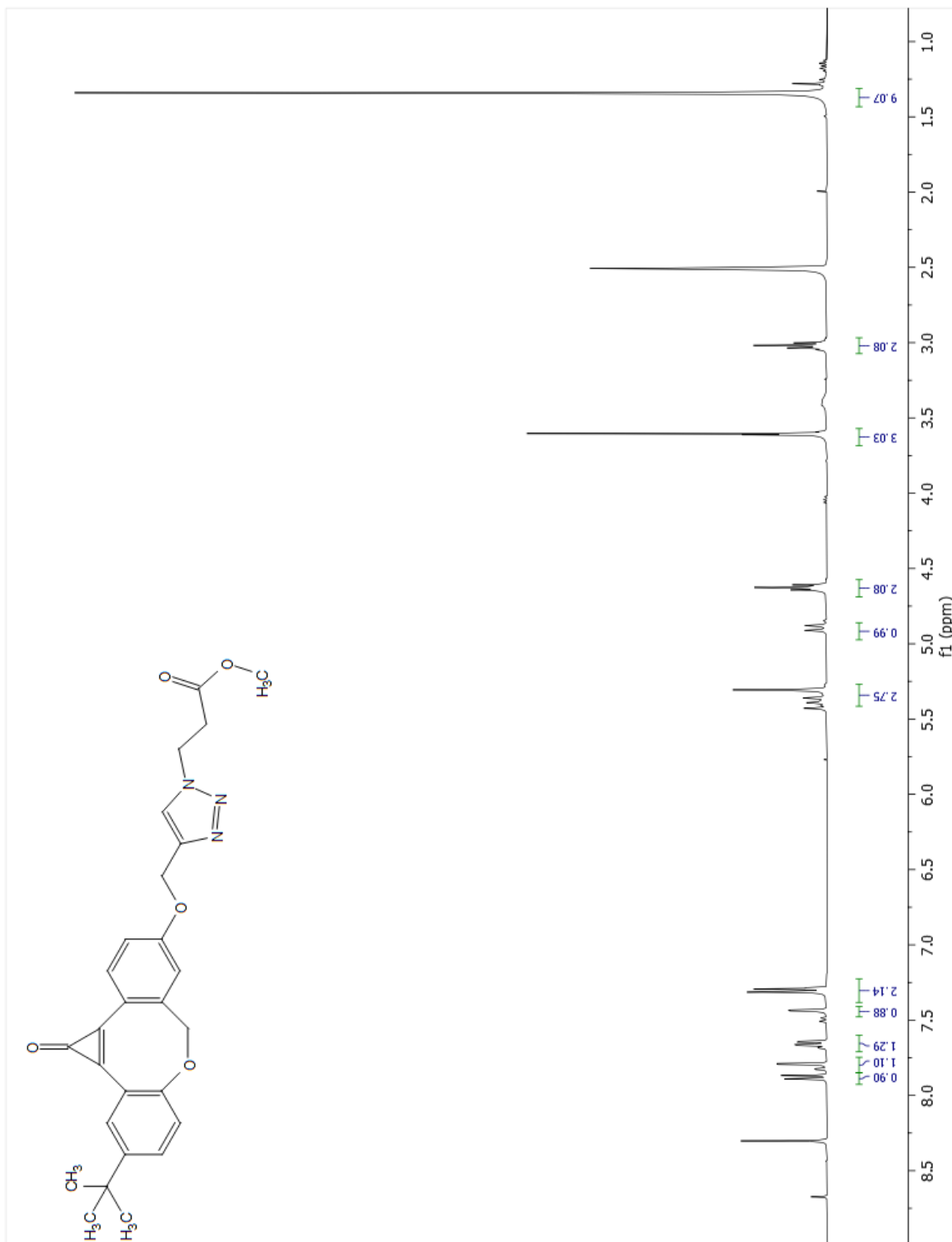


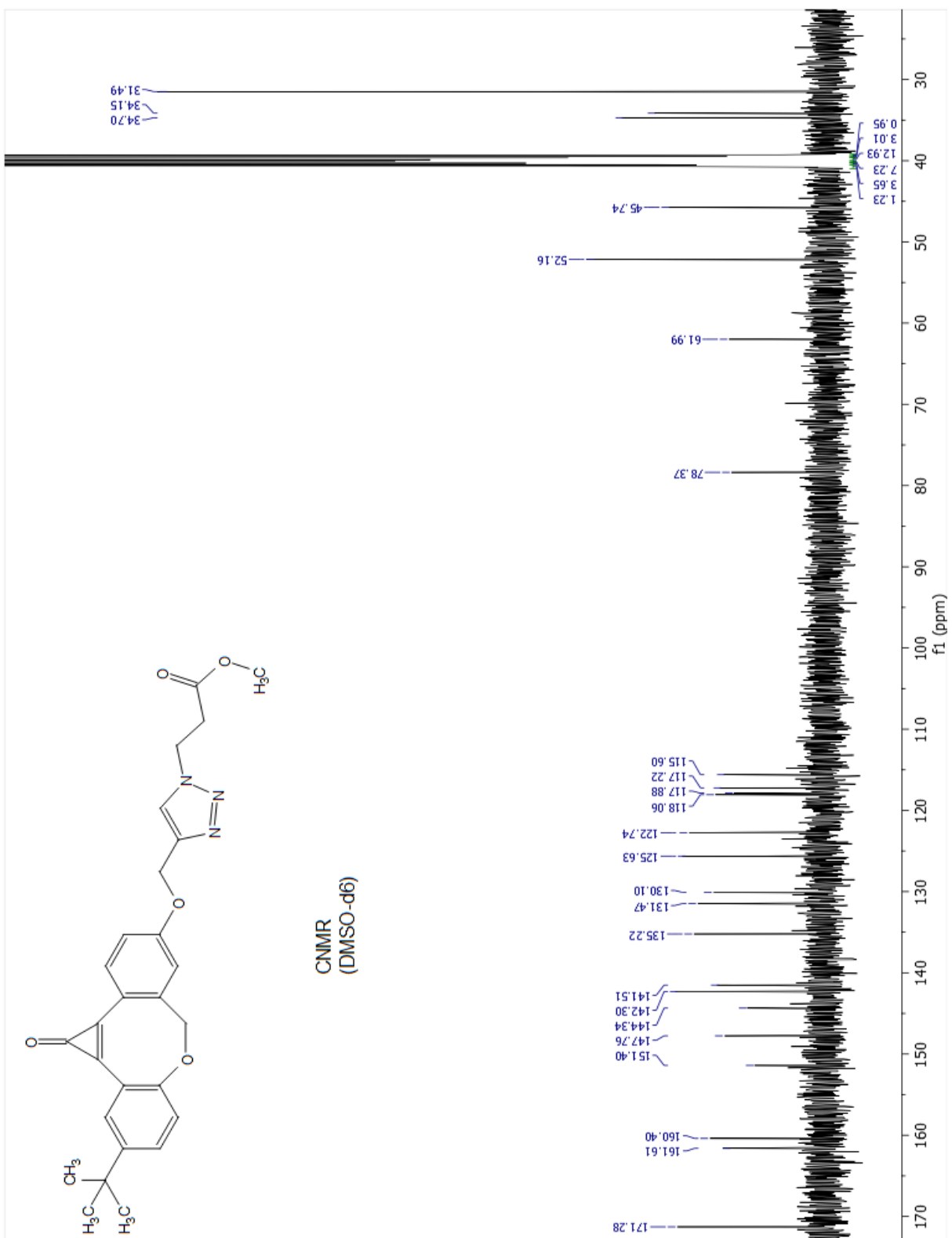
### 3.05 HNMR

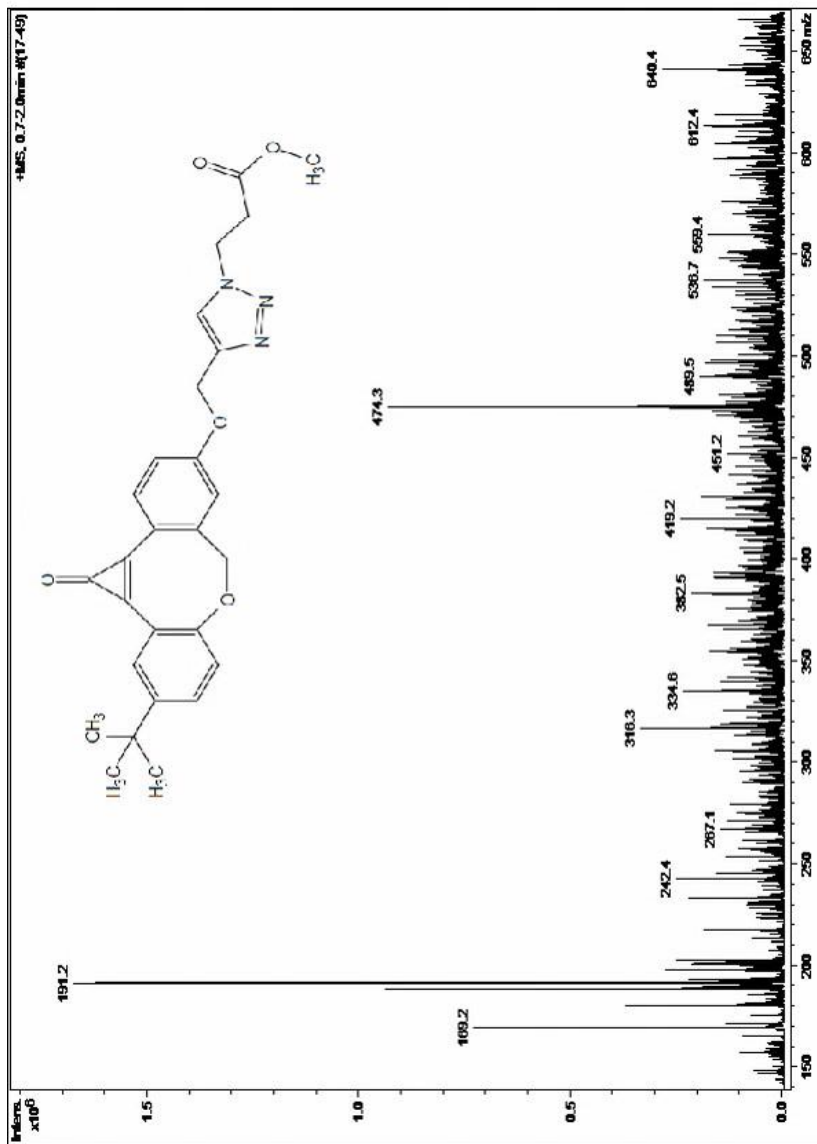


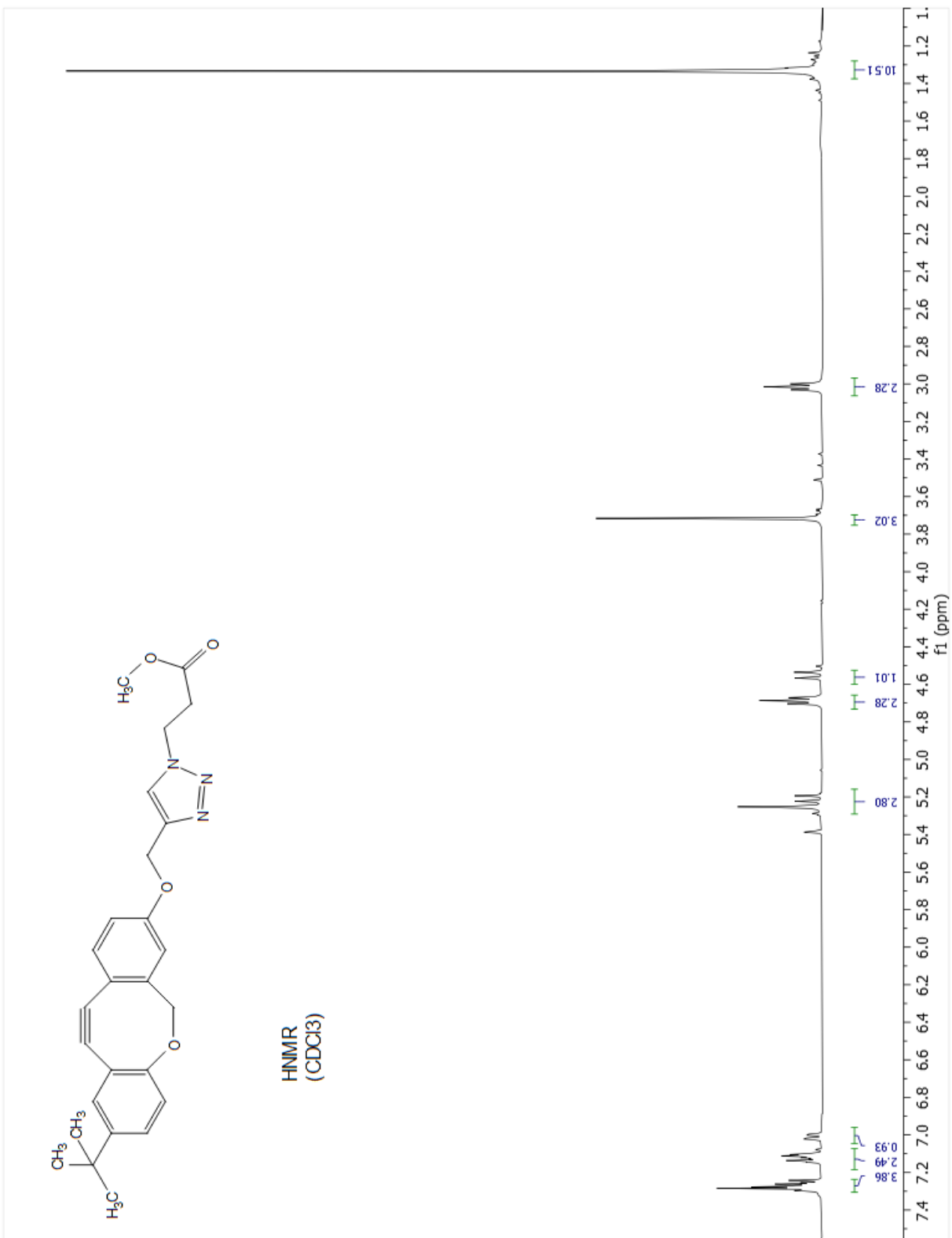
3.05 CNMR

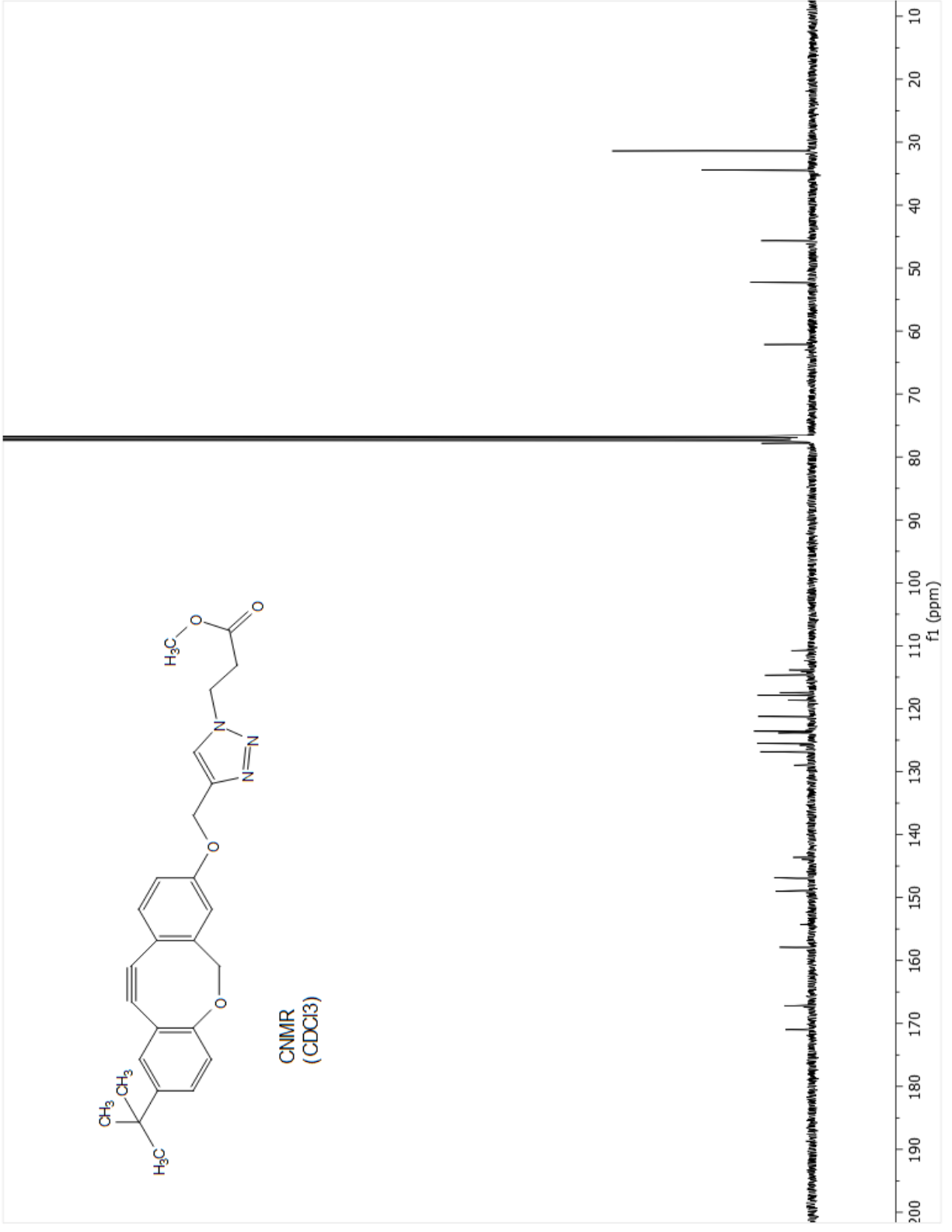


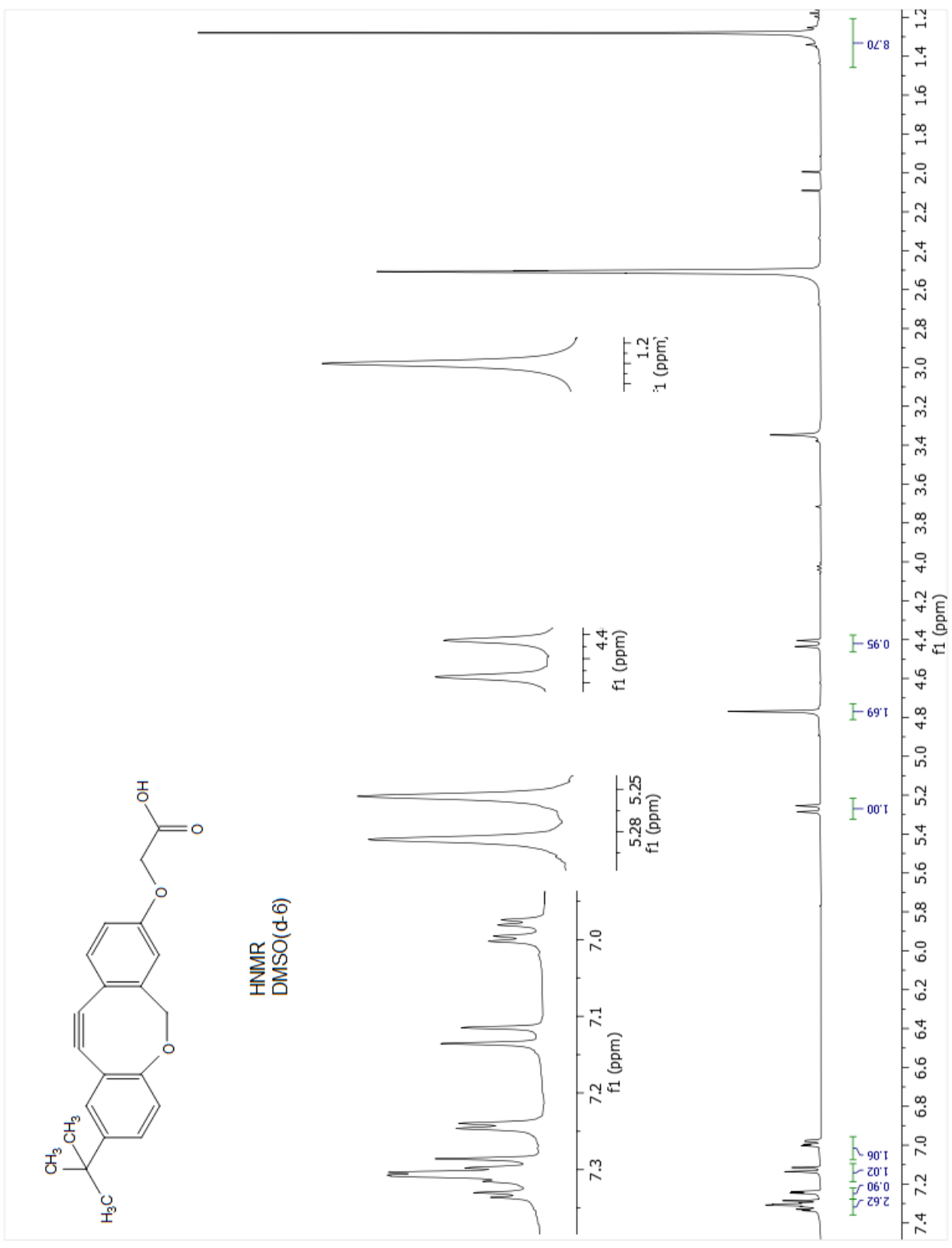


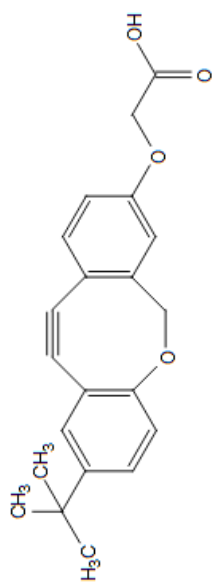




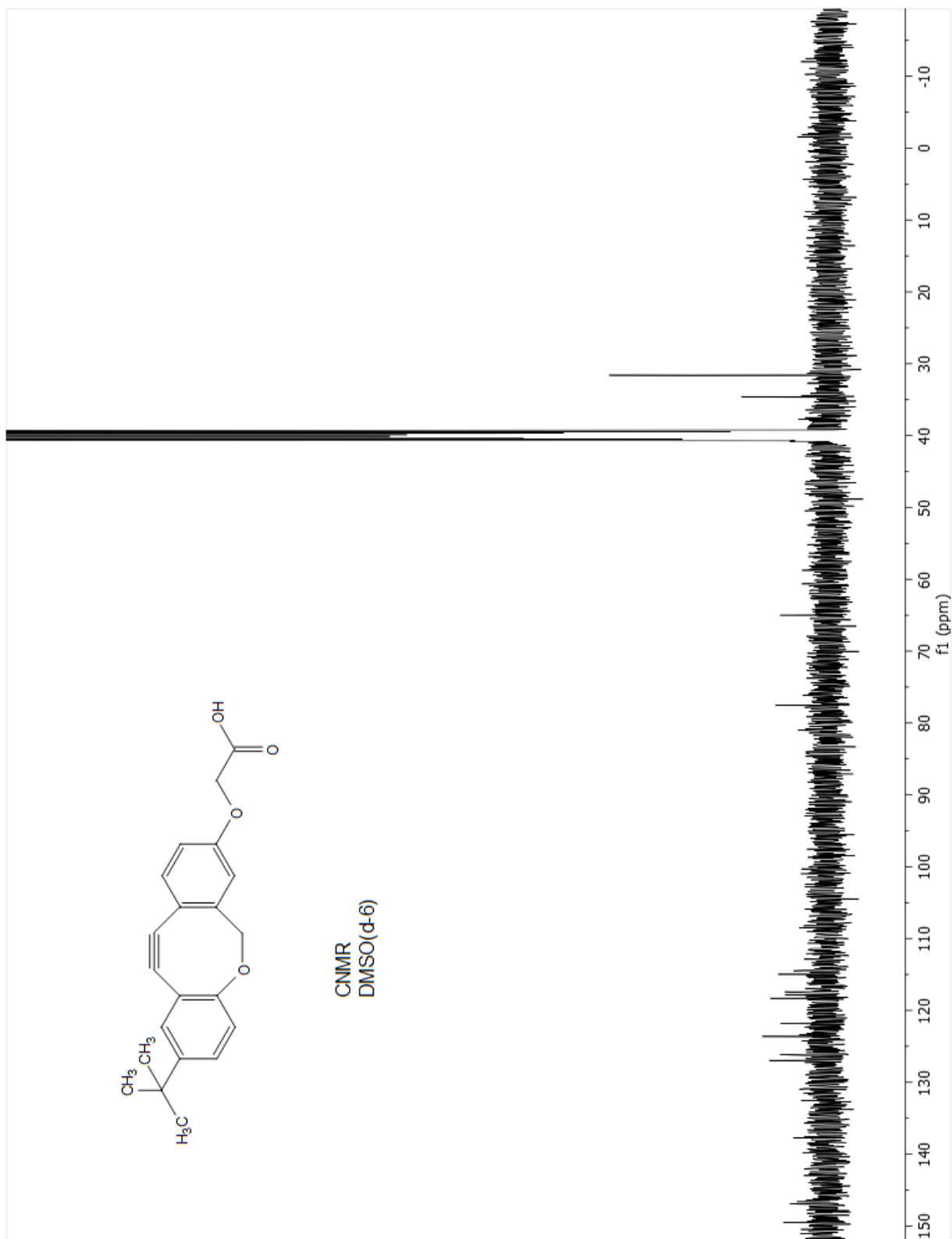


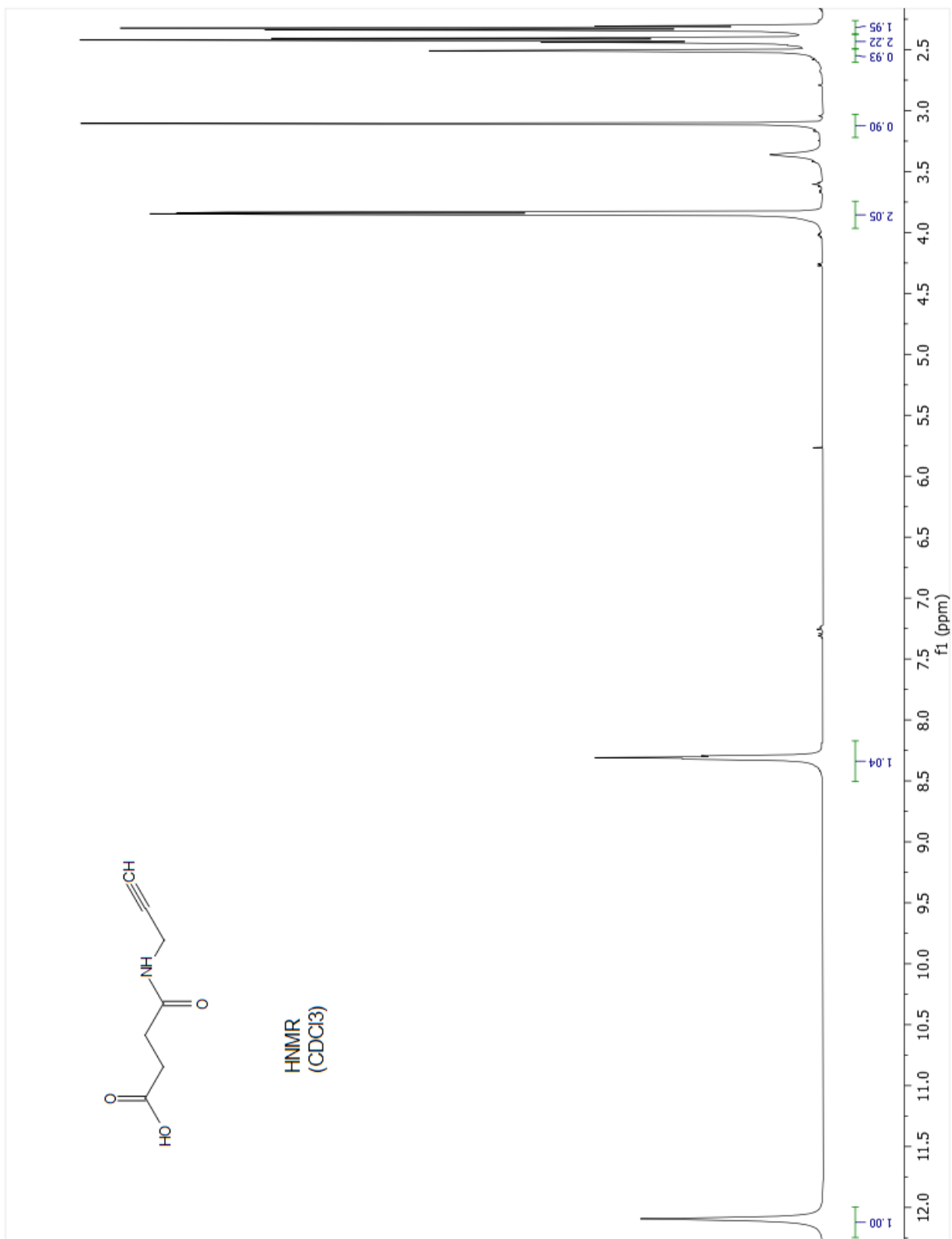


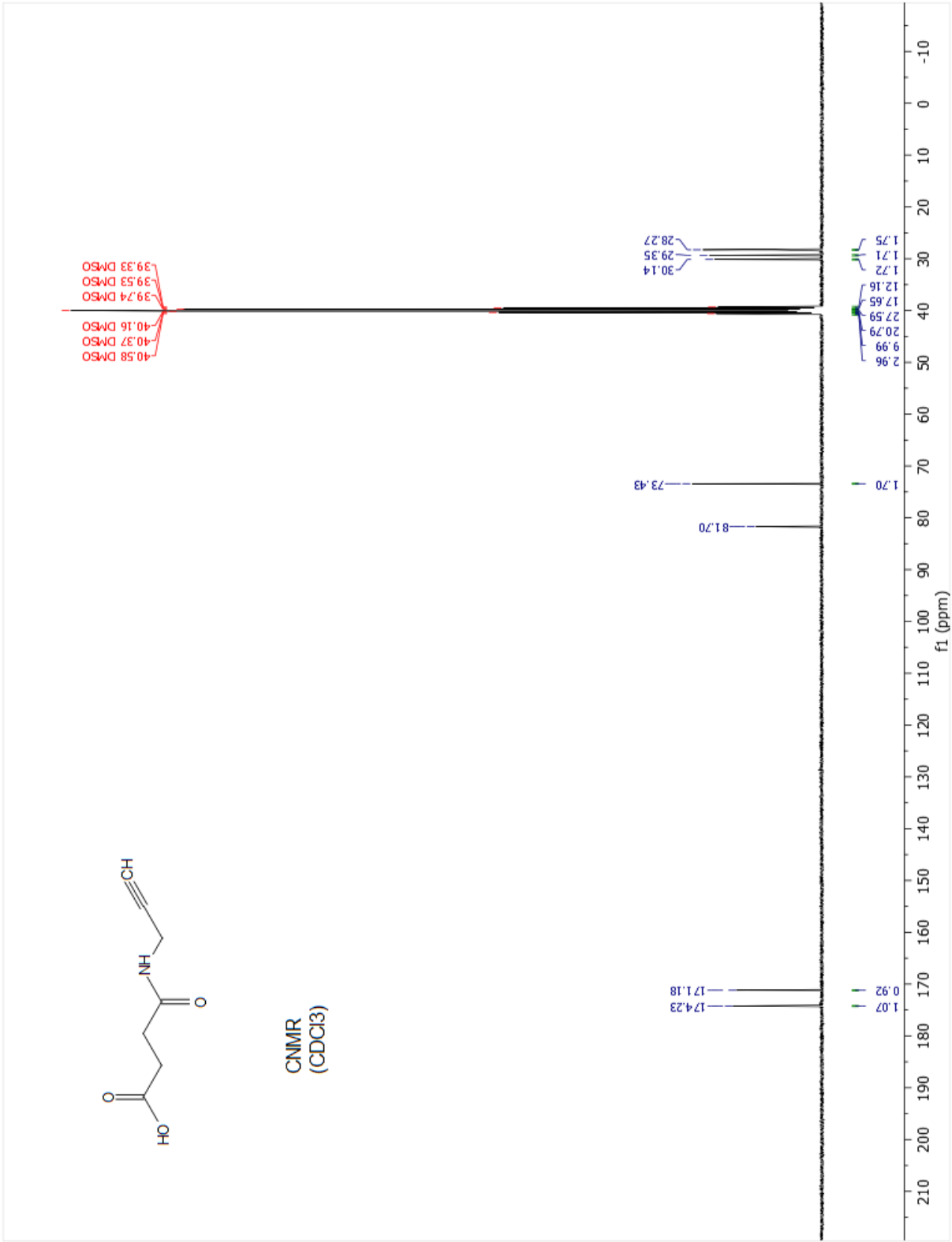


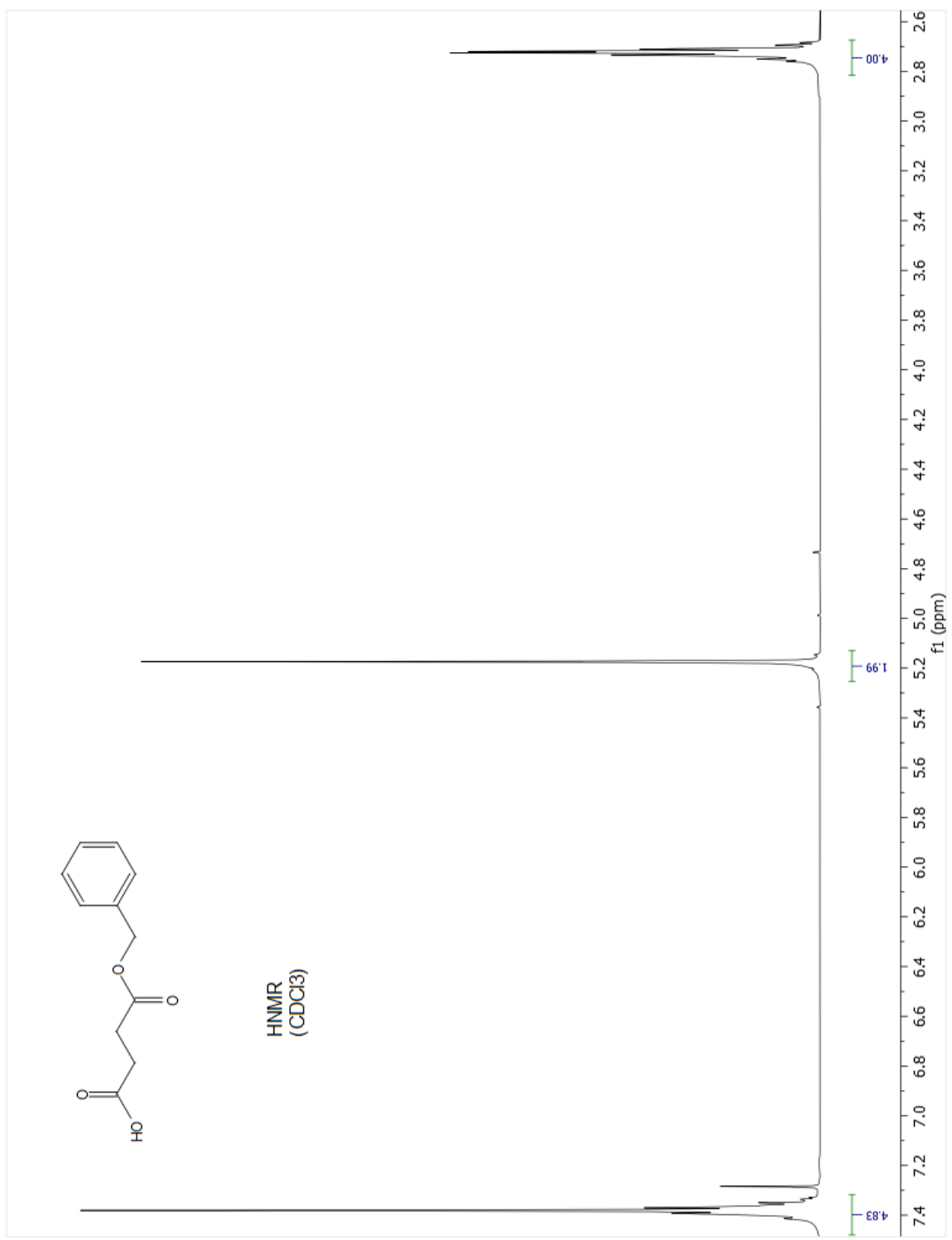


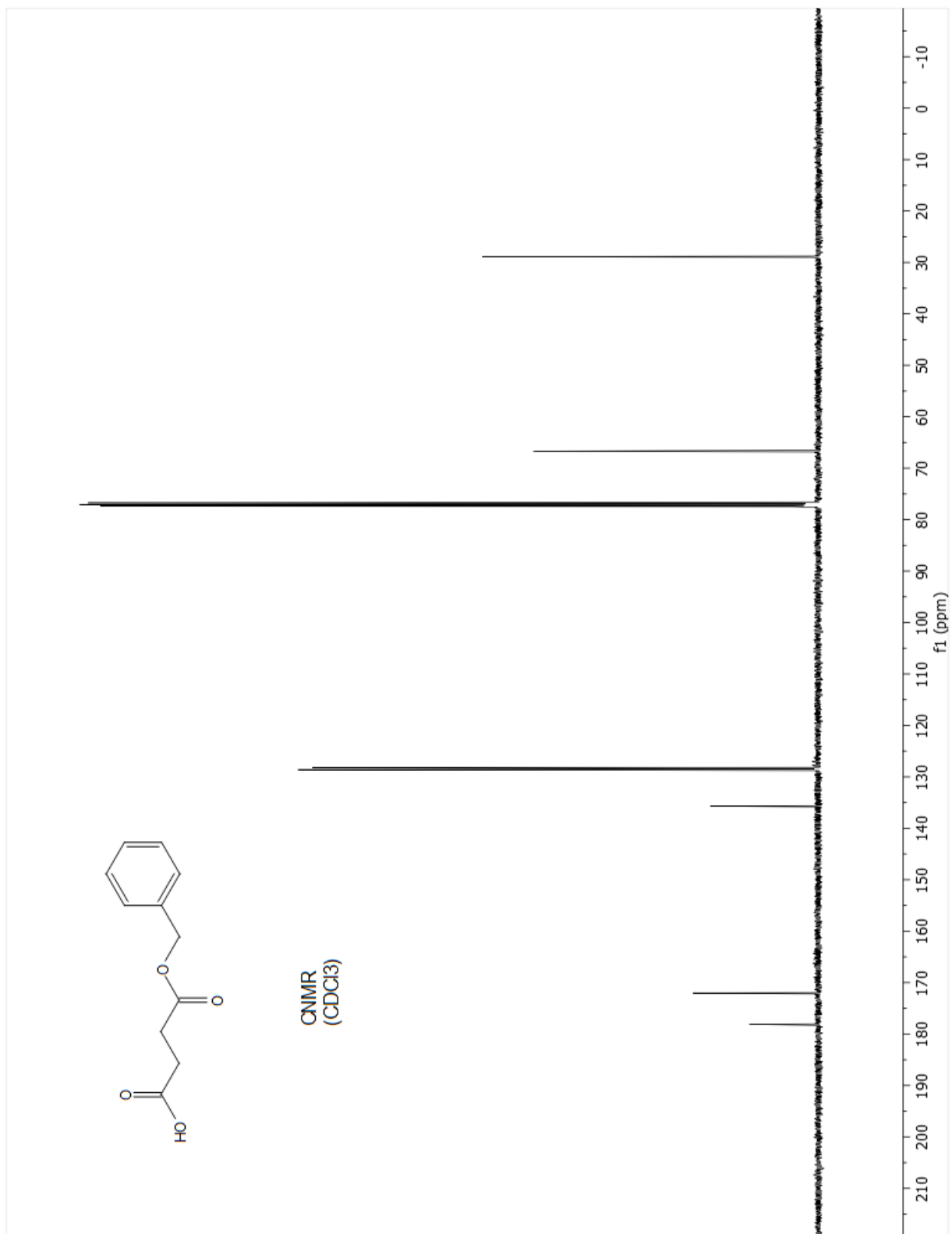
CNMR  
DMSO(d-6)

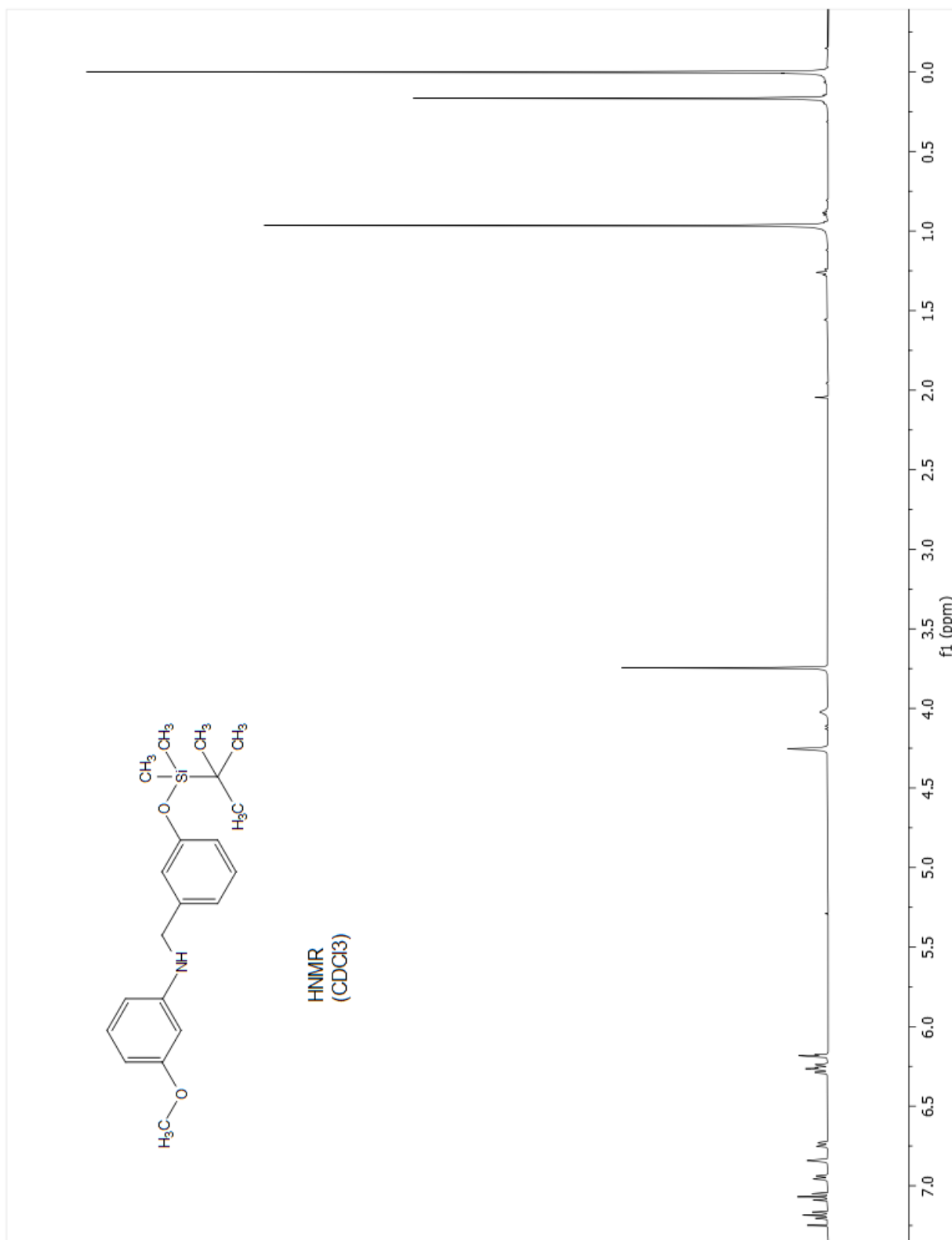


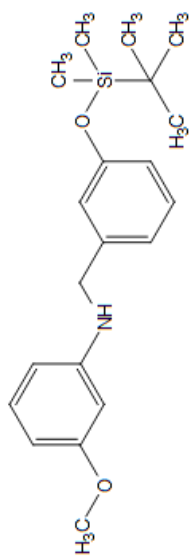




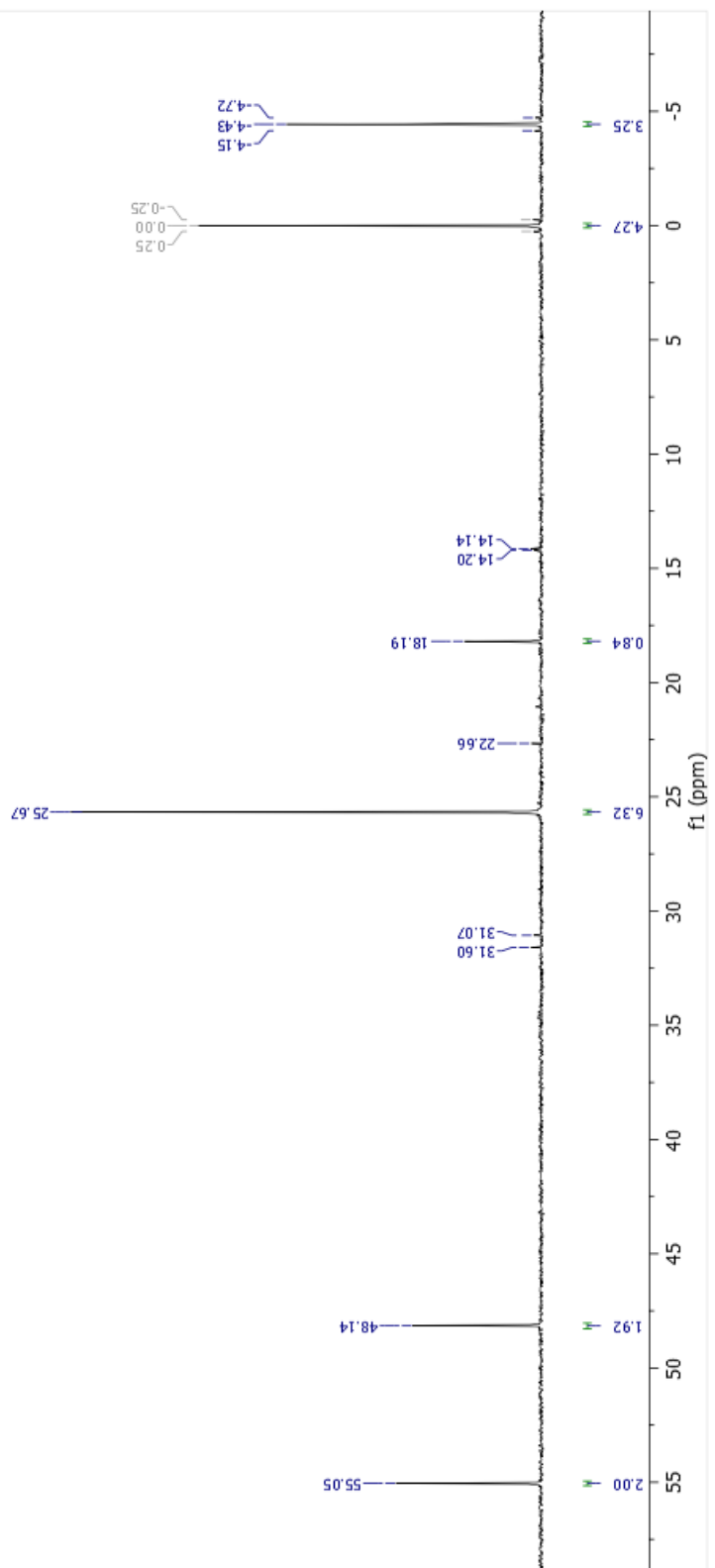




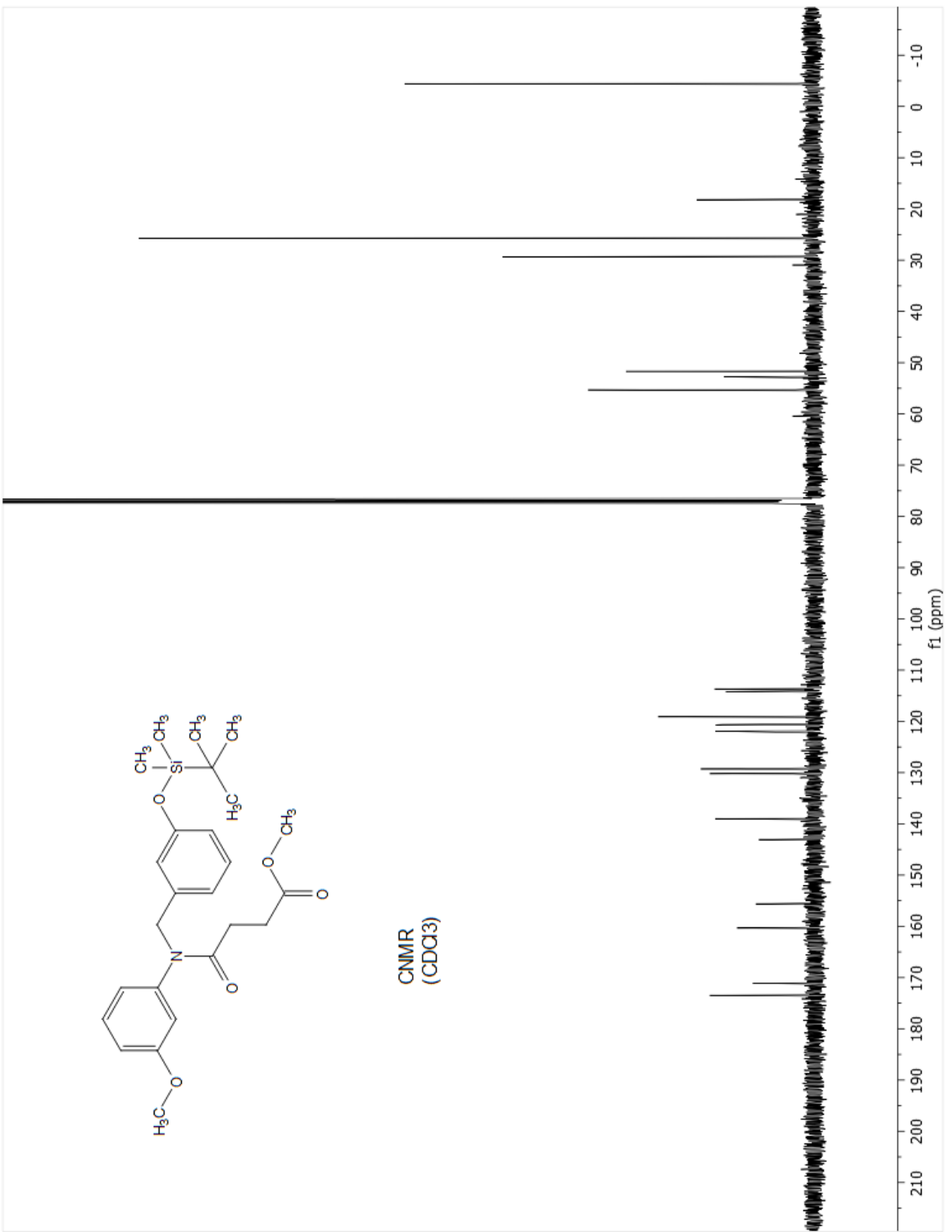


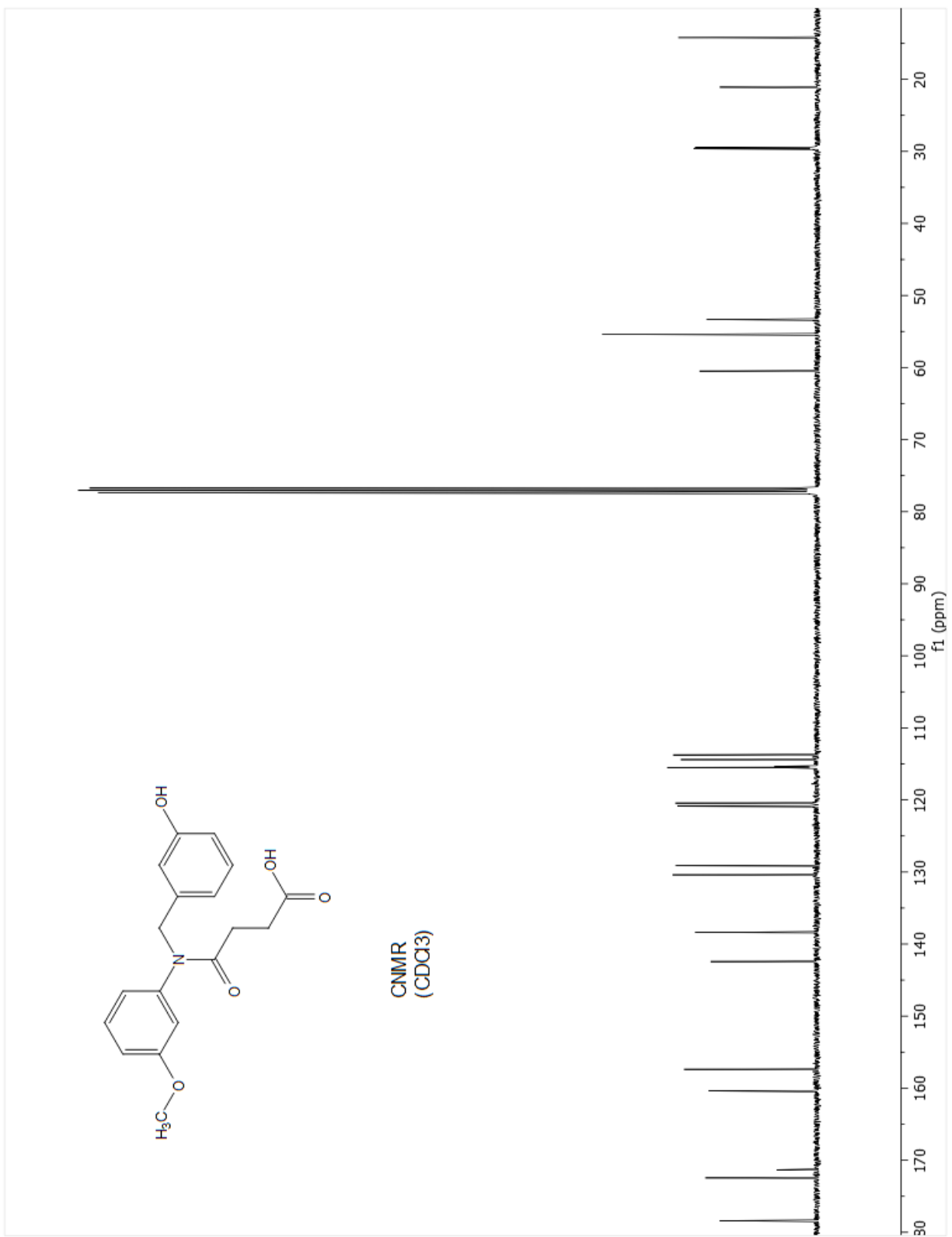


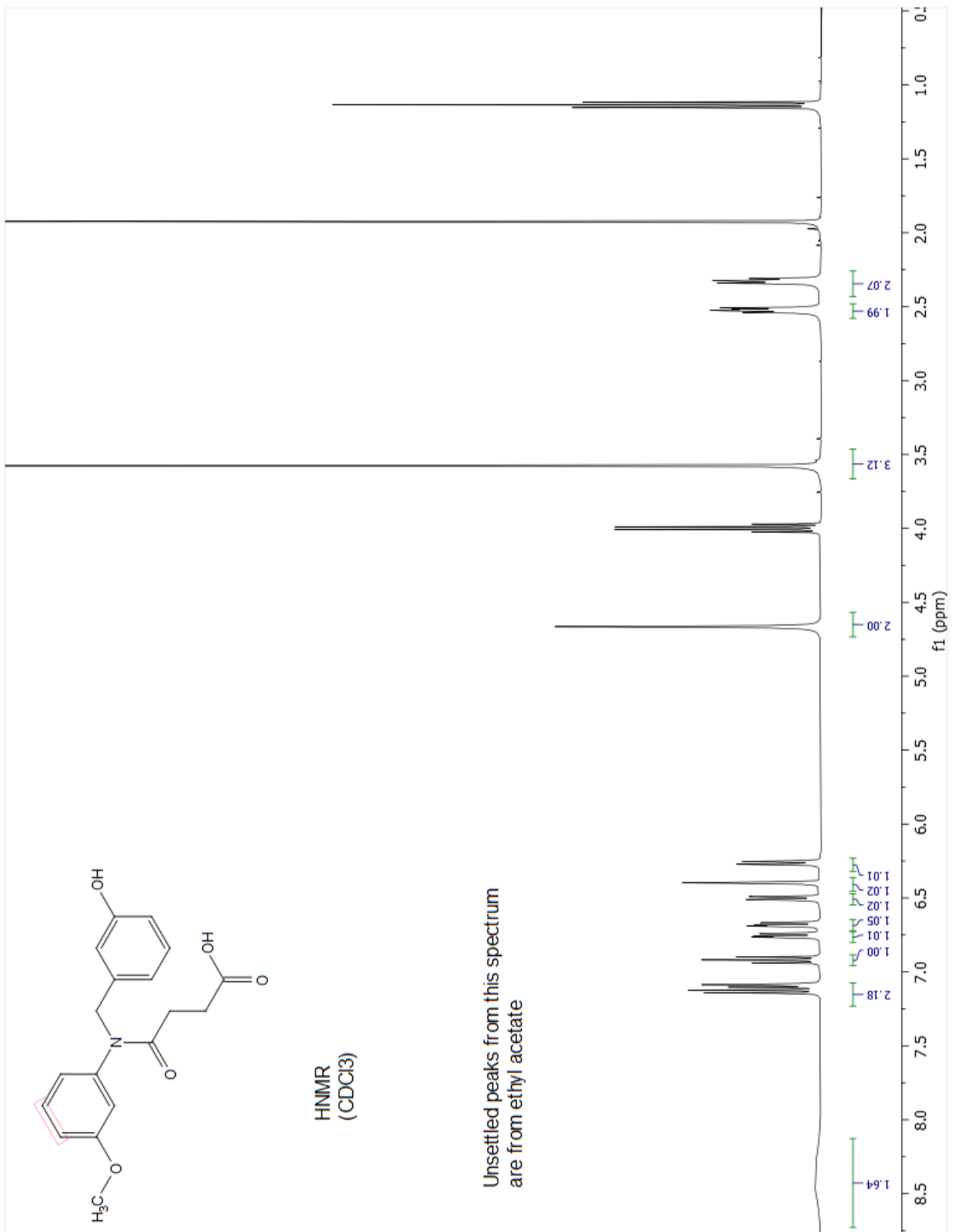
CNMR  
(CDCl<sub>3</sub>)

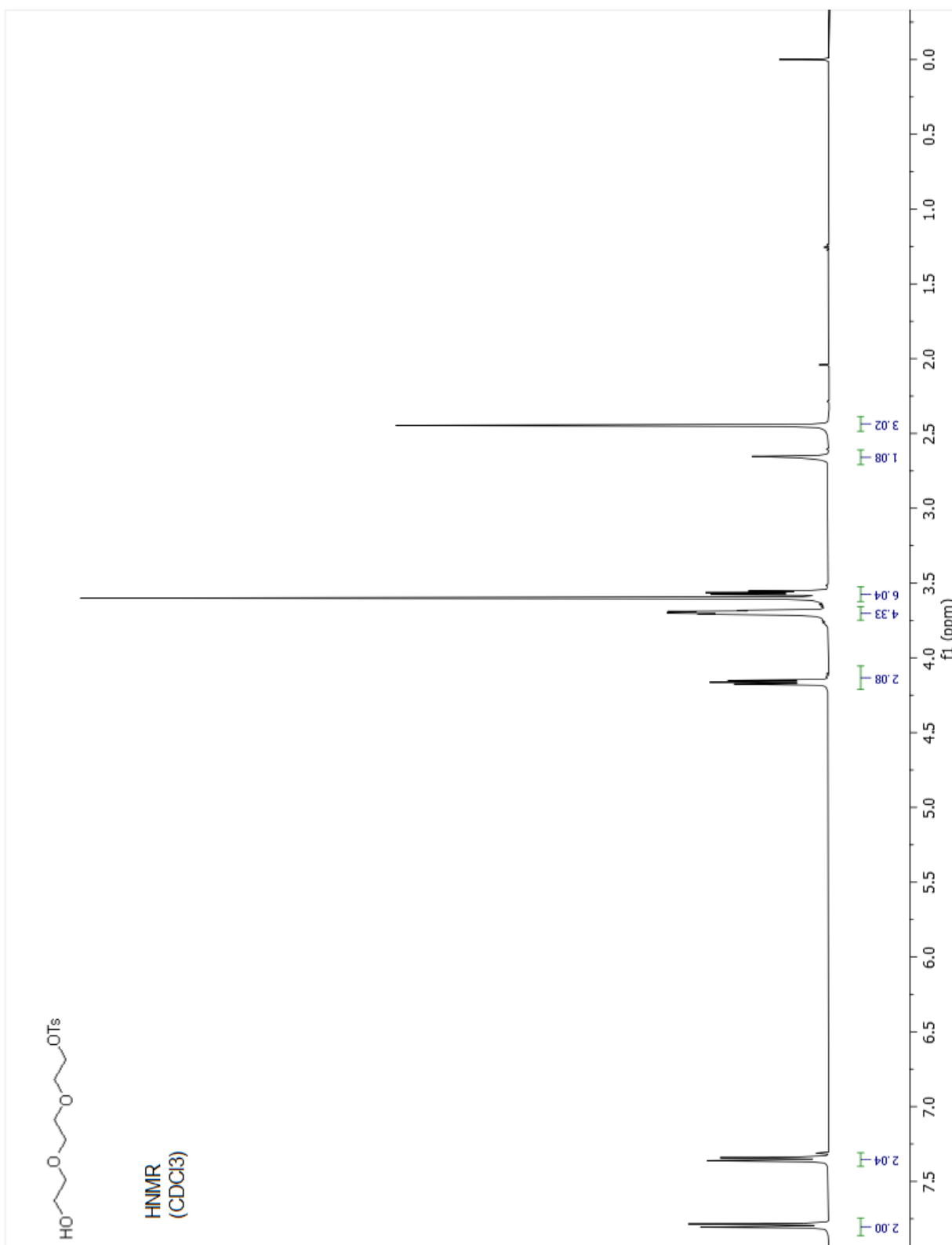




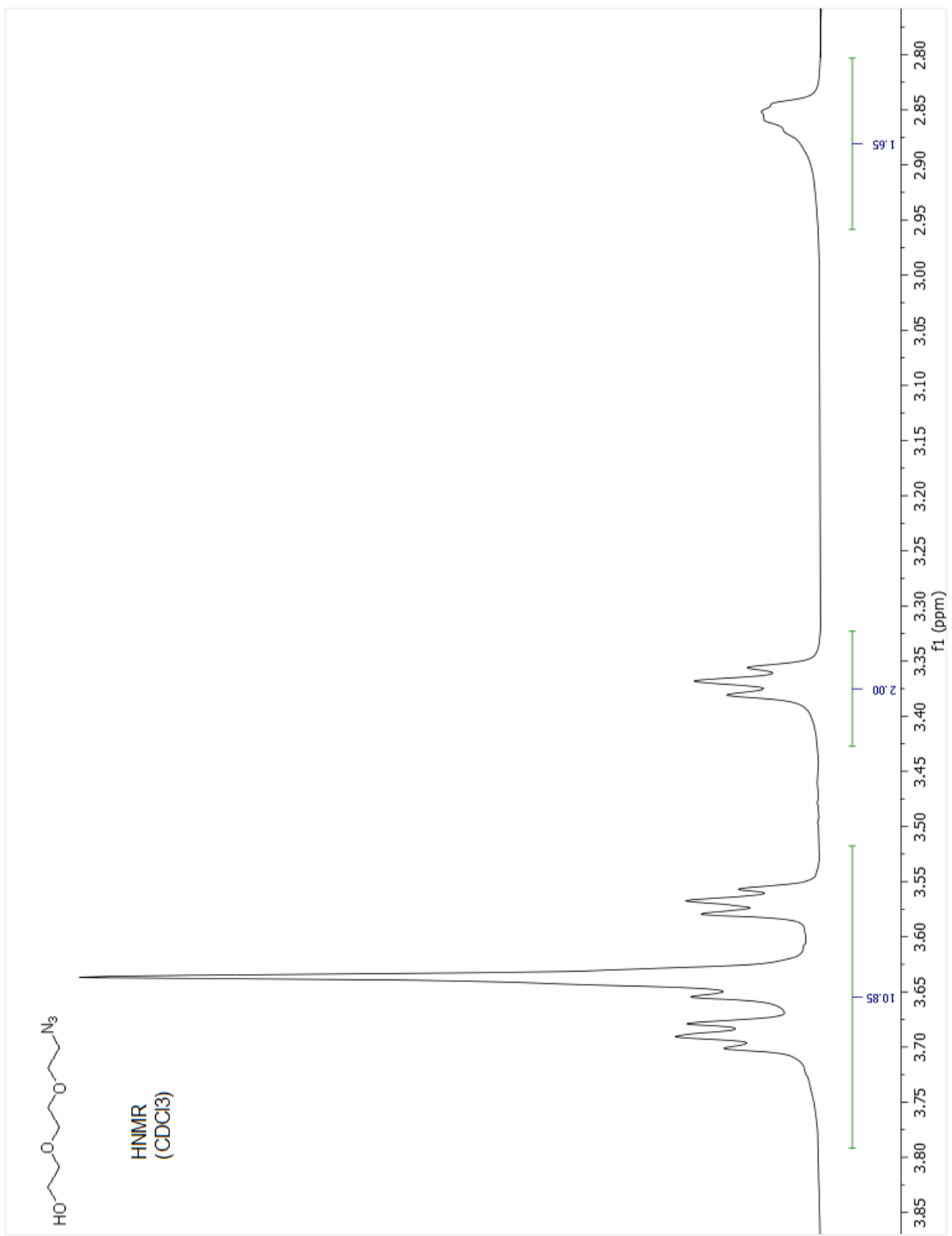


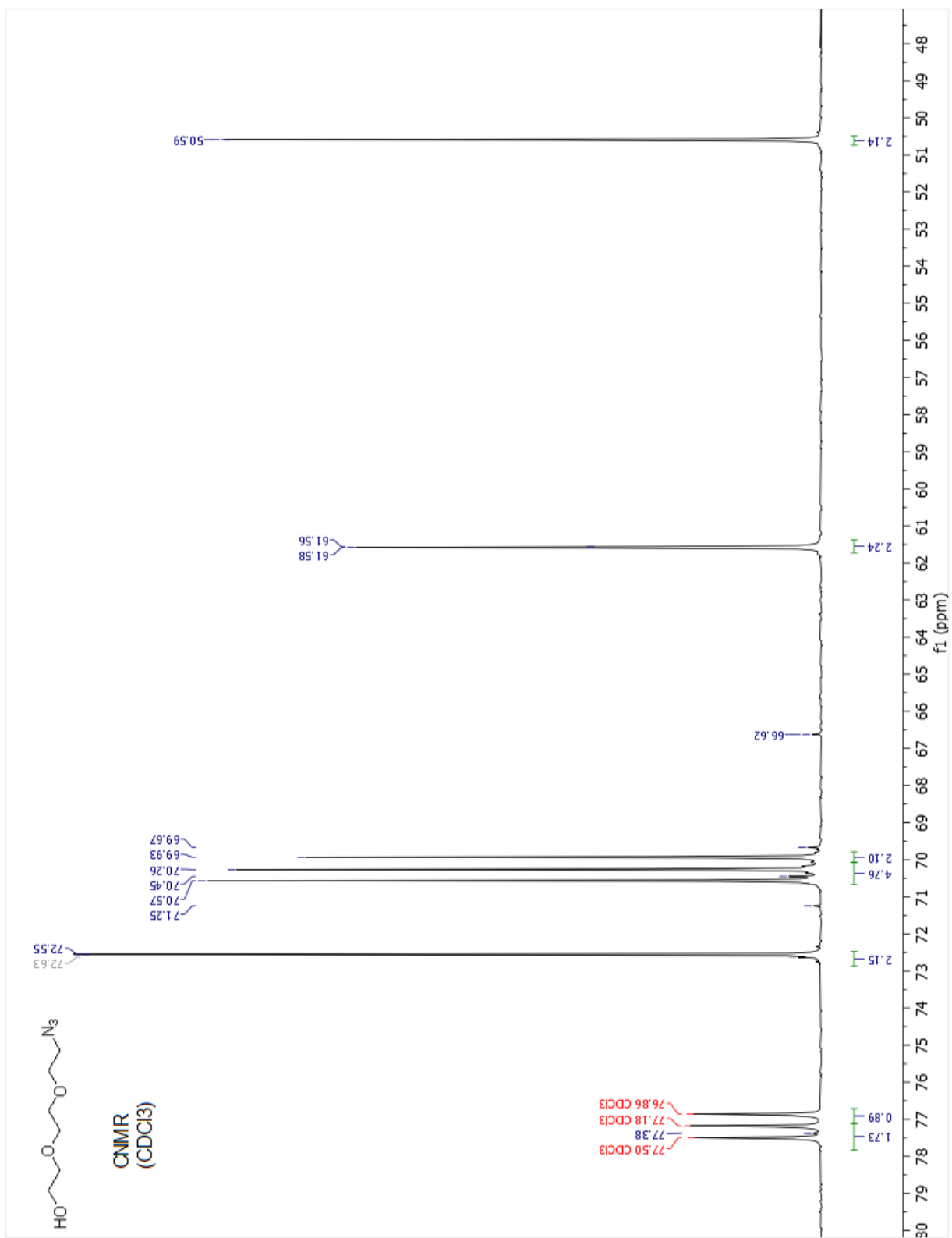


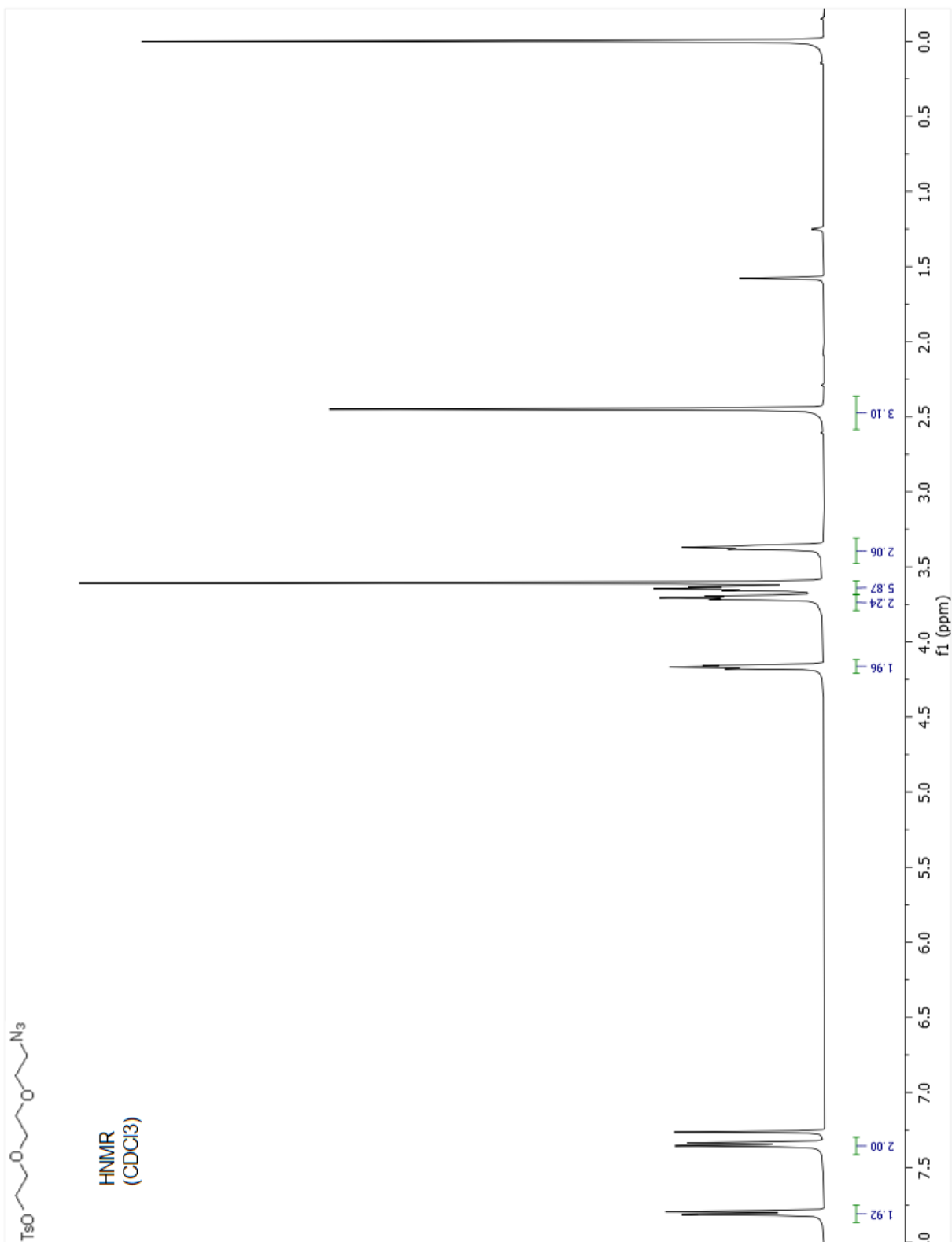


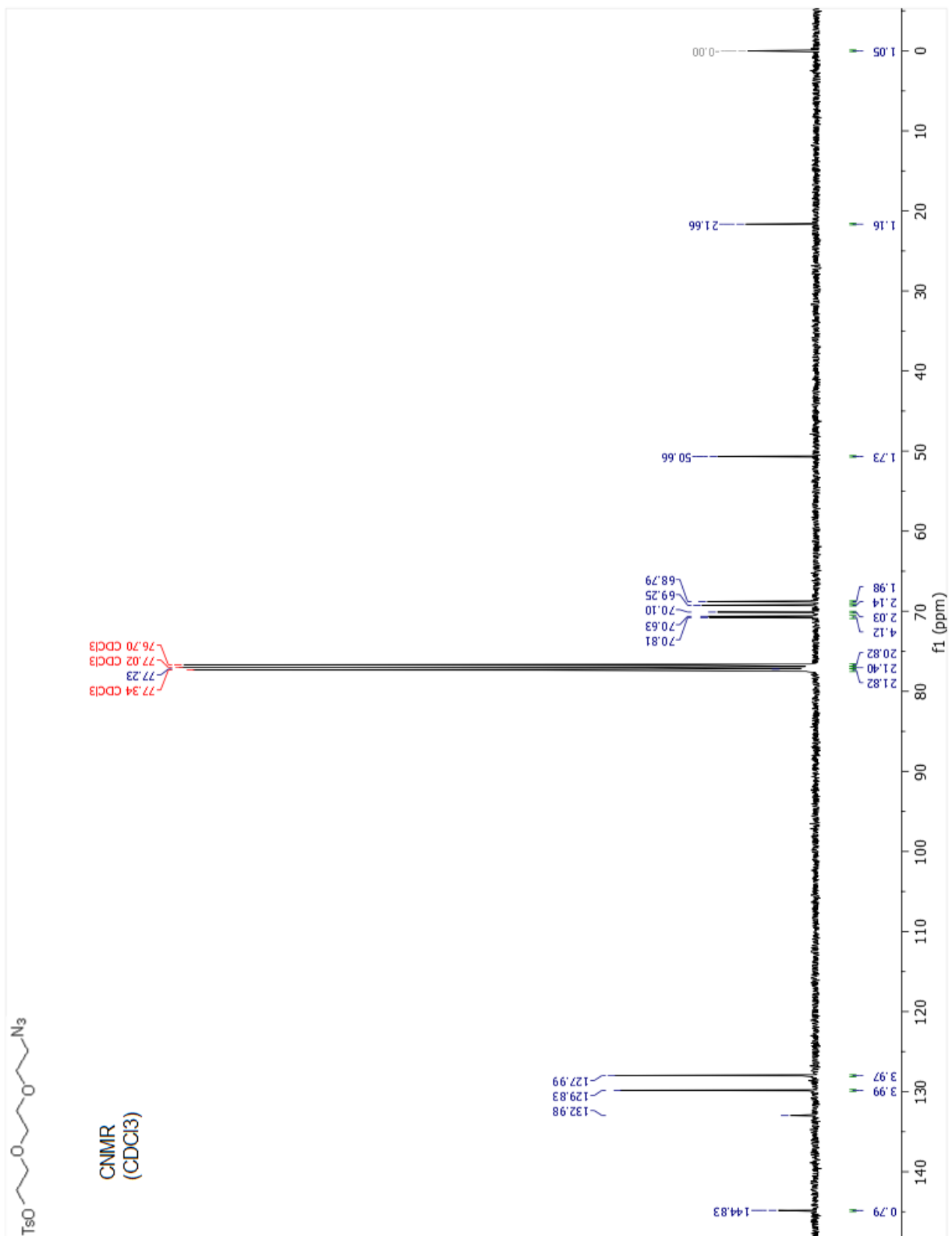






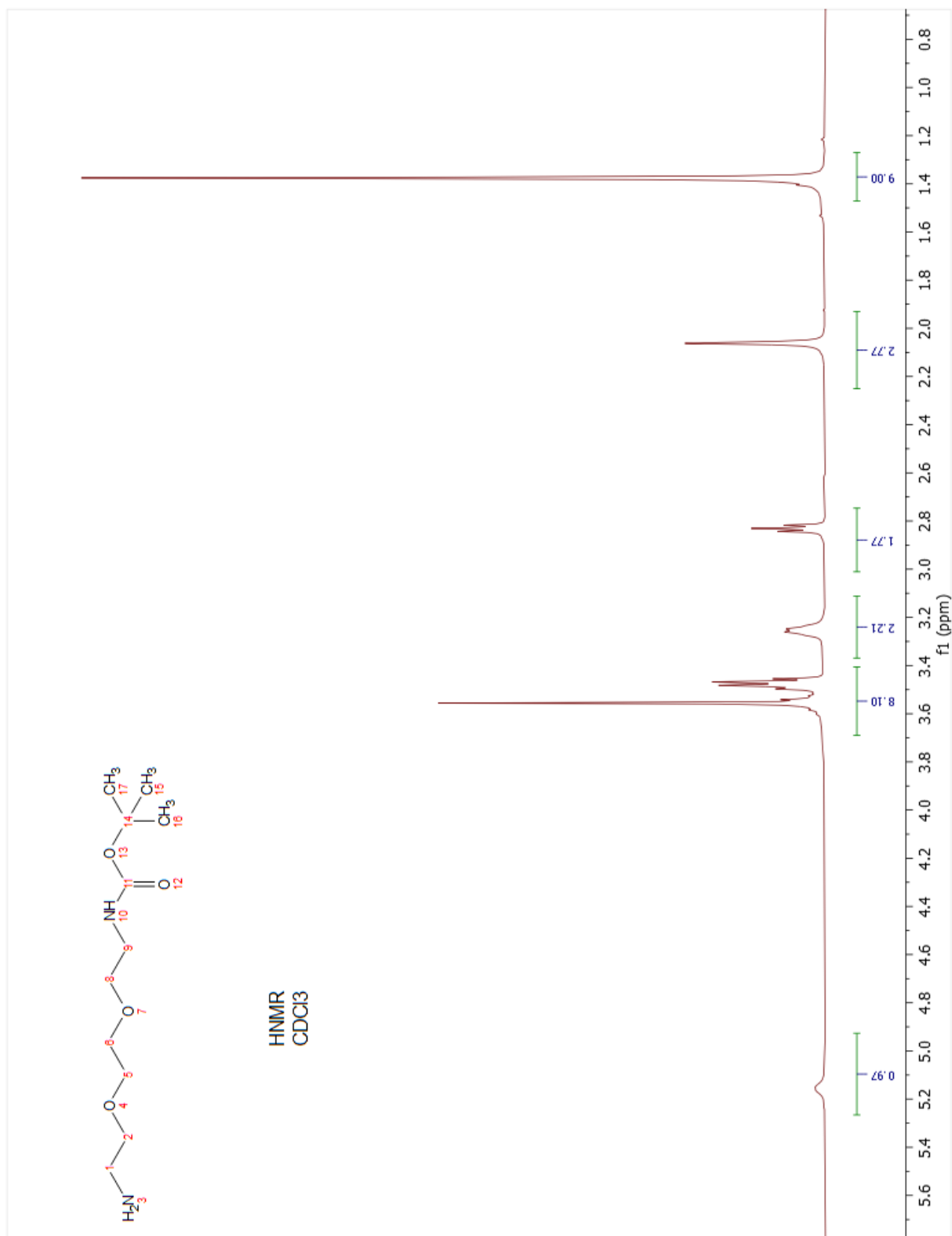


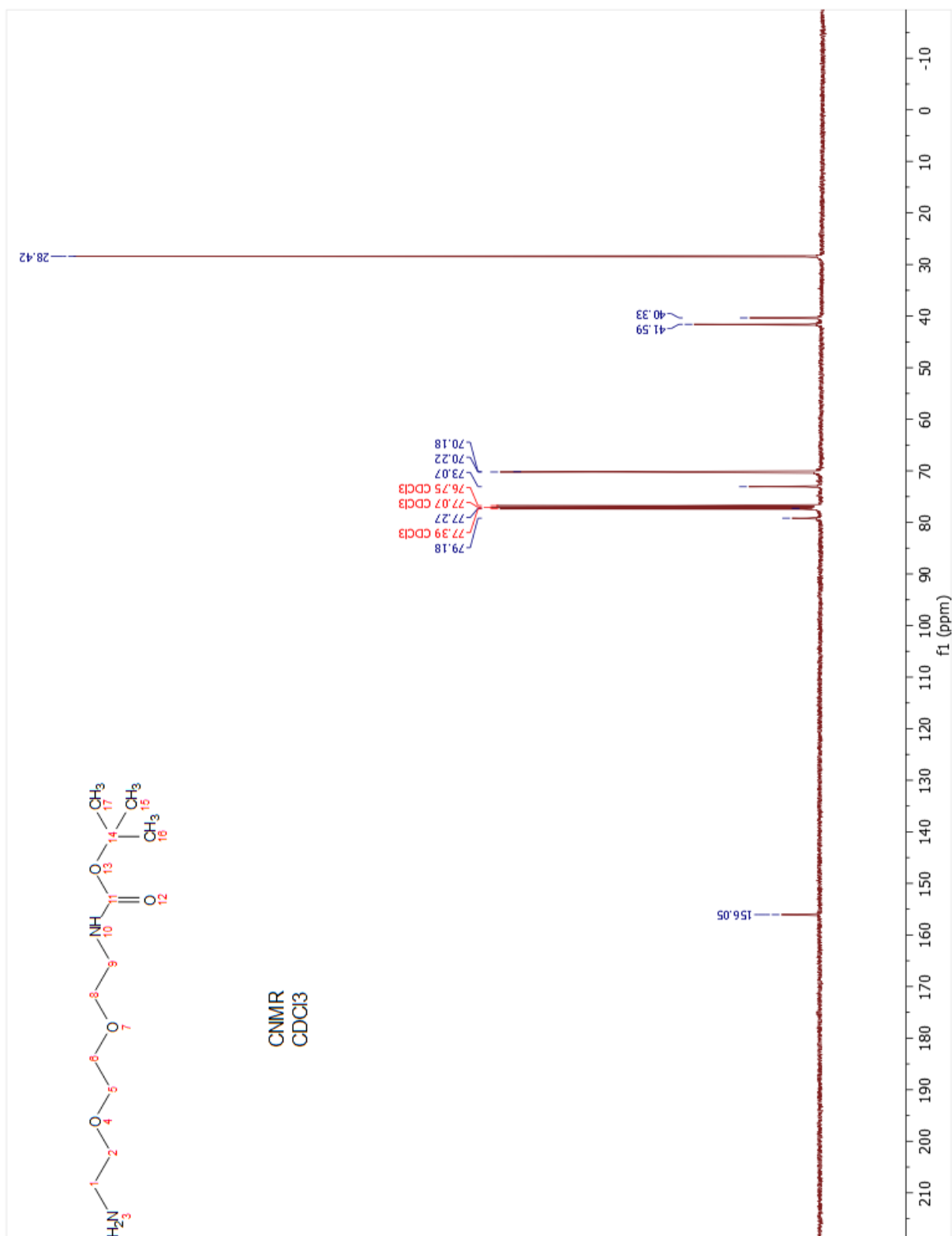


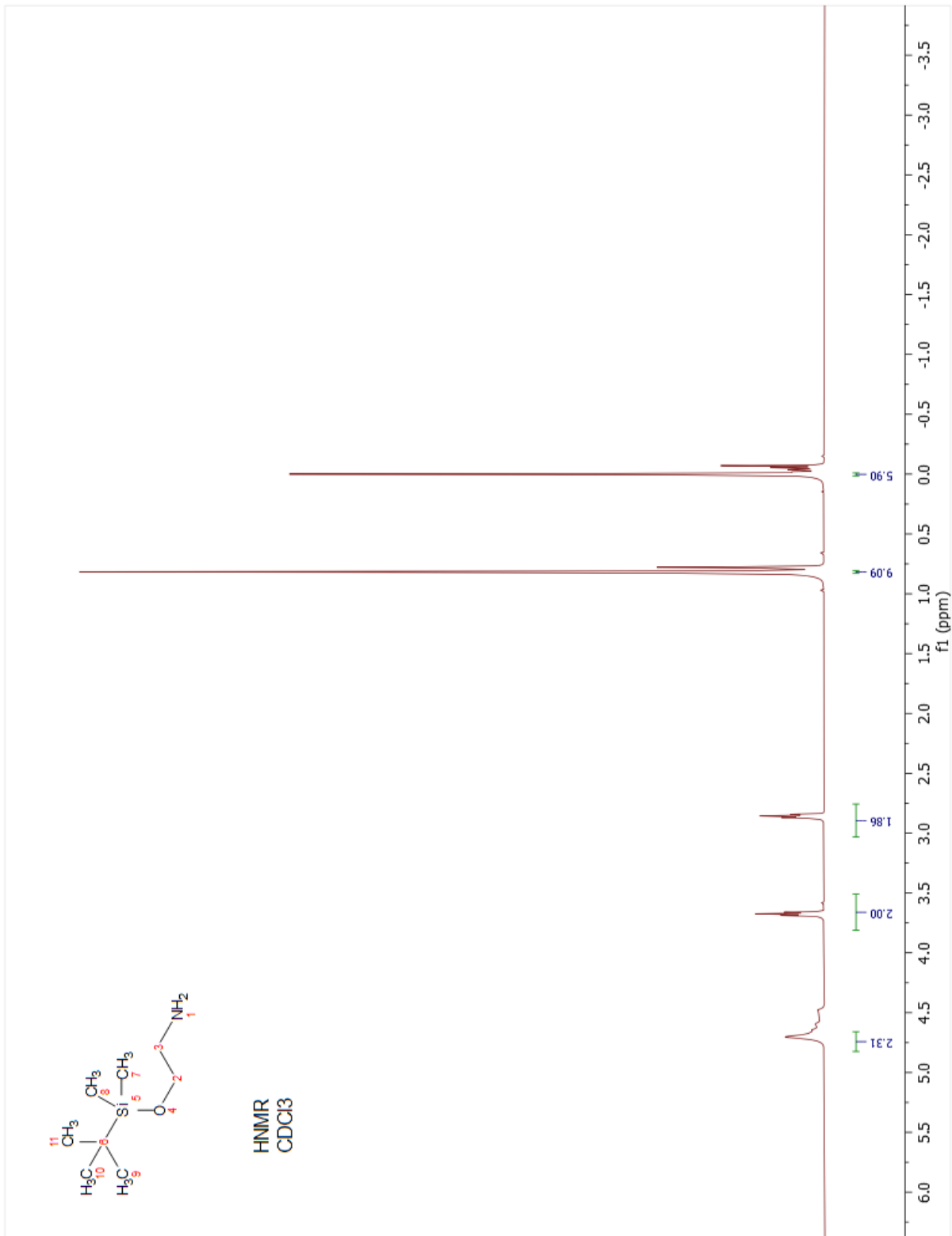


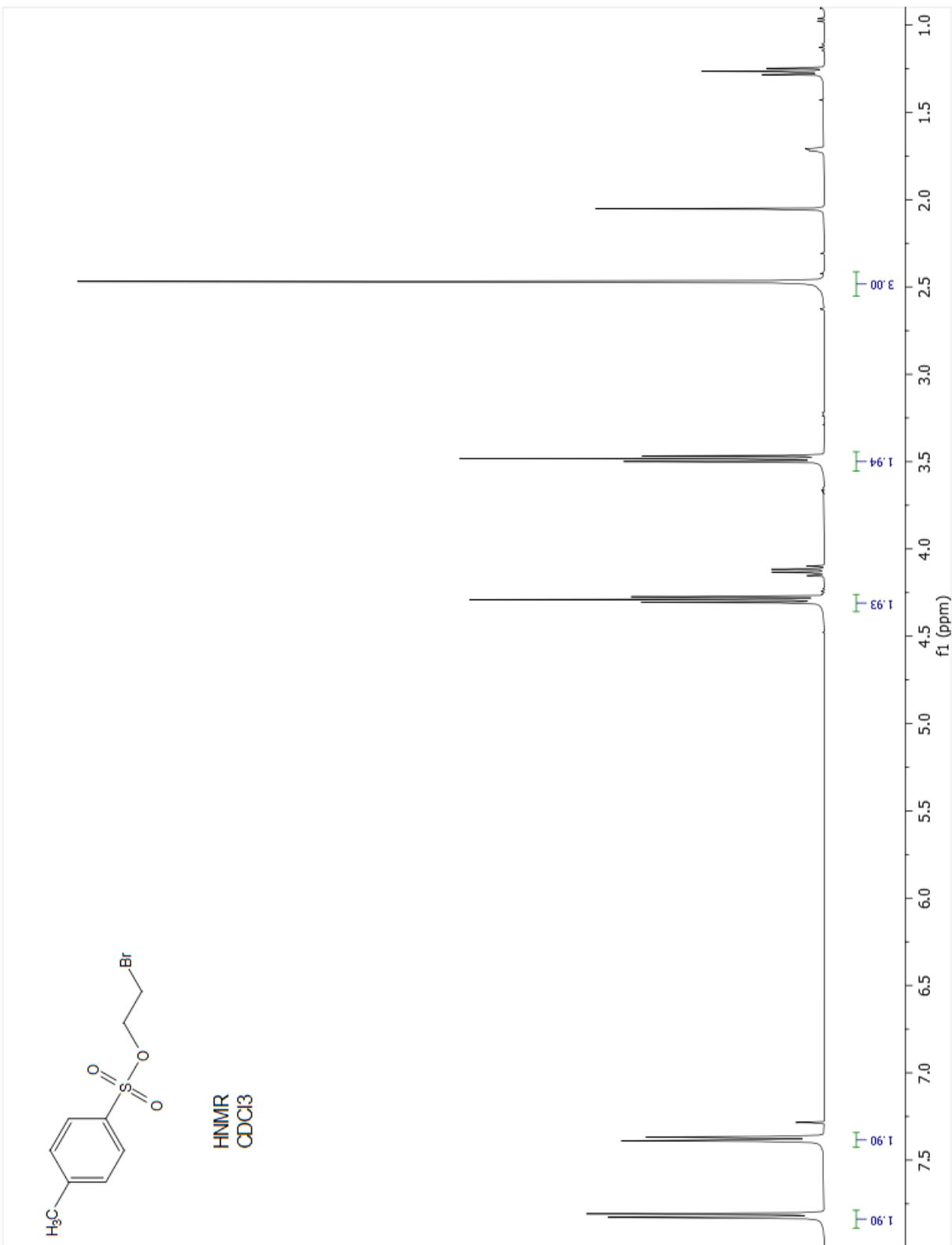


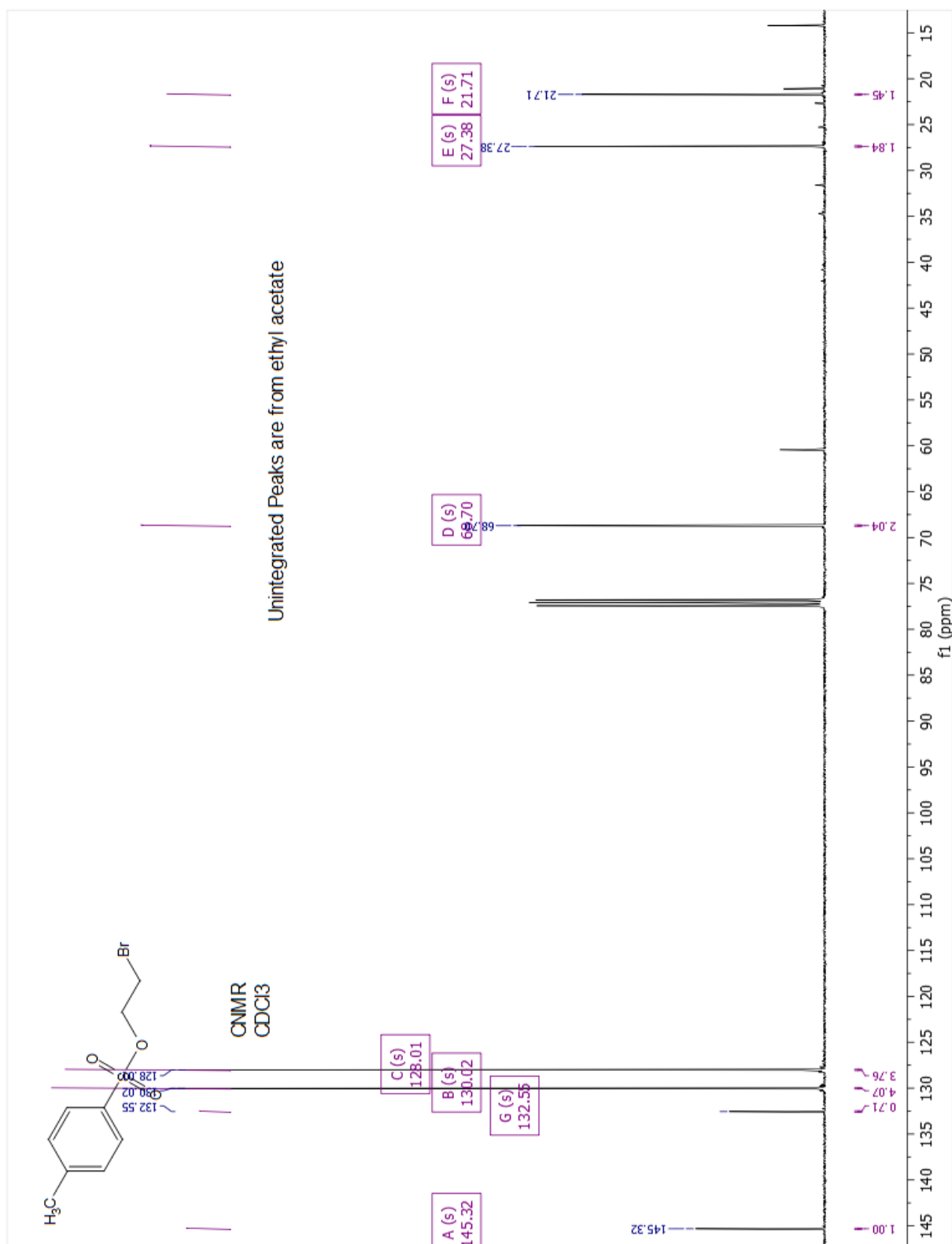


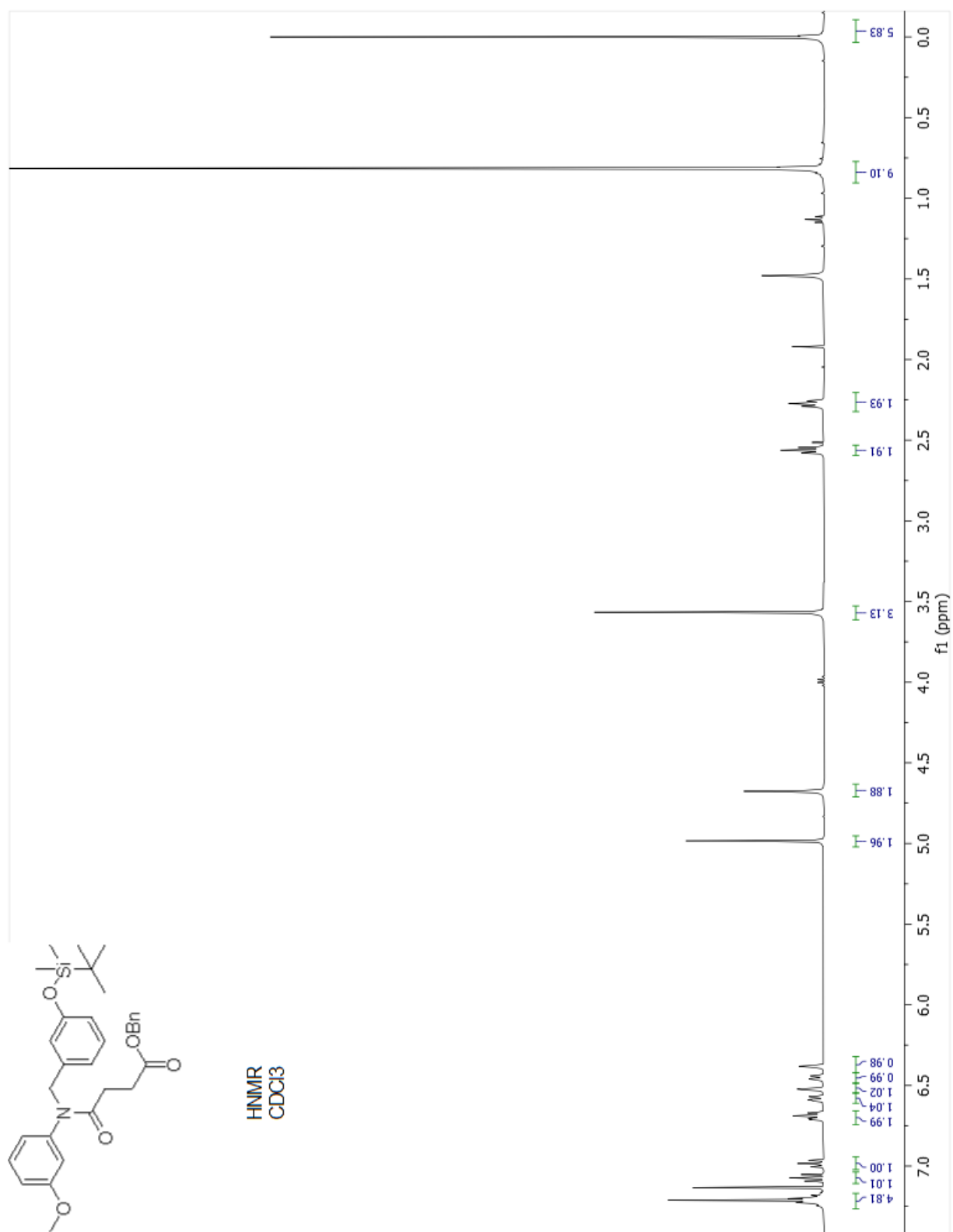


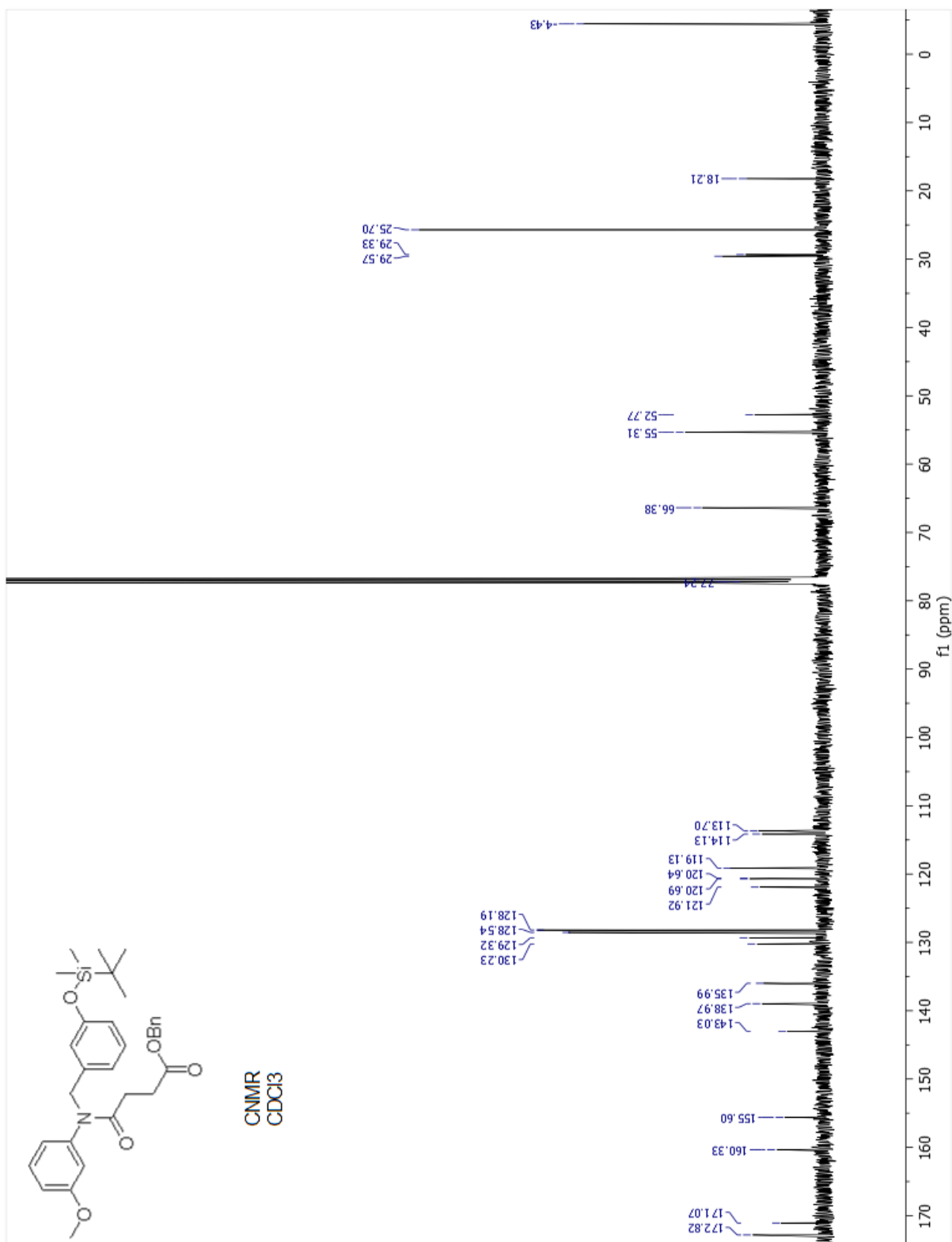


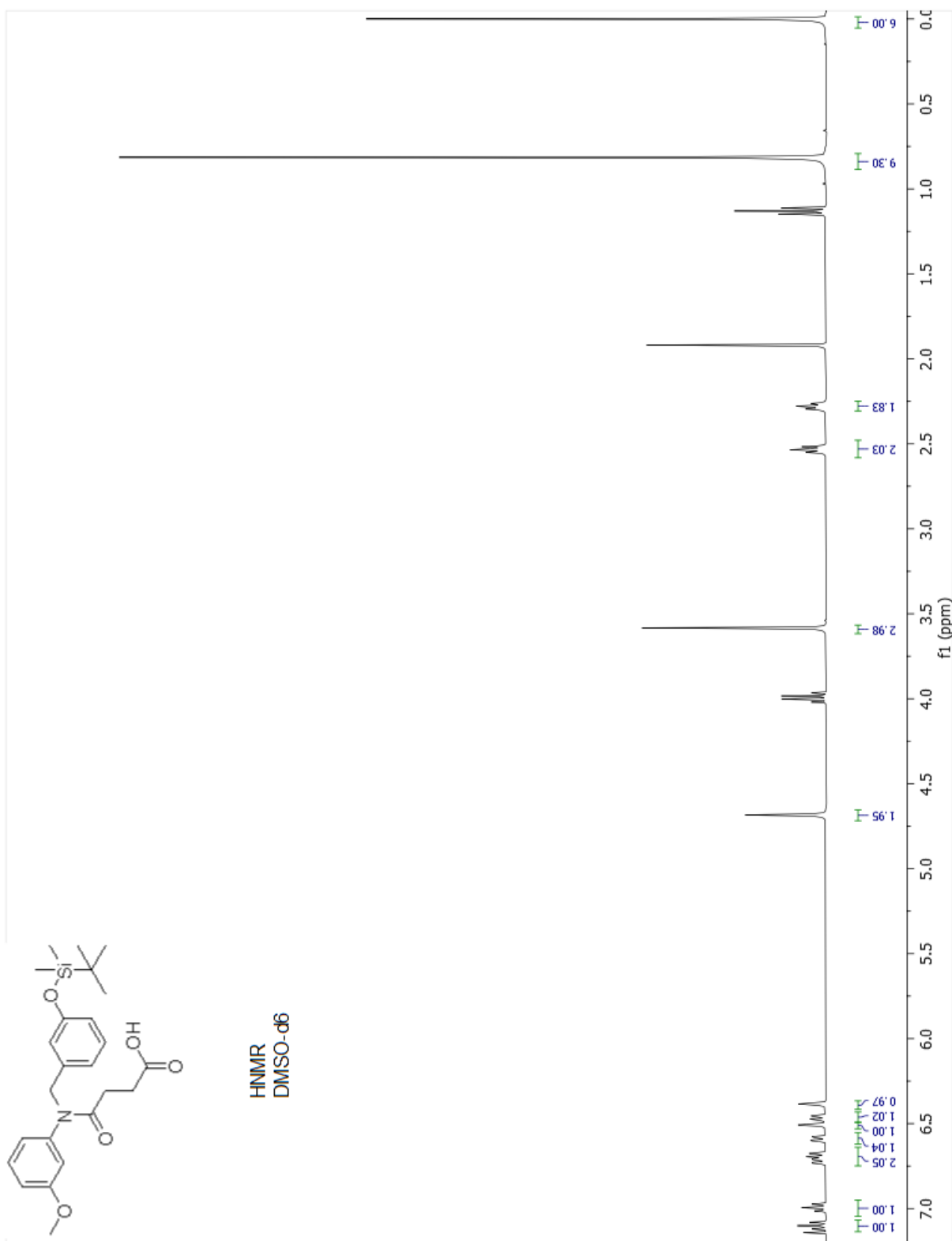




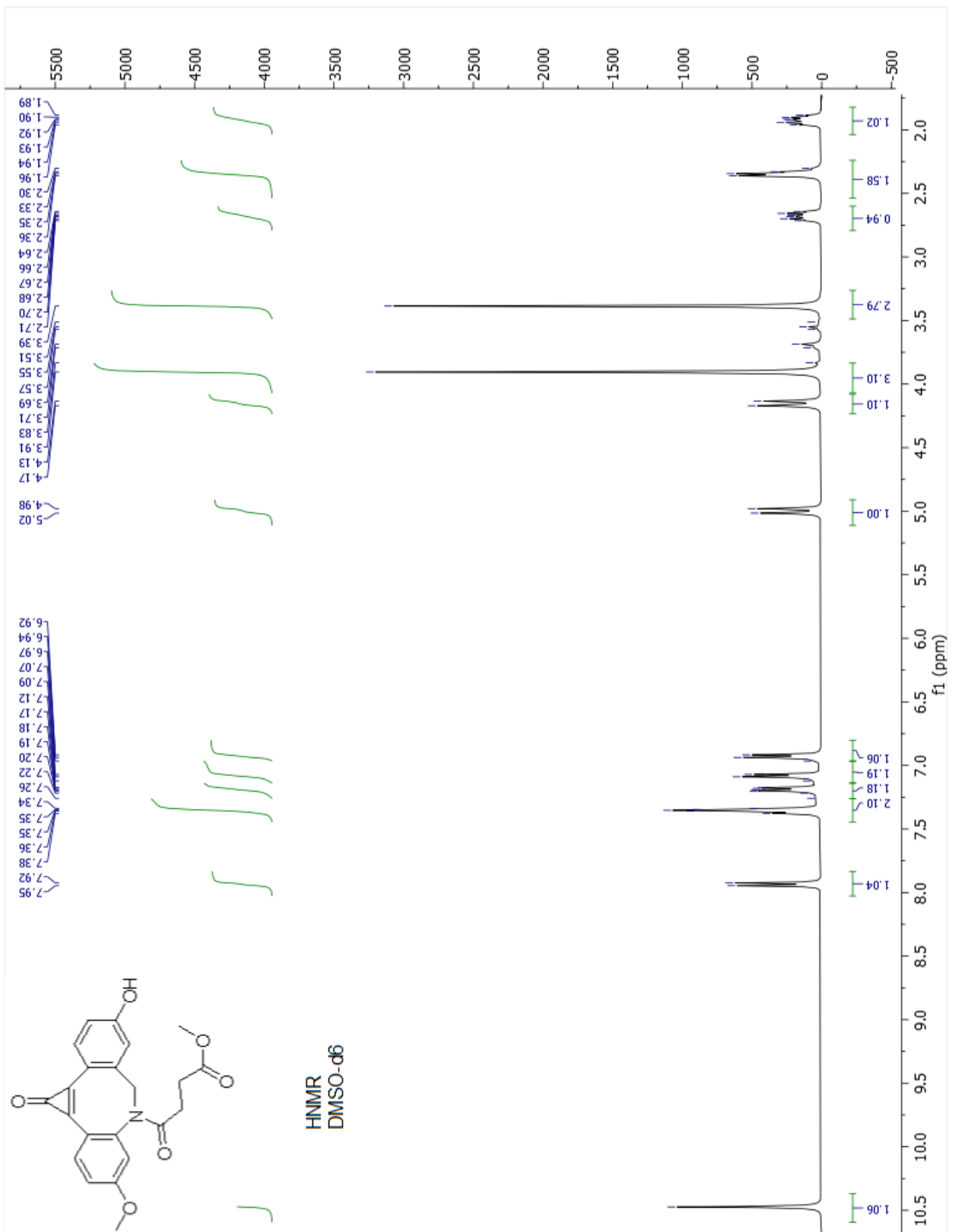


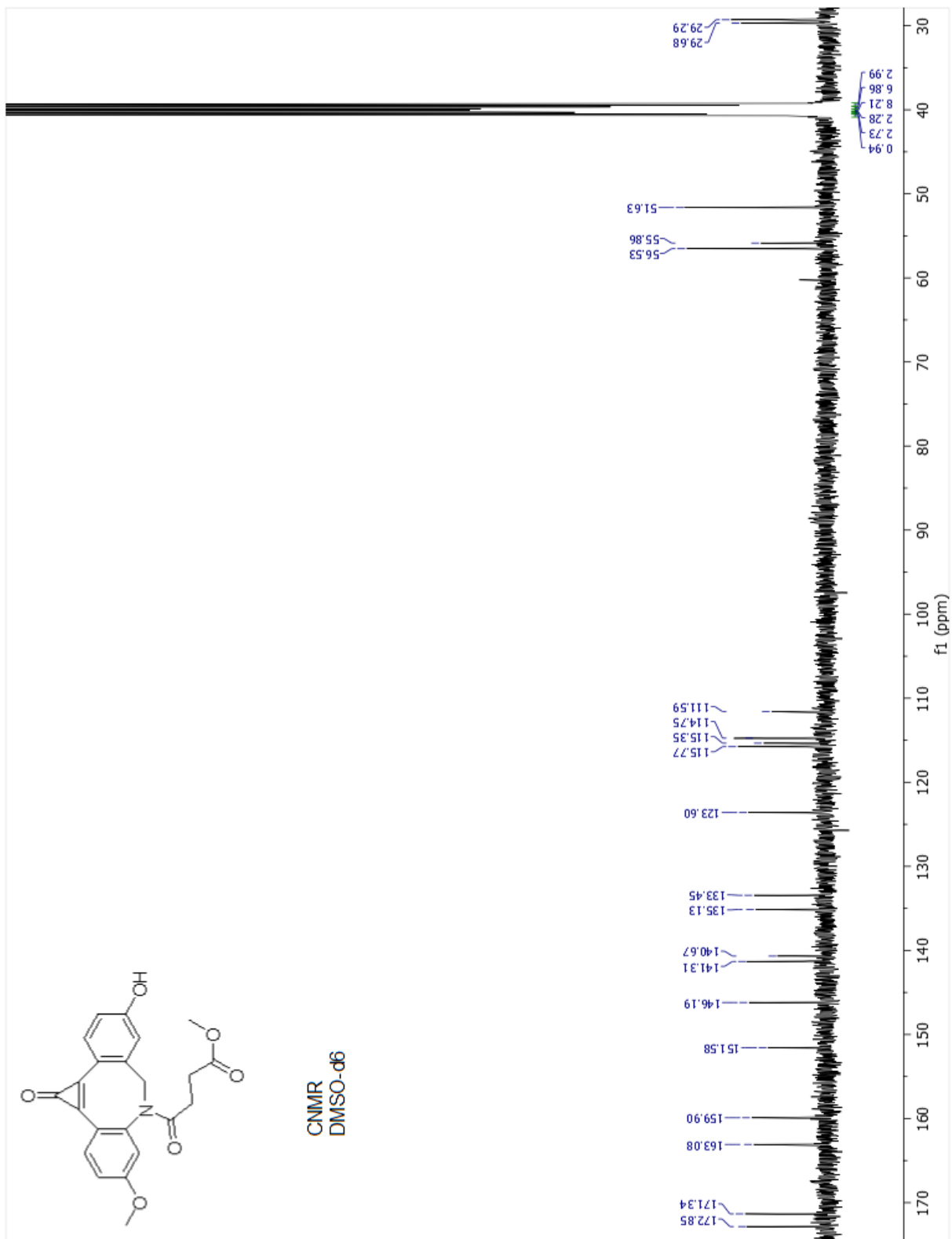


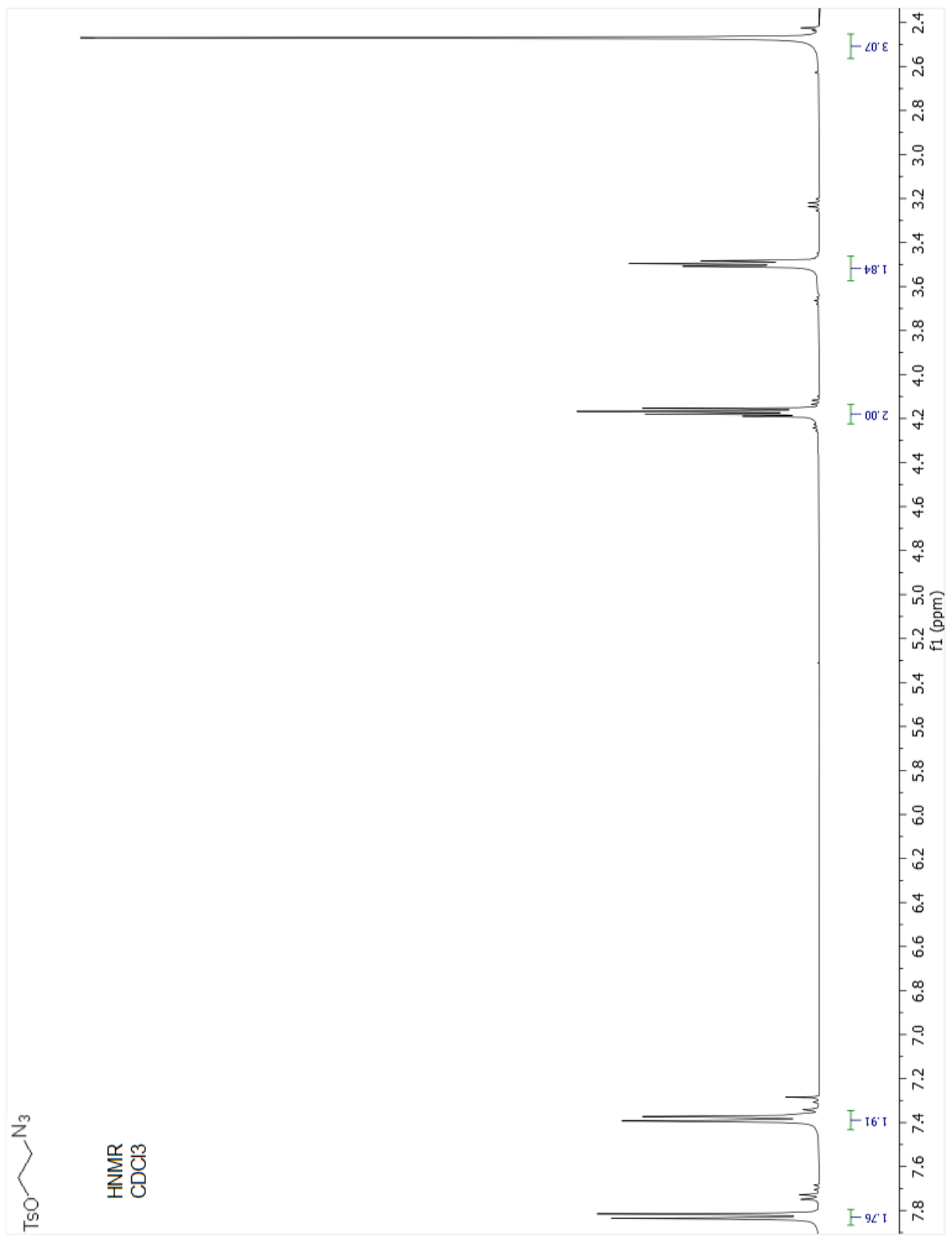


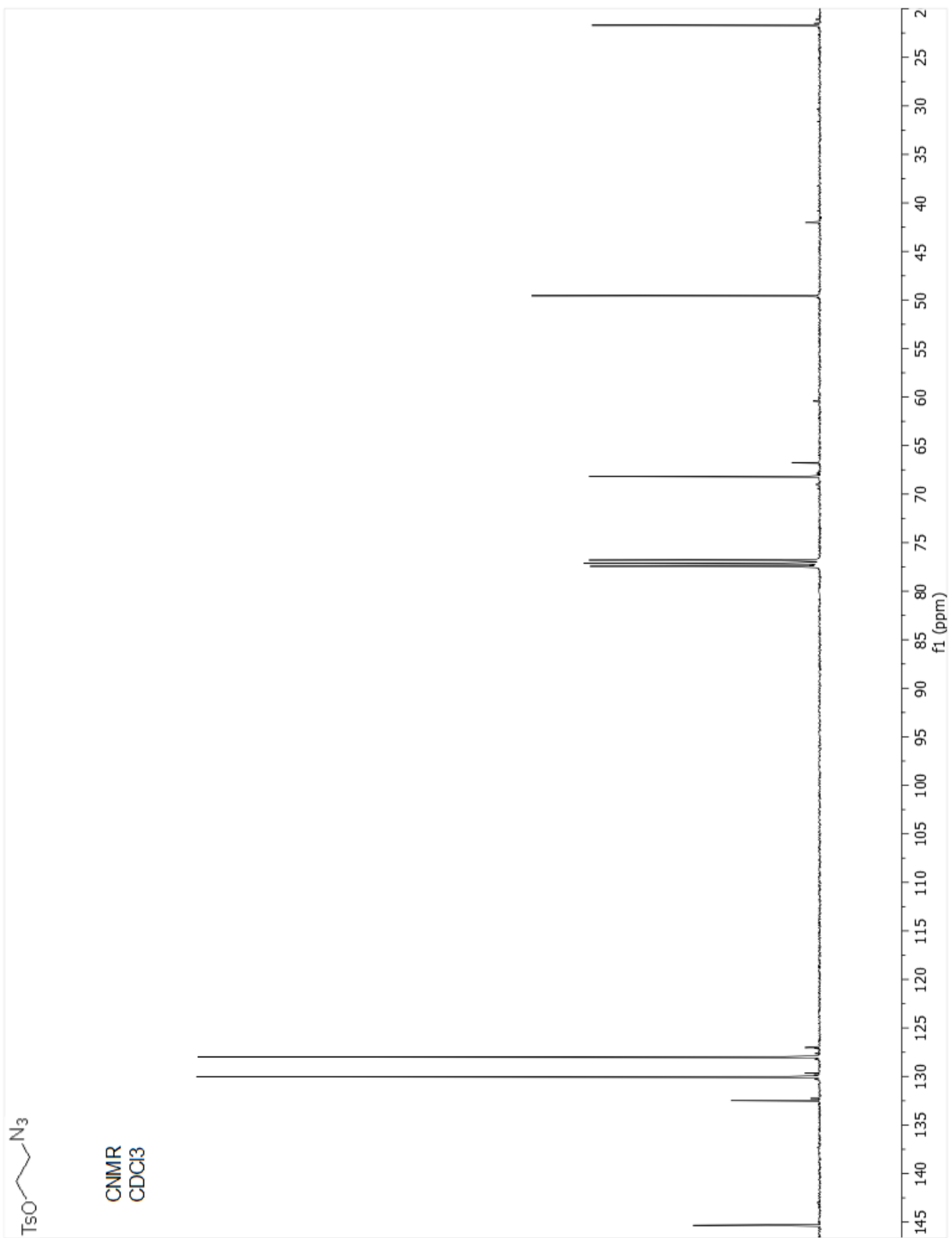


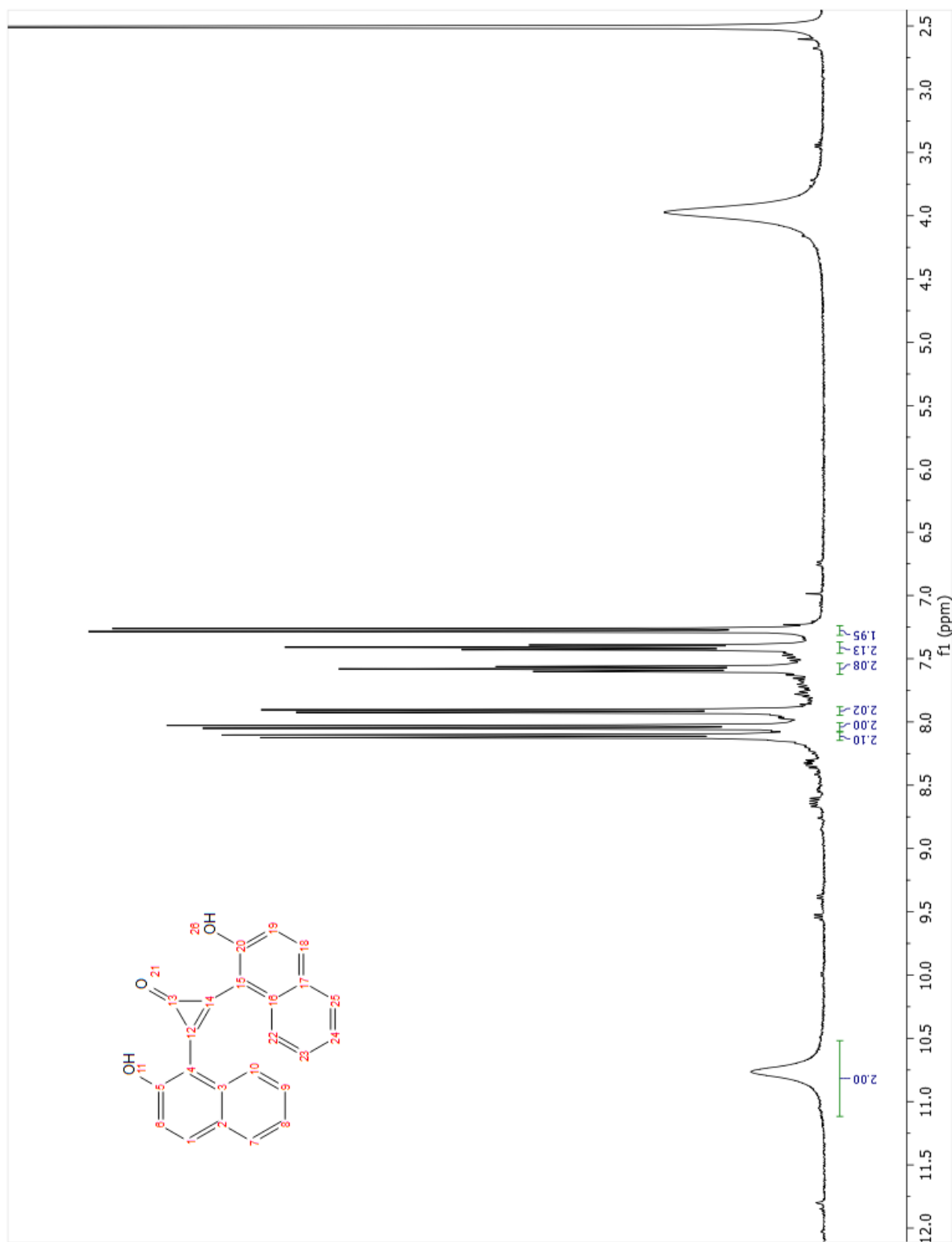


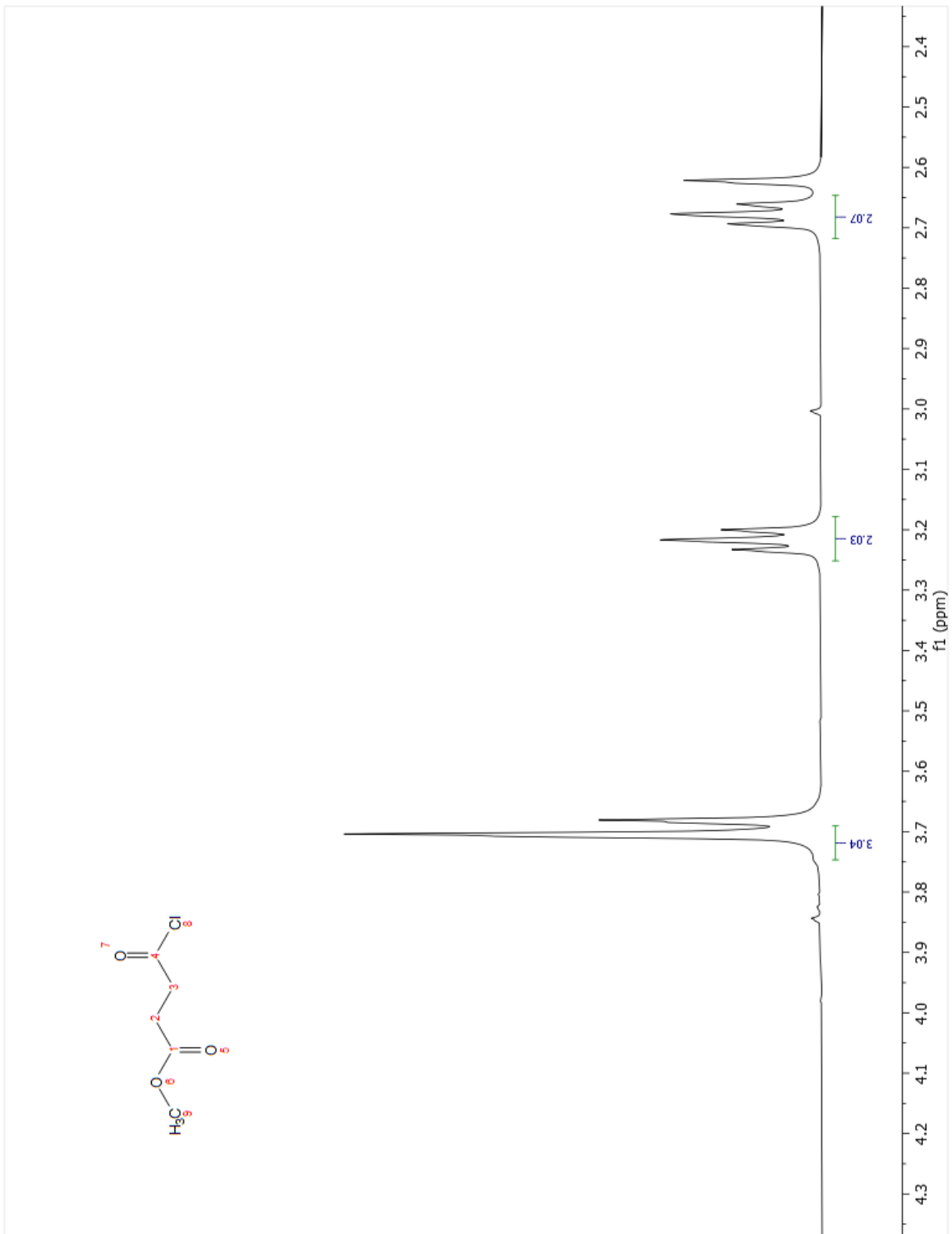
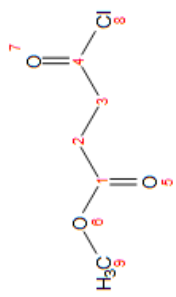














## 2. Measurement of pKa Value of 2.32

100  $\mu\text{L}$  2.40 mM Photo-ADIBO-Bis-OH methanol solution was added to the buffer (80.0  $\mu\text{L}$ ). UV-Vis spectra were taken immediately after solution preparation. UV spectra of compounds 1 and 2 looked very similar. Thus, it is hard to determine the pka of acid to carboxylate through UV-Vis spectrometry. For pka analysis, absorbance of spectra at 374 nm was used for analysis. Boltzmann fit was then applied to get approximate pka value. Pka (first phenol) value was expected to be  $6.97 \pm 0.01$  (from pH range 1.02 – 8.12).